

'I would like to dedicate this thesis to my parents '

'Thank you Mother and Father'

Exploration of a xenograft model of human prostate cancer to predict patient treatment response

Ramprakash Beekharry

MD Thesis

The University of York and The University of Hull,
Hull York Medical School

October 2014

ABSTRACT

For several years, docetaxel was the only treatment to improve survival of patients with metastatic prostate cancer. There are now many novel agents available but the optimal sequence of treatments remains undefined. The emergence of prostate cancer stem cells has brought a new way to elucidate the molecular mechanisms behind treatment failure and recurrence. Traditionally cell lines have been used in preclinical studies but recently 'near patient' derived xenografts (PDX), have been suggested to be a better way to investigate new therapies and investigate pathways in metastatic spread. First we used a subcutaneous and an orthotopic PDX model to determine which is most feasible in looking at the differences in the expression of basal and luminal cell markers. We then looked at the effect of docetaxel on hormone naïve and castrate resistant PDXs specifically measuring changes in the numbers of basal and luminal cells determining docetaxel resistance. Finally we tried labelling and fluorescent cell sorting PDX cells to track metastatic spread and monitor chemotherapy effects.

The mouse prostate microenvironment did not drastically change cellular phenotypes, allowing us to use the simpler subcutaneous method to assess chemotherapy effects on PDX. In fact the subcutaneous xenografts retained basal and luminal cells maintaining the clinical heterogeneity present in prostate cancers. In the docetaxel studies, alteration in AR expression and high levels of basal-like cells from the outset appeared to confer resistance. Although docetaxel had an overall detrimental effect, there was a typical decrease in the number of basal cells in both hormone naïve and resistant tumours. No trends were seen in the luminal populations. Side effects affecting continuation of treatment were evident. Lentiviral transduction was successful in PC3 cells where they maintained high levels of fluorescent (RFP) reporter expression. Transduction of PDX cells proved more challenging and requires further optimisation.

In the evolving area of new prostate cancer treatments, docetaxel chemotherapy continues to play an important role and could be given in hormone naïve cancers. This can also increase the chances of benefitting from the whole variety of new drugs. However, not all tumours are sensitive and resistance mechanisms remain unclear.

LIST OF CONTENTS

List of tables and figures	8
Presentations from this thesis and proposed publication	12
Acknowledgements	13
Author's Declaration	14

CHAPTER 1. INTRODUCTION

1.1 Anatomy of the prostate	16
1.2 Embryology and development of the prostate	19
1.3 Physiology of the prostate	20
1.4 Prostate Cancer	23
1.4.1 Incidence	23
1.4.2 Aetiology	25
1.4.3 Diagnosis Paradigms.....	27
1.4.3.1 PSA	
1.4.3.2 New Biomarkers	
1.4.4 Staging and Grading	31
1.4.4.1 Risk Assessment Methods	
1.4.5 Management	35
1.5 Castrate Resistant Prostate Cancer	39
1.5.1 Emergence.....	39
1.5.2 Targeting the Androgen-signalling axis and the molecular aspect of CRPC.....	40
1.5.3 AR amplification, mutations and splice variants.....	40
1.5.4 Ectopic androgen synthesis.....	41
1.5.5 Co-regulators of AR.....	41
1.5.6 AR independent pathways.....	42
1.6 CRPC treatment options.....	43
1.6.1 Docetaxel.....	43
1.7 Novel treatment options.....	46
1.7.1 Abiraterone Acetate.. ..	46
1.7.2 Enzalutamide.....	47
1.7.3 Radium-223 Chloride	47
1.7.4 Sipuleucel-T	47

1.7.5 Cabazitaxel.....	48
1.7.6 Denosumab	48
1.8 Clinical characteristics to predict treatment benefits.....	49
1.9 Chemotherapy in hormone naïve PC	50
1.10 Sequencing treatments in mCRPC.....	51
1.11 Cancer stem cells.....	52
1.11.1 Current concepts in PC stem cells.....	53
1.11.2 p63 in PC stem cells.....	55
1.11.3 CSC in CRPC.....	55
1.12 Models of studying PC.....	57
1.12.1 Cell lines.....	57
1.12.2 Primary cell cultures.....	58
1.12.3 ‘Near patient’ derived xenograft.....	58
1.12.4 PDX in other cancer models.....	59
1.12.5 In vivo mouse models.....	59
1.12.5.1 Xenografts in immunocompromised mice	
1.12.5.2 Genetically engineered mouse models	
1.12.6 The mouse prostate as an orthotopic model.....	62
1.13 Tracking PC stem cells.....	64
1.14 Hypothesis and Project Aims	66

CHAPTER 2. MATERIALS AND METHODS

2.1 Mammalian Cell culture	68
2.1.1 Cell lines	68
2.1.2 Live/dead cell count	68
2.2 Protein expression	69
2.2.1 Prostate and xenograft tissue	69
2.2.1.1 Tissue fixation and embedding	
2.2.1.2 Sectioning and mounting	
2.2.1.3 H&E staining	
2.2.1.4 Immunohistochemistry	
2.2.1.5 Cells counts and positive cell identification	
2.2.2 Flow cytometry	72
2.2.2.1 Cell surface protein detection	

2.2.2.2 Intracellular antigen detection	
2.2.2.3 Data analysis	
2.3 In vivo studies	75
2.3.1 General animal husbandry.....	75
2.3.2 Grafting of prostatic tumour cells	75
2.3.2.1 Depletion of mouse endothelial and lineage positive blood cells	
2.3.2.2 Subcutaneous engraftment of tumour cells	
2.3.2.3 Orthotopic engraftment of tumour cells	
2.3.3 Intraperitoneal injection of drug	79
2.3.4 Preparation of docetaxel	79
2.3.5 Analysis of treatment responses	80
2.3.6 Genotyping of PDXs.....	81
2.4 Tracking prostate epithelial cells	82
2.4.1 Lentivirus transduction of PC3 cells and selection with Blasticidin.....	82
2.4.2 Transduction of xenograft cells	82
2.4.3 Tumour initiation assay	82
2.4.4 Explant culture of tumour	83

CHAPTER 3. RESULTS I

Comparison between subcutaneous and orthotopic engraftment of PDXs using immunohistochemistry	85
3.1 Rationale.....	85
3.2 Setting up PDXs.....	87
3.3 Orthotopic engrafting of PC3 cells.....	89
3.4 Orthotopic engrafting of PDX cells.....	90
3.5 Histological analysis	92
3.6 Comparing cellular phenotypes between subcutaneous and orthotopic tumours	
3.6.1 Immunohistochemistry for p63	95
3.6.2 Immunohistochemistry for PSA	99
3.6.3 Immunohistochemistry for AR	101
3.6.4 Immunohistochemistry for Pancytokeratin	105
3.6.5 Immunohistochemistry for Vimentin	107

3.6.6 Immunohistochemistry for Ki67	111
3.7 Discussion.....	116

CHAPTER 4. RESULTS II

In-vivo targeting of a ‘near patient’ xenograft model with docetaxel	121
4.1 Rationale.....	121
4.2 Developing a protocol to determine the optimum dose of docetaxel.....	122
4.3 Treatment PDX Y019 with docetaxel	124
4.4 Effect of 15 and 20mg/kg docetaxel on the growth rate of PDX Y019	128
4.4.1 Histological analysis of Y019 xenograft following treatment	132
4.4.2 Immunohistochemistry of Y019 xenograft post treatment	134
4.4.3 Flow cytometry analysis of Y019 xenograft post treatment	137
4.4.3.1 Gating strategy	
4.4.3.2 FACS for CD24 and CD44	
4.4.3.3 FACS for Y019 proliferation	
4.5 Treatment of PDX H016 with docetaxel	141
4.5.1 Histological analysis of H016 xenograft post treatment	143
4.5.2 Immunohistochemistry of H016 xenograft post treatment	145
4.5.3 Flow cytometry analysis of H016 xenograft post treatment	147
4.5.3.1 FACS for CD24 and CD44	
4.5.3.2 FACS for AR	
4.5.3.3 FACS for H016 proliferation	
4.6 Treatment of PDX Y042 with docetaxel	151
4.6.1 Histological analysis of Y042 xenograft post treatment	153
4.6.2 Immunohistochemistry of Y042 xenograft post treatment	155
4.6.3 Flow cytometry analysis of Y042 xenograft post treatment ...	159
4.6.3.1 FACS for CD24 and CD44	
4.6.3.2 FACS for AR	
4.6.3.3 FACS for Y042 proliferation	
4.7 Summary of basal and luminal cell expression	162
4.8 Discussion.....	163
4.9 Docetaxel effects on basal cells.....	168
4.10 Docetaxel effects on luminal cells.....	169
4.11 Off target effects of docetaxel.....	170

CHAPTER 5. RESULTS III

Lentiviral transduction of PC3 and PDX cells for tracking metastatic spread

5.1 Rationale.....	172
5.2 The AMSBio™ lentiviral system.....	173
5.3 Generation of clonal, lentivirus transduced PC3 cell lines	175
5.4 Tumour initiation with transduced PC3 cells	177
5.5 Flow cytometry analysis of transduced PC3 tumours	178
5.6 Generation of lentivirus transduced patient derived xenograft cells	181
5.7 Tumour initiation with transduced Y042 cells	182
5.8 Flow cytometry analysis of transduced Y042 tumours	183
5.9 Discussion.....	184
5.10 Conclusion.....	186

CHAPTER 6. DISCUSSION AND CONCLUSION

6.1 Final Discussion.....	188
6.2 Conclusion and Future trends.....	190
REFERENCES	191
APPENDICES	206
ABBREVIATIONS	216

LIST OF TABLES AND FIGURES

	Page
TABLES	
Table 1: List of drugs used in medical castration for ADT.....	38
Table 2: Commonly used prostate cancer cell lines.....	57
Table 3: Series of immunocompromised mice used.....	60
Table 4: Gating strategy for FACS.....	74
Table 5: Summary of the advantages and disadvantages of the subcutaneous and orthotopic xenograft methods.....	86
Table 6: 'Near patient' derived xenografts.....	88
Table 7: Orthotopic injection of PC3 cells.....	89
Table 8: PDXs used for orthotopic prostate injections.....	90
Table 9: Outcomes of orthotopic prostate injections.....	91
Table 10: Comparison between the method of engraftment and the fraction of Ki67 positive cells.....	111
Table 11: Summary of the effect of docetaxel on basal and luminal populations in the 3 PDXs analysed.....	162
Table 12: Summary of the effect of docetaxel on p63 and AR populations.....	162

FIGURES

Figure 1.1: Lateral view of the adult prostate showing its pelvic location and anatomical relations.....	16
Figure 1.2: Schematic representation of the zonal anatomy of the adult prostate gland.....	17
Figure 1.3: Cross sectional views of the prostate gland showing the more clinically relevant lobes.....	18
Figure 1.4: Development of the prostate gland from the urogenital sinus of the male.....	19
Figure 1.5: The Hypothalamic-Pituitary-Gonadal Axis.....	21
Figure 1.6: Androgen action in the prostate.....	22
Figure 1.7: The ten most common cancers in males in the United Kingdom.....	23
Figure 1.8: New diagnoses of prostate cancer and age-specific incidence rates.	24
Figure 1.9: Proliferative inflammatory atrophy as a precursor to prostate intraepithelial neoplasia and prostate cancer.....	26

Figure 1.10: Tumour Nodal and Metastasis, staging of prostate cancer.....	32
Figure 1.11: Conventional and modified Gleason grading system.....	33
Figure 1.12: Development of CRPC.....	39
Figure 1.13: Chemical formula of docetaxel.....	44
Figure 1.14: Hierarchical or stem cell model of cancer.....	51
Figure 1.15: Phenotype of the prostate cancer stem cells and more differentiated prostate cancer cells.....	54
Figure 1.16: Diagram of the anatomy of the murine prostate.....	63
Figure 1.17: Simplified version of the retroviral life cycle.....	65
Figure 3.1: H016, H&E staining.....	93
Figure 3.2: Y042, H&E staining.....	93
Figure 3.3: Y018, H&E staining.....	94
Figure 3.4: Y019, H&E staining.....	94
Figure 3.5: p63 staining in subcutaneous and orthotopic Y042 tumours.....	96
Figure 3.6: p63 staining in subcutaneous and orthotopic H016 tumours.....	96
Figure 3.7: p63 staining in subcutaneous and orthotopic Y018 tumours.....	97
Figure 3.8: p63 staining in subcutaneous and orthotopic Y019 tumours.....	98
Figure 3.9: PSA staining in subcutaneous and orthotopic xenografts.....	100
Figure 3.10: AR staining in subcutaneous and orthotopic Y042 tumours.....	101
Figure 3.11: AR staining in subcutaneous and orthotopic H016 tumours.....	102
Figure 3.12: AR staining in subcutaneous and orthotopic Y018 tumours.....	103
Figure 3.13: AR staining in subcutaneous and orthotopic Y019 tumours.....	104
Figure 3.14: PCK staining in subcutaneous and orthotopic xenografts.....	106
Figure 3.15: Vimentin staining in subcutaneous and orthotopic Y042 tumours..	107
Figure 3.16: Vimentin staining in subcutaneous and orthotopic H016 tumours..	108
Figure 3.17: Vimentin staining in subcutaneous and orthotopic Y018 tumours..	109
Figure 3.18: Vimentin staining in subcutaneous and orthotopic Y019 tumours..	110
Figure 3.19: Ki67 staining in subcutaneous and orthotopic Y042 tumours.....	112
Figure 3.20: Ki67 staining in subcutaneous and orthotopic H016 tumours.....	113
Figure 3.21: Ki67 staining in subcutaneous and orthotopic Y018 tumours.....	114
Figure 3.22: Ki67 staining in subcutaneous and orthotopic Y019 tumours.....	115

Figure 4.1: Overview of the in vivo protocol to determine the effect of docetaxel on tumour growth.....	123
Figure 4.2: Time frame and schedule for docetaxel injection.....	123
Figure 4.3: Effect of docetaxel on mouse weight.....	125
Figure 4.4: Effect of docetaxel on PDX Y019 tumour growth.....	126
Figure 4.5: Kaplan-Meier curve of overall survival following treatment with docetaxel.....	127
Figure 4.6: Increasing the docetaxel dose has a detrimental effect on the weight of mice.....	129
Figure 4.7: Effect of increasing docetaxel on Y019 tumour growth.....	130
Figure 4.8: Kaplan-Meier curve of overall survival in the 3 groups.....	131
Figure 4.9: H&E staining of PDX Y019.....	133
Figure 4.10: AR staining of PDX Y019.....	134
Figure 4.11: p63 staining of PDX Y019.....	135
Figure 4.12: Ki67 staining of PDX YO19.....	136
Figure 4.13: Flow cytometry gating strategy.....	137
Figure 4.14: Flow cytometry analysis for Y019 xenograft after treatment with docetaxel.....	139
Figure 4.15: Percentage of dead Y019 cells after docetaxel.....	140
Figure 4.16: H016 tumour growth curve.....	142
Figure 4.17: External appearance of tumour mass of H016.....	143
Figure 4.18: H&E staining of H016 xenograft.....	144
Figure 4.19: AR staining of PDX H016.....	145
Figure 4.20: p63 staining of PDX H016.....	146
Figure 4.21: Ki67 staining of PDX H016.....	146
Figure 4.22: Flow cytometry analysis of H016 xenograft after treatment with docetaxel.....	148
Figure 4.23: FACS to show AR staining.....	149
Figure 4.24: Percentage of dead Y019 cells after docetaxel.....	150
Figure 4.25: Effect of docetaxel on PDX Y042 tumour growth.....	151
Figure 4.26: Survival curves of Y042 xenograft after treatment.....	152
Figure 4.27: External appearance of tumour mass of Y042 after treatment with docetaxel.....	153
Figure 4.28: H&E staining of Y042 xenograft.....	154

Figure 4.29: AR staining of Y042 xenograft.....	156
Figure 4.30: p63 staining of Y042 xenograft.....	157
Figure 4.31: Ki67 staining of Y042 xenograft.....	158
Figure 4.32: Flow cytometry analysis for Y042 xenograft after treatment with docetaxel.....	159
Figure 4.33: Flow cytometry analysis for AR on Y042 xenograft after treatment with docetaxel.....	160
Figure 4.34: Percentage of dead Y042 cells after docetaxel.....	161
Figure 4.35: Antitumour activity of docetaxel.....	164
Figure 5.1: The AMSBio lentivirus.....	173
Figure 5.2: Transduced PC3 cells post Blasticidin selection.....	176
Figure 5.3: Clonal selection of transduced PC3 cells.....	176
Figure 5.4: Explant of a transduced PC3 tumour.....	177
Figure 5.5: Flow cytometry analysis of transduced PC3 cells.....	178
Figure 5.6: Flow cytometry analysis of untransduced PC3 cells.....	179
Figure 5.7: Flow cytometry analysis of transduced PC3 clones.....	180
Figure 5.8: Lentivirus transduction of Y042 PDX cells.....	181
Figure 5.9: Explant of transduced Y042 tumours.....	182
Figure 5.10: LIN depleted Y042 tumour analysed by flow cytometry.....	183

PRESENTATIONS AND PUBLICATIONS FROM THIS THESIS

Part of this work has been presented to the following scientific meetings:

- Yorkshire Urology Group (YUAG), November 2012 – Poster presentation
- Association of Surgeons in Training (ASiT), April 2013 – Oral presentation
- Hull York Medical School Annual Scientific Meeting (HYMS), June 2013 – Oral presentation
- British Association of Urological Surgeons (BAUS) Annual meeting, June 2014 – Poster presentation
- EAU section of Urological Research (ESUR), September 2013 – Oral presentation (**Award Winner**)
- National Cancer Research Institute Conference (NCRI), November 2013 – Poster presentation
- EAU Annual Meeting, April 2014 – Poster presentation
- Yorkshire Cancer Research (YCR) Annual Scientific Meeting, June 2014 – Poster presentation
- EAU section of Urological Research (ESUR), October 2014 – Oral presentation
- British Association of Urological Surgeons (BAUS) Annual meeting, June 2015 – Poster presentation

Part of this work is under consideration for publishing:

- **Patient-derived Xenografts represent the clinical heterogeneity of human prostate cancer**

^{1,2} Ramprakash Beekharry, ³Paula Kroon, ¹Marie-Christine Labarthe-Last, ²Vincent Mann, ⁴Greta Rodriguez, ^{2,5}Matthew Simms., ¹Norman J Maitland, ¹Anne T Collins
Manuscript in preparation

ACKNOWLEDGEMENTS

I opted for time out of clinical urology training to pursue new goals and study the much-anticipated field of prostate cancer research. This thesis is the culmination of a rewarding period in the lab for which I am grateful to many people. First and foremost, I would like to thank Professor Norman J Maitland who gave me this unique opportunity. He took patience in guiding me through the new journey of research. His warm welcome and advice were a godsend. My deepest thanks go to Mr Matthew Simms, my clinical supervisor at Castle Hill Hospital. He is a great mentor and role model. I can only aspire to follow his steps. What a great surgeon!

Many thanks to Dr Anne Collins, whose relentless efforts guided me in performing in vivo experiments and flow cytometry. There are many people I wish to thank: Paul Berry, Hannah Walker, Catherine Hyde and Dr Fiona Frame for their technical support; Samantha Hansford for managing the lab; Michelle Scaife for secretarial assistance; Bert and Lisa for cleaning and tidying. I would also like to thank my thesis advisory panel, TAP members Dr Fabiola Martin and Professor Paul Kaye for their timely feedback. Thanks to Dr Graeme Park and Dr Karen Hogg from the Technology Facility for operating the cell sorter.

In the end, I especially want to thank the prostate cancer patients from Castle Hill Hospital and York District Hospital for consenting to provide tissue material. Special thanks to Dr Vincent Mann and Mr Michael Stower for making tissue provision a reality. Finally, I would like to express my gratitude to Yorkshire Cancer Research for funding this work.

AUTHOR'S DECLARATION

I confirm that this work is original and that if any passages or diagrams have been copied from academic papers, books, the Internet or any other sources these are clearly identified by the use of quotation marks and the references are fully cited. I certify that, other than where indicated, this is my own work and does not breach the regulations of HYMS, the University of Hull or the University of York regarding plagiarism or academic conduct in examinations. I have read the HYMS Code of Practice on Academic Misconduct, and state that this piece of work is my own and does not contain any unacknowledged work from any other sources. I confirm that any patient information obtained to produce this piece of work has been appropriately anonymised.

Ram Beekharry

October 2014

CHAPTER 1

INTRODUCTION

1.1 Anatomy of the prostate

The prostate gland is approximately 3cm in diameter and walnut sized. It is the largest accessory gland of the male reproductive system. The glandular part consists of approximately two-thirds of the prostate and the other third is fibromuscular. It has a dense fibrous capsule and sheath, which anchors it in the pelvis (Figure 1.1) with puboprostatic ligaments. The prostate has:

- A base, directly adjacent to the bladder neck

- An apex, in contact with the superior aspect of the urethral sphincter and deep perineal muscles

- A posterior surface that is related to the ampulla of the rectum

- A muscular anterior surface with muscle fibres continuous interiorly with the urethral sphincter

- Inferolateral surfaces related to the levator ani (Moore and Dalley, 1999).

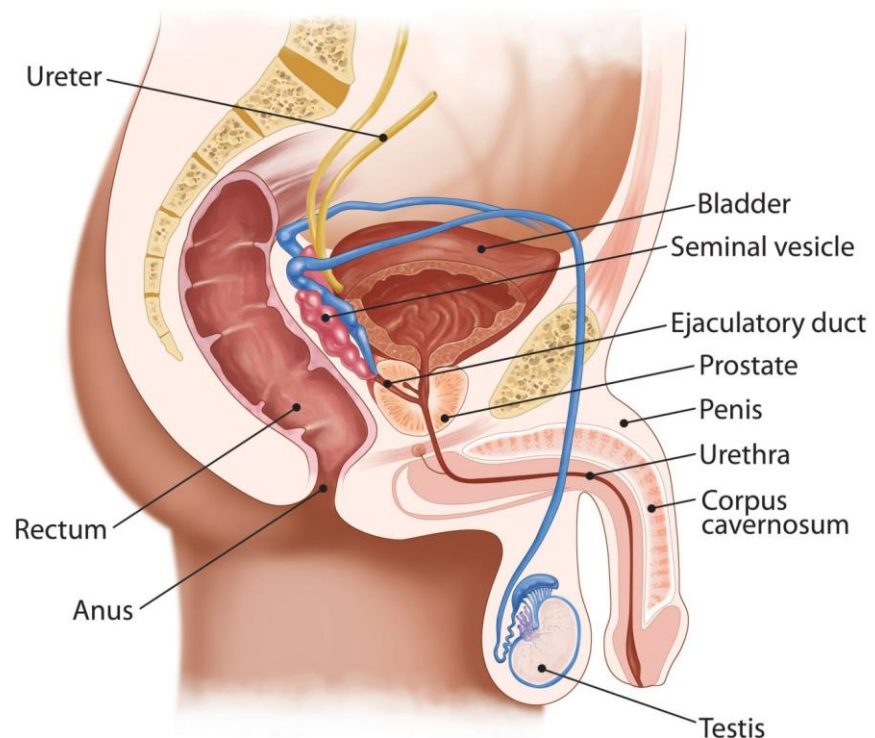


Figure 1.1: **Lateral view of the adult prostate showing its pelvic location and anatomical relations.** Image taken from <http://urologyinleeds.com/page1/>

The prostate can be described in two ways: as zones or lobes.

The zonal classification was first introduced by McNeal (McNeal, 1981). He divided the prostate into four distinct zones (Figure 1.2) as follows:

The transition zone surrounds the majority of the proximal urethra as it comes out of the bladder neck. It accounts for 5-10% of the glandular tissue of the prostate. This area continues to grow throughout life and is where benign prostatic hypertrophy develops (McNeal, 1988).

The central zone surrounds the ejaculatory ducts and comprises 25% of the glandular tissue. It lies directly in contact with the bladder base. It accounts for approximately 2.5% of prostate cancer cases, although they tend to be more aggressive and invade the seminal vesicles (Cohen et al., 2008).

The peripheral zone is the sub capsular portion of the posterior part of the prostate surrounding the transition zone, central zone and the rest of the prostatic urethra after the ejaculatory ducts. The majority of prostate cancers originate here (McNeal, 1988).

The fibromuscular zone is situated anteriorly and has very few glandular components. It is also known as the fibromuscular stroma. Only very rarely are prostate cancers found there.

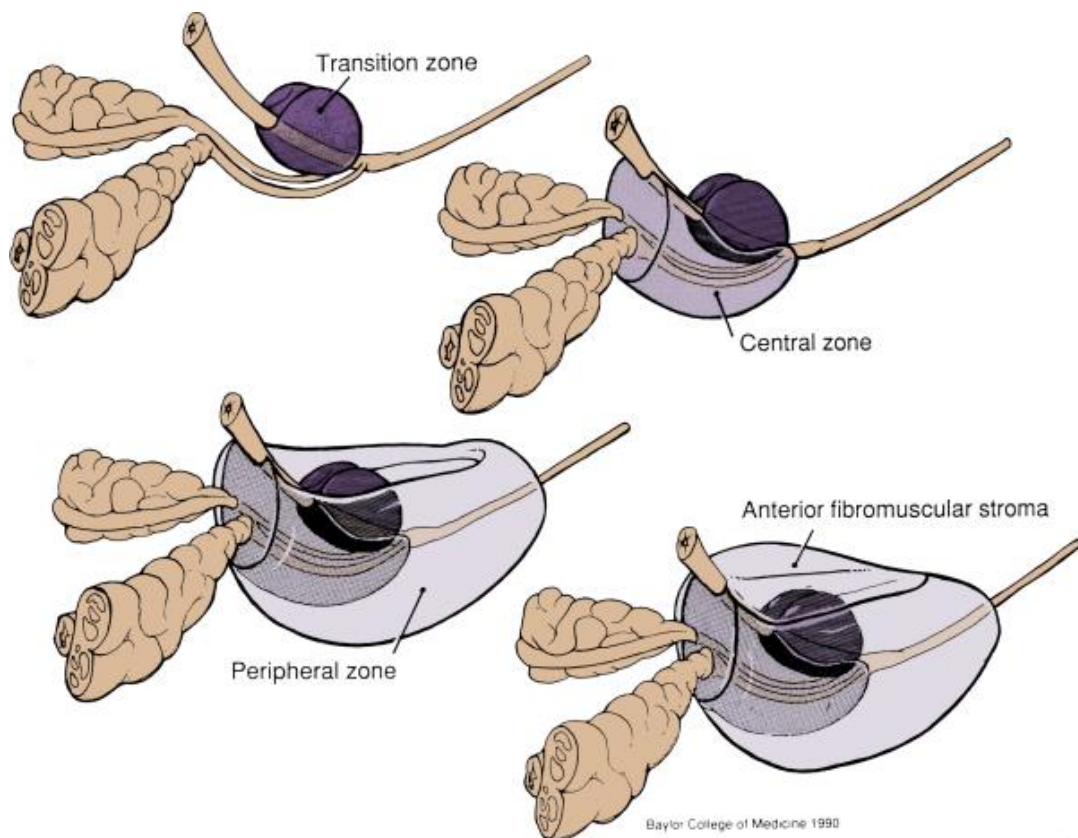


Figure 1.2: **Schematic representation of the zonal anatomy of the adult prostate gland.** As described by J.E. McNeal in 1981. Image taken from <http://www.aokainc.com/prostate-anatomy-pictures/>

The prostate gland can also be described in terms of lobes although these are not clearly distinct anatomically (Figure 1.3). This terminology is mainly used in clinical practice:

The anterior lobe or isthmus lies anterior to the urethra. This is mainly comprised of fibromuscular fibres, continuous with the urethral sphincter muscle.

The posterior lobe lies posterior to the urethra and inferior to the ejaculatory ducts. This is readily palpable by digital rectal examination.

The lateral lobes on either side of the urethra form the major part of the prostate.

The middle (median) lobe lies between the urethra and the ejaculatory ducts and is connected to the bladder neck.

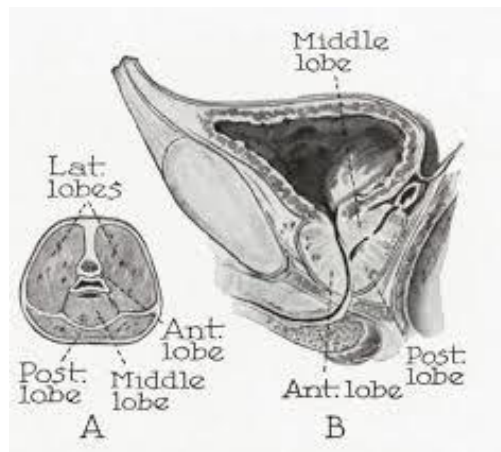


Figure 1.3: **Cross sectional views of the prostate gland** showing the more clinically relevant lobes. Image taken from <http://intranet.tdmu.edu.ua>

1.2 Embryology of the prostate

The prostate gland begins to develop in the 10th week of gestation. At the caudal end of the embryo lies the urogenital sinus, which is endodermal in origin. It comprises three unequal sized parts of which the largest forms most of the bladder and the lowest (or phallic) part forms the penis and penile urethra. The middle or pelvic part of the sinus forms the remainder of the prostatic urethra and the prostate gland. The surrounding mesoderm forms the fibromuscular stroma (Sinnatamby, 1999) (Figure 1.4). Prostate buds initiate as small epithelial projections that elongate into the surrounding stroma, undergo branching morphogenesis, and arborize into the mature ductal network (Keil et al., 2014).

This development depends on the conversion of secreted testosterone to dihydrotestosterone. Subsequent differentiation of the prostate epithelium occurs in a proximal to distal progression and is mediated by the expression of several transcription factors, including p63 (a tumour suppressor gene with homology to p53) and Foxa1 (Schoenwolf et al., 2008). This also helps to maintain the growth of the prostate gland during the foetal and neonatal period.

Until puberty, the prostate gland remains mainly in a quiescent state with few morphological changes taking place. An increase in testosterone at puberty causes prostatic enlargement and full maturation of ducts from the age of 12 to 18 years (Lee et al., 1995).

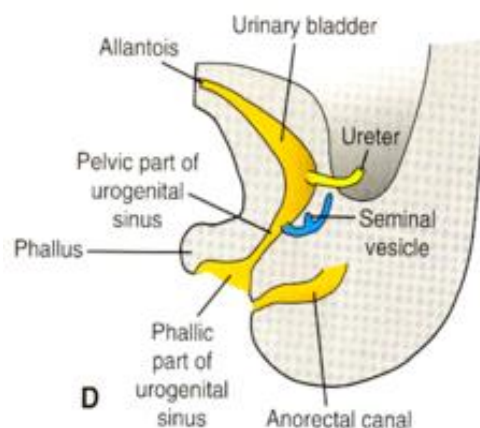


Figure 1.4: **Development of the prostate gland from the urogenital sinus of the male.** The pelvic part of the urogenital sinus forms the prostatic and membranous parts of the urethra. The phallic part of the urogenital sinus forms the spongy part of the urethra and the urethral vestibule. Illustration from: <https://web.duke.edu/anatomy/embryology/urogenital/urogenital.html>

1.3 Physiology of the prostate

The prostate gland secretes a thin, milky fluid that contains small molecules and multiple proteins. It has calcium, citrate ions, phosphate ions, polyamines, clotting enzyme and profibrinolysin. During emission, the capsule of the prostate gland contracts so that the secretions mix with sperm from the vas deferens. It is alkaline to neutralise the relative acidic contents of the vas and helps in sperm survival in the vagina where the pH is acidic (Hall and Guyton, 2000).

In the mature prostate, the main cell types are basal, secretory luminal and neuroendocrine (Aumuller, 1991). The luminal cells produce prostate specific antigen (PSA), prostate acid phosphatase (PAP) and human-kallikrein-2 which are all secreted into seminal fluid (McNeal, 1988). The fibromuscular tissue (noncellular stroma and connective tissue) makes up the ground substance and the extracellular matrix, which play an important role in the prostate physiology.

The function of the prostate gland depends on androgens. Testosterone is the most abundant of the androgens and is formed by the Leydig cells in the testicles and to a smaller extent in the adrenal glands. Production of androgens is in turn regulated by the hypothalamic-pituitary-gonadal axis. (Figure 1.5)

In the prostate, androgen is converted by the intracellular enzyme 5α -reductase into the more potent dihydrotestosterone (DHT), which binds to androgen receptors (AR) in the cell cytoplasm. The AR ligand complex induces translocation into the nucleus. This facilitates the binding of the AR with additional nuclear proteins to produce transcriptional complexes, which can bind to the androgen responsive elements (ARE) in the promoter region of target genes (Xu et al., 1998) (Figure 1.6). It is the target proteins that promote growth of the gland and control PSA and PAP secretion.

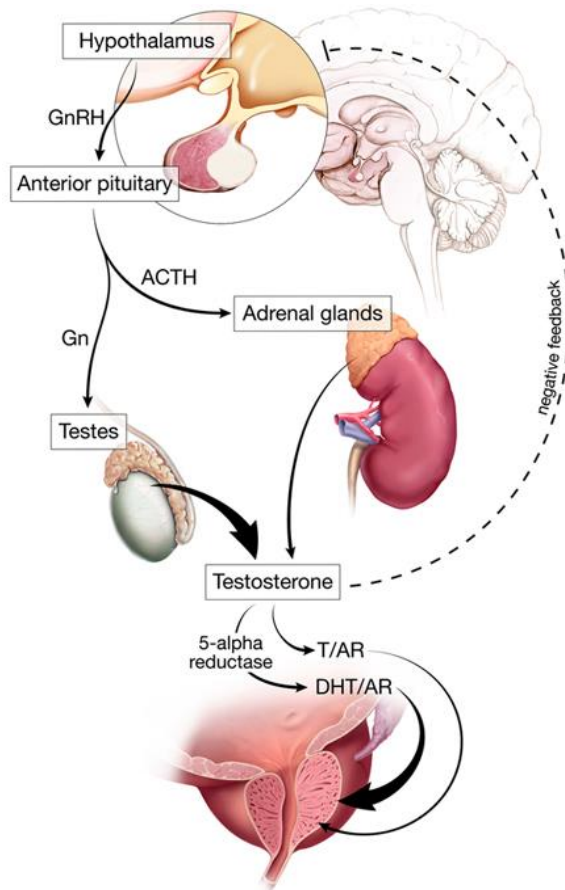


Figure 1.5: **The Hypothalamic-Pituitary-Gonadal Axis.** Gonadotropin-releasing hormone (GnRH) stimulates the secretion of gonadotropic hormone (Gn) from the anterior pituitary, which stimulates the production of testosterone. Circulating testosterone acts in a negative feedback loop to down-regulate the expression of GnRH. Adrenocorticotropic hormone (ACTH), also made by the pituitary, stimulates androgen synthesis in the adrenal gland. Testosterone (T) and DHT bind to the AR, causing increased expression of androgen-responsive genes and leading to cell growth. Illustration from: (Aragon-Ching et al., 2007)

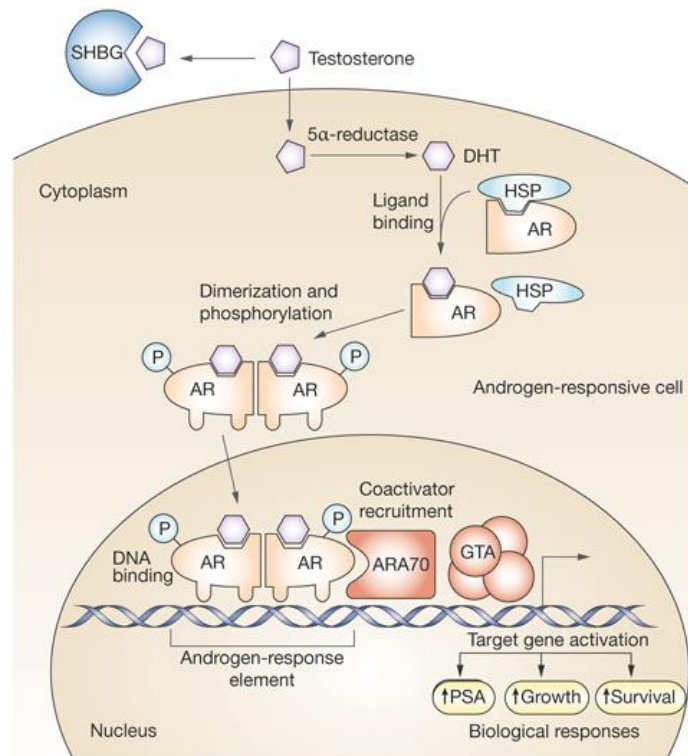


Figure 1.6: **Androgen action in the prostate.** Testosterone circulates in the blood bound to sex hormone binding globulin (SHBG). In androgen responsive cells testosterone is metabolised to DHT. Unbound AR forms a complex with Heat-Shock Proteins (HSP). The binding of testosterone to AR induces dissociation of the AR from the HSPs and subsequent receptor dimerization and translocation into the nucleus. Translocation is regulated by several coregulators, for example, the F-Actin binding protein (P): Filamin. Coactivators such as ARA70 (Androgen Receptor Coactivator) stabilise the process of ligand binding to AR and act as docking molecules with the general transcription apparatus (GTA). The AR complex then binds with the androgen responsive element on the DNA to mediate growth, secretion and survival by target gene activation. Illustration from: (Harris et al., 2009)

1.4 Prostate Cancer

1.4.1 Incidence of prostate cancer

Prostate cancer is the most common cancer in men in the UK. In 1990, both lung and bowel cancers were more common in males than prostate cancer, but by 1998 prostate cancer was the most common cancer in UK males. In 2011, there were 41,736 new cases diagnosed (Cancer Research UK) (CRUK, 2012) (Figure 1.7). The crude incidence rate shows that there are 134 new prostate cancer cases for every 100,000 males in the UK. Over 250,000 men are currently living with the disease in the UK (Prostate Cancer UK) (PCUK, 2013).

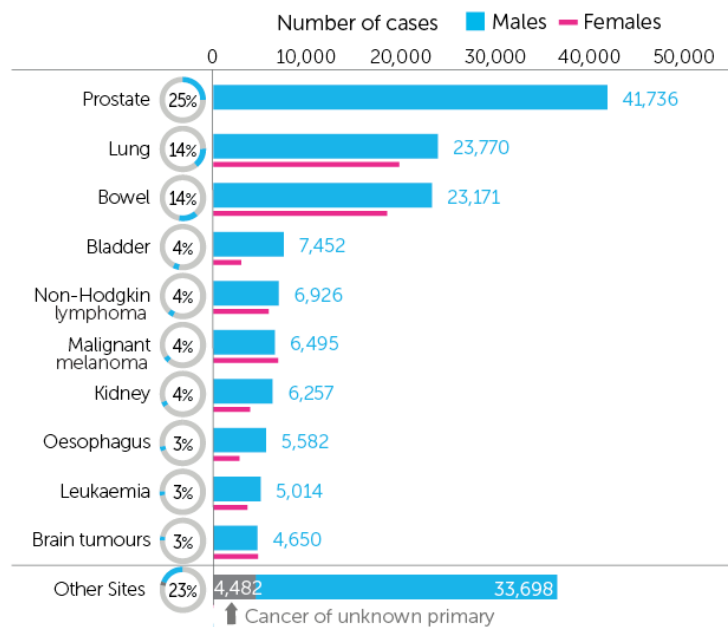


Figure 1.7: **The ten most common cancers** in males in the United Kingdom (Cancer Research UK, 2012). Prostate cancer is the most common cancer diagnosed.

Prostate cancer incidence is strongly related to age, with the highest incidence rates in older men. In the UK between 2009 and 2011, an average of 36% of cases was diagnosed in men aged 75 years and over and only 1% was diagnosed in the under-50s (Figure 1.8). The lifetime risk of developing prostate cancer is 1 in 8 (CRUK, 2012).

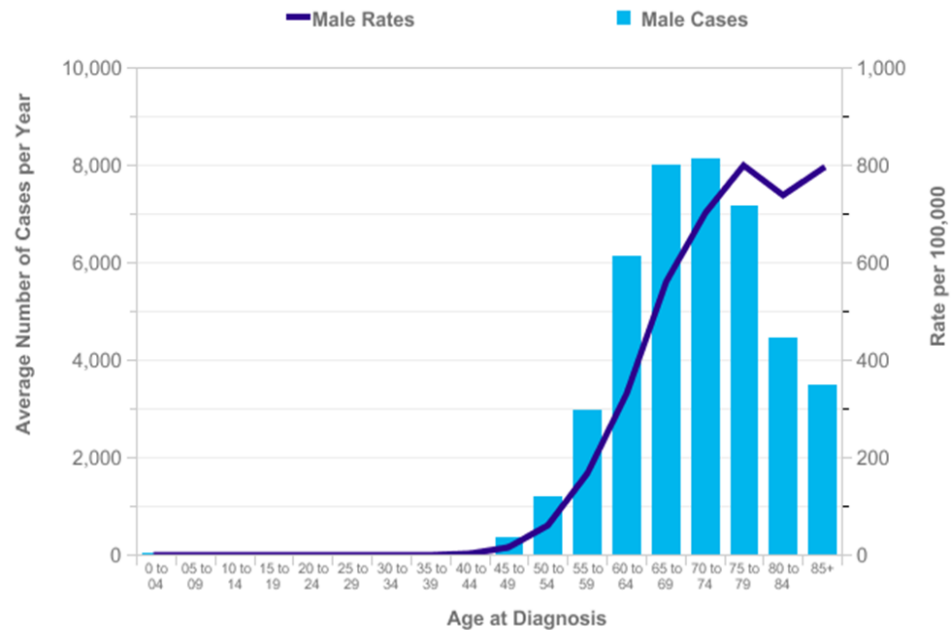


Figure 1.8: **New diagnoses of prostate cancer** and age-specific incidence rates in the United Kingdom (Cancer Research UK, 2012)

The incidence of prostate cancer varies widely between countries and ethnic groups. American Afro-Caribbeans have the highest incidence rates worldwide, whereas native Japanese have among the lowest (SEER, 2010). Thus it is most probable that there is a genetic predisposition to developing the disease. However, Japanese and Chinese men living in the United States have a higher risk of developing and dying from prostate cancer than their native counterparts (Muir et al., 1991). There is also some evidence now that the Chinese prostate cancer differs in its genetic changes from the Western disease (He et al., 2013, Shen et al., 2013). Hence environment factors can modulate the risk around the world with migration. There is also increasing evidence that diet and lifestyle play a crucial role in prostate cancer biology and tumourigenesis (Mandair et al., 2014).

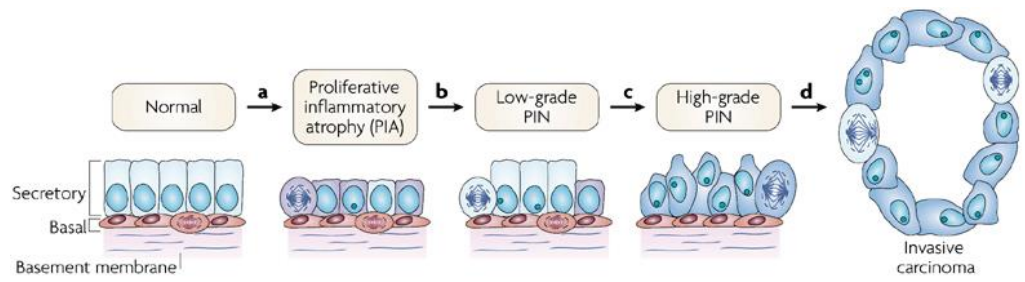
1.4.2 Aetiology of prostate cancer

In the UK, prostate cancer comprises almost a quarter of all cancer diagnosis in men. Older men, men with a family history of prostate cancer and men from an Afro-Caribbean background are more at risk (CRUK, 2012). Afro-Caribbean men have a 3 fold greater risk of developing the disease in the UK (Ben-Shlomo et al., 2008). Although both genetic and environmental factors are considered to play a role, specific gene–environment interactions have remained elusive (Neslund-Dudas et al., 2014).

Men with a family history are at higher risk of developing the disease than the rest of the population. For example men with their brother or father diagnosed are two and a half times more likely to get prostate cancer. This risk rises if the relative was diagnosed under the age 60 or if there is more than one close relative with prostate cancer. History of breast cancer linked to BRCA1 or BRCA2 in close relatives also increases the risk (Easton et al., 1997, Thompson et al., 2002).

Inflammation has also been suggested as a possible cause of prostate cancer. Chronic or recurrent inflammation of the prostate causing oxidative damage to DNA, and other cellular components, is believed to initiate the tumour. Both inflammation and carcinoma affect the peripheral zones where the majority of prostate cancer occurs (De Marzo et al., 2004). It is here that focal areas of epithelial atrophy containing proliferative cells called proliferative inflammatory atrophy (PIA) are found (De Marzo et al., 1999, Shah et al., 2001). It is a lesion frequently identified in prostate biopsies and can be involved in carcinogenesis.

PIA gives rise to prostate intraepithelial neoplasia (PIN) which in turn, due to continued proliferation of genetically unstable luminal cells, leads to progression towards invasive carcinomas (De Marzo et al., 2007). This hypothesis is illustrated in Figure 1.9.



Nature Reviews | Cancer

Figure 1.9: **Proliferative inflammatory atrophy (PIA)** as a precursor to prostate intraepithelial neoplasia (PIN) and prostate cancer. PIA gives rise to prostate intraepithelial neoplasia which in turn, due to continued proliferation of genetically unstable luminal cells, leads to progression towards invasive carcinomas (Illustration from (De Marzo et al., 2007))

1.4.3 Diagnostic paradigms

Patients with prostate cancer do not commonly present with any specific lower urinary tract symptoms. Late signs can be bone pain and general tiredness (Bower and Waxman, 2010). A suspicious prostate specific antigen (PSA) blood test or abnormal digital rectal examination (DRE) by the patient's general practitioner (GP) usually triggers referral to a urologist.

In the clinic, a careful history is taken and a full examination including a repeat DRE is carried out. The latter is performed to evaluate the size, consistency and presence of any lesions on the periphery of the gland, as this is the area that is palpable. Although DRE has a poor positive predictive value for low PSA ranges, it is still advocated in advanced cancer (Schroder et al., 1998).

When the results are suspicious, a transrectal ultrasound-guided (TRUS) biopsy of the prostate is carried out to produce a histopathological diagnosis. Traditionally, magnetic resonance imaging (MRI) has been applied as a staging investigation after histological diagnosis, but artefacts can last for 6 months after biopsy and so it has become frequent practice to carry out MRI first (Rouse et al., 2011). The addition of multiparametric sequences to anatomical T2-weighted images, such as diffusion-weighted imaging (DWI), dynamic contrast enhancement and magnetic resonance spectroscopy have shown potential in the diagnostic pathway for prostate cancer (Grey et al., 2015). Combining all the above MRI techniques, a structured reporting scheme has been published, called Prostate imaging reporting and data system (PI-RADS). This system involves the use of 5-point scales for grading the findings obtained with the different MRI techniques. As shown below, using an aggregated scoring, a diagnosis of suspected prostate cancer is made if the PI-RADS score is 4 or higher (Rothke et al., 2013). This points system helps to better guide biopsies in patients with suspected cancer.

PI-RADS 1: very low (clinically significant cancer is highly unlikely to be present)

PI-RADS 2: low (clinically significant cancer is unlikely to be present)

PI-RADS 3: intermediate (the presence of clinically significant cancer is equivocal)

PI-RADS 4: high (clinically significant cancer is likely to be present)

PI-RADS 5: very high (clinically significant cancer is highly likely to be present)

Recent studies have suggested that TRUS biopsy of the prostate is a flawed method in that a third of men with no or low-risk cancer diagnosed are found to have significant disease on transperineal biopsy (Ayres et al., 2012, Vyas et al., 2014). Hence, transperineal biopsies are now increasingly being considered in selected patients to enhance diagnosis especially of anterior and apical prostate tumours.

1.4.3.1 Prostate specific antigen (PSA)

PSA is a prostate-specific secretory product not specifically related to the presence of cancer. PSA plays a role as a marker for prostatic diseases and monitoring. PSA has not been perfected as a screening test. An elevated serum PSA concentration is not always consistent with prostate cancer. Raised levels are also detected in benign prostatic hyperplasia (BPH), prostatitis and other lower urinary tract infections. Conversely, not all prostate cancers produce an elevated PSA and approximately 40% of men who undergo radical prostatectomy have a normal serum PSA concentration (Oliver and Gallagher, 1995).

Therefore the specificity of PSA is not very good for early interventions. In patients with PSA between 2-4ng/ml, the chance of having PC is approximately 25%. At levels over 10ng/ml, the chance of diagnosing the disease increases to 40% (Boyle and Ferlay, 2005, Heidenreich et al., 2011). The European Randomised study of Screening for Prostate Cancer (ERSPC) showed that PSA-based screening significantly reduced mortality from PC but screening is controversial because of adverse events such as over diagnosis (Schroder et al., 2012). Increasing the PSA threshold results in a decrease in sensitivity and increase in specificity (Schroder et al., 2008, Thompson et al., 2004). Consequently, lowering the PSA cut off levels leads to a higher detection rate of PC but also leads to an increase in negative biopsies and over diagnosis of cancers which might otherwise not present clinically (Postma et al., 2007).

1.4.3.2 New biomarkers

New diagnostic methods include prostate cancer antigen 3 (PCA3) and Prostate specific Membrane Antigen (PSMA). PCA3 is a PC specific molecular marker in urine that has been evaluated in a multicenter clinical study to enhance the specificity of PSA for positive biopsy after a previous negative result (Haese et al., 2008). PSMA is a type II membrane protein with folate hydrolase activity produced by the prostatic epithelium. Mhaweck-Fauceglia et al have shown the sensitivity and specificity of PSMA in distinguishing PC from any other type of malignancy was 65.9% and 94.5% respectively. Despite its expression by subsets of various types of malignancies, PSMA is still considered to be fairly sensitive and highly specific (Mhaweck-Fauceglia et al., 2007).

At present there is no specific test that can differentiate between indolent and aggressive tumours. Genomic biomarkers are being developed to refine the risk for men with PC but most importantly they must be both valid and of clinical utility. PSA remains an important marker in diagnosing PC recurrence or relapse after radical treatment. If a biomarker gives a risk of biochemical recurrence after radical prostatectomy, it is considered to be prognostic. Conversely, if a biomarker predicts biochemical recurrence after radical prostatectomy plus success for adjuvant radiation therapy, it can be considered as predictive. Three such commercialised genomic tests for PC are illustrated below.

The Decipher test is a 22-gene panel corresponding to RNAs from coding and non-protein coding regions of the genome (Davis, 2014). It can be tested on radical prostatectomy tissue to address the question as to the likelihood of lymph node or bone metastases developing in the first 5 years after surgery.

The Oncotype Dx test is a 12-cancer related gene panel that reflects several pathways: stromal response, cellular organization, androgen signaling and proliferation (Klein et al., 2014). This test gives a direct prognosis for the finding of adverse pathology at radical prostatectomy such as T3 disease and/or upgrading the Gleason 4+3 or higher. It gives a unique genomic prostate score (GPS) on a scale of 0-100, which is then translated to a percentage risk of having unfavourable pathology.

The Prolaris test is a 46-gene panel of cell cycle progression genes that measure proliferation as cells go into their division cycles. The test is different from Decipher, in that the prognosis reported takes into account clinical parameters. To

predict outcomes on active surveillance, a Prolaris score for a low risk patient will report a 10-year probability of cancer related mortality with conservative management (Cooperberg et al., 2013). These new biomarkers have helped in the prognosis of PC but are not widely available and remain costly. With time it is hoped that genomic markers will be more specifically linked to a therapy and help us guide primary treatment better.

1.4.4 Staging and Grading

Clinical staging of the cancer is performed before treatment by taking into account the findings of a DRE, the PSA level, the results of the needle biopsies (Gleason score) and imaging studies.

Pathological staging is determined after removal of the prostate gland, seminal vesicles and regional lymph nodes, based on histopathological analysis.

The Tumour-Node-Metastasis (TNM) staging system is used based on the size of the primary tumour (T), whether cancer cells have spread to nearby (regional) lymph nodes (N) and whether metastasis (M), or the spread of the cancer to other parts of the body, has occurred (Schroder et al., 1992). This helps in risk stratification and predicting prognosis of disease (Figure 1.10). The TNM classification system was subdivided into T2a (unilateral tumour less than half a lobe), T2b (unilateral greater than half a lobe) and T2c (bilateral tumour). However, T2b disease almost never exists as by the time the tumour occupies more than half a lobe in the majority of cases there is bilateral (pT2c) tumour already. The pathological substaging of T2 disease fails on this account and lacks prognostic significance (Epstein, 2011). However it is still important in advanced tumours.

The conventional Gleason system classifies prostate cancer into 5 grades/scores depending on the glandular pattern and the degree of differentiation. As tumours often exhibit more than one pattern, the sum of the two most prominent cell growth patterns determine a combined Gleason grade or score (e.g. Gleason 3+4 gives a score of 7). Those tumours with only one pattern of differentiation are considered as if the primary and secondary grades were the same and the score is doubled, e.g 3+3 (Gleason, 1966). Figure 1.11A illustrates the originally developed, conventional Gleason grading system (Gleason, 1966). Combined with staging, this allows a more objective assessment of prognosis.

Since the introduction of the Gleason grading system more than 40 years ago, the classification of prostate cancer have changed. The Gleason system was updated in 2005 under the auspices of the International Society of Urological Pathology. Gleason score 1 and 2 is now rarely if ever diagnosed. Poorly formed glands originally considered Gleason pattern 3 are now considered Gleason pattern 4 and all cribriform cancer are graded pattern 4 (Figure 1.11B) (Epstein et al., 2005). Other changes include commenting on tertiary grade patterns which differ depending on whether the specimen is from needle biopsy or radical

prostatectomy. Although tertiary Gleason patterns are typically added to pathology reports, they are routinely omitted in practice since there is no simple way to incorporate them in predictive nomograms/tables, research studies and patient counseling (Epstein, 2010).

Stage	Definition
Primary tumor	
TX	Primary tumor cannot be assessed
T0	No evidence of primary tumor
T1	Clinically, the tumor is neither palpable nor visible with imaging
T1a	Tumor is an incidental histologic finding in 5% or less of tissue resected
T1b	Tumor is an incidental histologic finding in more than 5% of tissue resected
T1c	Tumor identified with needle biopsy (eg, because of an elevated PSA level)
T2	Tumor confined within the prostate
T2a	Tumor involves one-half of one lobe or less
T2b	Tumor involves more than one-half of one lobe but not both lobes
T2c	Tumor involves both lobes
T3	Tumor extends through the prostate capsule
T3a	Extracapsular extension (unilateral or bilateral)
T3b	Tumor invades seminal vesicle(s)
T4	Tumor is fixed or invades adjacent structures other than seminal vesicles: bladder neck, external sphincter, rectum, levator muscles, and/or pelvic wall
Regional lymph nodes	
NX	Regional lymph nodes were not assessed
N0	No regional lymph node metastasis
N1	Metastasis in regional lymph node(s)
Distant metastasis	
MX	Distant metastasis cannot be assessed (not evaluated with any modality)
M0	No distant metastasis
M1	Distant metastasis
M1a	Nonregional lymph node(s)
M1b	Bone(s)
M1c	Other site(s) with or without bone disease

Figure 1.10: **Tumour Nodal and Metastasis**, staging of prostate cancer. Adapted from (Han et al., 2000)

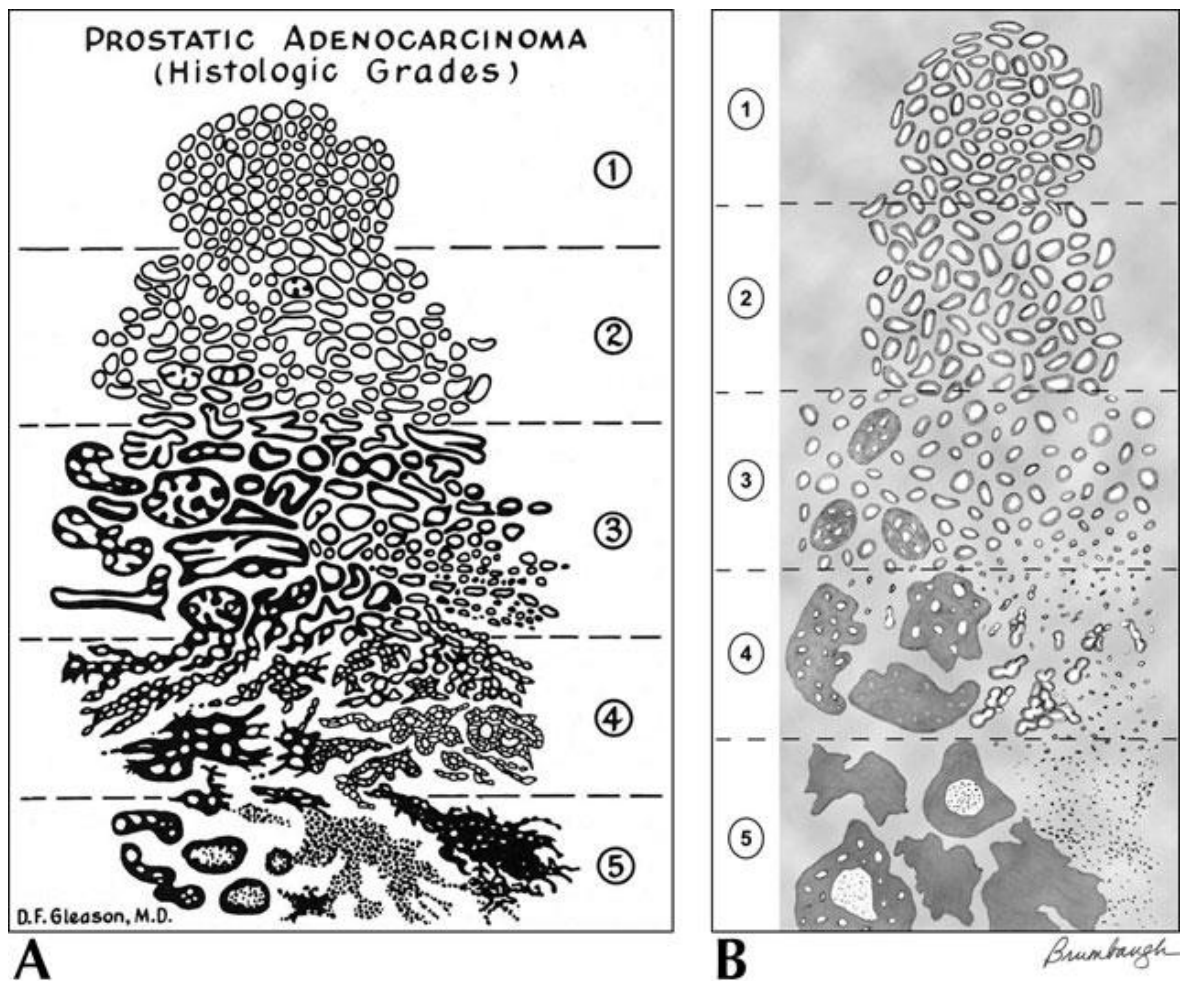


Figure 1.11: (A) Conventional and (B) modified Gleason grading system. At lower grades glandular structure is more organised and differentiated whereas at higher grades, structure breaks down. The most important changes between A and B are in patterns 3 and 4. In the modified system, most cribriform patterns and also poorly defined glands are included in pattern 4 (Epstein et al., 2005).

1.4.4.1 Risk Assessment Methods

Risk assessment systems are not intended to replace individualised patient assessment, but rather to provide a straightforward instrument for facilitating disease risk classification in clinical decision making and in future research.

The risk classification system developed by D'Amico and colleagues is one of the most widely used (D'Amico et al., 1998). It uses PSA level, Gleason grade, and T stage to group men as low, intermediate, or high-risk.

Low-risk: PSA less than or equal to 10, Gleason score less than or equal to 6, and clinical stage T1-2a

Intermediate risk: PSA between 10 and 20, Gleason score 7, or clinical stage T2b

High-risk: PSA more than 20, Gleason score equal or larger than 8, or clinical stage T2c-3a

However, it does not account for multiple risk factors. For example, a patient with Gleason 3+4, PSA 3.2, stage T1c cancer in one biopsy core and another patient with Gleason 4+3, PSA 19.2, stage T2b cancer involving eight cores. Both patients are classified as intermediate risk, although the second patient would have much higher disease risk.

Similarly Kattan et al created a nomogram based on similar preoperative disease characteristics (Korets et al., 2011). As illustrated above, several factors such as accuracy, generalisability and validity must be considered prior to widespread clinical implementation of risk stratification tools. In 2005, the University of California, San Francisco developed the Cancer of the Prostate Risk Assessment (CAPRA) score to assist in predicting recurrence free survival and pathological tumour stage after radical prostatectomy. The scores range from 0-10 considering age, preoperative PSA, Gleason sum, clinical T stage and percentage positive of biopsy cores (Cooperberg et al., 2005). This tool is externally validated by both national and international institutions and is simple to apply. Similar to the D'Amico classification scheme, CAPRA score can be collapsed with 3 risk groups. It has been shown to accurately predict both cancer specific mortality (CSM) as well as overall mortality (OM) (Cooperberg et al., 2009).

1.4.5 Management

The evolution of clinical practice in prostate cancer is affected by a number of factors. Of particular importance are treatment guidelines and the development of new treatment techniques. In Europe, the European Association of Urology (EAU) guidelines offer a regularly updated evidence-based source of recommendations for the optimal treatment (Wolff and Mason, 2012).

This is particularly important for prostate cancer, as unlike most cancers, some have a low risk of progression and a benign course. Hence patients may live normally with the tumour long before it becomes progressive. Older patients diagnosed with such tumours may even die of natural or unrelated causes.

Conversely, some patients undergo radical treatments, which carry a high morbidity risk only to find out later that their mortality has not reduced. Others with high-risk cancers have limited options and may rapidly succumb to the disease. The treatment here is mainly palliative and aimed toward symptoms control.

Primary treatment for clinically localised PC is a complex decision as there are various therapeutic options available often with equal oncological efficacy but differing adverse effects (Heidenreich et al., 2011). After this has been explained to the patient, an informed decision is made according to their wishes. The following treatment options are available:

- Active surveillance/Watchful waiting
- Radiotherapy/Brachytherapy
- Radical prostatectomy
- Minimally invasive therapies
- Androgen ablation therapy

Active surveillance/Watchful waiting

Currently, low-risk prostate cancer, defined as Gleason Score 6 or less with PSA <10 ng/ml, is diagnosed in about half of men undergoing screening (Klotz and Emberton, 2014). For this category, active surveillance is a recommended treatment option. It involves regular follow-up with repeat PSA and planned re-biopsies of the prostate. If the disease progresses, the patient is restaged and reassessed with a view to offering radical treatment with a curative intent.

The Prostate Cancer Intervention Versus Observational Trial (PIVOT) was a large RCT, which showed no prostate CSM benefit associated with surgery

compared to observation for patients with low-intermediate risk disease (Wilt, 2012). Watchful waiting is similar but reserved for elderly patients with high comorbidities, where disease progressions will trigger only palliative options.

Radiotherapy/Brachytherapy

Radiotherapy to the prostate lasts for approximately 6 weeks and in most cases is combined with neoadjuvant androgen ablation, which decreases the risk of local relapse and improves survival (Bolla et al., 2002). The format of radiotherapy includes conventional external beam radiotherapy (EBRT), 3-dimensional conformal radiotherapy, image guided radiotherapy and intensity modulated radiotherapy (IMRT). Brachytherapy is a slightly different technique where the local intensity of radiation is amplified by implanting radioactive ¹²⁵I seeds in the prostate gland. When used as monotherapy, the dose is 145 Gy of ¹²⁵I and when used in combination with EBRT 110 Gy is given. Recent studies have also shown increased survival with combined EBRT and transperineal prostate brachytherapy boost plus androgen deprivation therapy (ADT) (Hurwitz et al., 2011).

Radical Prostatectomy

Radical prostatectomy is the preferred treatment option for patients with a long life expectancy for Gleason score ≥ 7 adenocarcinomas, which is organ confined. It is optional for selected patients with T3a, PSA < 20 ng/ml, Gleason score ≤ 8 and life expectancy > 10 years (EAU, 2014). Approaches include open retro-pubic surgery, laparoscopic and robotic techniques. Increasing use of robotic-assisted prostatectomy has revolutionized surgery. However, while there is less blood loss, no functional or early oncological outcome data can be established with certainty (Prasad et al., 2011).

Minimally invasive therapies

In recent years the accuracy of cancer localisation within the prostate has improved considerably, which enables the increasing use of focal therapy techniques (Porres et al., 2012). These include cryotherapy and high intensity focused ultrasound (HIFU) therapy. Cryotherapy utilizes an argon-based freezing system delivered to focal areas in the prostate by cryoprobes. Its use has

increased significantly over the last 10 years with a trend towards focal ablation rather than whole gland ablation. 5 year biochemical disease free rates defined by PSA is reported to be as high as 92% for patients with low and intermediate risk disease (Barqawi et al., 2014).

HIFU is a technique that uses nonionizing energy to induce irreversible damage to the malignant lesion. It involves transrectal delivery of ultrasound under real-time imaging. The probe has a cooling balloon around it to protect nearby areas from the high temperature. The thermal and cavitation effects can be repeated with subsequent treatment administration and can be an option in cases of local relapse (Riviere et al., 2010). Long-term oncologic results for HIFU are sparse in the literature, and it is still considered investigational in the EAU guidelines (Heidenreich et al., 2011, Warmuth et al., 2010)

Androgen deprivation therapy (ADT)

This is reserved for patients with extensive cancer (T3-T4) with a high PSA (>25) and has a non-curative intent. ADT encompasses any treatment that results in suppression of androgen activity. This can be achieved by either decreasing testicular and/or extra-gonadal androgen production with medical or surgical castration or by using anti-androgens to block AR signaling (Grossmann et al., 2013). It is most commonly given with an injection of long acting gonadotrophin-releasing hormone (GnRH) agonists. Table 1 illustrates a list of drugs that are currently used. When using GnRH agonists, giving anti-androgens a few days before and after the injection prevents a tumour flare. This counteracts the negative feedback pathway caused by a surge in testosterone (Figure 1.5). In the case of starting with GnRH antagonists, anti-androgens cover is not required.

Anti-androgens directly interact with the AR, interfering with its trans-activation of target gene transcription. Anti-androgens have been used as monotherapy in an attempt to spare side effects of castration. Bicalutamide has showed similar survival benefit as bilateral orchidectomy for men with locally advanced but non-metastatic PC (Iversen et al., 2000). To neutralize the effects of adrenal androgens, non-steroidal anti-androgens are given in combination with bilateral orchidectomy or GnRH analogues, known as maximum androgen blockade or combined androgen blockade.

Class	Drugs
Non-steroidal antiandrogens	Bicalutamide
	Flutamide
	Cyproterone Acetate
GnRH agonists	Goserelin
	Histrelin
GnRH antagonist	Degarelix
Non-steroidal oestrogen	Diethylstilbestrol

Table 1: List of drugs used in **medical castration** for ADT

1.5 Castrate Resistant Prostate Cancer

1.5.1 Emergence

Castrate resistant prostate cancer (CRPC) occurs when hormone sensitive cancers become refractory after a period and resume growth despite castrate testosterone levels (Figure 1.12). It is the second most common cause of cancer-related death in men in the developed world (CRUK, 2012). CRPC has a poor prognosis with median survival times of 18 months. In addition, the morbidity increases as metastases to bone can lead to spinal cord compression, fractures, pain, cachexia, anaemia and ultimately death (Petrylak, 2014).

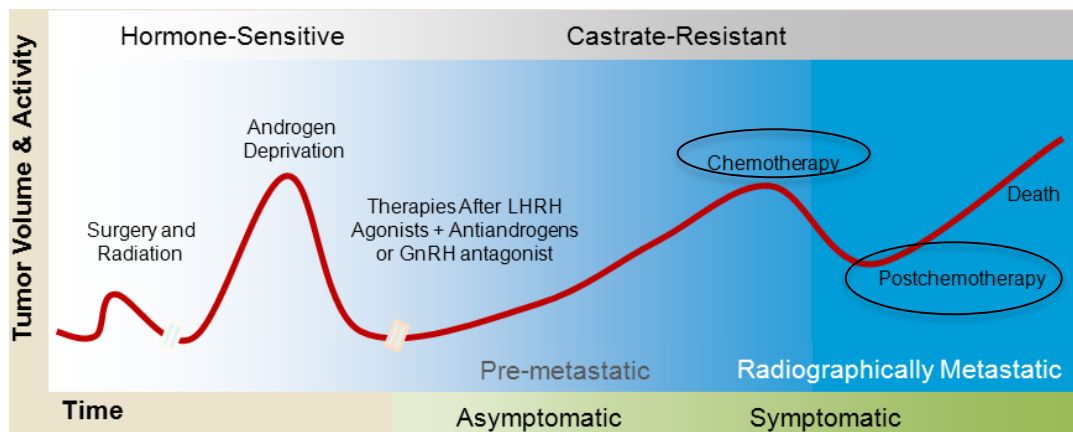


Figure 1.12: **Development of CRPC.** Despite ADT, prostate cancer recurs and resume grown. Relapse is usually rapid and catastrophic. Image adapted from http://www.webedcafe.com/extern/program_media/goldjournal.net. The stage when to give chemotherapy and postchemotherapy treatments are currently under not finalised.

Careful definition of clinical and therapeutic parameters that characterise the development of CRPC is important to further understand the evolving natural history and selection of potential treatments. More frequent diagnostic imaging has contributed to earlier detection of metastatic CRPC. Understanding the mechanisms of PC progression has provided the rationale for designing some of the most promising targeted treatments and further expanded the mCRPC treatment paradigm. The time when to give first line chemotherapy and newer anti-androgen drugs to have the maximum effects, are currently the subjects of important trials (see section 1.7 and 1.9).

1.5.2 Targeting the androgen-signaling axis and the molecular aspect of CRPC

The first systemic treatment offered to most men with PC targets the androgen-signaling axis accomplished by using androgen deprivation with anti-androgens or a combination GnRH analogues. In the normal prostate epithelium, androgenic hormones principally drive differentiation to a columnar secretory phenotype. However, in PC cells, the androgen signaling axis contributes to cell growth and survival as well as to differentiation. As a consequence, most men enjoy an initial benefit characterised by a fall in serum PSA and relief of symptoms. Unfortunately, the emergence of androgen-independent PC is common. In most cases these cancers maintain the expression and function of androgen receptors (AR) despite therapeutic reduction of serum androgen levels.

Human PC cells studies in xenografts models, have shown progression to androgen independence to be associated with increased expression of AR transcripts and increased abundance of ARs, presumably contributing to an increased sensitivity of the receptors to low levels of androgenic hormones (Feldman and Feldman, 2001). Whether this phenomenon occurs in men suffering from androgen independent PC has not been established. Nonetheless, AR is a known target for somatic genome alterations especially upon progression to androgen independence (Taplin et al., 1999). AR mutations with altered ligand specificity can result in agonist activity for anti-androgens, providing a molecular explanation for the “anti-androgen withdrawal” syndrome in which patients with PC progression whilst on maximum androgen blockade, benefit from discontinuation of the anti-androgens (Tilley et al., 1996). Androgen independent cells containing wild-type ARs appear to be capable of AR signaling, even at castration levels as a result of posttranslational modifications on the AR and/or its co-activators in response to other growth factor signaling pathways (Feldman and Feldman, 2001).

1.5.3 AR amplifications, mutations and splice variants

In the absence of androgens, AR is bound to heat-shock proteins and remains in the cytoplasm. Upon progression to castration resistance AR signaling is maintained through a variety of mechanisms including increased expression of AR, amplification of the AR gene (Tomlins et al., 2007) and structural changes in

AR caused by genetic mutations (Taplin et al., 1995) or mRNA splice variants (Sun et al., 2010).

The increased expression, greater stability and nuclear localization of AR in CRPC are all indicative of an overactive AR which can be stimulated by minute concentrations of circulating androgens (Nupponen and Visakorpi, 1999). Moreover, while wild type AR is only activated by androgens, the specificity of ligand binding can be broadened by somatic mutations usually occurring in the ligand-binding domain of AR. These mutations can lead to inappropriate activation of the AR by non-androgens, resulting in promiscuous AR phenotype that may lead to activation by oestrogens, progesterone, tyrosine kinases and other signaling molecules (Brooke and Bevan, 2009). Finally the castration state can promote alternative splicing of the AR gene, yielding variant mRNA transcripts lacking the ligand-binding domain, which are constitutively active (Watson et al., 2010). For example the splice variant AR V-7 may define which patients may or may not benefit from drugs targeting the AR pathway. Thus, there are a variety of AR- mediated mechanisms of resistance, each of which may require different therapeutic approaches.

1.5.4 Ectopic androgen synthesis

Although ADT decreases total testosterone levels by approximately 95% from gonadal synthesis, it does not affect extra-gonadal androgens. In CRPC there is a continuous production of androgens by the adrenal glands as well as de-novo intratumoural synthesis from the PC itself through increased expression of steroidogenic enzymes like cytochrome P450-17 (CYP17) (Montgomery et al., 2008). This enzyme is the target of Abiraterone acetate, one of the new drugs against CRPC.

1.5.5 Co-regulators of AR

Co-activators (co-repressors) function as signaling adjuncts for AR-mediated transcription influencing the binding of AR to androgen-response elements in promoter regions of DNA. Among the most important co-regulators is the p160 family of nuclear steroid receptor co-activator (Zhou et al., 2005) and nuclear receptor co-activator, (NCOA2) (Taylor et al., 2010).

1.5.6 AR independent pathways

Apart from the promiscuous pathways described above, another potential resistance mechanism against castration involves the activation of anti-apoptotic pathways associated with survival. Overexpression of the anti-apoptotic protein Bcl-2 has been found to confer resistance to androgen suppression (Raffo et al., 1995). Other factors related to Bcl-2 such as Bcl-XL and survivin are also frequently expressed in CRPC (Zhang et al., 2005). These biologic features lend themselves to a variety of treatment strategies that have been exploited to develop novel agents.

1.6 CRPC treatment options

The management of CRPC was solely limited to palliation of symptoms in the 1990s due to lack of effective treatments. Mitoxantrone was the first chemotherapy agent approved. It is a type II topoisomerase inhibitor and has effects against metastatic breast cancer, acute myeloid leukaemia and lymphoma as well. It disrupts DNA synthesis and repair in both healthy and cancerous cells by intercalation between DNA bases (Mazerski et al., 1998).

Three randomised trials demonstrated only modest benefits in time to progression when mitoxantrone was used with steroids compared to steroids alone (Tannock et al, 1996, Kantoff et al, 1999 and Berry et al, 2002) In the first trial, most responding patients had a decrease in serum PSA and an increase in pain control when treated with mitoxantrone and prednisolone (Tannock et al., 1996). In 1999, Kantoff et al. set out to look for a survival benefit with mitoxantrone and prednisolone versus prednisolone alone. They found no difference in overall survival despite a better quality of life (Kantoff et al., 1999). The third trial evaluated mitoxantrone and prednisolone in asymptomatic patients with progressive hormone refractory prostate cancer. A 50% or greater decrease in PSA was demonstrated compared to prednisolone alone. Time to treatment failure was significantly prolonged in the chemotherapy treated group but survival rates were not different (Berry et al., 2002). This study highlighted the fact that future studies should include patients with varying stages of advancing prostate cancer.

Overall, looking at the poor end points there was an urgent need for new drugs and novel therapies to improve survival although the intent of treatment for CRPC remains palliative.

In 2004, the results of two randomised trials (TAX 327 and the Southwest Oncology Group, SWOG 99-16) were published and revealed significant survival benefits for men treated with docetaxel (Cheung et al., 2013). This marked the beginning of a new era in CRPC.

1.6.1 Docetaxel

Docetaxel belongs to the class of taxanes and is a semi-synthetic analogue of paclitaxel which is an extract from the bark of the rare pacific yew tree, *Taxus Brevifolia* (Clarke and Rivory, 1999). As paclitaxel is scarce, docetaxel was

developed which is more readily available from the leaves of the European yew tree. Figure 1.13 demonstrates the chemical structure of docetaxel.

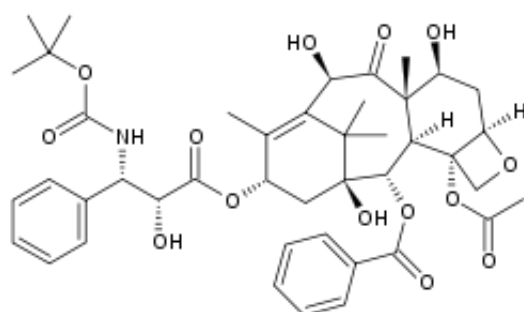


Figure 1.13: **Chemical formula of docetaxel** (Adapted from <http://www.answers.com/topic/docetaxel-taxotere>)

Docetaxel holds a European license as the first line chemotherapy agent for the treatment of CRPC. It is administered at a dose of 75mg/m² once every three weeks in a slow intravenous infusion over one hour (Tannock et al., 2004). Oral prednisolone tablets are started together at a dose of 5mg twice a day. This can be repeated up to 10 cycles if tolerated. It primarily induces tumour cell death by causing mitotic catastrophe, and caspase-2 and -3 dependent apoptosis following inhibition of microtubule depolymerisation (Mediavilla-Varela et al., 2009). Docetaxel has also been reported to induce non-apoptotic death in tumour cells, both in vitro and in vivo, depending on the dose, cell type, and tumour microenvironment (Morse et al., 2005).

Based on the TAX 327 trial, an international multi-centre randomised control study, the median survival was 18.9 months versus 16.4 months in the group of patients who received mitoxantrone and prednisolone (Tannock et al., 2004). Southwest Oncology Group (SWOG) led a second phase III trial comparing docetaxel/estramustine to mitoxantrone/prednisolone in 770 men with CRPC. The docetaxel experimental arm improved median survival by nearly two months (17.5 months versus 15.6 months) and progression-free survival by nearly 3 months (6.3 months compared to 3.2 months) (Petrylak et al., 2004). These two trials remain the cornerstone for adopting docetaxel as the first line cytotoxic agent for CRPC to this date.

Although docetaxel currently represents the most active chemotherapeutic agent, it only gives a modest survival advantage with most patients eventually progressing because of inherent or acquired drug resistance (O'Neill et al., 2011).

The mechanisms underlying resistance appear to be diverse and poorly understood. Proposed mechanisms are firstly prostate cancer cells are slow growing and unlikely to respond to drugs that are S-phase dependent (Raghavan et al., 1997). Secondly, a reduced intracellular drug concentration through increased efflux, decreased intake secondary to alterations in drug transporters. Multidrug resistance (MDR) mechanisms have been shown to protect cancer cells against cytotoxic drugs (van Brussel and Mickisch, 2003). Thirdly, changes in β -tubulin isotypes with different kinetics of microtubule formation has been shown to contribute to resistance (Makarovskiy et al., 2002). Fourthly, mutations in tumour suppressor proteins, such as phosphatase and tensin homolog (PTEN), which is a common event in about 60% of PC patients can activate intracellular signal transduction and increase cell proliferation (Shen and Abate-Shen, 2007). Finally, as PC progresses there is the expression of survival factors that inhibit the apoptotic cell death pathways (Feldman and Feldman, 2001).

The chemosensitivity of docetaxel is associated with the phosphorylation and inactivation of the bcl-2 protein. Its presence in tumour cells may serve as a prognostic indicator for responsiveness (Kraus et al., 2003). Through a detailed understanding of docetaxel induced cell death and its resistance in prostate cancer, new molecular targets and combination therapy can be further developed shedding light on the poorly understood mechanisms of chemoresistance.

1.7 Novel treatment options

For several years, docetaxel was the only treatment shown to improve survival of patients with mCRPC. Over the last few years, several new drugs licensed in mCRPC have become available. Abiraterone acetate plus prednisolone, cabazitaxel, sipuleucel-T, enzalutamide, denosumab and radium-223 dichloride have recently been added to the therapeutic arsenal. They offer improvement in survival while maintaining or improving the quality of life (Parker et al., 2013, Scher et al., 2012). The key challenge for clinicians is choosing the right drug for the right patient at the right time in their cancer journey as apart from survival benefits they also confer side effects. Currently there is no single accepted standard sequence of agents, as the choice varies depending on patient characteristics, such as the presence of symptoms, sites of metastasis, previous docetaxel exposure, comorbidities, patient preference, the cost and availability of different treatments. But as new data from ongoing trials are published the current practice is evolving.

1.7.1 Abiraterone acetate (AA)

Abiraterone acetate inhibits 17 α -hydroxylase/C17,20 and counteracts CYP17A1 which is a key enzyme in synthesising androgen. CYP17A1 is expressed by the testicles, adrenals and PC. In the COU-AA-301 phase III study in post docetaxel patients (n=1195), AA plus prednisolone improved median OS compared with prednisolone alone (14.8 vs 10.9 months) (Fizazi et al., 2012). In the COU-AA-302 study (n=1088) AA plus prednisolone showed an improvement in radiographic progression-free survival (PFS) compares with prednisolone alone in asymptomatic and mildly symptomatic docetaxel naïve men. The study was 'unblinded' at the planned interim analysis after 43% of expected death had occurred. The OS did not meet the pre-specified significance level but the difference in OS was considered to be clinically meaningful (Ryan et al., 2013) and the USA Food and Drug Administration (FDA) and the European Medicines Agency (EMA) approved AA plus prednisolone for docetaxel naïve men. In both studies side effects associated with mineralocorticoids excess (hypokalaemia, oedema, hypertension and cardiac disorders) were more common but deemed manageable.

1.7.2 Enzalutamide

Enzalutamide (formerly MDV3100) is an androgen-receptor-signaling inhibitor, which works on the basis of activity in PC models with overexpression of the AR (Scher et al., 2012). In CRPC it has five to eight fold greater affinity for AR compared with bicalutamide, which is the most widely used antiandrogen (Watson et al., 2010). Enzalutamide exhibited a median OS advantage (18.4 vs 13.6 months) compared with placebo in post-docetaxel men in the AFFIRM study (n=1199) (Scher et al., 2012). The most common side effects were fatigue, diarrhoea, hot flushes and a small increase in risk of seizures. Recently the PREVAIL study in asymptomatic and mildly symptomatic docetaxel naïve patients (n=1715) reported a 30% reduction in the risk of death with enzalutamide compared with placebo. The risk of progression was also significantly reduced, meaning a delay in chemotherapy initiation (Beer T.M, 2014).

Currently both AA and enzalutamide are approved as post docetaxel treatments in mCRPC and AA is also approved for docetaxel naïve patients. Regulatory approval of enzalutamide for chemotherapy naïve patients with mCRPC is anticipated.

1.7.3 Radium-223 dichloride

Radium-223, an alpha-emitting agent is the first bone targeting agent to show an improvement in OS compared with placebo. In the ALSYMPCA study, patients with symptomatic bone metastases, no visceral disease and no nodes >3cm (n=809) had a 3.6 months improvement in median OS with radium-223 compared with placebo (Parker et al., 2013). There was no increase in adverse events in the treatment arm compared with placebo. In the EU it is approved for men with bone metastases and no visceral metastases who are post docetaxel.

1.7.4 Sipuleucel-T

Sipuleucel-T is the first vaccine therapy to be approved for any advanced solid tumour and is indicated in asymptomatic and mildly symptomatic patients with mCRPC and no visceral disease. Sipuleucel-T is an active cellular immunotherapy consisting of patient's own mononuclear blood cells including antigen-presenting cells that have been activated ex vivo with a recombinant fusion protein. The latter consists of a prostate antigen, prostatic acid phosphatase

that is fused to an immune-cell activator (Kantoff et al., 2010). It acts like a personalized vaccine. Data from the IMPACT phase III trial (n=512) demonstrated a survival benefit of 4.5 months over placebo mCRPC patients (Kantoff et al., 2010). Currently, sipuleucel-T is approved in the USA and EMA has issued a positive opinion.

Another vaccine for prostate cancer is the Prostavac-VF which consists of a recombinant vector as a primary vaccination followed by multiple booster vaccinations employing a fowlpox vector (Madan et al., 2009).

1.7.5 Cabazitaxel

Cabazitaxel is a second-generation tubulin-binding taxane that has been shown to improve survival compared with mitoxantrone in post docetaxel patients. In the TROPIC study (n=755), cabazitaxel plus prednisolone achieved a better OS of 15.1 vs 12.7 months in the mitoxantrone group (de Bono et al., 2010). Cabazitaxel treatment was associated with myelosuppression, which was associated with toxic deaths in ~5% of patients in the TROPIC study. Prophylactic granulocyte colony-stimulating factor support may improve the safety and tolerability on this regimen. There are several ongoing phase III trials attempting to optimise cabazitaxel: FIRSTANA is a direct comparison study looking at docetaxel plus prednisolone with cabazitaxel plus prednisolone as first line chemotherapy in mCRPC. TAXYENERGY trial is evaluating the role of an early switch in taxane therapy based on suboptimal decline in PSA levels.

1.7.6 Denosumab

Denosumab is a human monoclonal antibody that inhibits osteoclast mediated bone resorption in bone metastases from solid tumours. A phase III study of 1904 patients showed that Denosumab was superior to Zoledronic acid in delaying the time to first skeletal related event (Fizazi et al., 2011). This can be used in CRPC patients with widespread bone mets.

1.8 Clinical characteristics to predict treatment benefit

With this increasing number of available agents, the timing of each is likely to be crucial. With no validated risk stratification or molecular biomarkers, clinical features such as presence of pain and disease characteristics may assist in making treatment decisions. Duration of response to previous therapy may also be of value in selecting patients for different treatments. Two retrospective cohort analyses showed that the survival benefit obtained with docetaxel or cabazitaxel may be most pronounced in patients with high Gleason scores (Buonerba et al., 2013, van Soest et al., 2014). Although the presence of visceral disease could aid in selecting patients, there are no comparative studies of chemotherapy and AR-targeting agents in mCRPC. Treatment sequencing also relies much on comorbidities, patient preference, cost and availability of agents. Although for several years docetaxel was the only treatment shown to improve survival, AA and enzalutamide are expected to be first-line treatments in many men based on tolerability, efficacy and convenience. However, the treatment paradigm still remains a dilemma.

1.9 Chemotherapy in hormone naïve PC

The ChemoHormonal Therapy vs Androgen Ablation Randomised Trial for Extensive Disease (CHAARTED) in PC is a phase III trial (n=790) looking at docetaxel before the development of mCRPC. A significant improvement was noted with 6 cycles of docetaxel in combination with ADT compared with ADT alone (57.6 vs 44 months). This trial was initially targeting patients with high volume disease only but was amended to allow even those with lower volume disease owing to slow accrual. The median survival in the high burden group improved by ~17 months from 32.2 to 49.2 months (Sweeney CJ, 2014).

In contrast the GETUG-AFU 15 study (n=385) looked at unselected patients with metastatic castrate sensitive PC randomized to ADT alone vs ADT with 9 cycles of docetaxel plus prednisolone. There was no difference in median OS between treatments. The major difference in patient population compared with the CHAARTED trial was that only 22% had high tumour burden at base line (Gravis et al., 2013). The emerging data from this trial support 6 cycles of docetaxel in chemotherapy eligible patients with disease burden castration sensitive disease.

STAMPEDE (Systematic Treatment in Advancing or Metastatic Prostate Cance; Evaluation of Drug Efficacy) is the largest randomized clinical trial of treatment for men with PC ever conducted, with more than 6,500 patients enrolled since 2005. This ongoing study has an innovative multistage, multiarm design that can be modified both to assess new therapies and adapt to changes in the standard of care. At the American Society of Clinical Oncology (ASCO) 2015 annual meeting, STAMPEDE researchers reported results on standard of care vs standard of care with docetaxel for six cycles. Overall survival was on average 10 months longer in the docetaxel arm compared with the standard of care arm (67 vs 77 months), with a relative improvement of 24%. For the subset of patients with metastatic disease, the average improvement in overall survival was even higher, 22 months (from 43 vs 65 months). Docetaxel also extended the time to relapse by 38% in all patients (James et al., 2015). The decision to use docetaxel based chemotherapy in men before the development of mCRPC awaits further publication of the CHAARTED and STAMPEDE trials.

1.10 Sequencing treatments in mCRPC

The availability of multiple non-chemotherapeutic agents for mCRPC patients will inevitably delay the time to initiation of docetaxel. The optimal trigger to docetaxel remains currently undefined. In the absence of predictive biomarkers, the American Urological Association (AUA) and EAU recommend that clinical symptoms (pain and change in the number or pattern of metastases) are a trigger for starting chemotherapy. On the other hand, asymptomatic patients with increasing PSA or a PSA doubling time of <6months may also benefit from docetaxel to extend OS although definitive data do not exist (Cookson et al., 2013, Mottet et al., 2011).

AA plus prednisolone (if not used before docetaxel), enzalutamide (if not used before docetaxel), radium-223 and cabazitaxel (second-line chemotherapy) are all possible treatment options, along with continuing ADT in patients progressing after docetaxel. Each has level 1 evidence, but no predictive factors exist on their optimum timing (Sonpavde et al., 2015). Until data become available from prospective RCTs using predictive biomarkers, the administration of all active agents in the most feasible sequence is likely to produce the best outcomes.

Systemic chemotherapy with docetaxel remains an important method in the treatment armamentarium for mCRPC or metastatic hormone naïve PC. However, given its toxicity profile, the window of opportunity is narrower than for the recently approved oral androgen inhibitors. Therefore consideration should be given in starting the most feasible sequence that permits the administration of all active agents and most importantly, all patients should be treated within the framework of a multidisciplinary team.

1.11 Cancer Stem Cells

From a treatment point of view, whether using ADT, novel antiandrogen agents or chemotherapy, we are assuming a uni-dimensional approach. Instead, identifying the tumour initiating cells and the heterogeneity of PC at the biological level can offer a better definition to the ideal treatment.

The existence of cancer stem cells (CSC) was first alluded to by Rudolph Virchow in 1855 who observed histological similarities between tumours and embryonic tissue which he termed the “embryonal-rest hypothesis”. Julius Cohnheim in 1867 later proposed that tumours arise from embryonal tissues (Sharifi et al., 2006).

The hypothesis that cancer is driven by tumour-initiating cells (popularly known as cancer stem cells) has recently attracted a great deal of attention, owing to the promise of a novel cellular target for the treatment of haematopoietic and solid malignancies (Zhou et al., 2009). The haematopoietic system is considered the gold standard for measuring and characterizing cancer stem cells (Bonnet and Dick, 1997, Huntly and Gilliland, 2005).

CSCs are defined as a population of cells found within a tumour that have characteristics similar to normal stem cells. Like normal stem cells they have the potential to self-renew and differentiate. The cellular origin of these cancer stem cells in spite of whether they originate from stem cells that have lost the ability to regulate proliferation, or if they arise from a more differentiated population of progenitor cells that have acquired abilities to self-renew, is still unclear (Bansal and Banerjee, 2009).

This model also predicts that eradication of the bulk of the tumour may result in remission, but if the tumour-initiating cells are not eliminated, the tumour will re-grow (Collins and Maitland, 2006). (Figure 1.14)

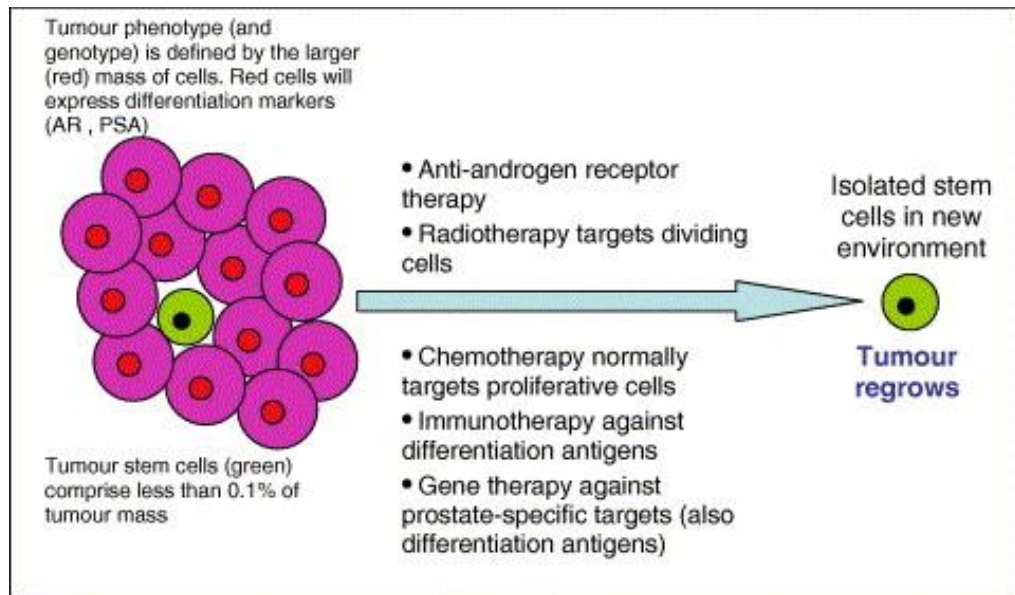


Figure 1.14: **Stem cell model of PC.** Eradication of the bulk of the tumour will result in remission, but if the cancer stem cells are not eliminated the tumour will re-grow. Reproduced from (Collins and Maitland, 2006).

1.11.1 Current concepts in PC stem cells

Multiple genetic and epigenetic factors have been implicated in the oncogenesis and progression of PC. The molecular mechanisms underlying the disease remain largely unknown. Like most other solid tumours, it represents a very heterogeneous entity (Maitland and Collins, 2005). Evidence of the presence of stem cells in the prostate first came from rat studies. After castration, the luminal cells undergo apoptosis leaving only basal cells and re-administration of androgens replenish the prostate epithelium to its functional state (DeKlerk and Coffey, 1978, Kyprianou and Isaacs, 1988). The basal layer therefore possessed the ability to fully regenerate the glands.

It has been suggested that PC arise from the differentiated luminal cells because the bulk population of tumour cells express luminal cell markers (CK8, CK18, AR, PSA and PAP) but lacks basal cell markers such as p63 (Nagle et al., 1987, Signoretti et al., 2000).

Collins et al. first isolated a putative PC stem cell from human prostatectomy specimens (Collins et al., 2005) (Figure 1.15). Here, they used the same phenotypic markers for normal prostate stem cells (CD44⁺, α 2 β 1^{hi}, CD133⁺). These cells do not express AR, but when exposed to

dihydrotestosterone (DHT), they exhibited more of a luminal epithelial phenotype with expression of AR, CK18 and PAP (Collins et al., 2001). These cells also contained and expressed transmembrane protease serine 2, TMPRSS2-ERG fusion (oncogene) and expressed alpha-methylacyl-CoA racemase (AMACR) (an enzyme which increased in PC) (Polson et al., 2013). These putative cancer stem cells also had a higher survival rate and were more invasive through Matrigel as compared to their CD44⁺, α2β1^{low} (control) counterparts.

More recently, Patrawala et al. characterized the tumorigenic properties of prostate cancer cell lines separated on the basis of CD44 expression (Patrawala et al., 2006). They found that across several prostate cancer cell lines, CD44⁺ cells are 10–100 times more tumorigenic in mice when compared with CD44⁻ cells from the same cell line. These findings suggest that the CD44⁺ population is enriched in cells with stem cell properties and tumorigenic potential. Importantly these were consistent with the results of Collins et al., 2005.

Ultimately, it will be necessary to determine whether prostate cancer cells that express α2β1^{hi}/CD133⁺ are tumour initiating in immune-deficient hosts and can recapitulate the original tumour heterogeneity in vivo (Collins and Maitland, 2006).

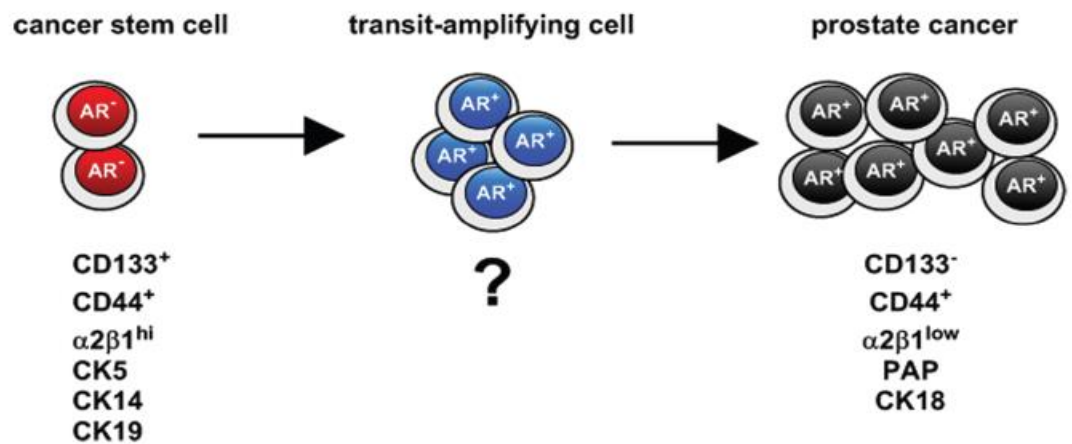


Figure 1.15: **Phenotype of the prostate cancer stem cells** and more differentiated prostate cancer cells. Prostate CSC are CD133⁺, CD44⁺, α2β1^{hi} and express CK 5, 14 and 19. These cells differentiate into CD133⁻, CD44⁺, α2β1^{low} and cytokeatin 18 (CK18) and prostatic acid phosphatase (PAP) expressing cells. The prostate cancer transit-amplifying cell phenotype has yet to be defined. Reproduced from (Sharifi et al., 2006)

1.11.2 p63 in PC stem cells

The p63 protein is a homologue of the p53 tumour suppressor gene (Levine et al., 2011, Yang et al., 1998). Early in development, the prostate consists exclusively of p63-expressing cells, which are induced to differentiate into a bilayer of basal and luminal secretory cells (Signoretti et al., 2000). The two major classes of p63 proteins are those containing (TAp63) and those lacking (Δ Np63) an N-terminal transcription-activating (TA) domain (Yang et al., 1998). Δ Np63 α is the most commonly expressed p63 isoform in the adult prostate and is only present in basal cells. Unlike p53 however, p63 lacks mutation in cancer development (Finlan and Hupp, 2007).

There is increasing evidence that p63, and specifically Δ Np63, plays a central role in tumorigenesis by promoting epithelial cell survival. Knockdown of p63 isoforms in prostate epithelial cells has been shown to cause a decrease in cell viability by inducing apoptosis without affecting the cell cycle (Sabbisetti et al., 2009).

1.11.3 Cancer Stem Cells in CRPC

Currently, the conventional treatments indiscriminately kill proliferating cells. In order to be more successful, therapy must first target all proliferating tumour cells then differentiate or eliminate CSC (Massard et al., 2006). Understanding the cellular signaling that controls stem cell proliferation and differentiation could lead to the development of new anticancer strategies.

As explained in section 1.11.1 above, the tumour cell populations in PC are constantly evolving with treatment. New populations can arise by random mutations and not always in the CSCs. In fact, stem cells whose aim is to survive in an unaltered form throughout appear to have evolved a hierarchy of gene inactivation, which allows them to be flexible in the responses to changing environments. They can fold their chromosomes to turn off unwanted genes, modify their cytosine bases when a gene is not required and inactivate a gene by point mutations. Hence, after first line castration has failed it is likely that there will be few different cell populations in the tumour (Maitland, 2015). This further limits treatment which use targeted agents normally directed against the most common tumour cells. It is the current therapies that therefore select for and define the resistant multiclonal cells, which are heterogeneous and lethal (Maitland, 2015).

The CSC concept implies that the founder cells of each cancer are defined in their malignant potential when the cancer emerges for the first time. All subsequent mutations and the gene rearrangements are an enhancement, which help the cancer prosper. Possible strategies that can help combat the treatment resistant phenotypes are (Maitland, 2015):

- i. Combination treatment with complementary and salvage cell signaling pathways to target new cancer cell populations forming.
- ii. Order and timing of such combinations as per the new treatment paradigms.
- iii. Tailoring the treatment to the patient's specific form of disease as a form of 'personalised' or 'precision' medicine.

The next generation of PC treatments should therefore be decided on a truly individual and patient centered basis. Development of patient derived PC xenografts can further help in elucidating some of these strategies and could potentially influence cancer management in the decades to come.

1.12 Models of studying prostate cancer

1.12.1 Cell lines

PC research has traditionally been conducted on established cell lines. They are easily cultured, adapt to various conditions, can be subcultured, passaged many times and are readily transfectable. Hence they have been used for decades to test hypotheses, screening and development of new treatments for prostate cancer. There is a wide range of normal, pre-malignant and malignant cell lines derived from various sites. Some of them are androgen sensitive and others not (Maitland et al., 2010).

Metastatic PC cell lines include LNCaP derived from lymph nodes (Horoszewicz et al., 1980), PC-3 derived from bone spread (Kaighn et al., 1979) and DU145 derived from brain metastases (Stone et al., 1978). These were all derived from metastatic cancers resistant to prior chemotherapy. The cell line P4E6 was derived from an early Gleason score 4, well differentiated prostate cancer (Maitland et al., 2001). Non-malignant prostate epithelial cell lines include PNT1a and PNT2.C2 established from normal prostate tissue of young male organ donors (Berthon et al., 1995) (Table 2). For each cell line, sub clones can also be engineered from the parent cells by phenotypic selection or genomic transduction. All non-malignant cells including P4E6 had to be immortalised with viral transforming genes, such as simian virus (SV40), human papilloma-18 (HPV) or telomerase (hTERT) (Webber et al., 1996).

Cell line type	Name
Metastatic PC	LNCaP
	PC3
	DU145
Early PC	P4E6
Benign prostate epithelial cells	PNT1a
	PNT2.C2

Table 2: Commonly used **prostate cancer cell lines**.

Although cell lines represent an excellent basis for testing scientific hypotheses, there are some concerns regarding how closely they represent the *in vivo* situation. They are limited in showing the inherently slow growth of early prostate tumours and the slow proliferation rate of normal prostatic epithelial cells (Isaacs and Coffey, 1989). They fail to demonstrate the heterogeneity and the stromal–epithelial interactions that are pivotal in many aspects of prostatic biology. It is of little surprise that some clinical trials fail to translate the excellent results achieved in pre-clinical cell line experiments. As a result, more robust models are urgently required that better mirror the cellular events in the individual prostate cancer patients. Two such models where recent breakthroughs have occurred are primary cell cultures and patient derived xenografts.

1.12.2 Primary cell cultures

Primary cultures of prostate cells are derived from patients' actual tissues obtained after surgical procedures. Directed needle biopsies of Gleason score 6 and 7 are received from radical prostatectomy samples. Resection biopsies from high Gleason score patients and CRPC are mainly from palliative transurethral resection of the prostate (TURP) operations. Non-cancerous cells are also derived from benign tissue obtained from TURP where only benign prostatic hypertrophy (BPH) was diagnosed. Single cell suspensions are then isolated from these tissues by collagenase digestion, trypsin treatment, differential fractionation and cellular marker separation depending on what specific populations are required. Enriched populations of prostate cancer stem cells can also be derived by using cell-surface markers such as CD133, CD44, integrin $\alpha 2\beta 1$ hi (Collins et al., 2005).

1.12.3 'Near patient' derived xenograft (PDX)

Xenografts derived from inoculation of PC cell lines fail to recapitulate the full dynamics of the disease. Hence a more clinically relevant model that captures the biological and molecular heterogeneity of PC is needed. A more precise model is provided by patient-derived xenografts, based on direct implantation of fresh cancer tissue specimens into immunodeficient mice (Lin et al., 2014). Such xenografts contain the cellular heterogeneity, architectural and molecular characteristics of the original cancer (Garber, 2009). They are viewed as the next generation models of PC to test molecular theories and preclinical drug trials.

1.12.4 PDX in other cancer models

In non-small cell lung cancers and colorectal cancers, the establishment of PDX in immunocompromised mice has been achievable with a success rate of more than 50% (de Cremoux et al., 2007, Fichtner et al., 2008). Breast cancer PDX have recently shown a high correlation between drug responses, which corresponded to the various outcomes found in the original tumours (Marangoni et al., 2007). Here, the PDXs better represented the vasculature, stroma, central necrosis and peripheral growth that are similar to that of the patient's tumour. There is also an extensive panel of non-small cell lung cancer derived from various grades of cancer. These have provided an excellent model to test marketed as well as novel drug therapies (Fichtner et al., 2008). The role of PDX displaying the original cancer heterogeneity has also been emphasized in pancreatic cancer models and development of personalised treatment approaches (Sjoquist et al., 2014).

1.12.5 In vivo mouse models

In order to engineer new potential treatments for prostate cancer, it is necessary to have biologically relevant models of prostate carcinogenesis. Although in vitro models provide an established means of studying prostate cancer, valuable information about its biology and pathology can be obtained from in vivo studies. Immunocompromised mouse is a commonly used in vivo model. The two main classes of mouse models are: xenografting or genetically engineered mouse models (GEMMs).

1.12.5.1 Xenograft in immunocompromised mice

Apart from the subcutaneous space, xenografting involves implantation of human tissue or cell lines into the sub-renal capsule or orthotopic space in immunocompromised mice. These methods have been used to study numerous different human cancers (Mattie et al., 2013, Shultz et al., 1995) and allow serial transplantation in parallel to numerous individual mice so that the efficacy of specific treatments can be evaluated. The first PC xenograft tissue, called PC-82 was demonstrated in 1977 from a primary prostatic adenocarcinoma implanted in

athymic nude mice. This model did not achieve widespread popularity as immortalized in vitro cell lines could not be derived from it (van Weerden et al., 1996).

Nude mice are one of the most commonly used mouse hosts of human tissue. They are deficient in T lymphocytes due to lack of a thymus. Severe combined immunodeficiency (SCID) mice are deficient in mature B and T cells, due to a defect in genetic recombination necessary for lymphoid development (Bosma and Carroll, 1991). In addition, NOD/SCID (non obese diabetic/SCID) mice also have low levels of NK cells, circulating complement, and functional antigen-presenting cells (Shultz et al., 1995). However, there is evidence of remnant NK cell activity in these mice (Yoshino et al., 2000). NOG/NSG mice offer complete deficiency of NK cells, after the NOD/SCID mice were crossed with interleukin 2 receptor γ (IL2R γ) null mice (Ohbo et al., 1996). Rag2 $\gamma^{-/-}$ C $^{-/-}$ is a genetic cross with a recombinase-activating gene 2 (RAG2) deficient strain (Goldman et al., 1998). RAG encodes enzymes that play an important role in the rearrangement and recombination of the genes of immunoglobulin and T cell molecules. The two recombination-activating gene products are known as RAG1 and RAG2 (Jones and Gellert, 2004).

Rag2 $\gamma^{-/-}$ C $^{-/-}$ mice lack B and T lymphocytes and most importantly NK cells. They are able to accept foreign tissue with a higher success rate and were more immunodeficient than SCID mice. Table 3 shows a list of immunocompromised mice generally used.

Mouse strain	Immune deficiency
Nude	Lacks T lymphocytes
SCID	Lacks T/B lymphocytes
NOD/SCID	Lacks T/B cells, complement factors, reduced NK cells and APCs
NOG/NSG and Rag2$\gamma^{-/-}$C$^{-/-}$	Complete lack of T/B and NK cells

Table 3: Series of immunocompromised mice used.

1.12.5.2 Genetically engineered mouse models

The genetic modifications in the GEMM are constructed to be equivalent to those associated in human tumours. Genetically modified mice involve the introduction of DNA constructs designed to induce the expression of genes under the control of tissue-specific promoters. Mice only develop PC after engineering prostate specific oncogene expression or suppressor gene knockout. In the transgenic adenocarcinoma of the mouse prostate (TRAMP) model, the SV40 tumour antigens were regulated by the prostate-specific rat probasin promoter. These mice develop PC together with metastases by 28 weeks (Gingrich et al., 1997, Greenberg et al., 1995).

Several transgenic models exist but so far they have not been able to accurately induce all stages of epithelial PC. This is most likely because prostate cancer probably requires more than one genetic event involving multiple molecular pathways. Furthermore, human prostate cancer is not mutation driven, but typified by gene rearrangement (Valkenburg and Williams, 2011).

Mouse models have also helped looking at gene deletion studies. Genetic lineage marking has demonstrated that rare luminal cells expressing Nkx3-1 in the absence of androgens (castration-resistant Nkx3-1-expressing cells, CARNs) were bipotential and can self-renew in vivo. Single-cell transplantation assays showed that CARNs could reconstitute prostate ducts in renal grafts. These observations indicate that CARNs represent a new luminal stem cell population that can be an efficient target for oncogenic transformation in PC (Wang et al., 2009). So far substantial evidence has supported only the existence of a basal stem cell population (Lawson and Witte, 2007) however, Wang et al. suggested the relevance of this new luminal stem cell population as a cell type of origin for PC. Another recent study showed that deletion of phosphatase and tensin homologue (PTEN) in basal cells, does not result in advanced PC as found on PTEN deletion in luminal cells, but can induce prostate intraepithelial neoplasia possibly through the differentiation into luminal intermediates (Choi et al., 2012). In normal prostate development, clonal analysis has also shown the existence of multipotent basal progenitors which contrasts with the distinct pools of unipotent basal and luminal stem cells that mediate adult prostate regeneration (Ousset et al., 2012). The microenvironment of epithelial cells has been suggested to have an important role

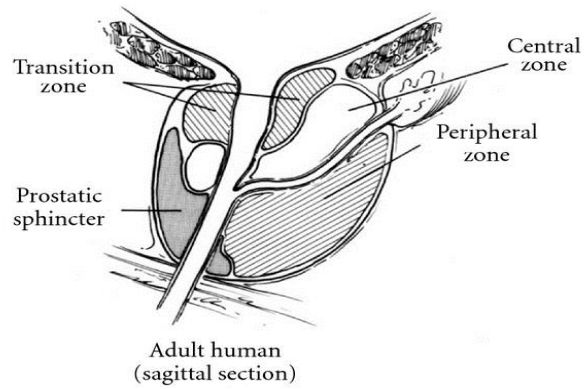
in imposing intrinsic 'stemness' features and in maintaining multipotency (Blanpain et al., 2004).

1.12.6 The mouse prostate as an orthotopic model

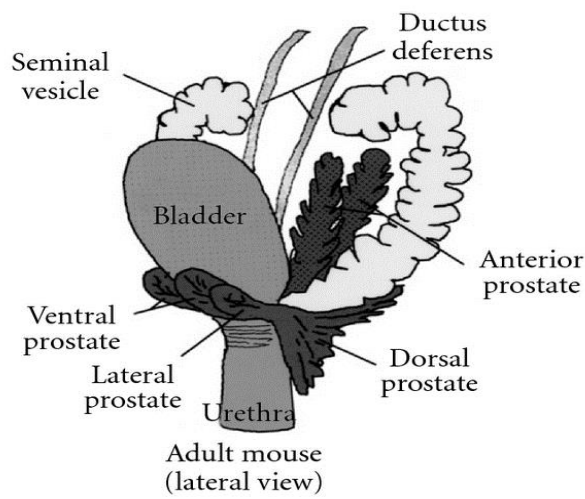
In vitro studies of clonal cell lines do not provide the opportunity to examine the dynamic interactions between the various cellular compartments that comprise the intact prostate gland. These include the prostatic epithelium, endothelium, neuroendocrine cells and stroma (Abate-Shen and Shen, 2002, Greenberg et al., 1995, Huss et al., 2001, Kaplan-Lefko et al., 2003, Winter et al., 2003). Orthotopic implantation (engraftment at the original site of the tumour) has been suggested to be more representative of prostate cancer due to the interaction of tumour cells with the prostate microenvironment.

Certain similarities between the mouse and human prostate gland support the use of mouse prostate models for elucidation of key molecular alterations that accompany PC development and progression. However, there are also anatomical differences which impact on the pathological analysis (Abate-Shen and Shen, 2002, Greenberg et al., 1995, Huss et al., 2001). The mouse prostate has a single epithelial layer with the luminal cells in contact with the basement membrane compared to human prostate epithelium where it is the basal cells that align first, below a distinct upper luminal layer.

The rodent prostate is divided into four distinct lobes: the anterior prostate, ventral prostate, dorsal prostate, and lateral prostate (Figure. 1.16b). Each lobe is surrounded by and separated from the others by fibrous and adipose connective tissue. Compared to the capsule and stroma surrounding the central, transitional and peripheral zones in the human prostate (Figure 1.16a). The mouse ventral lobe is easily amenable for injection and grafting, as the bladder provides a good landmark. The size of the mouse stromal compartment is modest compared to the robust human fibromuscular stroma (Harmelin et al., 2005). Nonetheless the mouse model provides an advantage in studying the prostate carcinogenesis including function of oncogenes and tumour suppressor genes.



(a)



(b)

Figure 1.16: Schematic illustration of the **anatomy of the human prostate** (a) and the **mouse prostate** (b). Adapted from (Abate-Shen and Shen, 2002, McNeal, 1988).

1.13 Tracking PC stem cells

Cancer cells often metastasize to several foci, which can be local or distant organs. They are robust and versatile surviving in various changing environments outside the prostate. Lentiviral vectors encoding for identifiable marker genes can be used to track CSC. Lentiviruses constitute a subgroup of retroviruses, which include oncoretroviruses and foamy viruses (Bukrinsky et al., 1992). The defining characteristic of retroviruses is their ability to convert single-stranded RNA into double stranded DNA in the course of their reproductive cycle (Figure 1.17). The resultant transcribed viral genome can then be translocated into the nucleus and integrated into a host cell genome by the viral enzyme integrase (Bukrinsky et al., 1992). Lentiviruses possess the ability to stably integrate into the genome of host cells, allowing long-term and stable transgene expression in their progeny (Bukrinsky et al., 1992). They have proved to be a versatile tool for gene delivery, as they can infect both dividing and non-dividing cells. Due to this unique ability to infect quiescent cells, they are ideal for genetic modification of stem cells. To 'mark' stem cells, a fluorescent gene indicator such as green fluorescent protein (GFP) is now frequently used (Frame et al., 2010). The reporter gene is normally expressed from a strong promoter, which is non-tissue specific, highly expressed in all cell types and less likely to be silenced after long-term culture. Current applications of lentiviral vectors include delivery of therapeutic genes (Gerolami et al., 2004) as well as reporter constructs for the purpose of cell tracking and monitoring (Suter et al., 2006, van den Brandt et al., 2004). High transgene expression is of great importance in targeted gene therapy and requires high efficiency at the levels of transcription, post-transcriptional mRNA processing and translation (Hager et al., 2008). Since no single post-transcriptional enhancer is optimal for all vector contexts and expression cassettes, there is an ongoing need to develop further sequence elements. A critical event in post-transcriptional processing of mRNA is polyadenylation, as addition of a poly(A) tail increases mRNA stability and translational efficiency (Jackson and Standart, 1990). However internal transcription units are commonly cloned without a poly(A) signal in order to avoid truncation of the viral genome (Blo et al., 2008). The possibility of integrating an internal poly(A) signal and its effect on functional viral titre have been recently shown to stably increase transgene expression in primary prostatic epithelial cells

(Hager et al., 2008). Lineage tracking lentiviruses for use in PDX are not currently available and are the next step to contribute to the study of PC stem cells.

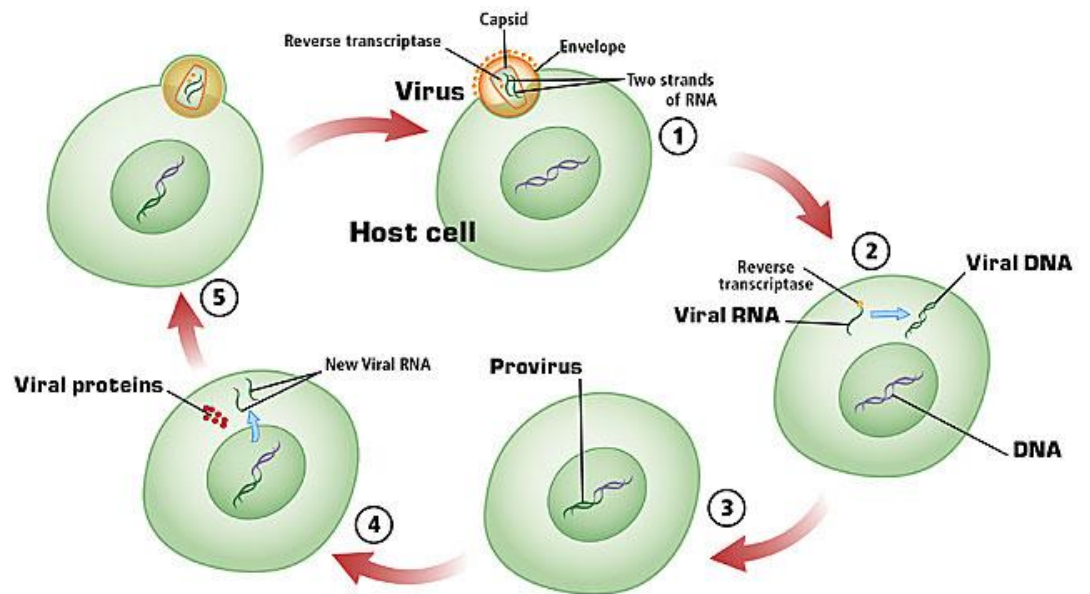


Figure 1.17: **Simplified version of the retroviral life cycle.** 1. Entry of the virus in host cell by endocytosis. 2. Reverse transcription of viral RNA to DNA. 3. The reverse transcribed genome integration into the host cell genomic DNA. 4. Nuclear export of lentiviral genome and viral protein synthesis. 5. Gathering of viral capsid and budding from host cell. (Adapted from <http://ewbiology.blogspot.co.uk/2006/10/replication-cycle.html>)

1.14 Hypothesis and Project Aims

Traditional methods of studying PC are based on cell lines, which do not fully represent the heterogeneity seen in the actual disease. PDXs are better predictors of PC and its relapse as they can mimic the wide plethora of cells in a cancer. They provide a 'near patient' technique which mirrors a personalised approach to individual treatment and are better than a 'one size fits all' treatment.

Xenografting is commonly performed in the subcutaneous (s/c) space of immunocompromised hosts however, there have been suggestions that the orthotopic method (intraprostatic) better represents carcinogenesis and metastatic spread. In the first results section, I have looked at whether orthotopic engraftment is superior to the s/c inoculation and if they provide a better method to look at IHC for candidate markers.

The focus was to find targets that can inhibit the normal functioning of CSC using in vivo techniques. Whether the long exposure to ADT makes the PDX model more sensitive to docetaxel. Looking at the phenotype of CSC, I evaluated whether some PC are predestined for treatment resistance. I tested the hypothesis that changes in basal or luminal cells determine docetaxel sensitivity.

In the third results section, I looked into lentiviral transduction of PDX cells with fluorescent and luciferase markers, which would allow live monitoring and locating spread of PC. If this was to be successful, transduced PDX cells could then be used to look at metastatic spread or to monitor therapy effects.

CHAPTER 2

MATERIALS

AND

METHODS

2.1 Mammalian cell culture

2.1.1 Cell lines

LNCaP and PC3 cells were purchased from the American Type Culture Collection (ATCC; Manassas, VA, USA). LNCaP cells were derived from a human prostatic adenocarcinoma metastatic lesion in a supraclavicular lymph node by (Horoszewicz et al., 1980). They were cultured in Roswell Park Memorial Institute-1640 (RPMI) (Invitrogen) supplemented with 10% foetal calf serum (FCS) (PAA) and 2mM L-Glutamine (Invitrogen), collectively known as R-10 media. They were regularly subcultured in a ratio of 1:10 when fully confluent.

PC3 cells were originally derived from a human bone metastasis by (Kaighn et al., 1979). The cells were cultured in Ham's F-12 medium (Lonza) supplemented with 7% FCS and 2mM L-Glutamine (H7). All cells were routinely grown in cell culture tissue flasks (Corning) T-25 at 37°C in 5% CO₂. Appendix 1 includes a list of all the different cell culture media that were used.

2.1.2 Live/dead cell count

The cells were detached from the tissue flask using 0.05% trypsin/EDTA (Ethylene-diamine-tetra-acetic acid) in PBS. Following 10 minutes of trypsination at 37°C, all cells were washed in R-10 media. A known volume of the cell suspension was mixed in a 1:1 ratio with 0.4% Trypan Blue stain (Sigma). After mixing, the cells were carefully injected into a two-chamber haemocytometer (10µL per chamber). The non-stained cells (live cells) were counted and the value determined in the original volume of the cell suspension. To calculate the dead cell numbers, the stained cells were counted from the same field of the haemocytometer. The addition of both species gave the total cell number.

2.2 Protein expression

2.2.1 Prostate and xenograft tissue

2.2.1.1 Tissue fixation and wax embedding

A sample of xenograft tissue (5-10mm) or prostate tissue (needle core or resection chips) was fixed in 10% formalin (Fluka) for at least 24 hours. For subcutaneous xenografts, a tissue sample free from necrotic areas and fat towards the core of the tumour was dissected out from the subcutaneous space in the mouse. For orthotopic xenografts, a laparotomy was performed revealing the prostate mass from which a tissue sample was cut and put in 10% formalin.

After 24 hours, the tissue was transferred to 70% Ethanol (Fisher Scientific) overnight. It was then placed in an embedding cassette (Cell Path) and dipped in fresh 70% ethanol for 10 minutes, on a shaker. As the needle cores were too small for the slits of the cassette, they were put in a protective net first then into a cassette. After 10 minutes in 70% ethanol baths, the cassettes were placed in absolute ethanol for 10 minutes, on a shaker. This process was repeated twice more. The cassette was then submerged in Propan-2-ol (Fisher Scientific) for 2x 10 minutes, in a fume cupboard followed by 4x 10 minutes in fresh xylene (Fisher Scientific). The cassette was then blotted onto tissue paper to soak up excess xylene.

The cassette was placed in Histoplast paraffin at 60°C (Thermo Scientific) for 4x 15 minutes. The tissue sample was then removed from the cassette or net protector and embedded in metal moulds with molten wax. Care was taken to orientate the tissue so that the largest surface was placed face down. The metal mould was allowed to set for 20-25 minutes on a freezing plate at -10°C after which the embedded cassette was carefully removed and stored at room temperature in a dry place until sectioning.

2.2.1.2 Sectioning and mounting

Paraffin embedded tissue blocks were placed (for 30 minutes) on a freezing plate to harden the wax. SuperFrost Plus slides (Merck) were coated with 2% (3'aminopropyl triethoxysilane) (v/v) (Sigma) (APES). The blocks were then cut with a microtome at 5µm thickness and sections carefully lowered onto lukewarm water. The sections were then mounted onto APES coated slides, labelled and left to dry on a hot plate. After drying, they were stored at room temperature in a slide box.

2.2.1.3 Haematoxylin and Eosin (H&E) staining

The dewaxing procedure was started by placing the paraffin embedded tissue slides on a hot plate at 40°C for 30 minutes. Next, they were transferred to a metal rack and placed in a fume cupboard in 2x 10 minutes and 2x 1 minute xylene baths. A different bath was used after each step. Sections were re-hydrated using absolute ethanol (3x 1 minute) followed by 1 minute, in 70% ethanol. Then they were washed under running tap water for 1 minute while still in the rack. The slides were placed in haematoxylin (Mayers) for 1 minute and rinsed under running tap water for 1 minute. The slides were then stained in Scott's tap water (0.2% Sodium Bicarbonate and 0.2% Magnesium Sulphate) for 1 minute and rinsed in tap water for a 1 minute. They were then stained in Eosin (Harris) for 30 seconds and washed in running tap water for 1 minute. Slides were dehydrated for 1 minute in 70% ethanol, 3x 1 minute absolute ethanol and 2x 1 minute Xylene. The slides were removed individually from the rack and placed on absorbent roll before mounting in Distrene, Plasticiser, Xylene (DPX) mounting medium (Sigma). A cover slip was lowered carefully onto the slide and pressed down to remove air bubbles. After leaving to dry in the fume cupboard overnight, the slides were stored in slide boxes or analysed immediately. Pictures were taken on an Olympus BX51 light microscope.

2.2.1.4 Immunohistochemistry

Following dewaxing, an antigen retrieval step was performed by boiling twice in 0.01M sodium citrate buffer (2.94g trisodium citrate/1L pH 6.0, 0.05% tween 20) for (2x 6 minutes) and leaving the slides to cool for 20 minutes. The boiling was carried out in a microwave at 900W. After cooling, slides were rinsed in tris-buffered saline (TBS) (150mM NaCl, 50mM TrisHCl, pH 7.5) for 5 minutes and then the tissue sections were encircled with a PAP-pen (Sigma). Depending on which species the secondary antibodies were raised in, the slides were blocked with 20% blocking serum at room temperature for 10 minutes. Following blocking, the sections were incubated in primary antibody (Appendix 1) or an isotype (negative) control (Appendix 2) (diluted in blocking buffer) for 1 hour. All the slides were then washed in TBS (3x 5 minutes). Biotinylated secondary antibodies (Appendix 3) were added to all sections and left at RT for 45 minutes followed by 3x 5 minutes TBS washes. Then slides were incubated in streptavidin-HRP conjugate (1:100 Thermo Scientific) for 30 minutes at RT followed by 3x 5 minutes TBS washes. 3, 3' Diaminobenzidine (DAB) substrate (Sigma) was then added for 7 minutes. Slides were washed twice in ddH₂O and running tap water for 5 minutes. Counterstaining was performed with Haematoxylin (Vector Laboratories), rinsed and dehydrated as described in section 2.2.1.3 before mounting in DPX. After drying, slides were analysed using and images taken. Pictures were taken on an Olympus BX51 light microscope.

2.2.1.5 Cell counts and positive cells identification

Cell counts were performed at high magnification fields (x200) on 3 different slides of the same group or PDX. Each of the slides were prepared in an identical way and each time more than 100 cells were counted with a cell counter using an Olympus BX51 light microscope. The mean and the standard deviation were then calculated. Where there was a difference between two groups, the Student's t test was used to determine statistical significance.

Dr G Rodriguez, histopathologist initially examined the mounted slides and taught us how to identify original PDX cells and their positive staining after

immunohistochemistry or H&E. She also reported the actual tumour specimens from the patient. In addition during my early days in the lab, Dr A Collins provided further guidance.

2.2.2 Flow cytometry

2.2.2.1 Cell surface protein detection

For flow cytometry or fluorescence-activated cell sorting (FACS), tumour cells from xenografts were used. A xenografted tumour excised from the mouse host was first depleted of mouse cells, as described in section 2.3.2.1. The resulting cells were washed once in MACS buffer (PBS supplemented with 2mM EDTA and 0.5% FCS) and cell labelling was performed in a MACSmix Tube Rotator (Miltenyi Biotec). Cells were mixed with primary conjugated antibodies (Appendix 1) and 20% FCR blocking buffer (Miltenyi Biotec) in a total volume of 100 μ L MACS buffer for 30 minutes at 4°C. Unlabelled or non-specific isotype were used as negative controls.

For dual labelling of cell surface markers, antibodies were added simultaneously in a total volume of 100 μ L. Following incubation cells were washed in MACS buffer and pelleted in a centrifuge at 323 xg relative centrifugal force (rcf) for 3 minutes. The labelled cells were resuspended in 1ml of MACS buffer and stored in a dark box at 4°C until analysis. 1:1000 sytox blue cell dead stain (Invitrogen) was used as a live/dead cell stain and was added five minutes before analysis, which was performed on a Cyan ADP flow cytometer (DAKO), using 495, 488 and 633nm lasers (Appendix 4). Summit v4.4 software (Beckman Coulter) was used to analyse the data.

2.2.2.2 Intracellular antigen detection

Detection of intracellular antigens involves permeabilisation to render the cell membrane porous. Cell suspensions were first incubated with 1:1000 Live/Dead Fixable Violet Dead Cell Stain (Invitrogen) for 30 minutes at 4°C. If detection of cell surface antigens was required, step 2.2.2.1 was followed. Then

the cells were fixed in 1.5% (v/v) formaldehyde for 10 minutes at 4°C. After a washing step in MACS buffer, ice-cold methanol was used to permeabilise cells for 10 minutes at 4°C. Cells were again washed and labelled with intracellular antibody for 30 minutes at 4°C. Cells were washed in MACS buffer and resuspended in 1ml ready for analysis on the Cyan ADP flow cytometer.

If unconjugated primary antibody was used, it was mixed in 20% serum from the secondary antibody species first then added to the cells for incubation. After a washing step, secondary antibodies (Appendix 3) were added and incubated for 30 minutes at 4°C.

When required, specific cell populations were isolated by processing the labelled cells in a cell sorter, the MoFlo Astrios™ (Beckman Coulter, Inc). Staff from the technology facility department operated the cell sorter.

2.2.2.3 Data analysis

For analysis of flow cytometer data, the following gates were set (Table 4). Firstly, pulse width to exclude doublets and debris. Secondly, Violet 1 channels to exclude dead cells. The latter would have been labelled with live/dead stain or Sytox blue, which has a wavelength of 405nm. Thirdly, a Forward scatter/Side scatter (FS/SS) dot plot was used to depict cell size and granularity. Fluorescein isothiocyanate (FITC), phycoerythrin (PE) and allophycocyanin (APC) channels were used to analyse the fluorescently labelled and control cells. The FITC emission spectrum overlaps into the PE spectrum (Appendix 4) and hence compensation was performed when analysing cells that were dual labelled with these fluorescent antibodies.

FACS	Gates	Reason
1	Pulse width	To exclude doublets and debris
2	Violet 1	To remove dead cells
3	Forward/Side scatter	To select similar size cells and the right population

Table 4: **Gating strategy for FACS.** Steps used for data analysis after scanning cells using flow cytometry.

2.3 In vivo studies

2.3.1 General Animal Husbandry

All animal studies were performed in the Biological Service Facility (BSF) a section of the Department of Biology, University of York. Experiments were in accordance with the scientific procedures act of 1986 where mice were checked daily for adverse clinical signs after tumour engraftment and treatment. Mouse colonies were managed on the Jackson Laboratory's Colony Management System (JCMS). This is a multi-user relational database in the research environment used to maximise the potential of the mouse colonies, through continuous monitoring of breeding performance and tracking mouse pedigrees. JCMS was updated every time a mouse changed status to maintain compliance with the Home Office licence regulations.

All mouse experiments were approved by the University of York Animal Procedures and Ethics Committee and performed under a United Kingdom Home Office Licence. The project licence holder is Dr Anne Collins who provided training on all the surgical procedures. Training had to be complete before unsupervised work was allowed. Support was also provided by Mr Paul Berry and the BSF staff. The Home Office project licence number is 60/3701 and my personal licence number 60/13426. The overall severity band attached to this licence is moderate and if the practice of the individual procedures exceeds this severity limit, then it required adjustment after discussion with the Home Office inspector, who did regular checks at the animal lab. This licence also covered the procedures (outlined below) and animal types, which may be used.

2.3.2 Grafting of prostatic tumour cells

Human prostatic tissues were obtained under full ethical permission (Ethics no. 07/H1304/121) and patients individually signed a consent form. This covered sample processing, storing and publishing with anonymisation. Samples were from patients undergoing radical prostatectomy and trans-urethral resection for prostate

cancer. Biopsies were taken immediately following surgery and the site of each biopsy was determined by previous pathology, imaging and palpation. Tissues were transported in RPMI-1640 with 5% FCS and 100U/ml antibiotic/antimycotic solution at 4°C and processed within 12hr. Biopsies were verified by subsequent histopathology of the full specimen by consultant pathologists. Tissue pieces were directly engrafted subcutaneously into recipient Rag2^{-/-}γC^{-/-} mice. For specimens from hormone naïve patients' mice were engrafted with dihydrotestosterone tablets at the time of tissue implantation. Once tumours reached 15mm, which was considered a humane endpoint, the mice were sacrificed and the tumours were either re-implanted into further mice or the tissue was processed for further experiments. To maintain the tumour xenograft as 'near-patient,' tumours were re-established from frozen cells after 5 passages in mice.

2.3.2.1 Depletion of mouse endothelial and lineage positive blood cells

Once tumours from serially transplantable xenografts reached 15mm, they were processed in the following way. The tissue was placed into a 10cm petri dish and washed in PBS. Fresh collagenase was weighed out to give a final concentration of 200IU/ml in 2.5 ml of KSFM/per 1g of tissue together with 5ml of R-10 with antibiotic-antimycotic (ABM). The collagenase solution was added to the petri dish containing the tissue and the tumour was diced into small pieces (~1 mm³) using forceps and a scalpel. The resultant mixture was transferred into a 125mls sterile Erlenmeyer flask and incubated at 37°C overnight in an orbital shaker for digestion.

Following digestion, repeated pipetting and syringing with a 21G blunt needle was performed to breakup larger tissue pieces. The mixture was centrifuged at 988 xg rcf for 10 minutes to sediment cells. The pellet was resuspended in 10mls PBS to wash out collagenase followed by a further centrifugation at 988 xg rcf for 10 minutes.

The pellet was suspended in 10mls of trypsin (concentration) and incubated at 37°C for 30 minutes in an orbital shaker. The digestion was stopped by adding

10mls of R-10. After a short centrifugation, the mixture was passed through a 21G needle and strained in a 40µm nylon cell sieve (Falcon). Further centrifugation was carried out in 5mls of MACS buffer before lineage depletion (MACS Lineage Cell Depletion Kit; Miltenyi Biotec catalogue number: 130-090-858) as outlined in the manufacturer's instructions. Due to possible infiltration of murine cells into tumours, depletion of mouse cells using a cocktail of blood lineage antibodies linked by magnetic beads was performed by MACS cell sorting. During this procedure, mature haematopoietic cells (macrophages, dendritic cells, monocytes, granulocytes and erythroid cells) are removed using this lineage depletion kit (Miltenyi Biotec). Endothelial cells and fibroblasts were depleted by antibodies CD31 (clone ER-MP12) and Sca-1 (clone D7) respectively, by MACS.

80µl of MACS buffer were used to resuspend the pellet with 20µl of Biotin Antibody cocktail and 5µl of CD31 antibody (AbD Serotec). This mixture was incubated for 10 minutes at 4°C on a rotating spinner. 60µl of MACS buffer, 40µl of Anti-Biotin MicroBeads were added, for incubation for 15 minutes at 4°C on a rotating spinner. Cells were washed with 4mls of MACS buffer and pelleted by centrifugation.

For magnetic separation, cells were resuspended in 500µl of MACS buffer and placed in a washed LS column (Miltenyi Biotec). LIN⁻/CD31⁻/Sca-1-cells were collected after washing the column 3 times with 3mls of buffer. LIN⁻/CD31⁻ cells were pelleted and used immediately for FACS labelling, sorting or setting up further experiments in mice.

2.3.2.2 Subcutaneous engraftment of tumour cells

Rag2^{-/-}γC^{-/-} mice with a mean age of 5-6 weeks were used. They were housed in groups of 5 per cage. LIN⁻/CD31⁻ tumour cells were counted and divided into equal aliquots in 1.5ml Eppendorf tubes. 2x10⁵ irradiated STO (feeder and stromal) cells were added to each aliquot and this suspension was centrifuged (336 rcf for 3 minutes in a bench top centrifuge) to obtain a cell pellet which was mixed with 100µl of ice cold Matrigel basement membrane complex (BD Biosciences) prior to injection. The samples were kept on ice until subcutaneous

injection in both flanks of a mouse using a 27G insulin needle (BD Biosciences). The surgical procedure was carried out under general anaesthesia with 2.5% Isoflurane (Abbott) and Oxygen (BOC gases).

Another method for subcutaneous tumour engraftment involved cutting 4mm discs of tissue from a freshly excised tumour using a cylindrical punch biopsy. A small incision was cut on both flanks of a mouse under general anaesthesia. The 4mm disc was then implanted subcutaneously and the incision closed on 4-0 nylon sutures (Ethicon). Prior to this type of surgery, Rimadyl (Pfizer) (a non-steroidal anti-inflammatory painkiller) was given at 4.5mg/kg subcutaneously as well. Mice were monitored carefully during the procedure and returned to the incubation room after full recovery.

2.3.2.3 Orthotopic engraftment of tumour cells

For orthotopic prostate injections, each batch of LIN-/CD31- epithelial cells was counted and mixed with irradiated 2×10^5 STO cells in a 1.5ml Eppendorf tube. After centrifugation, the pellet was carefully suspended in 20 μ l Matrigel (BD Bioscience). The cells were kept on ice until injection into the murine prostate.

On an anaesthetised mouse, the abdominal region was shaved with an electric shaver taking care to remove the hair from the surgical area. A midline incision was made with a scalpel, and the subcutaneous area was bluntly dissected. Using sharp scissors, the muscle wall was opened and the bladder exposed, lifting it out of the cavity with blunt forceps. An operating microscope (Leica) was used to identify the prostate gland and push away the fat. Holding the bladder up with blunt forceps, the ventral prostate was injected with a 29G needle. The lobe inflates as the cells are injected. This indicated a satisfactory targeting of the ventral prostate. The syringe was then rotated before withdrawing to prevent leakage. The abdominal cavity was irrigated with sterile water, to kill any cells that have spilled out of the prostate. The muscle wall was closed with a 4-0 absorbable suture (Vicryl, Ethicon) and then the skin with 4-0 non-absorbable sutures. Subcutaneous analgesic drug was given and the mouse was allowed to recover in a heated cage. In all cases the ventral lobe of the prostate was injected. Mice

were monitored carefully as this method did not produce a measurable tumour lump but instead an externally palpable prostate mass. At the end of the experiment, a laparotomy was performed and only the prostate tumour meticulously excised.

The proliferation index was estimated after counting Ki67 positive cells on paraffin embedded slides after immunohistochemical staining. Counting was done in triplicates and represented as a mean and standard deviation.

2.3.3 Intra-peritoneal injection of drug

Mice were randomised into groups of 10, which were either treated with vehicle control, 10mg/kg docetaxel or 20mg/kg docetaxel. Power calculations were not used as each xenograft was unique and was used only once. Treatment was started when the subcutaneous tumours reached approximately 5mm (section 2.3.5). Injections were administered intraperitoneally (i.p) by scuffing the mouse and carefully injecting the lower abdomen while pulling gently on the hind leg. This was a two-person procedure. A 27G needle on a 1ml insulin syringe was used. Treatment schedules were once a week for 4 weeks.

2.3.4 Preparation of docetaxel for injection

Docetaxel (Taxotere) used for this experiment was purchased from Tocris Bioscience. R&D Systems Company, UK as a prepared sterile powder of 50mg ready for dilution. Fresh docetaxel solution was prepared on the day of injections from a stock solution, which was stored at -20°C in aliquots of 50mg/ml dissolved in absolute ethanol. Homogenous docetaxel solution was mixed with an equal volume of polysorbate 80 (Sigma) and eighteen times in excess with 5% glucose to prepare a final solution of 2mg/ml. Thorough mixing was achieved with a vortex mixer and the stock was kept in an incubator at 37°C away from light until injected. Particular care was taken to maintain the docetaxel in solution until injection on the same day.

Vehicle control solution was similarly prepared by mixing an equal volume of absolute ethanol (diluent of docetaxel) to the same concentration as the docetaxel solution.

2.3.5 Analysis of treatment responses

The dimensions of tumours were measured in two perpendicular sides using a digital calliper (Duratools DC150) and volumes were calculated using the formula: $0.5 \times \text{length} \times \text{width}^2$ (mm³). Tumours were measured every 3-4 days. The difference between the two measurements was then calculated as the percentage difference over time. Mice without tumours, at the start of treatment were excluded from the experiment. Tumour volumes were then averaged per treatment group. Growth curves were generated and the error bars represented by the standard error of the mean (SEM).

Mice were monitored and weighed twice a week to assess wellbeing until the tumour volume reached 15mm in maximum diameter, when they were humanely killed using a schedule 1 method. Mice that lost more than 10% of their body weight or showed signs of distress were more closely assessed and rehydration gels were added to the cage. However, if they showed no signs of improvement, they were humanely killed. A treatment holiday was allowed if deterioration occurred during treatment.

Kaplan-Meier survival analysis was used to determine which xenografts were sensitive to treatment (Sigmaplot Systat Software, Inc). Dots on the curves represent censored events, which could be due to excessive weight loss, inflammation around tumours and general ill health in the mice. The software also provided further detailed statistical analysis (95% confidence interval and Log-Rank test) and significance tests.

2.3.6 Genotyping of PDXs

To check their identity, the PDXs have been genotyped (PowerPlex 16, Promega) in comparison with the patients' own lymphocyte. This is the process by which a unique genetic fingerprinting is obtained from cells using short tandem repeats (STR). This confirmed that the PDX cells were still the same as those removed from the patient by comparing back to the lymphocyte DNA. Miss Hannah Walker performed the genotyping experiments.

2.4 Tracking prostate epithelial cells

2.4.1 Lentivirus transduction of PC3 cells and selection with Blasticidin

Confluent PC3 cells from a T-25 flask was trypsinised and counted. 1×10^5 PC3 cells were aliquoted into 5ml falcon tubes (BD Biosciences). The medium was aspirated and fresh medium with AMsBio lentiviral particles (EF1a-Luciferase-“A-RFP) in a ratio of 1:5 at 37°C was added. The lentivirus expressed luciferase and red fluorescent protein (RFP) under the control of an EF1a promoter. Incubation was performed in 4 batches for 2hrs, 4hrs, 8hrs and 24hrs. Every 30 minutes the tube was agitated to resuspend the virus. After the respective times, the cells were diluted with medium, pelleted and resuspended in fresh medium. An aliquot of infected cells was cultured in a 10cm round dish. 48hrs post transduction, culture medium was supplemented with Blasticidin (4µg/ml) and selection was applied until the cells became confluent. Blasticidin containing medium was replenished every 3 days. Miss Hannah Walker performed the transduction procedures.

2.4.2 Transduction of ‘near patient’ derived xenograft cells

A freshly excised serially transplantable xenograft was first depleted from mouse cells as described in section 2.3.2.1. 4×10^4 (LIN-/CD31-) cells were transduced for 2hrs in a ratio of 1:5 virus particles at 37°C. Xenografts cells were cultured in D10 medium supplemented with Blasticidin (4µg/ml). The rest of the procedure was carried out as described in section 2.4.1 by Miss Hannah Walker.

2.4.3 Tumour initiation assay

Transduced PC3 and xenograft cells were received from Miss Hannah Walker, counted, resuspended in ice-cold matrigel and kept on ice prior to injection. For each mouse an aliquot of 50µl cells in matrigel suspension was used. Subcutaneous injections were performed in Rag2^{-/-}γC^{-/-} mice to assess tumour induction and growth.

2.4.4 Explant culture of tumour

Once the tumour size reached 15mm in diameter, the mouse was humanely killed and a piece of tumour dissected. It was placed on a 35mm collagen dish (Becton Dickinson) containing 2ml of medium (H7 or D10). After 2 days Blasticidin containing medium (4µg/ml) was added and this was changed every 3 days.

86)

CHAPTER 3

RESULTS I

3. Comparison between subcutaneous and orthotopic engraftment of patient derived xenografts

3.1 Rationale

The subcutaneous implantation of cells or pieces of tissue in the flank of immunocompromised mice is by far the most widely used method of xenotransplantation (Cramer, 2013). Its advantages are the ease in implantation, being labour and time economic. It is easy to monitor early tumour growth by palpation and with callipers. This method is inexpensive compared to the orthotopic method. However, it can be argued that calliper measurements are relatively inaccurate and encumbered with size dependent bias and that micro-CT is a more accurate way of tumour measurement (Jensen et al., 2008). Unfortunately, there was no such facility of imaging in the laboratory I was working in. Other disadvantages of the subcutaneous method are not being organ specific, inability to study interactions between the tumour and the prostate and difficulty in studying the formation and spread metastatic spread.

On the other hand, orthotopic implantation is thought to be the ideal site as it mimics the originating environment of the tumour (Chung et al., 2007). Interactions between the host and tumour cells can be better studied. Metastasis formation and spread can also be closely followed. Disadvantages of this method are the need for longer time to set up experiments, labour intensive, higher costs and surgical skills requirements. Mice exhibit the same prostate epithelial cell types (basal, luminal and neuroendocrine) as humans, but in different ratios. In the human prostate, the ratio of basal to luminal cells is 1:1, whereas in mice the columnar epithelium predominates (El-Alfy et al., 2000). Moreover, in humans the basal cells form a continuous layer and are situated on the basement membrane. In contrast, basal cells are sporadically located in between luminal cells in the mouse, which means that luminal cells are anchored to the basement membrane. Table 5 summarises the different advantages and disadvantages of the subcutaneous and orthotopic xenograft methods.

In this chapter, I have compared the two models in differences in their histological morphology and immuno-histochemical expression of prostate specific markers. In preparation for looking at drug response studies (next chapter), I have investigated how the orthotopic model of PC might be used to monitor therapy effect and if the results are comparable to the subcutaneous way. Staining for candidate prostate epithelial markers were performed: p63 for basal cells, PSA and AR for luminal cells, PCK for epithelial cells, Vimentin for epithelial-mesenchymal transition (EMT) and Ki67 for proliferation.

Since the orthotopic model allows the study of metastasis, successful transduction of 'near patient' derived xenografts (PDX) cells with a lentivirus containing luciferase can help in live monitoring of cancer spread using the in vivo imaging system (IVIS) and D-luciferin. Chapter 5 describes an attempt at transducing PDXs with a dual labelled lentivirus (luciferase and RFP) and in chapter 4, PDXs were used to measure the therapeutic effects of docetaxel.

Xenograft method	Advantages	Disadvantages
Subcutaneous	Easy	Not organ specific
	Inexpensive	No tumour and organ interaction
	Labour economic	No natural mets.
	Time economic	Cannot analyse immune system interactions
	Widely used	
	Easy to monitor	
Orthotopic	Relevant tumour/host interactions	Surgical expertise needed
	Metastatic spread studies	Expensive
		Longer time
		Experiments with fewer numbers

Table 5: **Summary of the advantages and disadvantages of the subcutaneous and orthotopic xenograft methods**

3.2 Setting up 'Near patient' derived xenografts, (PDXs)

PDXs were derived by engrafting different grades of prostate cancer tissue into the subcutaneous space of Rag2^{-/-}γC^{-/-} mice. This development was introduced in the lab since 2006 and Dr A. Collins has been mainly responsible for generating several PDXs. Primary tumour fragments, from 121 patients, were implanted and primary tumour outgrowths were generated from 38 of 121 (32%). 19 patients yielded a stable xenograft (Table 6). They are serially transplantable and can be re-derived from frozen cells. Stable lines represented 8 hormone naïve patients and the remainder were from patients that had undergone hormone therapy. To confirm their identity, the PDX were routinely genotyped (PowerPlex 16) by checking them against the respective patient's lymphocytes. This set of PDXs was established over a long period of time and the ones that were used in this study are highlighted in table 6. Two PDXs were from hormone naïve and two from CRPC prostate cancer specimens. These two classes were deemed to represent the possible case mix that might be receiving docetaxel in the clinical setting.

Patient	Pathology	Latency/days
Y042	G7, T2	28
H024	G7, T3b	55
H042	G7, T2c	32
H087	G7	72
H050	G7, T2	61
H084	G7, T3a	84
H070	G7, T2c	71
H082	G7, T3a	125
H075	G7, T2c	200
H288	G7, T2c BM	29
H016	G9, T3a BM	33
Y019	G9, CRPC	45
H027	G9	53
Y056	G9, CRPC	81
Y018	G9, CRPC	40
H107	G8, T2b	91
H135	G9, CRPC	68
H149	G9, CRPC	143
H279	G9, T4 BM	84

Table 6: 'Near patient' derived xenografts generated in this lab from primary patient tissues. G7- total Gleason score of 7. T- Tumour stage, BM- bone metastasis, CRPC- castrate resistant prostate cancer and Latency- time taken for first tumours to appear when engrafted. The highlighted ones were used in this study together with their respective grade and hormone status.

3.3 Orthotopic engrafting of PC3 cells

As orthotopic engrafting required specific surgical skills, PC3 cells were used first to learn and master the technique (outcomes are shown below). After enough confidence was gained, PDXs were used at low passages to set up comparison experiments.

Cells were injected into the ventral prostate of the mouse as described in section 2.3.2.3. Table 7 shows the number of PC3 cells injected and their latency period (time from setting up the experiment until the first tumours appear). Tumours were derived from 1 out of 3 mice injected, with a latency period of 30 days. This latency period was similar to those from subcutaneous PC3 tumours.

PC3 cells	Tumour status	Latency/days
5×10^5	No Tumour	Ear infection after 10 days
6×10^5	Tumour	30
2×10^5	Died post procedure	n/a

Table 7: **Orthotopic injection of PC3 cells.** The surgical procedure for orthotopic engraftment of cells was optimised using PC3 cells before starting experiments on PDXs. Each injection was performed on three separate days lasting around 40 minutes each.

3.4 Orthotopic engrafting of PDXs cells

Subsequently, tumours were derived from two hormone naïve PDXs (Y042 and H016) and two castrate resistant PDXs (Y018 and Y019) (Table 8). The outcomes of the orthotopic experiments are shown in Table 9. Out of 16 orthotopic injections, only 4 failed to yield tumours. Engraftment of each PDX was set up at least four times except Y018 which had a long latency and hence even a high number of cells resulted in a slow tumour growth (see Table 9). Calliper measurements of orthotopic tumours were not possible, as the tumour masses lay deep in the pelvis. However, over the observation period, mice had the following external signs and symptoms, which indicated that there might be a prostate tumour:

- Palpable tumour in the pelvis area
- Weight loss or gain (>20% of body weight)
- Unkempt appearance (pilo-erection and withdrawn)
- Reduced mobility or limb paralysis

Xenograft	Gleason grade	Nature
Y042	Gleason 3+4	Hormone naïve
H016	Gleason 4+5	Hormone naïve
Y019	Gleason 4+5	CRPC
Y018	Gleason 4+5	CRPC

Table 8: **PDXs used for orthotopic prostate injections.** Two xenografts originally from hormone naïve prostate cancers and two from hormone resistant, CRPC patients were used.

PDX Id.	No. of cells injected	Latency/days
Y042	8x10 ⁴	35
	1x10 ⁶	39
	1x10 ⁶	39
	1x10 ⁶	No tumour after 3 months
Y018	1x10 ⁶	No tumour after 3 months
	7x10 ⁵	67
Y019	5x10 ⁵	41
	5x10 ⁵	32
	1x10 ⁶	No tumour after 3 months
	1.2x10 ⁶	32
	1.2x10 ⁶	33
	7x10 ⁵	35
H016	2x10 ⁶	No tumour after 3 months
	1.5x10 ⁶	38
	1.5x10 ⁶	31
	1x10 ⁶	34

Table 9: **Outcomes of orthotopic prostate injections.** LIN-/CD31- cells from PDXs were generated as described in section 2.3.2.1. The cells were mixed with Matrigel together with irradiated STO cells and injected into the ventral prostate. Mice were observed up to 3 months for clinical signs of tumours, such as palpation, weight loss or gain (>20% of body weight), unkempt appearance. Mice were euthanised if any of these end points were reached.

3.5 Histological analysis

Subcutaneous xenografts were analysed alongside their orthotopic counterparts by H&E staining of tumour sections (Figure 3.1-3.4). Changes in morphology and cell architecture were particularly looked at. Dr G Rodriguez, histopathologist initially examined the H&E slides and taught us how to identify original PDX cells and mouse macrophages. Tumours from the orthotopic sites had more of the original tumour cells and less invasion from mouse cells, such as macrophages. The numbers of mouse cells were quantified using high power fields and a mean and standard deviation is represented below. The differences in the mean showed no statistical significance between s/c and orthotopic way of engraftment in all the 4 PDXs. Individual numbers are represented at the bottom of each figure.

On dissection, it was noted that the tumours derived from orthotopic sites were highly vascularised and had invaded local structures around the prostate. This was from general observation and could not be formally quantified. Subcutaneous tumours were often discrete structures and could be dissected easily from the abdominal wall, apart from PDX Y042, which was highly invasive.

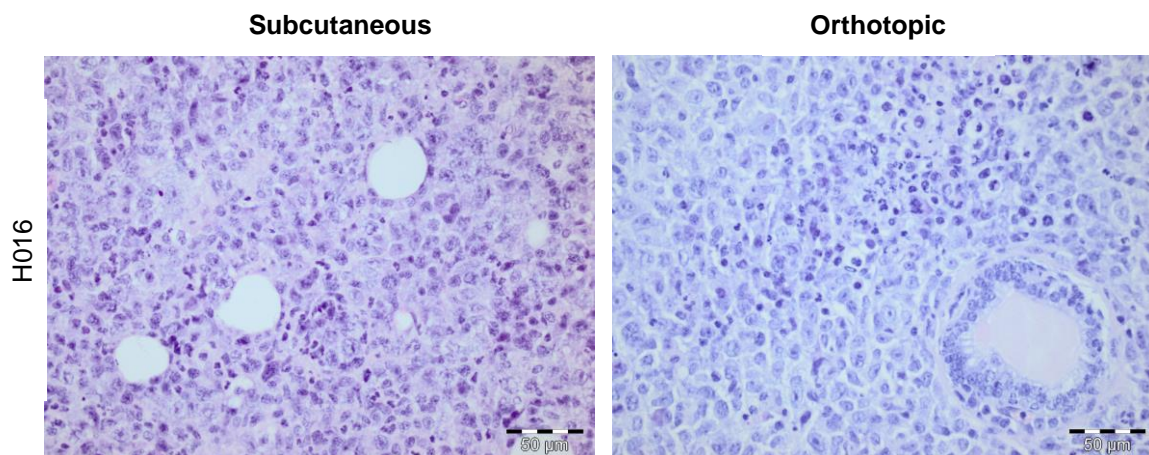


Figure 3.1: **H016**, H&E staining sections of subcutaneous and orthotopic xenografts embedded in paraffin wax. The mean number of mouse cells in the orthotopic sections v/s subcutaneous section was 3.4 (± 0.6) v/s 7.6 (± 0.8) per 100 cells counted. Despite the smaller number of mouse cells invasion in the orthotopic sections, no statistical significance was found using the Student's t test, $p = 0.96$. Cell counts and staining were done in triplicate. Images were taken on an Olympus BX51 light microscope at x40 magnification, with scale bars representing 50 μ m. Of note a mouse prostate epithelial gland was also present in the orthotopic section.

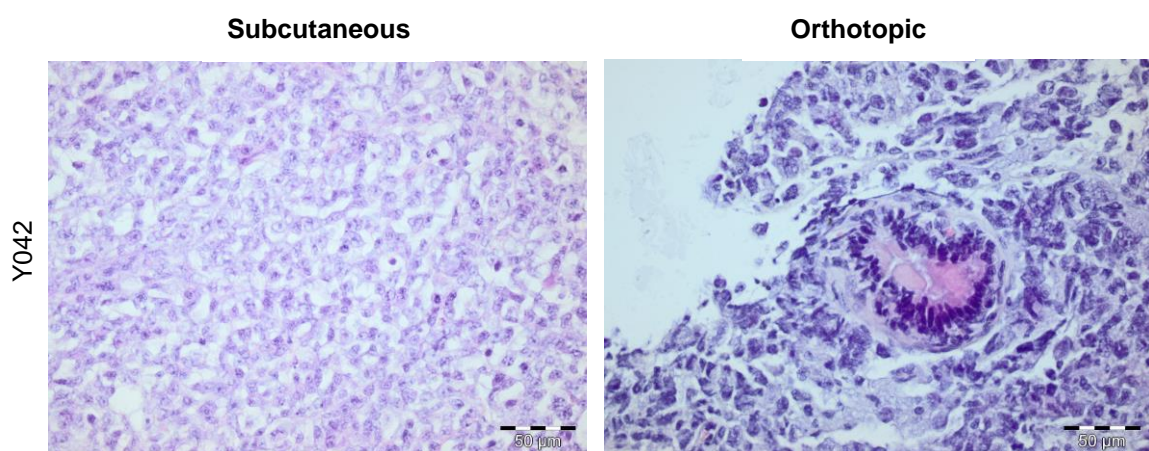


Figure 3.2: **Y042**, H&E staining sections of subcutaneous and orthotopic xenografts embedded in paraffin wax. Y042 was a very invasive xenograft and there were fewer invasions from mouse cells even in the subcutaneous section. There was a mean of 2.4 (± 0.9) mouse cells per 100 cells in each group after cell counts and staining were done in triplicate. A mouse prostate epithelial gland was also present in the orthotopic section. Images were taken on an Olympus BX51 light microscope at x40 magnification, with scale bars representing 50 μ m.

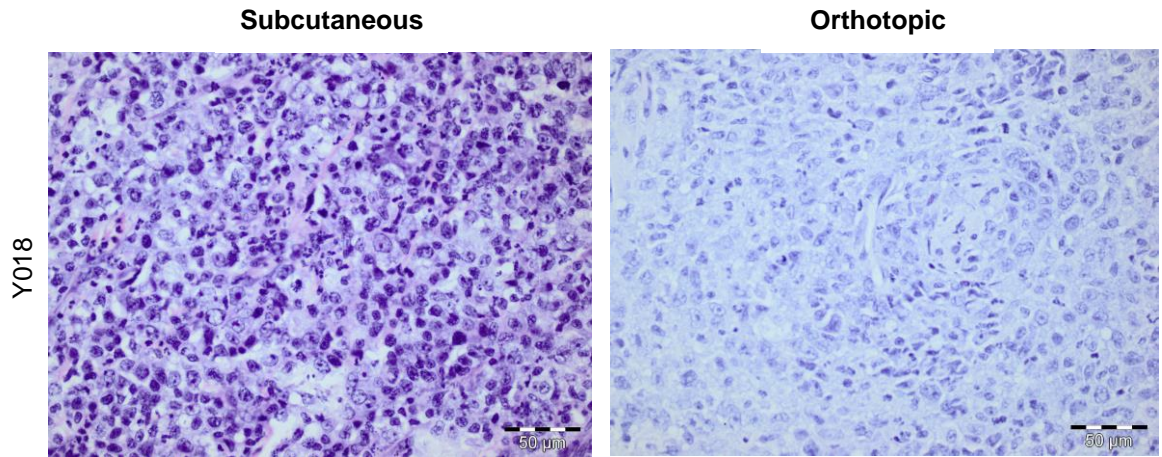


Figure 3.3: **Y018**, H&E staining sections of subcutaneous and orthotopic xenografts embedded in paraffin wax. The mean number of mouse cells in the subcutaneous sections v/s orthotopic section was 15.1 (± 3.8) v/s 8.6 (± 2.1) per 100 cells and no statistical significance was found, $p = 0.89$. Cell counts were done in triplicate. Images were taken on an Olympus BX51 light microscope at x40 magnification, with scale bars representing 50 μ m.

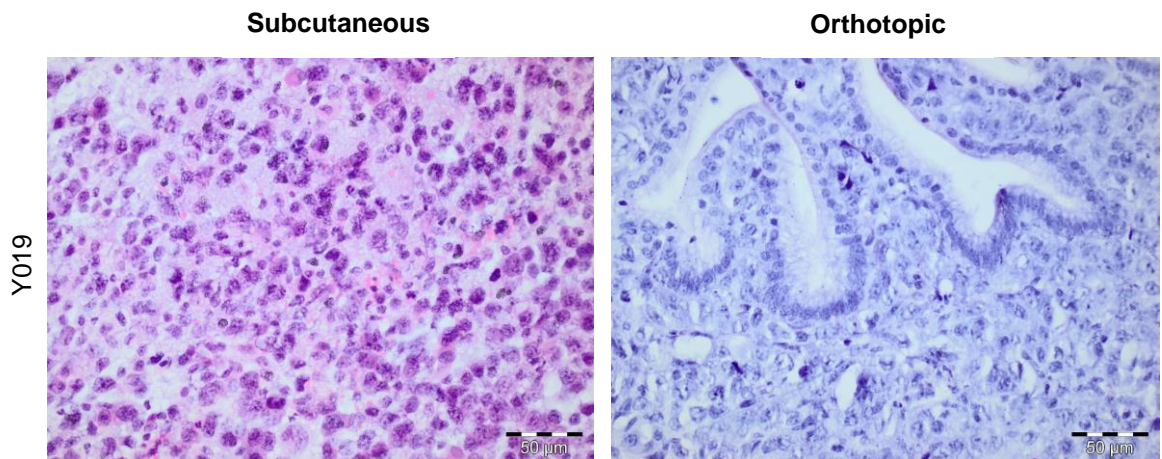


Figure 3.4: **Y019**, H&E staining sections of subcutaneous and orthotopic xenografts embedded in paraffin wax. Despite mean number of mouse cells in the subcutaneous sections v/s orthotopic sections was 10 (± 2.1) v/s 6.4 (± 0.9) per 100 cells, no statistical significance was found, $p = 0.99$. Several mouse prostate epithelial glands were also present in the orthotopic section. Cell counts and staining were done in triplicate. Images were taken on an Olympus BX51 light microscope at x40 magnification, with scale bars representing 50 μ m.

3.6 Comparing cellular phenotypes between subcutaneous and orthotopic tumours

3.6.1 Immunohistochemistry for basal cell marker, p63

Immunohistochemistry was performed to determine human p63 expression in tumours derived orthotopically and subcutaneously (Figure 3.5-3.8). p63 is specifically a basal cell marker. PDX H016 was negative in both s/c and orthotopic tumours. PDXs Y042 and Y019 were positive in both. In the CRPC xenograft Y018, p63 was only present in the orthotopic tumours, which was the only change in phenotype seen between the two methods of engraftment showing the only statistically significant change seen among the 4 PDXs. Where there was positive staining, the mean and statistical significance were represented. All staining were checked against a BPH positive control and isotype IgG negative control (Appendix 6).

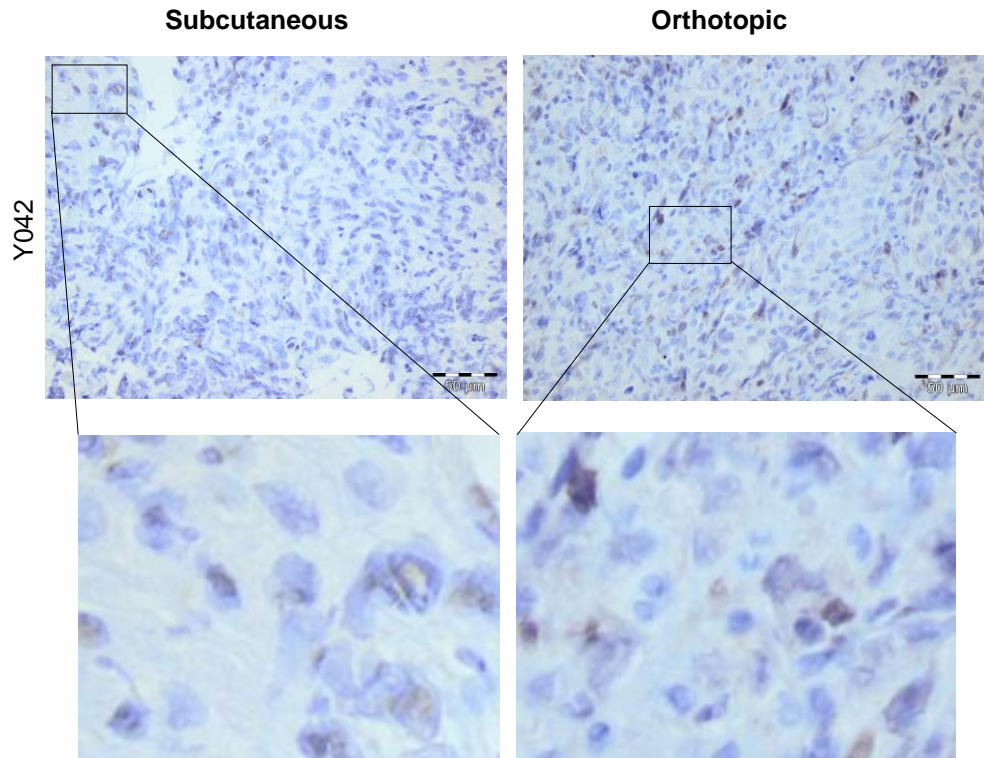


Figure 3.5: **p63 staining in subcutaneous and orthotopic Y042 tumours.** The s/c sections had a mean of 25.5 (± 3.4) p63 cells compared to 15.5 (± 2.5) cells in the orthotopic sections per 100 cells counted. This difference was not statistically significant, $p=0.06$ using the student's t test. Cell counts were done under high power magnification fields and in triplicate. An isotype IgG negative control was used each time alongside the primary antibodies (Appendix 2 and 6). Images were taken x40 and x200 magnification, with scale bars representing 50 μ m. The close up pictures represent positive cells.

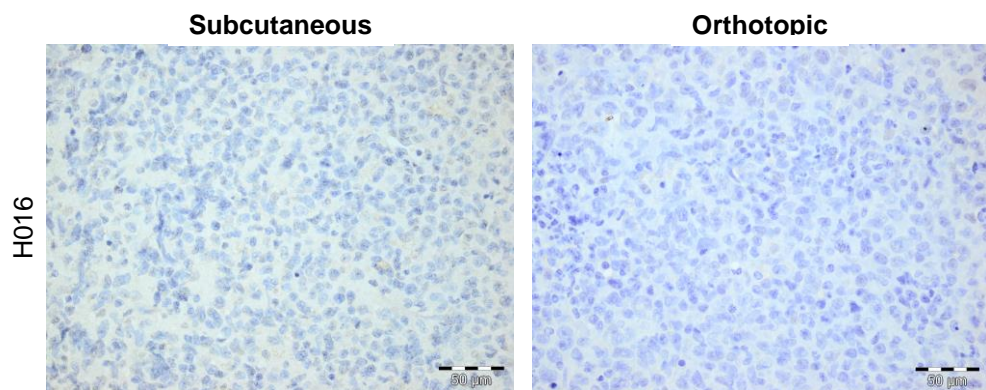


Figure 3.6: **p63 staining in subcutaneous and orthotopic H016 tumours.** p63 was not expressed in H016. Staining was done in triplicate. Images were taken x40 magnification, with scale bars representing 50 μ m.

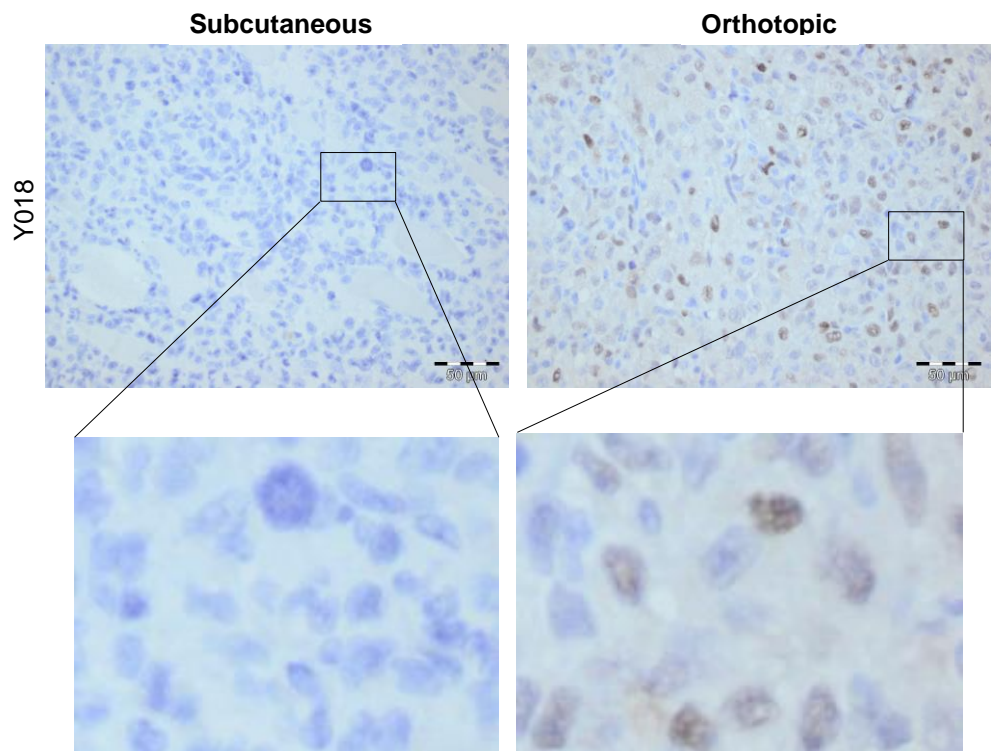


Figure 3.7: **p63 staining in subcutaneous and orthotopic Y018 tumours.** The pictures represent close up of positive cells in the orthotopic tumour and negative in the subcutaneous tumour. This represented a significant change. p63 staining was performed in triplicate. Images were taken x40 and x200 magnification, with scale bars representing 50µm.

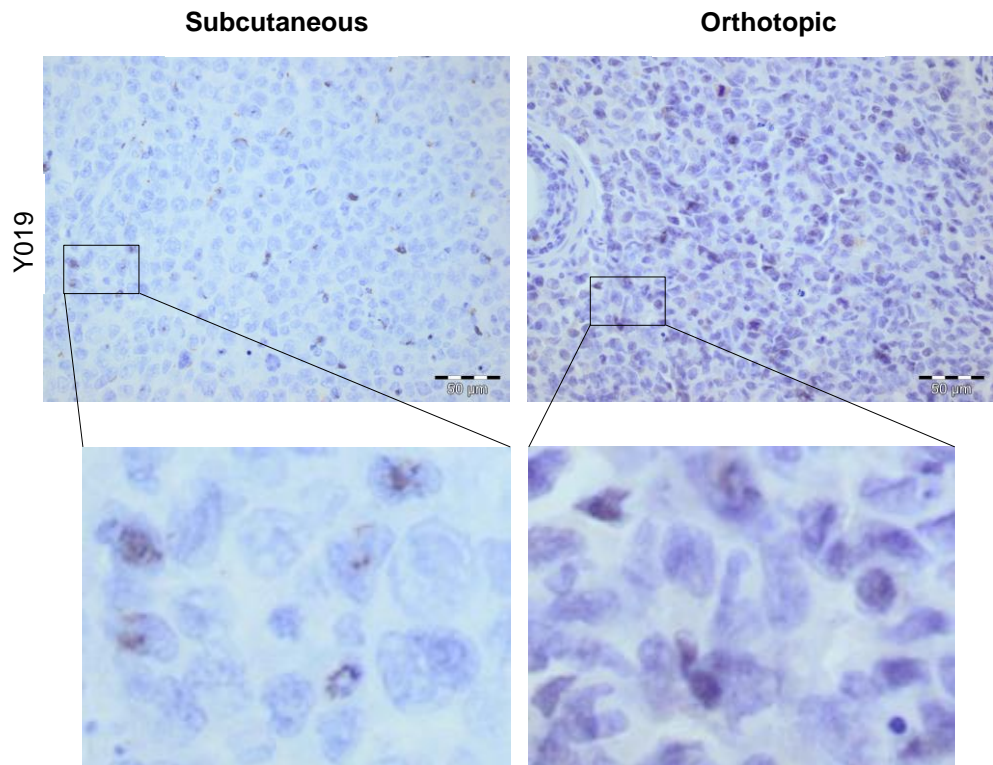


Figure 3.8: **p63 staining in subcutaneous and orthotopic Y019 tumours.** The s/c sections had a mean of 9.5 (± 2.3) p63 cells compared to 11 (± 3.2) cells in the orthotopic sections per 100 cells counted. This difference was not statistically significant, $p=0.74$. The close up pictures represent positive cells. Cell counts and staining were done in triplicate. Images were taken x40 and x200 magnification, with scale bars representing 50µm.

3.6.2 Immunohistochemistry for luminal cell marker, PSA

Prostate specific antigen (PSA) is secreted by luminal cells of the prostate gland. It is often elevated in prostate cancer and BPH. However none of the tumours from the four PDXs used, expressed PSA in the subcutaneous or orthotopic forms (Figure 3.9). Therefore, no difference was seen between the two methods of engraftment. Staining was performed in triplicate and results were checked against a BPH positive control (Appendix 6).

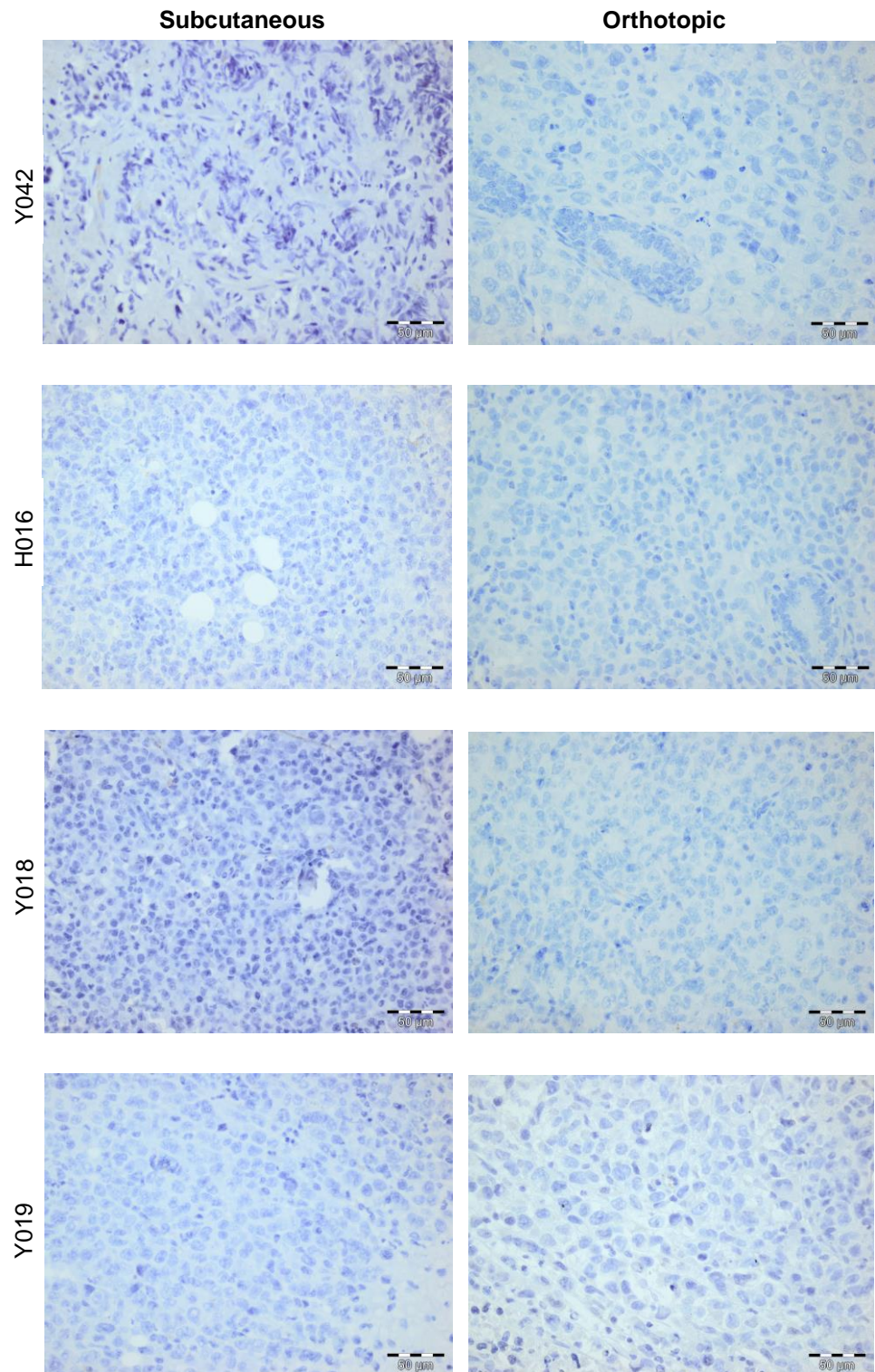


Figure 3.9: **PSA staining in subcutaneous and orthotopic xenografts.** None of the PDXs in either the s/c or orthotopic form expressed PSA. A BPH positive control and an isotype IgG negative control were used each time alongside (Appendix 6). Images were taken at x40 magnification with scale bars representing 50µm.

3.6.3 Immunohistochemistry for the luminal cell marker, androgen receptor

Androgen receptor (AR) signaling is necessary for the maintenance of the structural and functional integrity of the prostate gland. AR action contributes to the development and progression of prostate cancer (Yadav and Heemers, 2012). AR was present in all the orthotopic and subcutaneous xenograft except in Y019 (Figure 3.10-3.13). The proportions of positive cells were greater in the s/c tumours. This difference was only statistically significant in the hormone naïve PDXs (H016 and Y042).

Overall, AR staining was mostly nuclear. Some of the staining in the H016 orthotopic tumour and Y018 subcutaneous tumour were also cytoplasmic (Figure 3.11 and 3.12). Background staining was frequently seen despite repeating the experiments with reduced DAB time. The results were checked against a BPH positive control and isotype IgG negative control (Appendix 6).

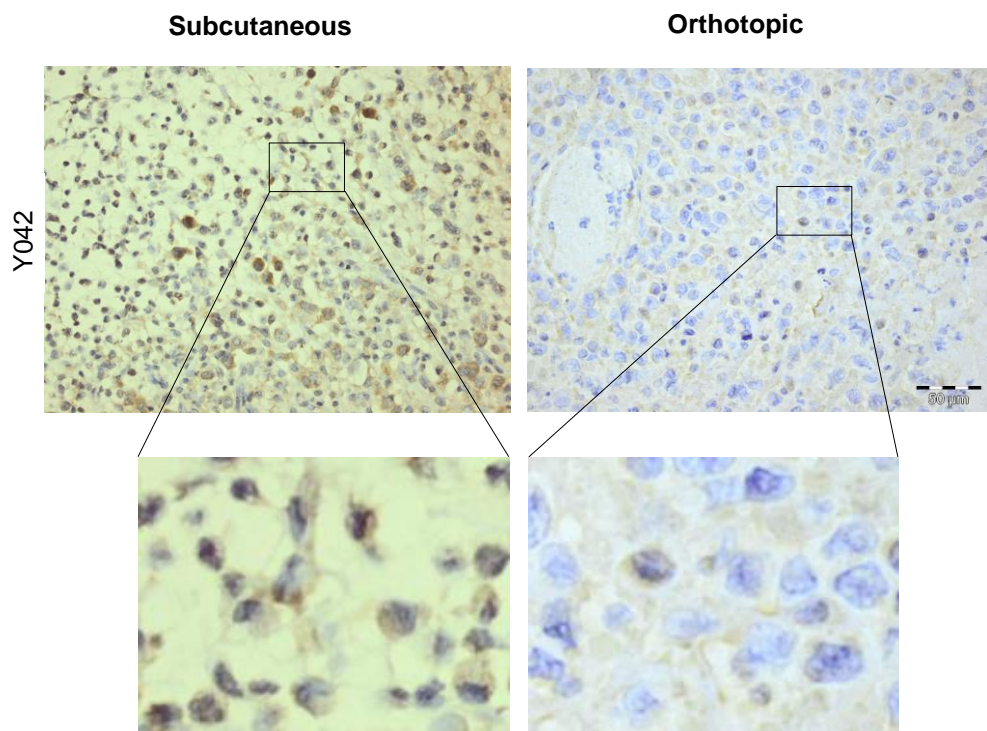


Figure 3.10: **AR staining in subcutaneous and orthotopic Y042 tumours.** The s/c method had more AR cells compared to the orthotopic engraftment with a mean of $27.7 (\pm 3.2)$ v/s $7.1 (\pm 1.5)$ positive cells per 100 cells counted. This difference was statistically significant with $p=0.0006$. The higher magnification slides below show its nuclear distribution. Cell counts were done under high power magnification fields and in triplicate. Images were taken at x40 and x200 magnification with scale bars representing $50\mu\text{m}$.

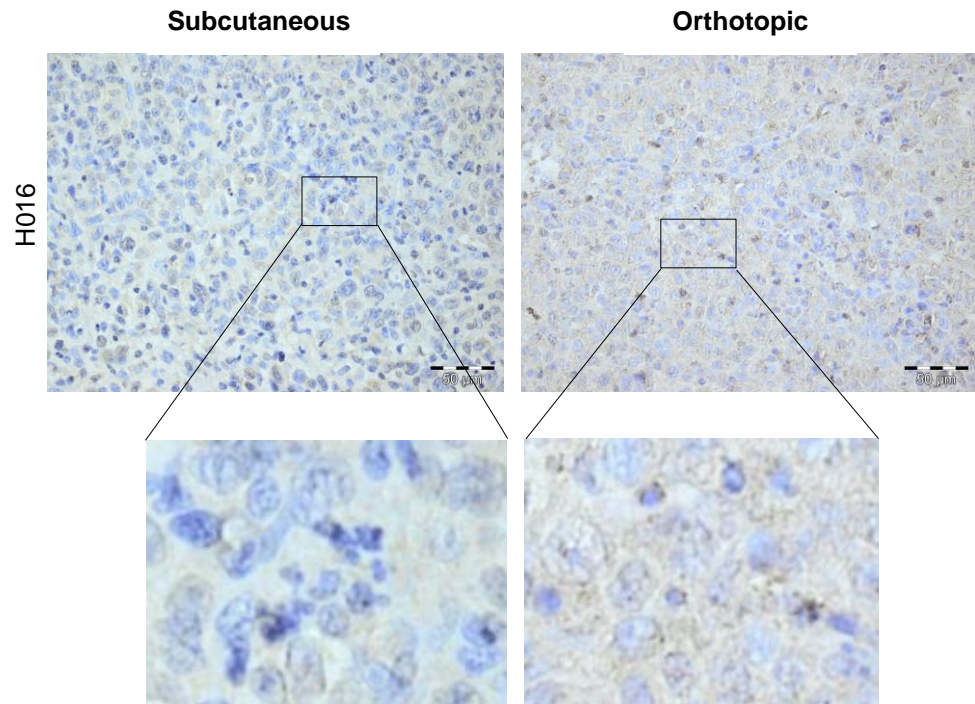


Figure 3.11: **AR staining in subcutaneous and orthotopic H016 tumours.** The s/c method had more AR cells compared to the orthotopic engraftment with a mean of 18.1 (± 1.5) v/s 8.0 (± 1.5) positive cells per 100 cells counted. This difference was statistically significant with $p=0.002$. The s/c images show its nuclear distribution and the orthotopic images show cytoplasmic AR distribution. Cell counts were done under high power magnification fields and in triplicate. Images were taken at x40 and x200 magnification with scale bars representing 50 μ m.

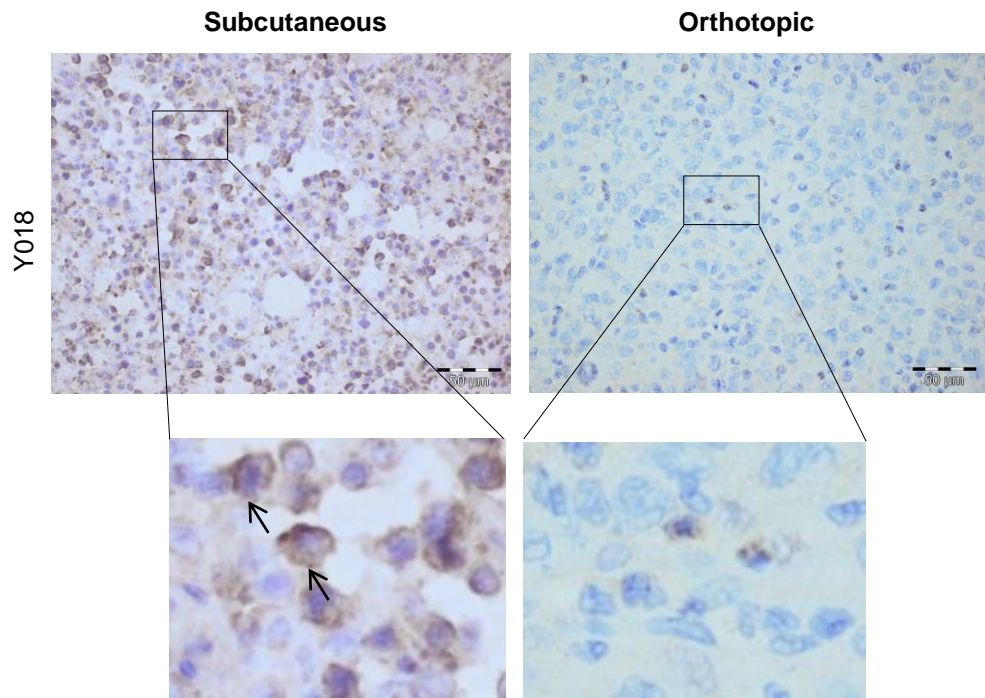


Figure 3.12: **AR staining in subcutaneous and orthotopic Y018 tumours.** The *s/c* method had more AR cells compared to the orthotopic engraftment with a mean of 18.1 (\pm 12.6) v/s 13.7 (\pm 1.5) positive cells per 100 cells counted. This difference was not statistically significant with $p=0.07$. AR was present in both sets of tumours. The subcutaneous images show its cytoplasmic distribution (black arrows) and the orthotopic images show nuclear AR distribution. Cell counts were done under high power magnification fields and in triplicate. Images were taken at x40 and x200 magnification with scale bars representing 50 μ m.

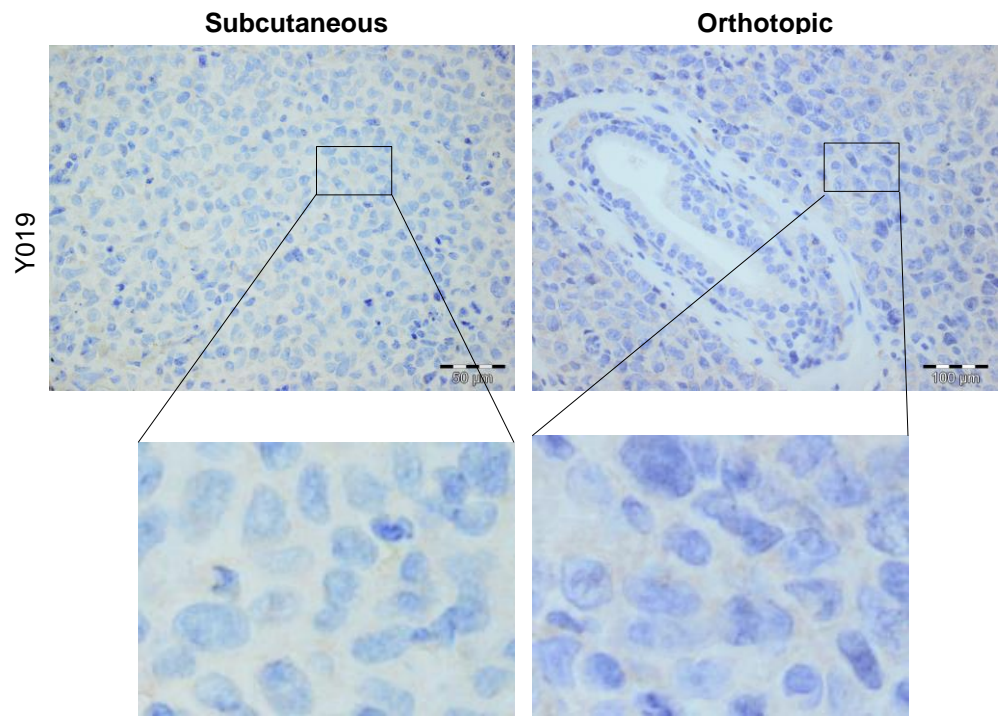


Figure 3.13: **AR staining in subcutaneous and orthotopic Y019 tumours.** AR was not expressed in both the subcutaneous and the orthotopic tumours. AR staining was repeated 3 times. Images were taken at x40 and x200 magnification with scale bars representing 50µm.

3.6.4 Immunohistochemistry for Pancytokeratin

Pancytokeratin (PCK) is strongly expressed in basal and luminal cells of benign prostatic acini and prostate adenocarcinoma. It is a broad-spectrum antibody with cytokeratins 5, 6, 8, 17 and 19 (Chu and Weiss, 2002). None of the 4 PDXs stained for PCK in either the subcutaneous or orthotopic methods. The results were checked against a BPH positive control and isotype IgG negative control (Appendix 6).

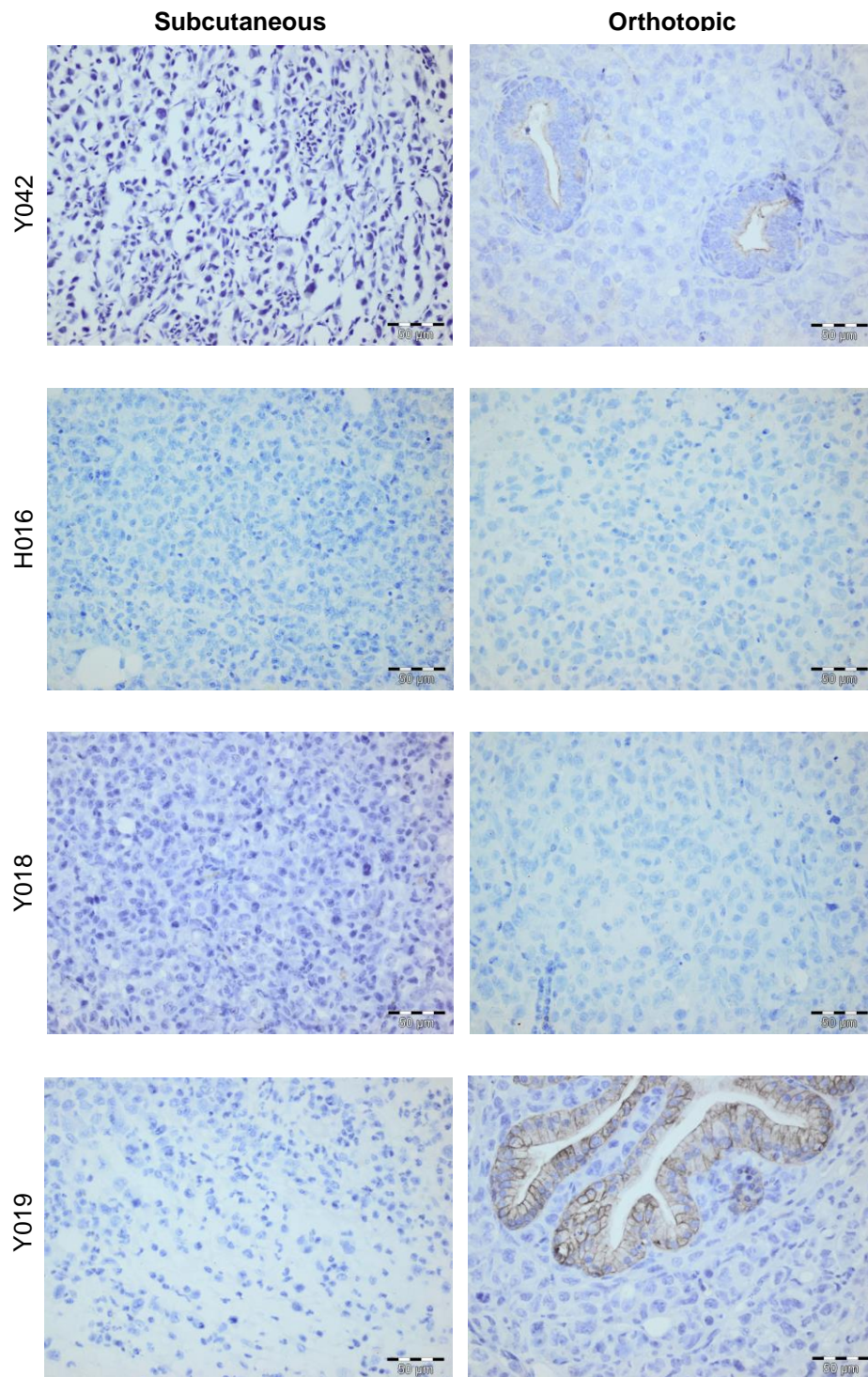


Figure 3.14: **PCK staining in subcutaneous and orthotopic xenografts.** PCK was negative in both methods of engraftment. Staining was observed in mouse prostate epithelial glands suggesting that the antibody is not human specific. Images were taken at x40 magnification with scale bars representing 50µm. Staining of all slides were done in triplicate.

3.6.5 Immunohistochemistry for Vimentin

Vimentin is a marker for cells undergoing epithelial to mesenchymal transition (EMT), which happens during normal development or metastatic spread. It is overexpressed in various epithelial cancers including PC (Shao et al., 2014). Vimentin was present in all the xenografts (Figure 3.15-3.18). The results were checked against a BPH positive control and isotype IgG negative control (Appendix 6).

In HO16 and Y019, the orthotopic method had more vimentin positive cells than the s/c method showing a statistically significant change. But in Y042 and Y018, the s/c method had more vimentin positive cells. Therefore no conclusion could be reached with this antibody.

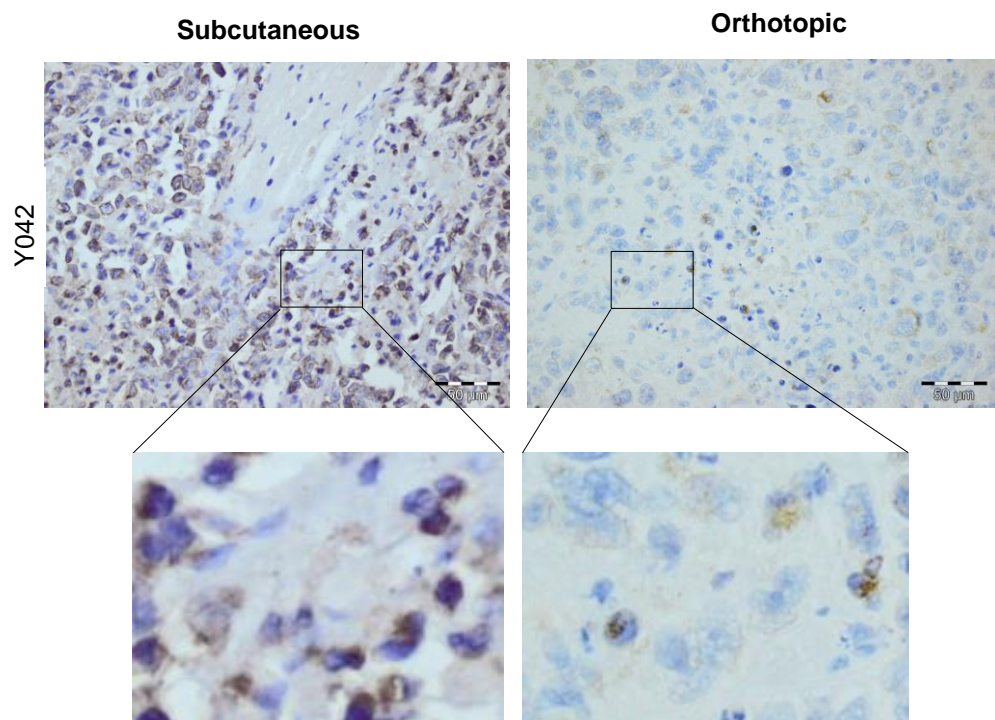


Figure 3.15: **Vimentin staining in subcutaneous and orthotopic Y042 tumours.** Both methods were positive. The s/c method had a mean of 35.3 cells (± 3.2) v/s 22 cells (± 1.7) in the orthotopic method per 100 cells counted. This difference was statistically significant $p=0.002$. The close up pictures represent positive cells. Cell counts and staining were done in triplicate. Images were taken x40 and x200 magnification, with scale bars representing 50 μ m.

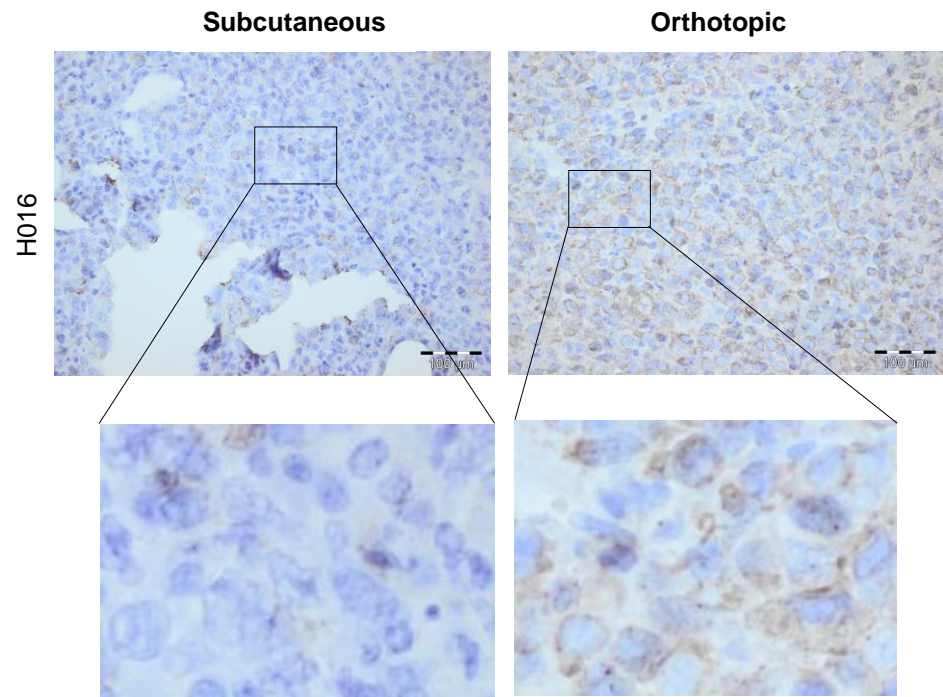


Figure 3.16: **Vimentin staining in subcutaneous and orthotopic H016 tumours.** In this PDX the s/c method had less positive cells with a mean of 36.7 cells (± 3.5) v/s 88 cells (± 2.6) in the orthotopic method per 100 cells counted. This difference was statistically significant $p=0.00004$. Cell counts and staining were done in triplicate. Images were taken x40 and x200 magnification, with scale bars representing 50 μ m.

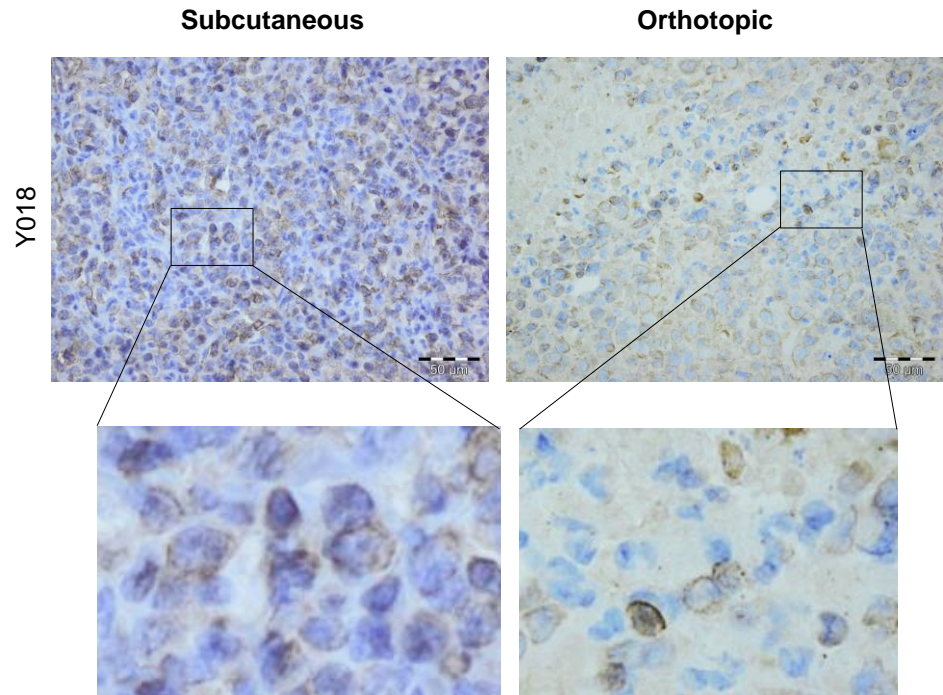


Figure 3.17: **Vimentin staining in subcutaneous and orthotopic Y018 tumours.** The s/c method had a mean of 32 positive cells (± 2.6) v/s 31.3 positive cells (± 1.5) in the orthotopic method per 100 cells counted. This difference was not statistically significant $p=0.72$. Cell counts and staining were done in triplicate. Images were taken x40 and x200 magnification, with scale bars representing 50 μm .

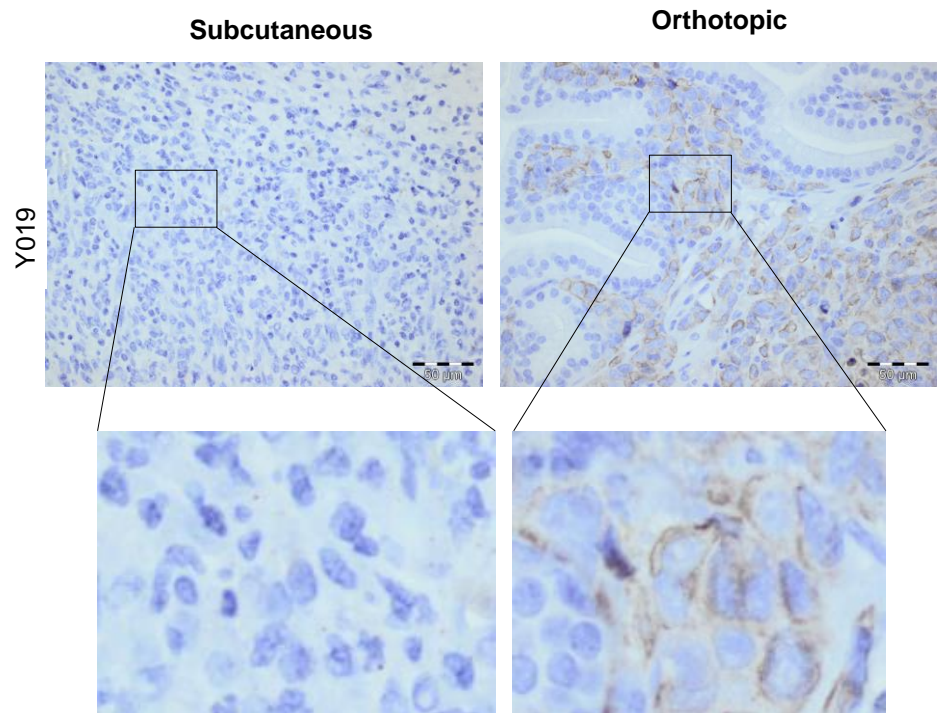


Figure 3.18: **Vimentin staining in subcutaneous and orthotopic Y019 tumours.** The s/c method had a mean of 11.7 (± 2.1) cells positive compared to 61.7 (± 2.3) cells in the orthotopic method (per 100 cells counted). This difference was highly significant at $p = 0.00001$. Cell counts and staining were done in triplicate. Images were taken x40 and x200 magnification, with scale bars representing 50 μm .

3.6.6 Immunohistochemistry for Ki67

Ki67 is a marker of cellular proliferation (Scholzen and Gerdes, 2000). Ki67 is present during all active phases of the cell cycle (G1, S, G2 and mitosis) but absent in the resting cells, G0. Ki67 can be detected in the cell nucleus. Both methods of engraftment showed positivity for Ki67 (Figure 3.19-3.22) across all the PDXs and this was represented as the proliferative index.

The proliferative index represents the number of cells in a tumour that are dividing. It can be used to give a more complete understanding of how fast a tumour is growing. The fraction of cells expressing Ki67 increased in all the orthotopic tumours compared to the subcutaneous tumours. Table 10 gives a summary of the proliferative indices of the 4 PDXs. The difference between the two groups was statistically significant in all 4 PDXs. The results were checked against a BPH positive control and isotype IgG negative control (Appendix 6). Staining and cell counts were performed in triplicate.

PDX	Subcutaneous	Orthotopic	p value
Y042	50% (5)	71% (1.5)	0.002
H016	12% (2)	44% (2.6)	7.5x10 ⁻⁵
Y018	26% (4)	46% (4)	0.002
Y019	30% (2.5)	39% (4)	0.03

Table 10: **Comparison between the method of engraftment and the fraction of Ki67 positive cells.** The standard deviation is represented in brackets. All counting were done in triplicate.

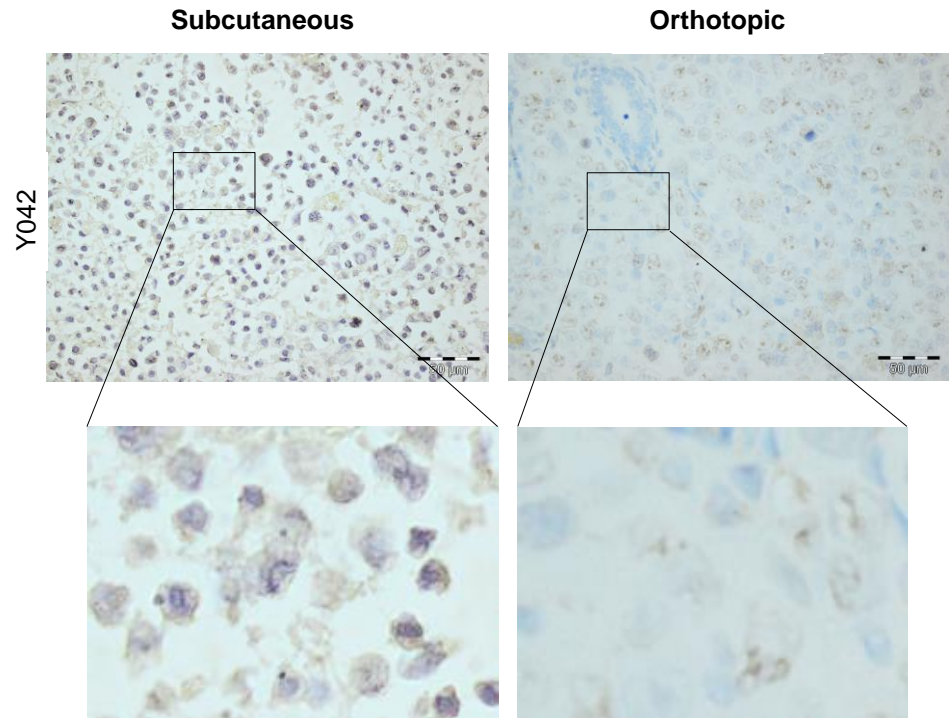


Figure 3.19: **Ki67 staining in subcutaneous and orthotopic Y042 tumours.** See Table 10 for proliferative indices including the statistical significance seen. The close up pictures represent positive cells. Images were taken x40 and x200 magnification, with scale bars representing 50 μ m.

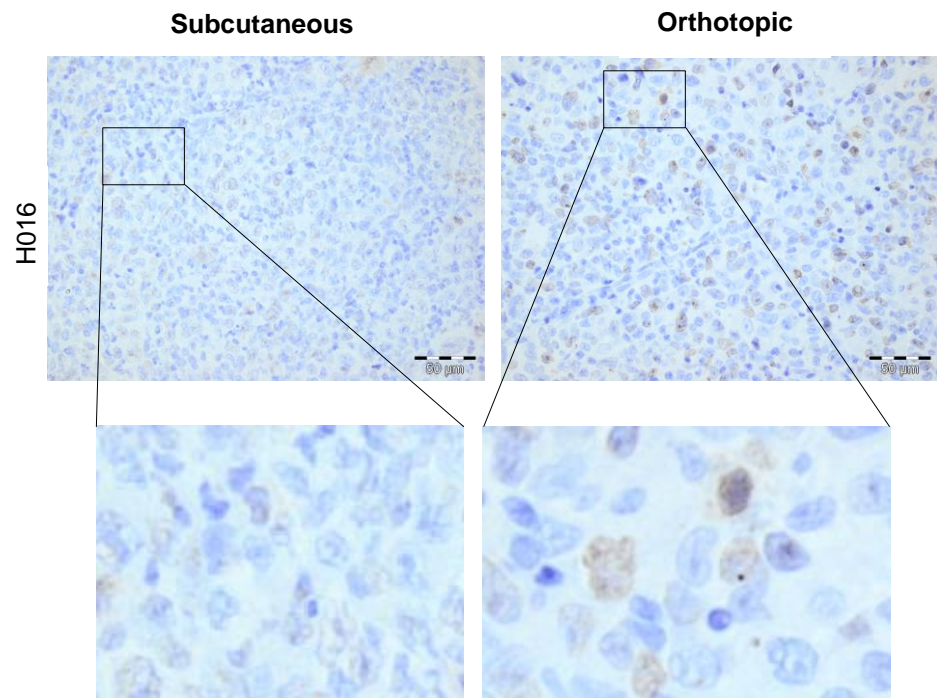


Figure 3.20: **Ki67 staining in subcutaneous and orthotopic H016 tumours.** The close up pictures represent positive cells. See Table 10 for proliferative indices including the statistical significance seen. Images were taken x40 and x200 magnification, with scale bars representing 50µm.

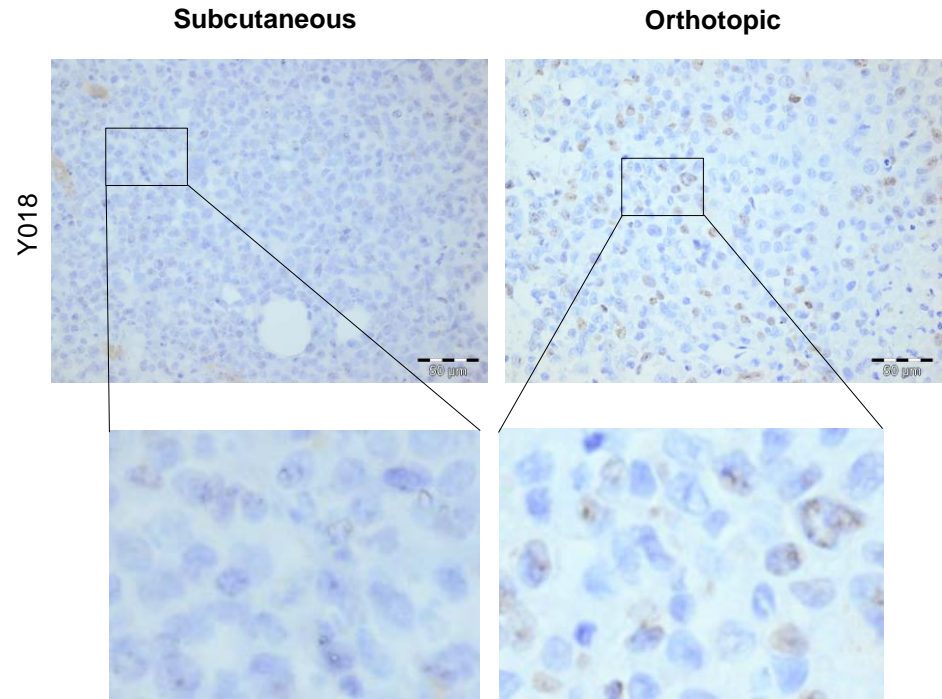


Figure 3.21: **Ki67 staining in subcutaneous and orthotopic Y018 tumours.** The close up pictures represent positive cells. See Table 10 for proliferative indices including the statistical significance seen. Images were taken x40 and x200 magnification, with scale bars representing 50µm.

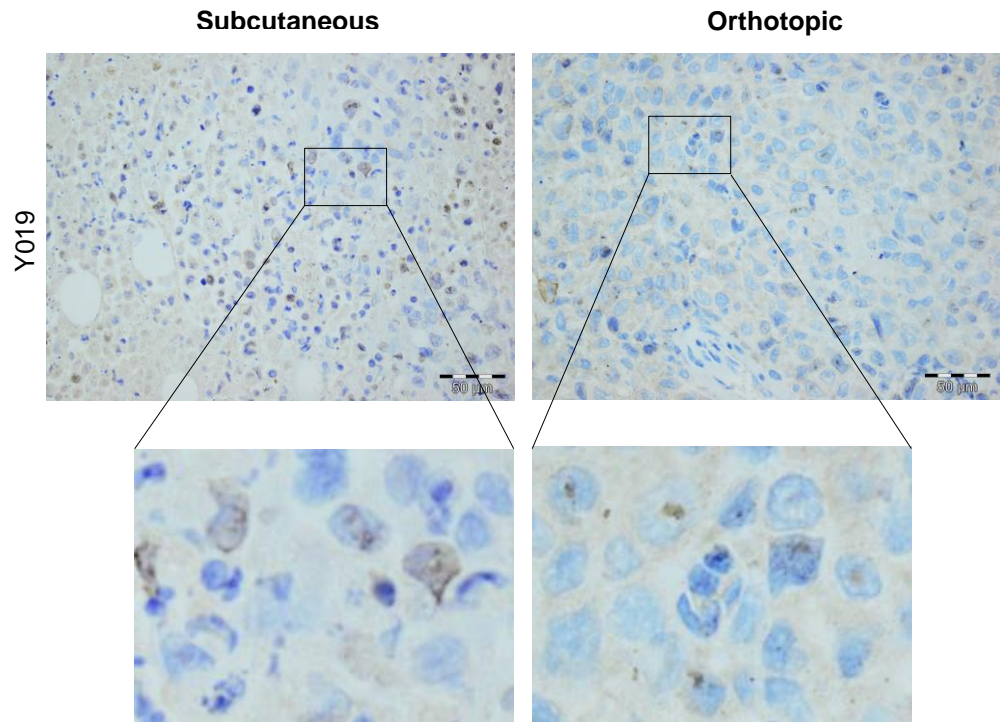


Figure 3.22: **Ki67 staining in subcutaneous and orthotopic Y019 tumours.** The close up pictures represent positive cells. See Table 10 for proliferative indices including the statistical significance seen. Images were taken x40 and x200 magnification, with scale bars representing 50µm.

3.7 Discussion

Translational research into the progression and treatment of prostate cancer depends significantly on robust in-vivo models of the disease. Prostate carcinogenesis and metastatic spread are intricate and rely on changes within the epithelial cells, interaction between the stromal and epithelial tissues and between the tumour microenvironment as a whole (Wang et al., 2005).

In mouse studies, the immune response to the tumour and the hormone status of the host are important. Xenografting studies have traditionally used three major grafting techniques; sub-cutaneous, sub-renal and orthotopic (Lubaroff et al., 1995). The purpose of this study was to look at 'near patient' derived xenografts, which represent the various stages of clinical prostate cancer and to determine whether the grafting techniques affect the differentiation profile of the originally engrafted tissue.

The generation of a substantial number of relevant prostate cancer xenografts and cell lines with stage-specific characteristics has significantly improved the potential application of preclinical models for testing of therapy efficacy (van Weerden et al., 2009). The use of the orthotopic prostatic site for xenografting has not been widespread, due largely to the technical difficulties in reaching and implanting tissue in this location (Corey et al., 2003). In this study, we demonstrate that in skilled hands, grafting the mouse ventral prostate is achievable with high efficiency and reproducibility (only 4 mice out of 16 did not yield tumours). The histology of the harvested tissues was found to be more representative of the original human tumour in the orthotopic samples. Subcutaneous xenografts had more mouse cell infiltration and were less vascularised, giving a poorer histopathological profile. The difference in mouse cell invasion had no statistical significance in all the 4 PDXs used. However, only by developing models that more closely mirror human tissues will we be able to design better clinical trials and further treatments for prostate cancer (Maitland et al., 2010).

The orthotopic tumour take rate was not 100%, which is the case in the subcutaneous technique as well. This can be explained by local influences including injection of a tiny gland in the orthotopic method and easily missing the target due to adjacent tissues. There were differences in pelvic anatomy and difficulties in finding the ventral prostate gland in some mice especially as they develop fat pads around the pelvis. Indeed, grafting pieces of tissue on the mouse prostate has been shown to have a better take rate than dispersed cells (Wang et al., 2005). On the other hand, the subcutaneous site is easily accessible offering a high capacity space to work with. But poor vascularisation of this space can explain low tumour take rates (van Weerden and Romijn, 2000).

3.7.1 Ki67 as a marker of proliferation

Ki67 expression was seen across all the xenografts, showing the cells were in the active phases of the cell cycle using both methods of grafting. Orthotopic, tumours from all 4 PDXs had significantly higher proliferative indices indicating that the prostate microenvironment favoured cell division.

3.7.2 Basal and luminal cell markers

Looking at the epithelial cell markers, all the xenografts engrafted did not express PSA and PCK irrespective of the method of engraftment. On a cell-by-cell basis PSA levels fall in cancers. But the overall levels are normally higher because there are more luminal cells and fewer basal cells in cancers and the tumour is more vascularised, allowing more PSA into the bloodstream (van Weerden and Romijn, 2000). Therefore, when looking at individual cells they could appear to be negative.

p63 expression increased in the PDXs Y019, Y018 and Y042 with the orthotopic method. This could be explained by the highly aggressive nature of CRPC samples (Y018 and Y019) and the mouse prostate microenvironment could have favoured activation of cancer stem cells present in those two xenografts.

Looking at AR in more detail, all the orthotopic and subcutaneous tumours expressed this steroid receptor molecule except in Y019. Further work in this lab has confirmed AR expression by RT-PCR to be high in these PDXs (personal communication). Androgen stimulation is a key component of prostate biology. Without androgens the prostate does not develop (Wang et al., 2005). In a microenvironment high in androgens (only male mice used), luminal cells from the xenografts might have been activated or amplified. This could explain why both nuclear and cytoplasmic staining was seen in H016 (Figure 3.11) and Y018 (Figure 3.12). Variations in androgen levels could also have favoured specific AR mutants with increased cytoplasmic/perinuclear staining compared to the wild type receptor (Simental et al., 1991). The AR expression in the two hormone naïve PDXs was more statistically significant in the s/c form than the orthotopic. Hence the s/c method proved equally efficient in eliciting AR. PDX Y019 was from a CRPC sample and AR could have been silenced or undergone mutation explaining its absence.

In summary, the constitution and expression patterns of basal and luminal cells in human epithelial cancers are complex. No convincing presence of a specific cellular phenotype was confirmed in either the subcutaneous or the orthotopic method.

The PDXs had neither a basal nor a luminal origin, suggesting an intermediate phenotype. This point was further evident by the fact that vimentin was expressed in all the xenografts, signifying they were undergoing epithelial to mesenchymal transition. Recent evidence suggests that mammary cancer cells undergoing EMT gain stem cell-like properties, thus giving rise to cancer stem cells. Mani et al showed that a subpopulation of CD44^{high}/CD24^{low} immortalised human mammary epithelial cells as well as cancer cells that possess stem-like properties increased with the concomitant induction of EMT (Mani et al., 2008).

In order to perform pharmacodynamics and drug treatment studies it is extremely important to have in vivo models which can be monitored and compared to molecular characteristics of the source tissue (Wang et al., 2005). Hence models, which retain epithelial interactions, are more accurate. In the present study, we have provided a side-by-side comparison of the results from both

subcutaneous and orthotopic methods of engraftment. No definite difference in phenotype has been demonstrated between them.

The use of orthotopic graft sites has been suggested to represent the best approach. However, this method has not been widespread due to technical difficulties. In this study the s/c method has been shown to have good expression of the candidate prostate epithelial markers to be able to assess treatment effects presented in the next chapter. We also took account of the fact that the grafting sites by different research groups are mainly based on their experience and also the estimated sample sizes. Setting up large groups with orthotopic PDXs would have been time consuming and less economically feasible. Grafting underneath the renal capsule follows the same level of complexity. Therefore, the subcutaneous model was deemed to offer a reliable graft site to be used in our further experiments of docetaxel treatment in PDXs.

CHAPTER 4

RESULTS II

4. In-vivo targeting of the 'near patient' xenograft model with docetaxel

4.1 Rationale

Metastatic PC have been treated for a long time with various hormonal therapies and in 2004, docetaxel was found to prolong overall survival (OS) in CRPC. This revolutionised PC chemotherapy for the next decade. However, for many patients this treatment does not work and we still do not know why. Often it is a hit and miss treatment and there is still no reliable biomarker for docetaxel sensitivity. In this chapter I have used the PDX model as a tumour avatar to investigate possible markers of docetaxel response.

The next logical step was to ask whether using docetaxel earlier when starting hormonal therapy would slow the disease down and increase overall survival even further. In fact recently three such trials have published their results. The CHARTED study showed an increase in OS from 44 to 57.6 months (Sweeney CJ, 2014). This benefit was more important in patients with a higher volume of disease who were hormone naïve. With the results of the GETUG-AFU 15 and STAMPEDE trials, we now have a lot of data to define the benefits from early chemotherapy. Hence in this chapter, I have investigated reasons as to why there might be differences in the docetaxel responses between hormone naïve PDXs and CRPC PDXs. I looked into factors determining chemo sensitivity and whether the long exposure to androgen deprivation therapy makes the CRPC PDX model more sensitive to docetaxel.

4.2 Developing a protocol to determine the optimum dose of docetaxel in murine xenografts

Optimisation studies were first carried out to determine the tolerable dose of docetaxel. In previous studies athymic nude mice were used (Fizazi et al., 2004), and not the Rag2^{-/-}γC^{-/-} strain. In this paper, the authors injected PC3 cells subcutaneously and waited 4 weeks for tumours to appear and reach a measureable size. They then used a weekly injection of docetaxel for 3 weeks and found good tolerance with 15mg/kg. In our lab, previous in vivo treatment on the Rag2^{-/-}γC^{-/-} mice with 5mg/kg and 10mg/kg of weekly docetaxel intraperitoneally had shown good sensitivity and tumour size reduction in PC3 tumours (personal communication). Hence, in the PDX models a similar regimen was used to begin with. PDX cells were injected subcutaneously into both flanks of Rag2^{-/-}γC^{-/-} mice and 4-5 weeks (latency period see table 6) was given for tumours to establish (Figure 4.1). Treatment was initiated once tumours reached ~5mm. After randomization, weekly docetaxel intraperitoneal injections at a dose of 5mg/kg and 10mg/kg were administered. Figure 4.2 illustrates the treatment schedule, devised from gathering information from previous studies and our own experience in the lab (personal communication).

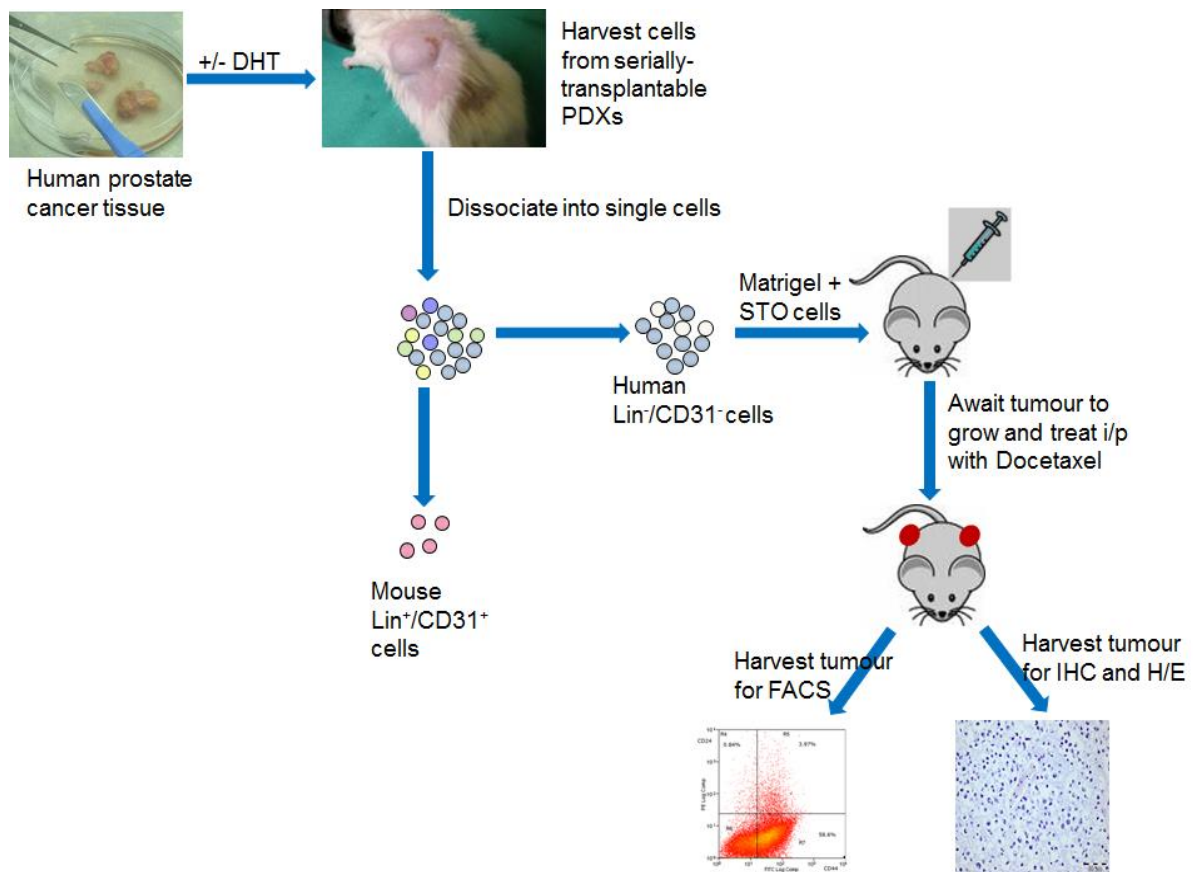


Figure 4.1: **Overview of the in vivo protocol to determine the effect of docetaxel on tumour growth.** PDXs were dissociated and depleted from mouse cells before implanting into Rag2^{-/-}γC^{-/-} mice (both flanks) (see section 2.3.2.1 and 2.3.2.2). Treatment with docetaxel started once tumours reached ~5mm in diameter. Resultant tumours were analysed. DHT- dihydrotestosterone tablet, FACS- fluorescent assisted cell sorting, IHC- immunohistochemistry and H/E- haematoxylin and eosin staining.

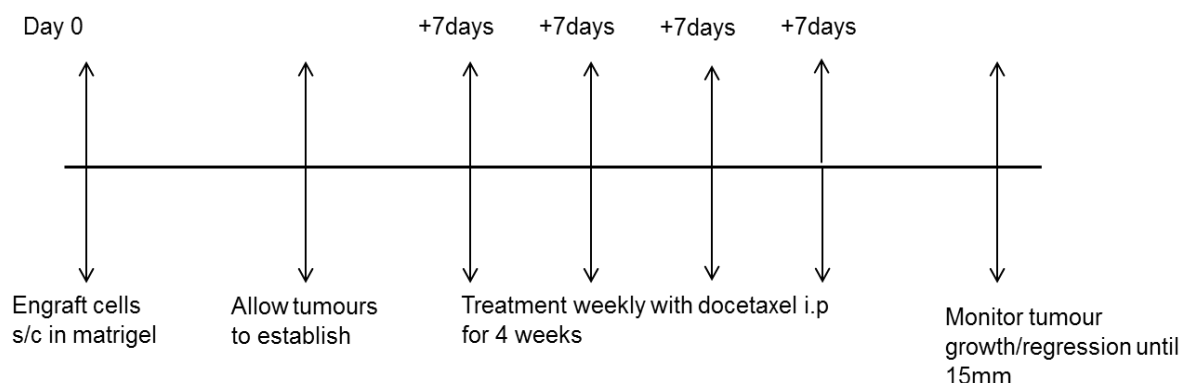


Figure 4.2: **Time line** of the experiment and schedule for docetaxel injection. This was developed after studies with PC3 cells using nude mice (Fizazi et al, 2004) and previous Rag2^{-/-}γC^{-/-} mice experiments in this lab where latency for PDX tumour induction and docetaxel dosage was recorded.

4.3 Treatment of PDX Y019 with docetaxel

The first experiment was performed on the Y019 xenograft (originally from a CRPC patient). This involved three groups of 10 mice each:

- Control group
- 5mg/kg group
- 10mg/kg group

1.6×10^4 Y019 (LIN-/CD31-) cells were injected into both flanks of 30 mice. Once tumours reached approximately 5mm the mice were randomly assigned to treatment or control arms. All mice had tumours at the beginning of treatment. 4 mice had tumours only on one flank and the remainder had bilateral tumours. The mean tumour volume at initiation of treatment was 82mm^3 . Figure 4.3 shows the mean weights of each group over time. No mice (even in the higher dose docetaxel treatment group (10mg/kg) showed any decrease in weight or ill health during the dosing period. One mouse from the control group had an adverse reaction to general anaesthesia and died. As a result, the control group had 9 mice at the beginning of the treatment schedule.

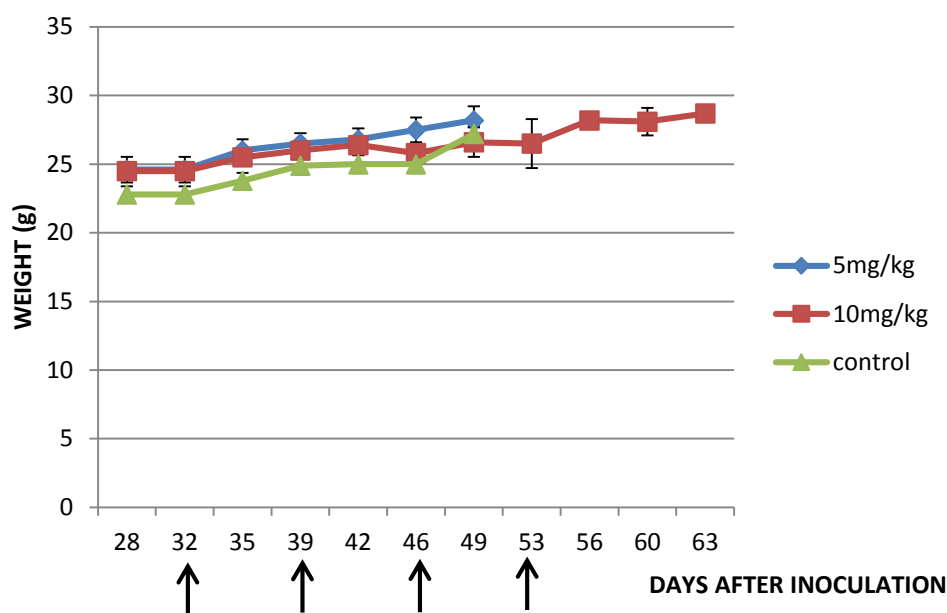


Figure 4.3: **Effect of docetaxel on mouse weight.** Mice were weighed twice weekly following treatment with docetaxel (5mg/kg and 10mg/kg) or vehicle control. The mean (weight) \pm the standard deviation is shown. $n= 20$ and 18 (treatment groups), $n= 18$ in the control group. The arrows below the x-axis indicate the dosing period.

Figure 4.4 shows the mean tumour volumes from each group over time. Docetaxel treatment at 5mg/kg was not effective as tumours grew at the same rate as those from the control arm. In contrast, tumour growth was affected by 10mg/kg of docetaxel. Indeed, after the third dose of 10mg/kg docetaxel, tumours regressed. At day 53 only 4 mice remained, but 3 had to be killed due to adverse side effects of the docetaxel. The last mouse to be sacrificed (due to growth of the tumour) was 10 days after the completion of the fourth docetaxel injection. Figure 4.5 illustrates the survival curve. The average survival for mice in the control group was 46 days, 47 days for the 5mg/kg group and 50 days for the 10mg/kg group. Although there was a small survival advantage with 10mg/kg docetaxel, this was not statistically significant (Log-rank test yielded a $p>0.05$, $p=0.338$).

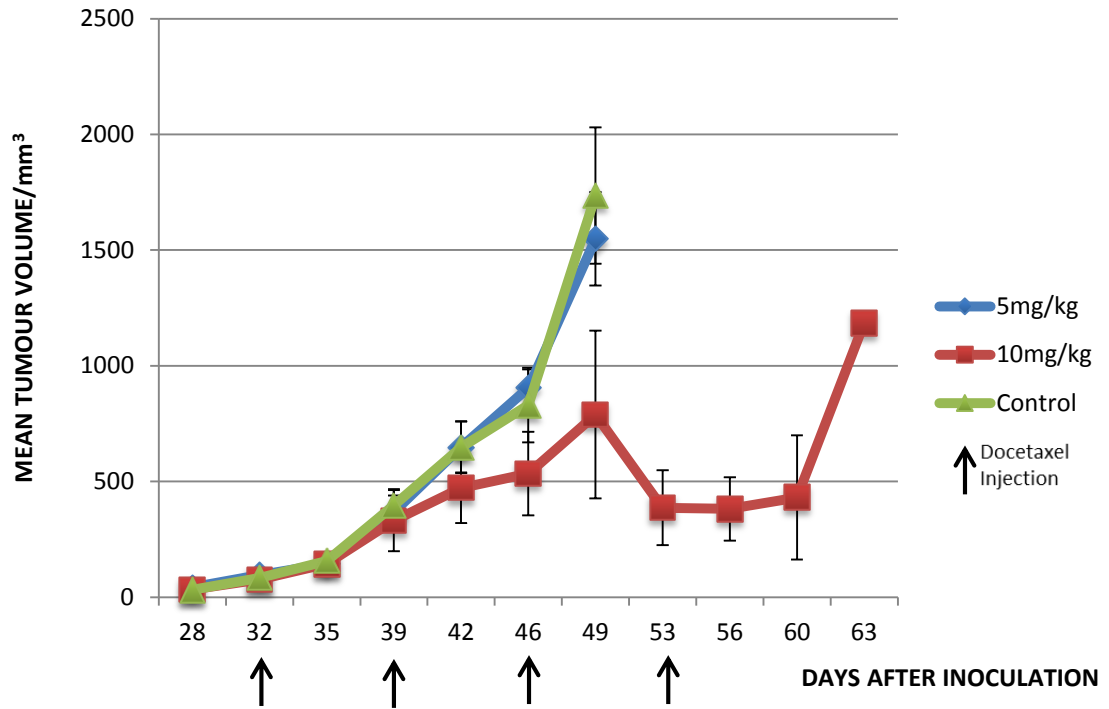


Figure 4.4: **Effect of docetaxel on PDX Y019 tumour growth.** Mean (\pm SD) tumour volumes in mice administered with 5mg/kg docetaxel (n=20), 10mg/kg docetaxel (n=18), control (n=18) were recorded at the times indicated for docetaxel treatment. The black arrows below indicate the dosing period. Of note only one mouse survived until day 63, explaining the absence of error bars.

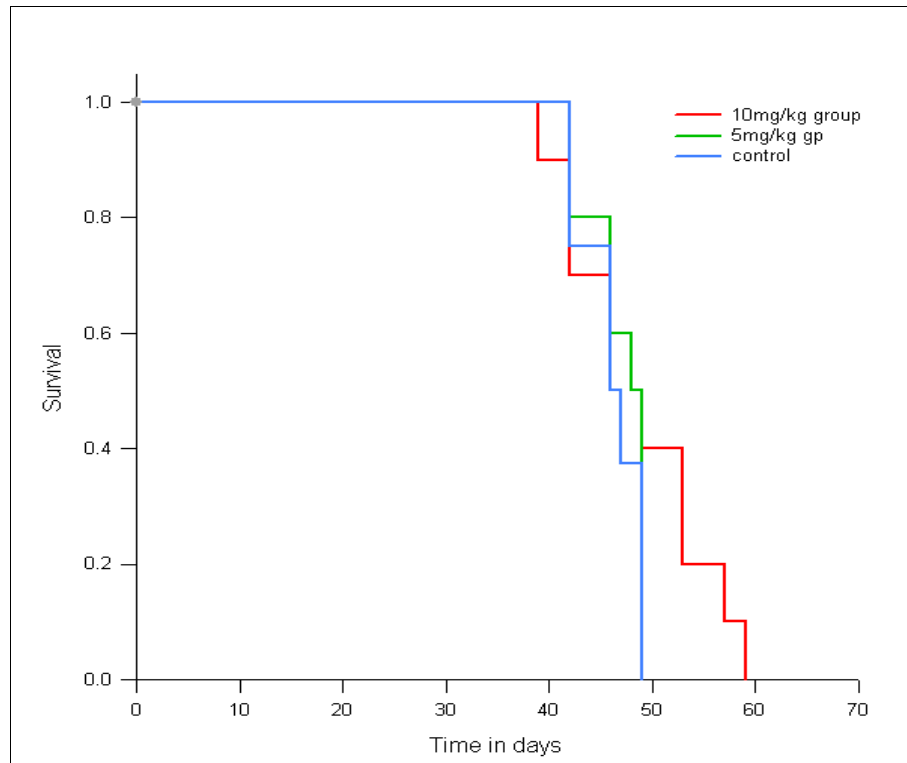


Figure 4.5: **Kaplan-Meier curve** of overall survival following treatment with docetaxel. The 10mg/kg group survived marginally longer, than those mice treated with the lower dose. The log-rank test was used giving a p value > 0.05 (p=0.338) showing that there is not a statistically significant difference amongst the 3 groups.

As survival was not significantly increased, despite the slower growth rate at 10mg/kg, a second experiment was set up with higher dosages (15mg/kg and 20 mg/kg). This optimization was necessary to find the right balance between maximum tumour response and minimum side effects, as no previous studies used these PDXs against docetaxel. Particular attention was paid to the 3Rs (Replacement, Refinement and Reduction) of animal welfare.

4.4 Effect of 15 and 20mg/kg docetaxel on the growth rate of PDX Y019 xenograft

7×10^4 Y019 (LIN-/CD31-) cells were injected into both flanks of Rag2^{-/-}γC^{-/-} mice. Once tumours reached ~5mm the mice were assigned to 3 arms, with 10 mice in each arm. Power analysis was not undertaken at this time, as this experiment was considered preliminary. Tumours were established in all 30 mice. They had established bilateral tumours except one mouse from the 15mg/kg group, which had only a unilateral tumour. This gave an effective sample size of n=19 for the 15mg/kg group, n=20 for the 20mg/kg and control group.

Reduction in the rate of tumour growth was noticed in the two docetaxel treatment groups. The mean tumour volume at initiation of treatment was 59mm³ in all the groups. Mice from the 15mg/kg and 20mg/kg groups showed weight loss of more than 10% over a week and other side effects after the third dose of docetaxel was administered. In the early stages of the experiment, the mice did not appear to be in distress. Compared with the first Y019 experiment where weight was not affected, increasing the docetaxel dose had a detrimental effect on the weight of the mice (Figure 4.6)

2 mice from the control group had to be euthanized early due to the tumour mass becoming haemorrhagic and forming a wound in the centre. 4 mice from the 15mg/kg group lost weight and had diarrhoea. 2 were also found dead from the same group. This was despite close monitoring and oral supplementation with rehydration gels. From the 20mg/kg group, 2 mice had to be terminated earlier than expected due to weight loss and ill health. The fourth dose of docetaxel was omitted during that period in an attempt to encourage recovery and weight gain. One was found dead after the third dose of docetaxel was injected. The remaining mice were culled when their tumours reached 15mm in diameter. The last mouse to complete the experiment was 14 days after the completion of the fourth injection and was from the control group.

Figure 4.7 shows the mean tumour volumes of each treatment group over time. 20mg/kg had the maximum effect in reducing tumour growth. Figure 4.8 illustrates the survival curve with the average survival for mice in the control group of 64 days, 58 days for the 15mg/kg group and 61 days for the 20mg/kg group. There was a slower tumour growth rate in both the docetaxel groups however, this was not statistically significant compared to control when analysed on a Kaplan-

Meier curve, figure 4.8 (the Log-rank test yielded a p value of, $p=0.1$). Although there was no survival advantage, there was a clear effect on growth rate and to test drug efficacy we calculated T/C % where T is the mean tumour weight in the treated group and C the mean tumour weight in the control group. Treatment is considered sensitive when T/C is $<50\%$. At day 55, T/C was 32% (20mg/kg) which was the optimal dose compared to 15mg/kg which gave a T/C value of 60%.

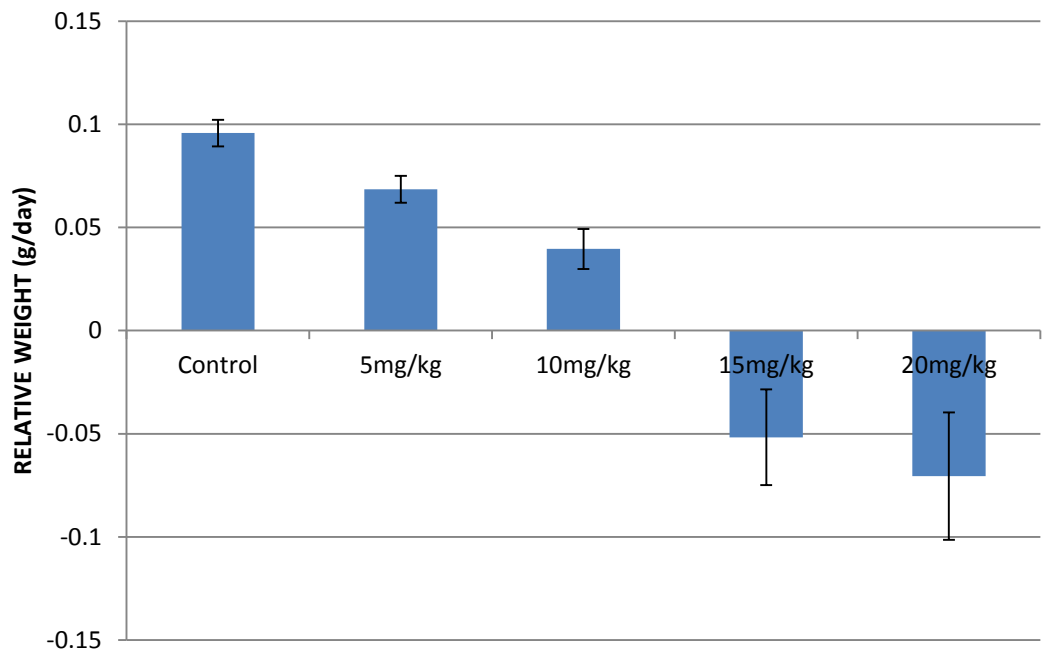


Figure 4.6: **Increasing the docetaxel dose has a detrimental effect on the weight of mice** (combined data from both Y019 experiments). Mouse weights over the entire follow up period according to different treatments administered: control, 5mg/kg, 10mg/kg, 15mg/kg and 20mg/kg Docetaxel groups. Relative growth rates of 10 mice per each treatment group and 9 mice in the control group are represented along the standard deviation (SD).

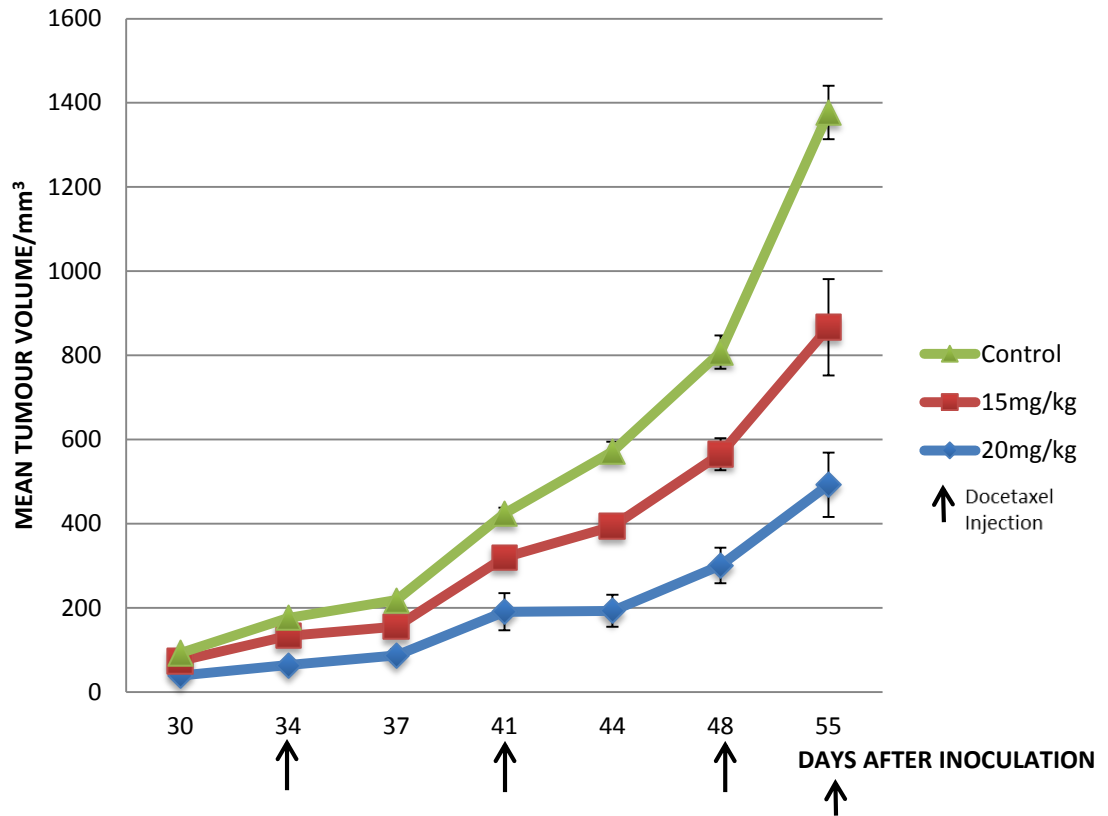


Figure 4.7: **Effect of increasing docetaxel on Y019 tumour growth.** Mice were treated with 15mg/kg docetaxel (n=19), 20mg/kg docetaxel (n=20), or vehicle control (n=20) once tumours reached ~5mm, at the times indicated (black arrows). The results are expressed as mean (\pm SD) tumour volumes at times relative to tumour volume at day 34, first docetaxel injection.

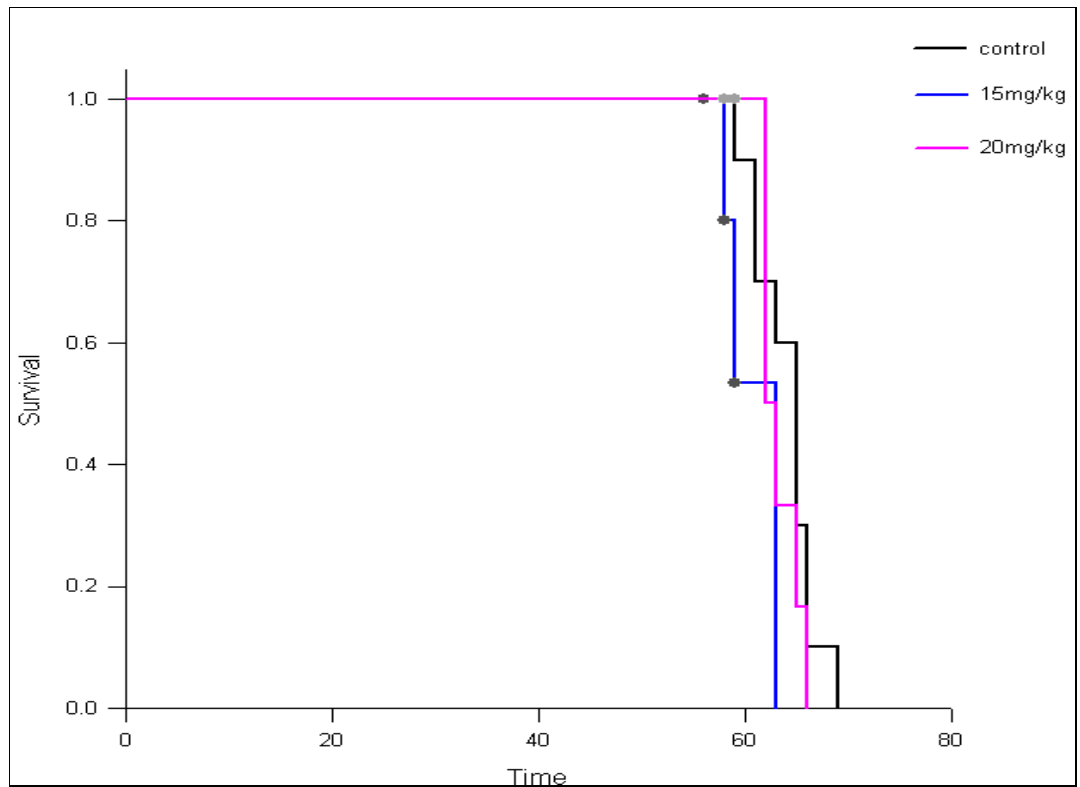


Figure 4.8: **Kaplan-Meier curve** of overall survival in the 3 groups, following initiation of docetaxel therapy. There was no survival benefit with docetaxel; the dots on the curves represent censored mice, which had to be culled because of side effects from treatment. Comparing groups together, a log-rank test was used giving a p value > 0.05 (p=0.1) showing that there is not a statistically significant difference amongst the 3 groups.

Although 20mg/kg had the maximum effect on tumour growth, severe side effects compromised the results. As those mice were censored, the survival advantage was not apparent. Experiments with 10mg/kg had an effect but the suppression was not long lasting. Therefore, we decided to use 10mg/kg and 20mg/kg as optimum doses to yield maximum data in future in vivo docetaxel experiments

4.4.1 Histological analysis of Y019 xenografts following docetaxel treatment

Sections of tumour tissue from PDX Y019 were analysed by Haematoxylin and Eosin (H&E) staining to determine histological changes following docetaxel treatment. The results are shown in Figure 4.9. As treatment dose increased there was a striking change in the overall cellular content and morphology with fewer actively dividing cells (mitotic nuclei) and blood vessels within the tumour section. There was an average of 33 (± 2.65) actively dividing cells seen in the control group compared to 5 (± 1) cells in the 20mg/kg group. This difference was statistically significant with a $p=0.004$.

Moreover, while dissecting the tumour mass from the mice, the edges of the 20mg/kg tumours were well demarcated and less vascularized compared to the control tumours. The latter were very adherent to the skin and abdominal muscles. This was a general observation and could not be quantified.

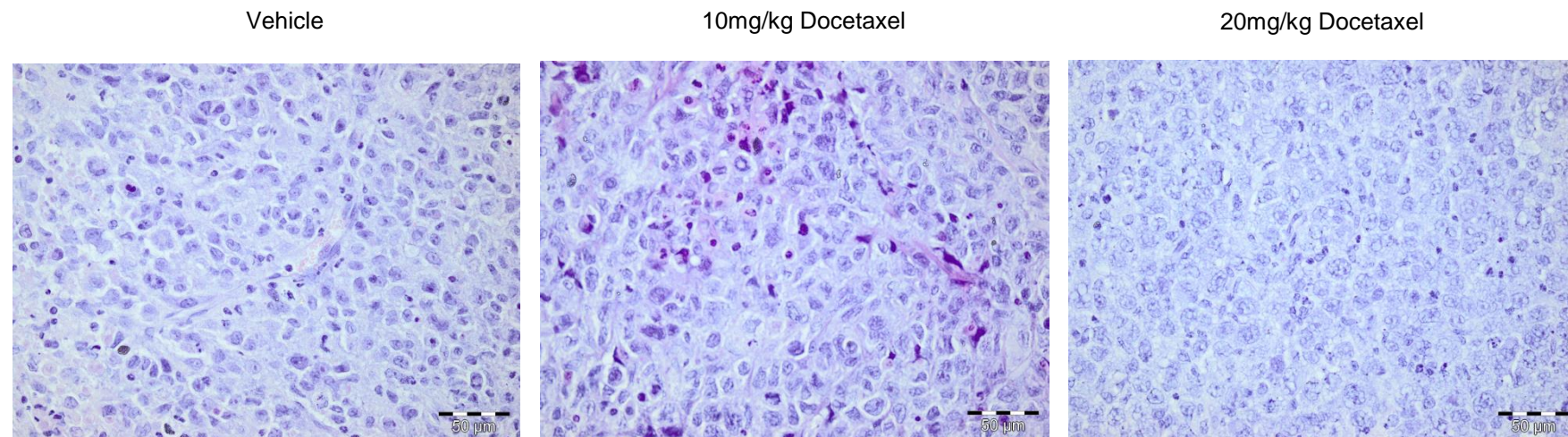


Figure 4.9: **H&E staining of Y019 xenograft paraffin embedded tissue sections.** Representative sections after treatment with vehicle control, 10mg/kg docetaxel and 20mg/kg docetaxel. Less nuclei are seen in the 20mg/kg tumour (mean of 5 ± 1 cells) as opposed to the control group (mean of 33 ± 2.65 cells). Staining and counting were done in triplicate with at least 100 cells counted each time. Images were taken on an Olympus BX51 light microscope at x40 magnification, with scale bars representing 50 μ m.

4.4.2 Immunohistochemistry of PDX Y019 post docetaxel treatment

Immunohistochemistry was performed to look at what happens to the basal and luminal cell numbers in the two classes of PDXs with docetaxel. p63 (basal cell marker) and AR (luminal cell marker) were used to look for differentiation within the cell types in the PDXs. The proliferation marker, Ki67 was used to look at how the actively proliferating cells were affected with docetaxel.

AR (Figure 4.10) was not expressed in tumours from both the control and 20mg/kg groups.

p63 was expressed in both treated and untreated PDX samples (Figure 4.11). However, not all xenograft cells were p63 positive: only rare p63⁺ cells were observed. There was no statistical difference between the control and 20mg/kg groups with a mean of 17.7 (\pm 1.5) v/s 15 (\pm 3.6) positive p63 cells ($p=0.4$). This corresponded to p63 staining previously reported in poorly differentiated human prostate cancers (Parsons et al., 2001).

The only difference seen with docetaxel treatment was in Ki67 staining, as only the control group was positive (proliferative index of 30.7%, \pm 3.8) compared to those from the 20mg/kg group (Figure 4.12).

BPH tissues were used as a positive control to show that the techniques had worked and the IgG negative showed that the staining was specific for each primary antibody used (Appendix 6).

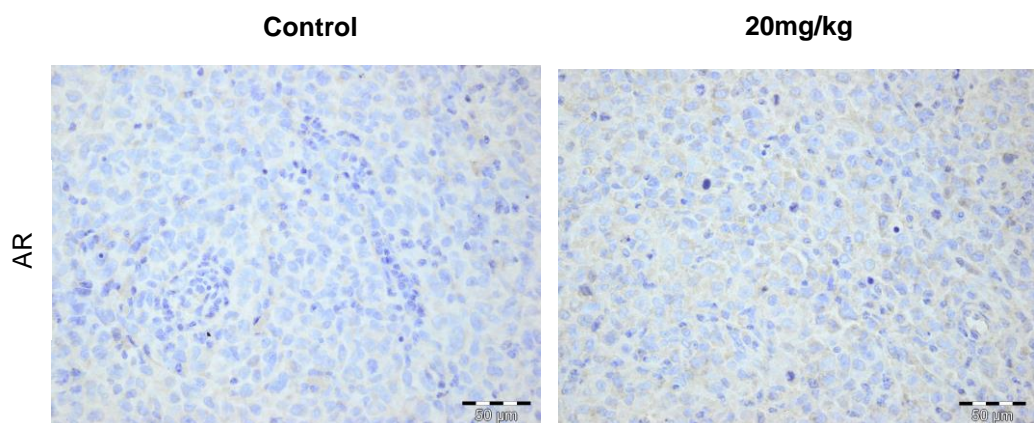


Figure 4.10: **AR staining of PDX Y019 on paraffin embedded tissue sections.** Representative sections from the control and 20mg/kg groups showing no AR staining. An isotype IgG negative control was used each time alongside the primary antibodies (Appendix 2 and 6). Images were taken on an Olympus BX51 light microscope at x40 magnification with scale bars representing 50 μ m.

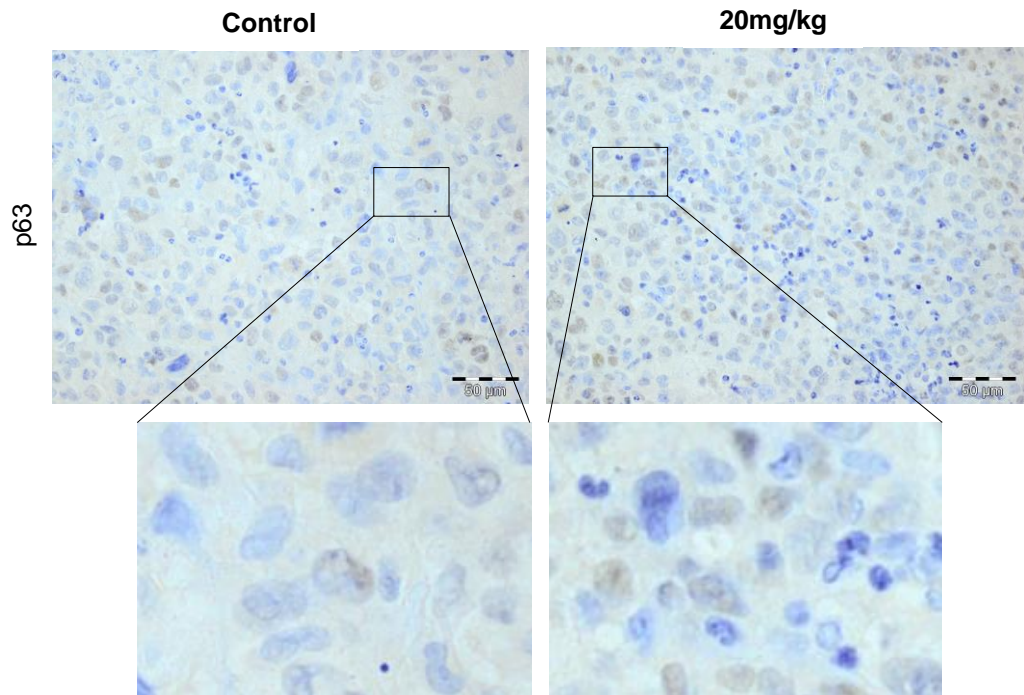


Figure 4.11: **p63 staining of PDX Y019 on paraffin embedded tissue sections.** Representative sections of control and 20mg/kg group with p63. There was no statistical difference between the control and 20mg/kg groups with a mean of 17.7 (± 1.5) v/s 15 (± 3.6) positive p63 cells ($p=0.4$). Counting and staining were done in triplicates. An isotype IgG negative control was used each time alongside the primary antibodies (Appendix 2 and 6). Images were taken on an Olympus BX51 light microscope at x40 and x200 magnification with scale bars representing 50 μ m. The close up pictures represent positive cells in both groups.

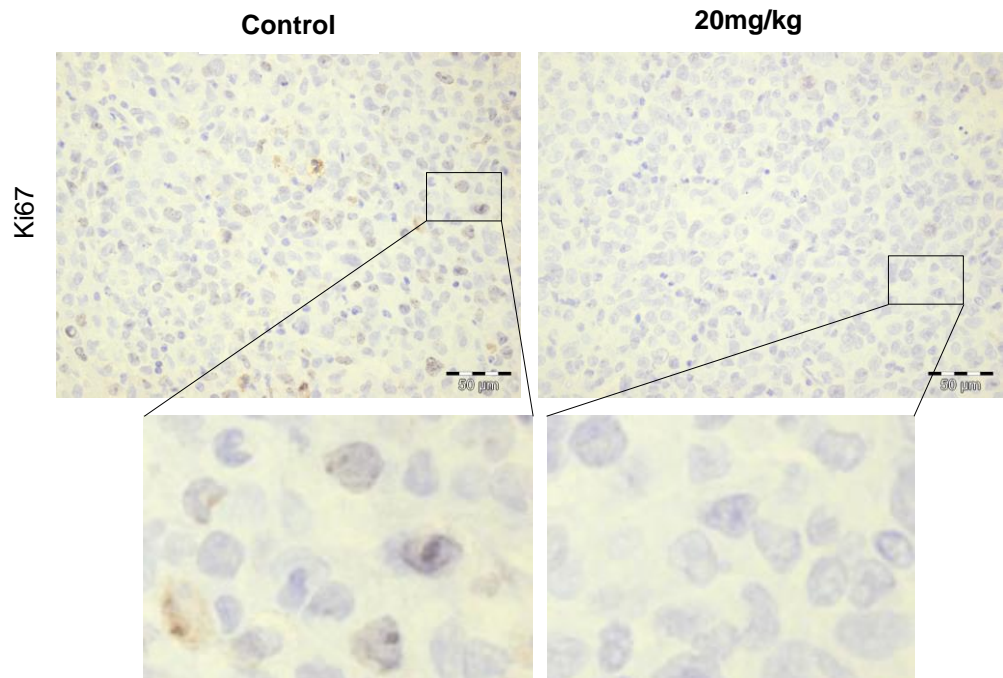


Figure 4.12: **Ki67 staining of PDX Y019 on paraffin embedded tissue sections.** Representative sections of control and 20mg/kg group showing Ki67 was positive only in the control group with a proliferative index of 30.7% (± 3.8). An isotype IgG negative control was used each time alongside the primary antibodies (Appendix 2 and 6). Images were taken at x40 and x200 magnification with scale bars representing 50 μ m. The pictures represent close ups of positive cells in control group and negative in the treated group. Staining and counting were done in triplicate.

4.4.3 Flow cytometry analysis of PDX Y019 post docetaxel treatment

To provide an alternative quantification of expression of antigens in xenografts, disaggregation and fluorescent-activated cell sorting (FACS) analysis was also performed.

4.4.3.1 Gating strategy

Once tumours from the treatment and control groups were excised, they were depleted of lineage positive blood cells and mouse endothelial cells (LIN-/CD31-). The human tumour cells were then analysed by flow cytometry after staining with respective antibodies. The first step was to select only cells of the correct size and granularity for epithelial cells (Figure 4.13A). Then dead cells were gated out using a live/dead stain (sytox blue) (Figure 4.13B). Thirdly, doublets and debris were gated out using pulse width (Figure 4.13C). This gating strategy was used for analyzing all xenografts.

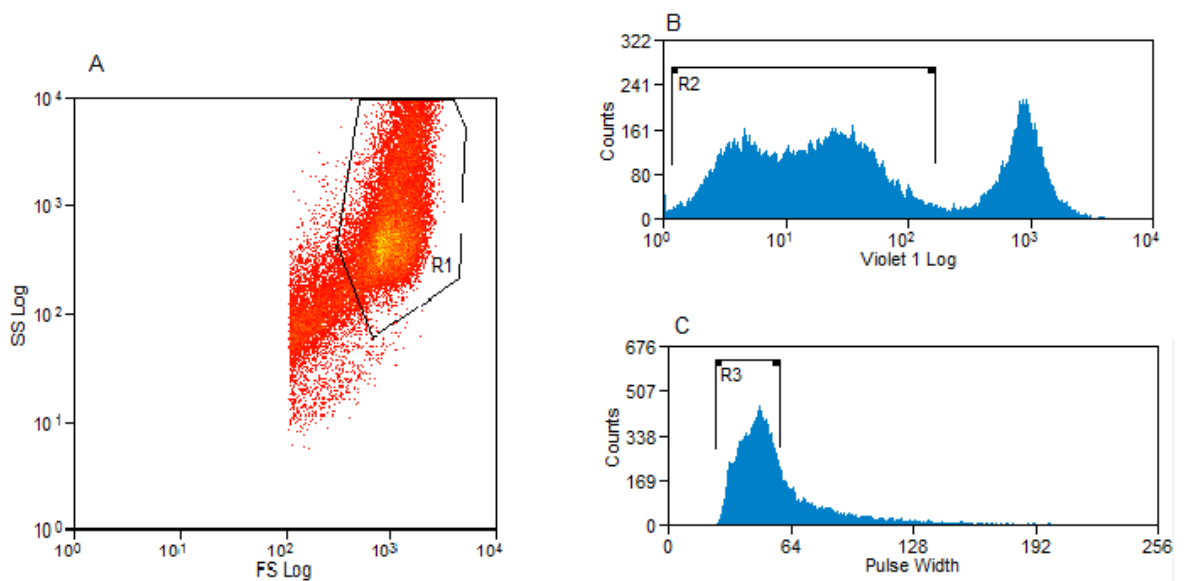


Figure 4.13: **Flow cytometry gating strategy.** LIN-/CD31- human tumour cells labelled and analysed. A. Dot-plot of forward (cell size) and side scatter (cell granularity) to include only cells with the correct size and granularity, R1. Debris was excluded in this way. B. Cells stained with sytox blue to exclude dead cells (take up the blue stain, R2) as opposed to live cells, which remain unlabelled. C. Histogram of pulse width to exclude debris and doublets.

To assess differences in biological response amongst the treatment groups, tumour specimens were examined by flow cytometry for:

1. CD44 used to label the basal-like cells
2. CD24 used to label the luminal-like cells
3. Live/dead stain to assess PDX proliferation

CD44 is a cellular hyaluronate receptor; widely expressed and known to exist in at least 12 different splice variant forms. In human prostate cancers, the normal epithelial forms are often upregulated in the basal compartment and increase the cells propensity to metastasise (Gunthert et al., 1995, Leong et al., 2008). CD24 is another cell surface molecule, which was initially discovered in B-cells and neutrophils. In B-cells, CD24 acts as an adhesion molecule and facilitates the rolling of leukocytes on endothelial cells during the process of inflammation. More recently, CD24 has been described as a marker for luminal epithelial cells of the human prostate (Goldstein et al., 2011, Liu et al., 2002).

The number of xenograft tumours analysed by flow cytometry was at least 3 from each group. The remaining tumours obtained from these experiments were kept for histological analysis, IHC staining and some were frozen after dissociation.

4.4.3.2 Flow cytometry analysis of PDX Y019 for CD24 and CD44 expression

Only the live cells are shown in the following analysis, e.g. those that had survived docetaxel treatment. Results from the control and 20mg/kg group showed a decrease in basal cells after docetaxel treatment. There was a proportional decrease from 79% to 53% in these particular samples (Figure 4.14). The luminal population also reduced from 3% to 1.5% with docetaxel treatment. Further analyses of the other tumours from the respective groups are shown in Appendix 7.

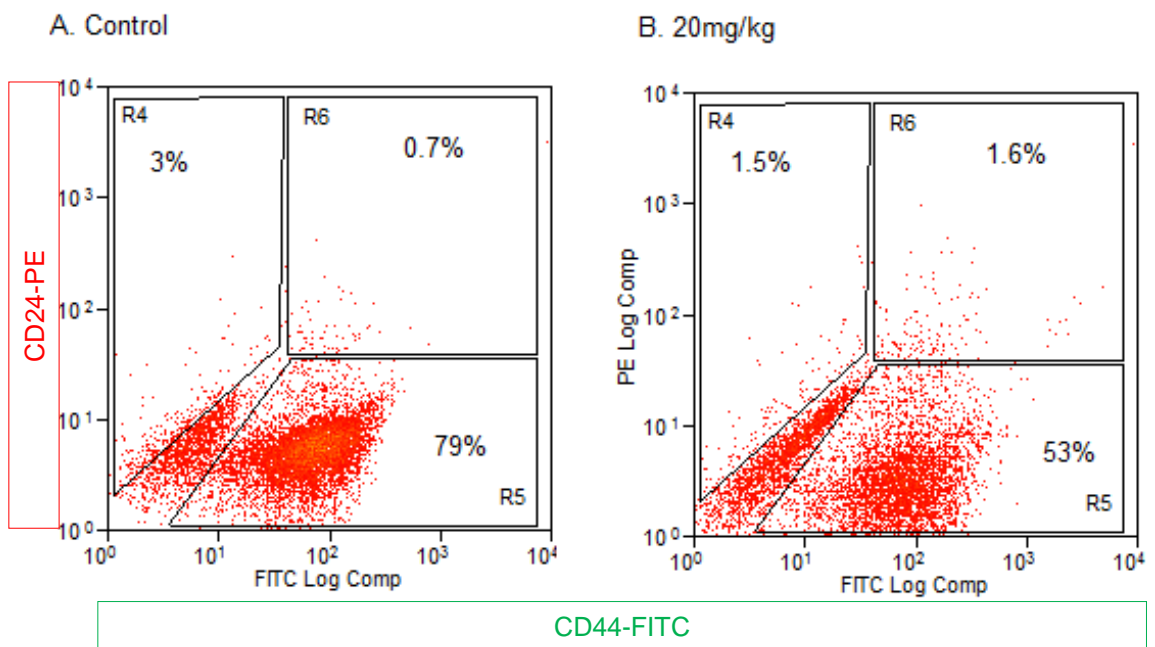


Figure 4.14: **Flow cytometry analysis for Y019 xenograft after treatment with docetaxel.** Tumours from the control and 20mg/kg treatment group were analysed. Dot plots of the LIN-/CD31- tumour cells dual labelled for CD44-FITC (x-axis), which labelled basal-like cells and CD24-PE (y-axis), which labelled luminal-like cells. With treatment a reduction of basal cells was seen. The number of positively labelled cells was set against a control of IgG labelled cells or cells only. Staining and counting were done in triplicate.

4.4.3.3 Flow cytometry analysis of PDX Y019 proliferation

Reduction of basal cell numbers could be a marker of docetaxel response. However, one other possibility is the reduction in the global cell numbers with docetaxel (off target effects). Hence tumours were examined with a live/dead stain. Comparing a typical tumour from the control group to one from the 20mg/kg group showed an increase from 21.7% to 42.5% (Figure 4.15) dead cells. More dead cells were sorted from the treatment groups confirming that the docetaxel treatment did have a detrimental response in the overall Y019 cell numbers.

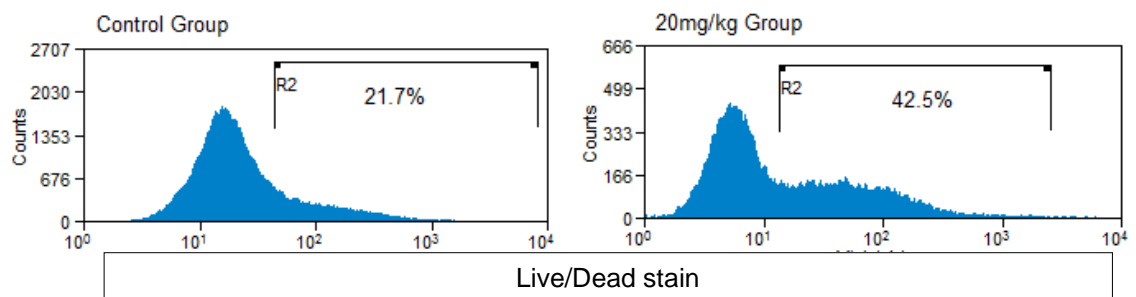


Figure 4.15: **Percentage of dead Y019 cells after docetaxel** using flow cytometry. The first peak represents the live cell population and region R2 represents the percentage of dead cells in the tumour analysed. The proportion of dead cells sorted increased from 21.7% to 42.5%. Experiments were repeated 3 times.

4.5 In vivo Treatment of PDX H016 with docetaxel

From the results of the previous experiment, 10mg/kg and 20mg/kg docetaxel were deemed to represent a good balance between the fewest side effects on the mice and maximum treatment response in the tumours. Therefore, three groups (control, 10mg/kg and 20mg/kg docetaxel) were included in this experiment.

PDX H016 was obtained from a patient who had undergone radical prostatectomy for organ confined prostate cancer. At diagnosis the tumour was graded Gleason score 4+5. At xeno-transplantation the patient was hormone naïve. 3×10^4 cells were injected subcutaneously in both flanks of 27 mice. The mice were randomly divided into the three groups:

- Control group, 8 mice
- 10mg/kg group, 10 mice
- 20mg/kg group 9 mice.

After a tumour establishment period of 50 days, 38 out of 54 flanks had tumours at the start of docetaxel treatment. They had grown at varying rates and the range was from 2-12mm. The mean tumour volume at the start of treatment was 43mm^3 . 6/8 mice from the control group, 9/10 mice from the 10mg/kg group and 7/9 mice from the 20mg/kg group had tumours in at least one flank.

After the third docetaxel injection, 4 mice from the 10mg/kg group and 3 mice from the 20mg/kg group had severe side effects of weight loss, diarrhoea and pilo-erection. Since they lost more than 20% of their body weight, they were terminated early.

Figure 4.16 shows the mean tumour volumes of each treatment group over time. Neither 10mg/kg nor 20mg/kg of docetaxel had an effect on the PDX H016 tumour. The progression of tumours was unaltered despite the three docetaxel injections.

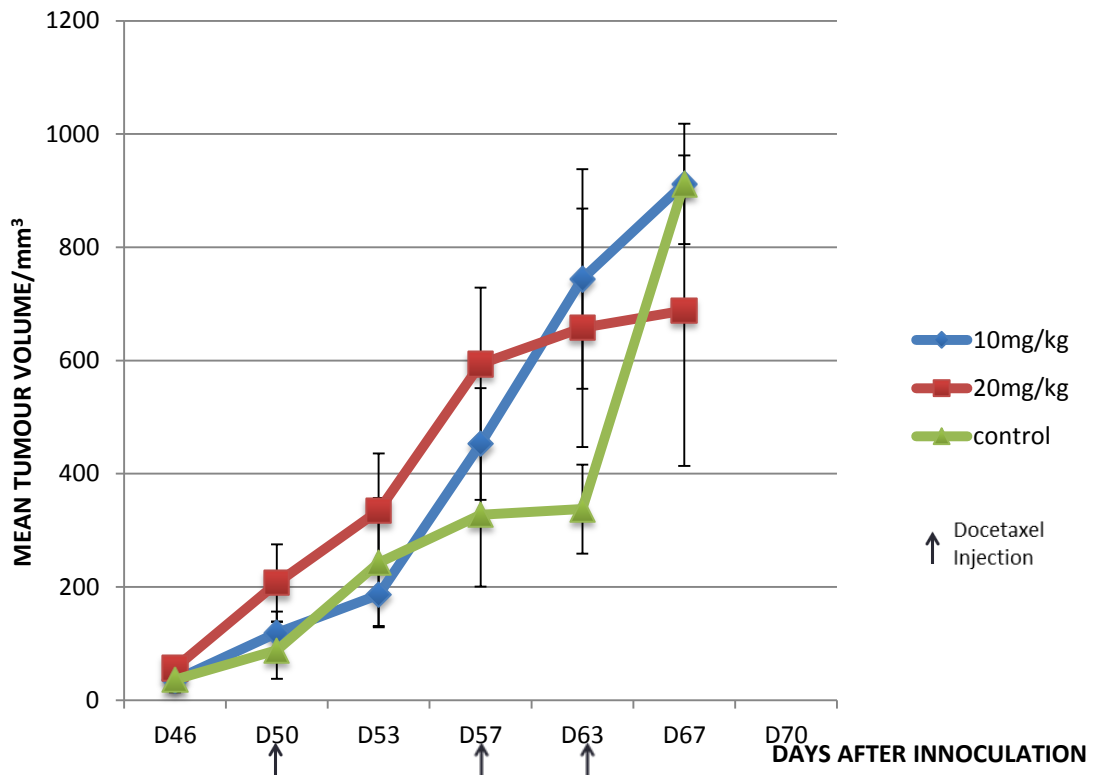


Figure 4.16: **H016 tumour growth curve.** Mice were administered with 10mg/kg docetaxel (n=20), 20mg/kg docetaxel (n=18), control (n=16) at day 50, once tumours reached ~5mm. The black arrows (the x-axis) indicate the dosing period. The results are represented as mean (\pm SD) tumour volume.

4.5.1 Histological analysis of PDX H016 post treatment

On dissecting the tumour mass from the flank and abdominal wall, there were no striking differences between the groups compared to the Y019 experiment where tumours from the treated group could easily be separated from the flanks or abdominal wall. The H016 tumours from the 20mg/kg group were equally adherent as those from the control group (Figure 4.17).

After dissection, tumour pieces from each group were stained with H&E (Figure 4.18). The tumour cell architecture was preserved. Cells continued to be closely packed together with abundant nuclei and blood vessels despite treatment with 10mg/kg and 20mg/kg docetaxel. No specific histological differences were identified. The control group had a mean of 49.6 (± 5.1) actively dividing cells compared to 32.3 (± 4.1) in the 20mg/kg group. This difference was not statistically significant ($p=0.06$) using the student t-test.

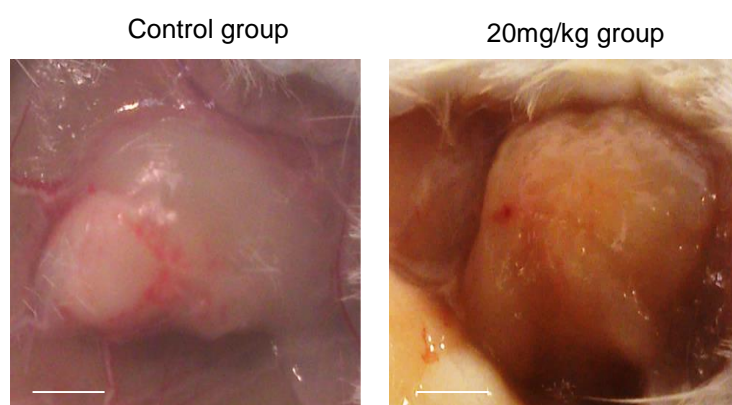


Figure 4.17: **External appearance of tumour mass of H016 after treatment with docetaxel.** Control group and 20mg/kg group: All tumours from both groups were seen to invade the abdominal muscles and flanks. Scale bars represent 5mm.

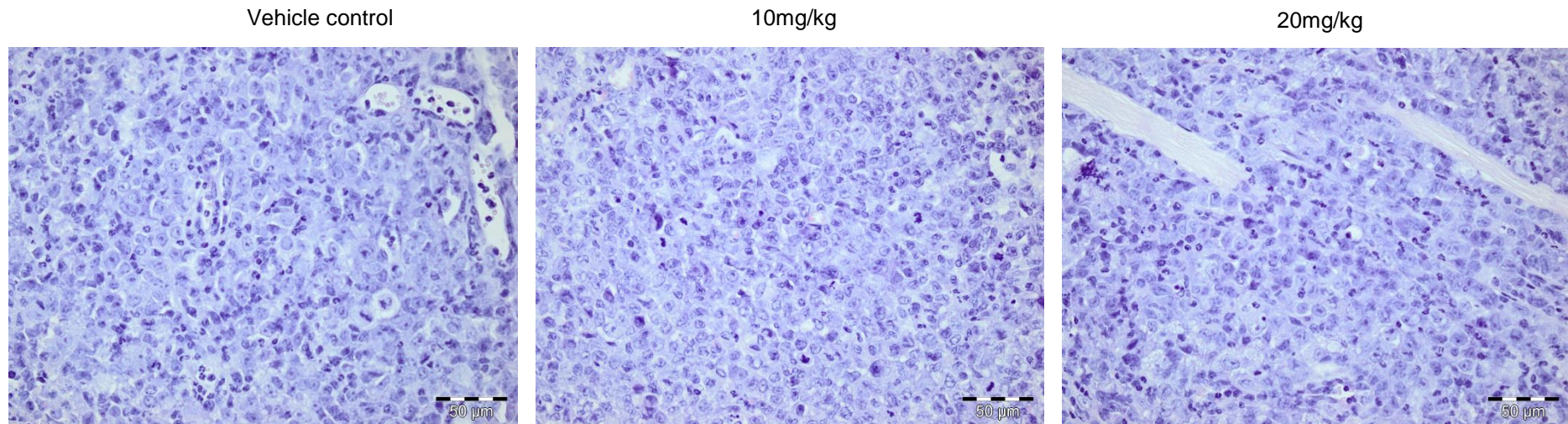


Figure 4.18: **H&E staining of H016 xenograft paraffin embedded tissue sections.** Representative sections after treatment with vehicle control, 10mg/kg docetaxel and 20mg/kg docetaxel. Tumour cells remain closely packed with abundant nuclei and blood vessels despite docetaxel treatment. No histological differences are seen in tumours from all three groups. The control group had a mean of 49.6 (± 5.1) actively dividing cells compared to 32.3 (± 4.1) in the 20mg/kg group. This difference was not statistically significant ($p=0.06$) using the student t-test. Staining and counting were done in triplicate with at least 150 cells counted each time. Images were taken on an Olympus BX51 light microscope at x40 magnification, with scale bars representing 50µm.

4.5.2 Immunohistochemistry of H016 xenograft post treatment

Androgen receptor staining was weakly positive in the control group and mainly nuclear. This changed to a more cytoplasmic distribution with treatment with 20mg/kg docetaxel (Figure 4.19). There was a mean of 50.3 (± 4.1) AR cells in the control group compared 55.3 (± 4.5) AR cells in the 20mg/kg group. This increase was not statistically significant ($p=0.4$).

No p63 staining was seen in the two groups indicating a more luminal cell phenotype in this xenograft (Figure 4.20).

Looking at the proliferation marker Ki67, both the control and docetaxel treated tumours were positive, showing continued active growth despite treatment (Figure 4.21). There was no statistical difference noted between the proliferative indices: Control group 35% (± 2) compared to 32.3% (± 2.5) in the 20mg/kg group.

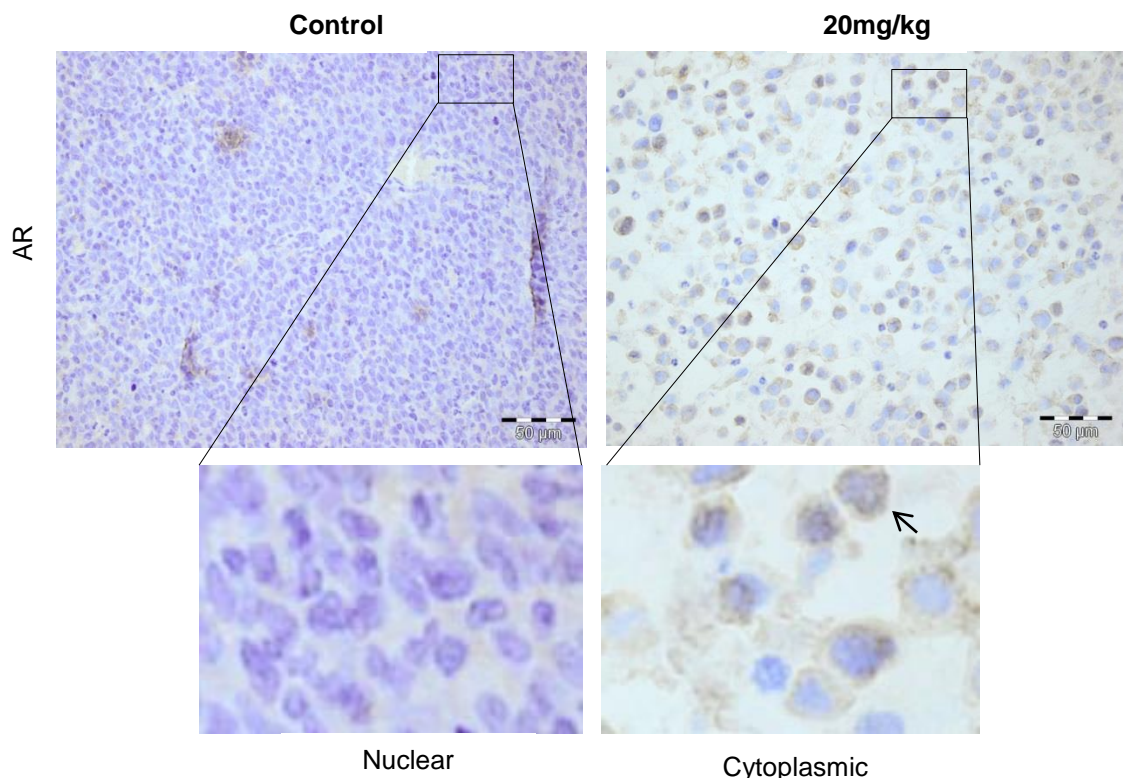


Figure 4.19: **AR staining of PDX H016 on paraffin embedded tissue sections.** Representative sections of control and 20mg/kg group with a change from nuclear to cytoplasmic staining (black arrow). An isotype IgG negative control was used each time alongside the primary antibodies (Appendix 2 and 6). Images were taken at x40 and x200 magnification with scale bars representing 50µm.

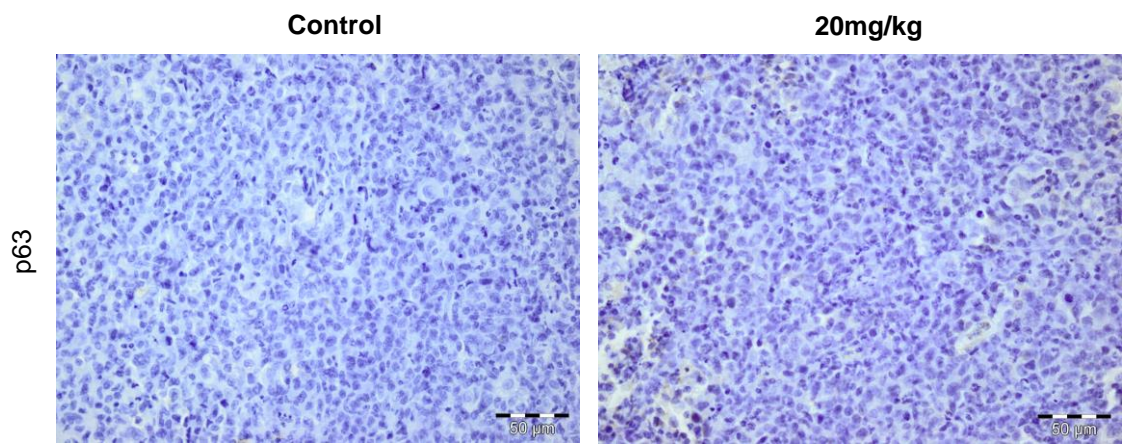


Figure 4.20: **p63 staining of PDX H016 on paraffin embedded tissue sections.** Representative sections of control and 20mg/kg group not expressing p63. An isotype IgG negative control was used each time alongside the primary antibodies (Appendix 2 and 6). Images were taken at x40 magnification with scale bars representing 50μm.

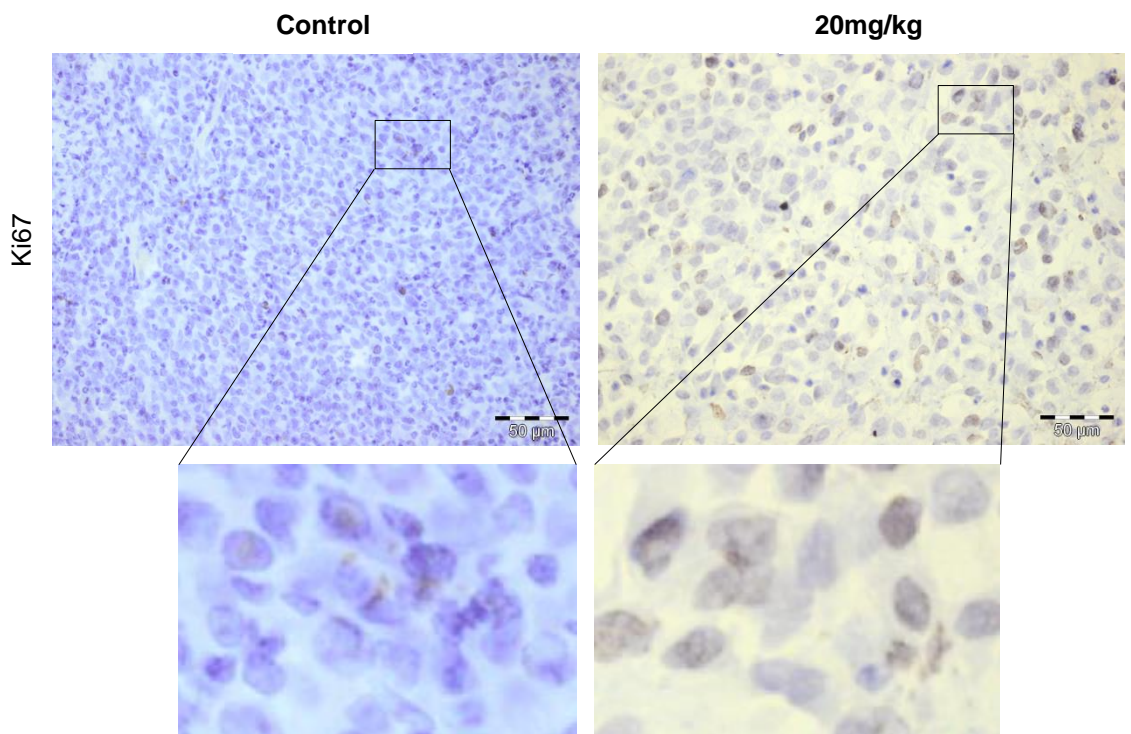


Figure 4.21: **Ki67 staining of PDX H016 on paraffin embedded tissue sections.** Both groups were positive for Ki67 with a proliferative index of 35% (± 2) v/s 32.3% (± 2.5). An isotype IgG negative control was used each time alongside the primary antibodies (Appendix 2 and 6). Images were taken at x40 and x200 magnification with scale bars representing 50μm. The pictures represent close ups of positive cells in both groups and staining was done in triplicate.

4.5.3 Flow cytometry analysis of PDX H016 post docetaxel treatment

4.5.3.1 FACS for CD24 and CD44

Tumours from all the three groups were analysed and 2 sets of xenografts from the control and 20mg/kg group are presented in Figure 4.22. In contrast to the differences observed in the proportion of CD44/CD24 cells in the previous experiment, in H016 there was an increase in the proportion of CD44 expressing cells with treatment (Figure 4.22A, B). However, in another H016 tumour a decrease in the percentage of cells expressing CD44 with 20mg/kg docetaxel was observed (Figure 4.22C, D). Thus no conclusions could be drawn from this experiment except that the expression of CD44⁺ cells remained high with treatment. No striking difference was seen in the proportion of CD24⁺ cells.

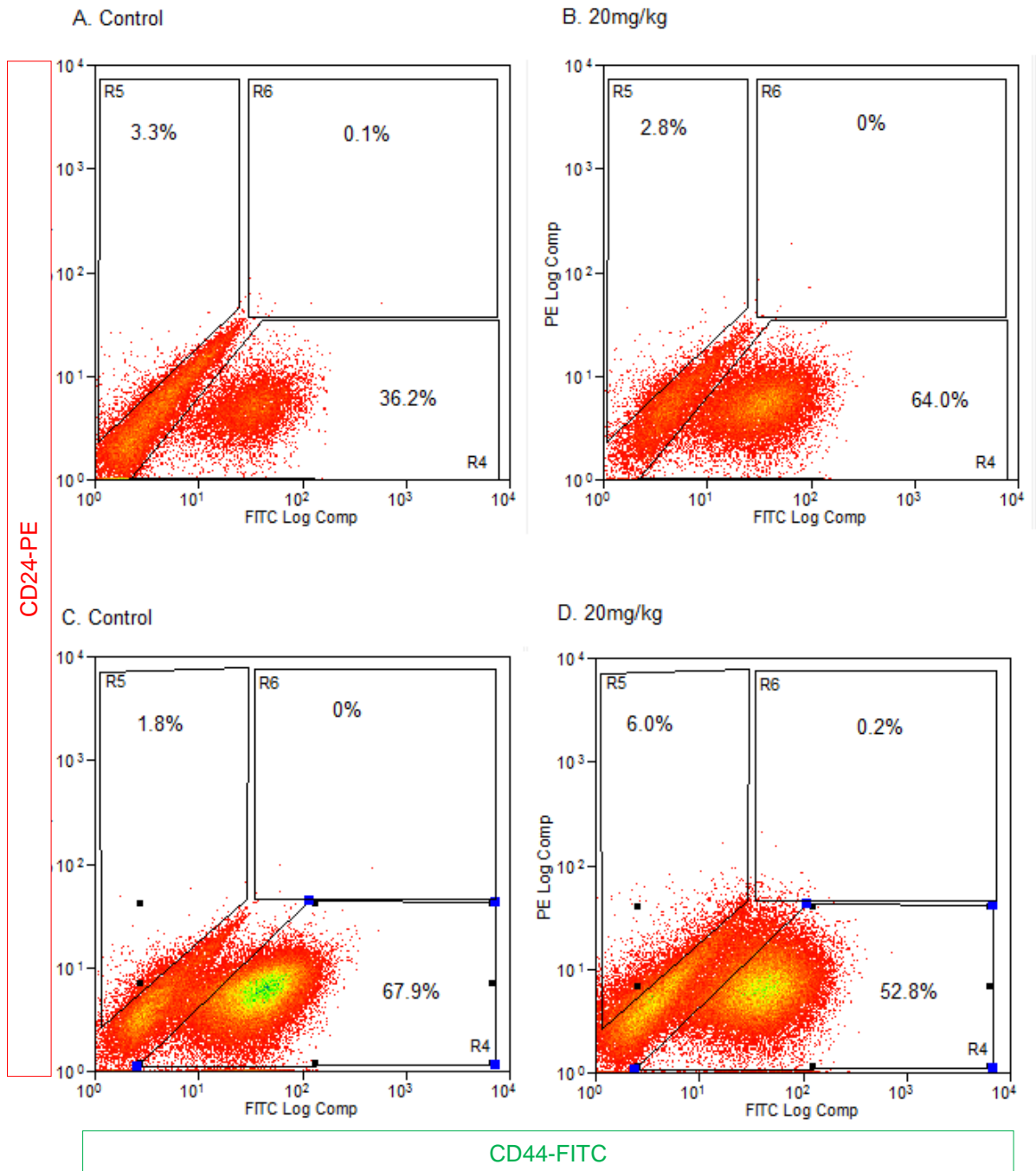


Figure 4.22: **Flow cytometry analysis of H016 xenograft after treatment with docetaxel.** Tumours from the control and 20mg/kg treatment group were analysed. Dot plots of the LIN-/CD31- tumour cells dual labelled for CD44-FITC (x-axis), which labelled basal-like cells and CD24-PE (y-axis), which labelled luminal-like cells. No correlation between the CD24 or CD44 population was seen as illustrated by the polygons R4, R5 and R6. The number of positively labelled cells was set against a control of IgG labelled cells or cells only.

4.5.3.2 FACS analysis of H016 xenografts for AR

As there was no difference in the CD24 and CD44 proportions with docetaxel treatment, AR staining was looked at. No gross difference was seen in this population in the control group compared to the 20mg/kg group (Figure 4.23) despite repeating the experiments 3 times. However, there were few high AR expressing cells in the control group (blue circle), which disappeared with 20mg/kg docetaxel.

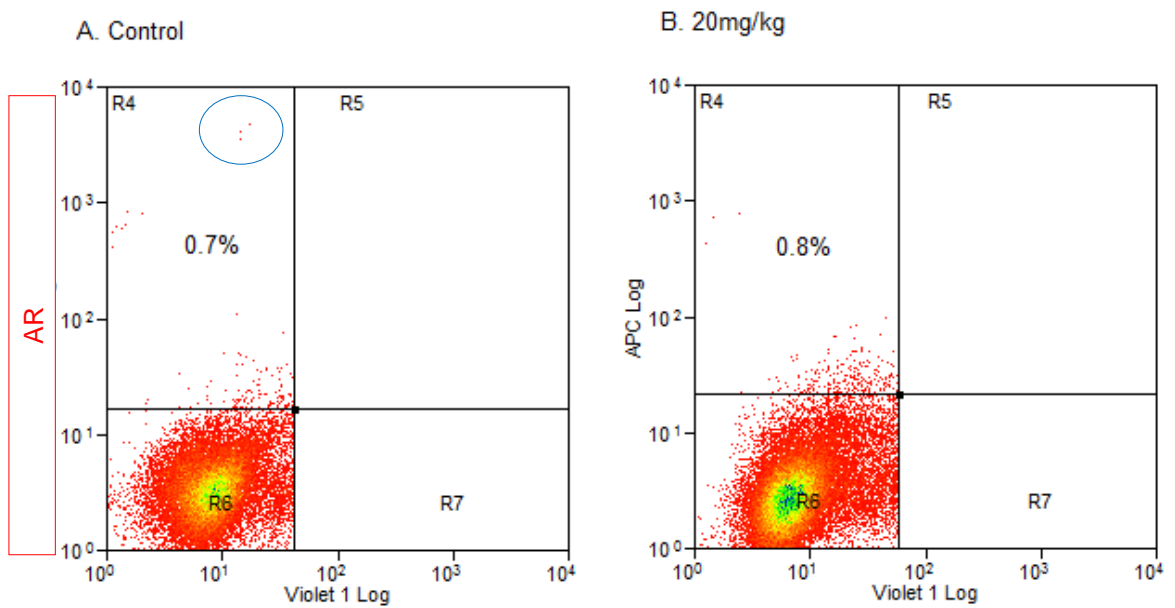


Figure 4.23: **FACS to show AR staining.** Rectangles R4 represent the APC labeled AR positive cells (y-axis). No gross difference is seen between the R4 proportions (0.7% and 0.8%). In figure A, R4 contains few high expressing cells (blue circle) which disappear in the R4 region of B. LNCaP cells were used as positive control for AR in the same experiment (Appendix 9).

4.5.3.3 Flow cytometry analysis of H016 proliferation

Flow cytometry was used to examine the response to docetaxel on the global PDX cell numbers. Although, from the tumour growth curve (Figure 4.16), there were no responses seen, analysis of the number of dead H016 cells showed an increase with treatment. Comparing a typical tumour from the control group to one from the 20mg/kg group there was an increase from 21.4% to 41.5% (Figure 4.24) dead cells indicating that docetaxel was having an effect.

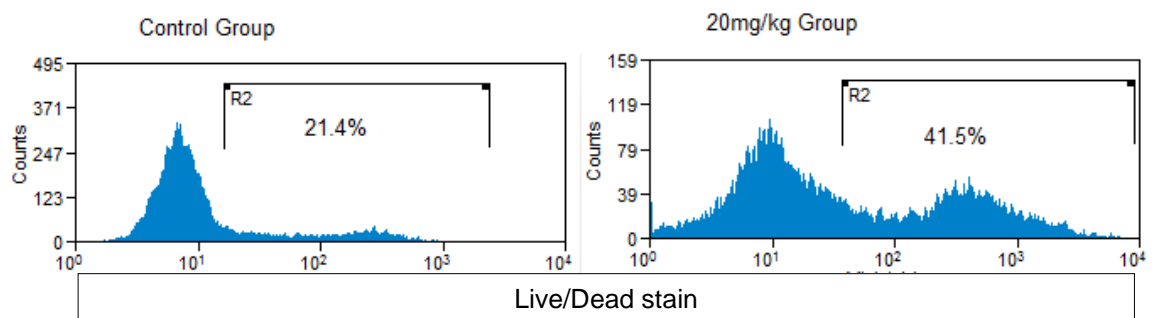


Figure 4.24: **Percentage of dead H016 cells after docetaxel** using flow cytometry. The first peak represents the live cell population and region R2 represents the percentage of dead cells in the tumour analysed. Experiments were repeated 3 times.

4.6 Treatment of PDX Y042 with docetaxel

The Y042 xenograft was obtained from a 56 year old patient who had undergone a radical prostatectomy for organ confined prostate cancer. At diagnosis the tumour was graded Gleason 3+4. At xeno-transplantation, the patient was hormone naïve. 9×10^4 cells of Y042 (LIN-/CD31-) were injected subcutaneously into both flanks of 30 mice. The mice were randomly divided into three groups of control, 10mg/kg and 20mg/kg containing 10 mice each.

After 29 days, 58 out of 60 flanks had tumours ranging from 4 to 6mm. The mean tumour volume at the start of injections was 150mm^3 . 10mg/kg and 20mg/kg of docetaxel slowed tumour progression. This xenograft was responsive from early in the experiment, as the difference in tumour volume was observed from day 38 (Figure 4.25).

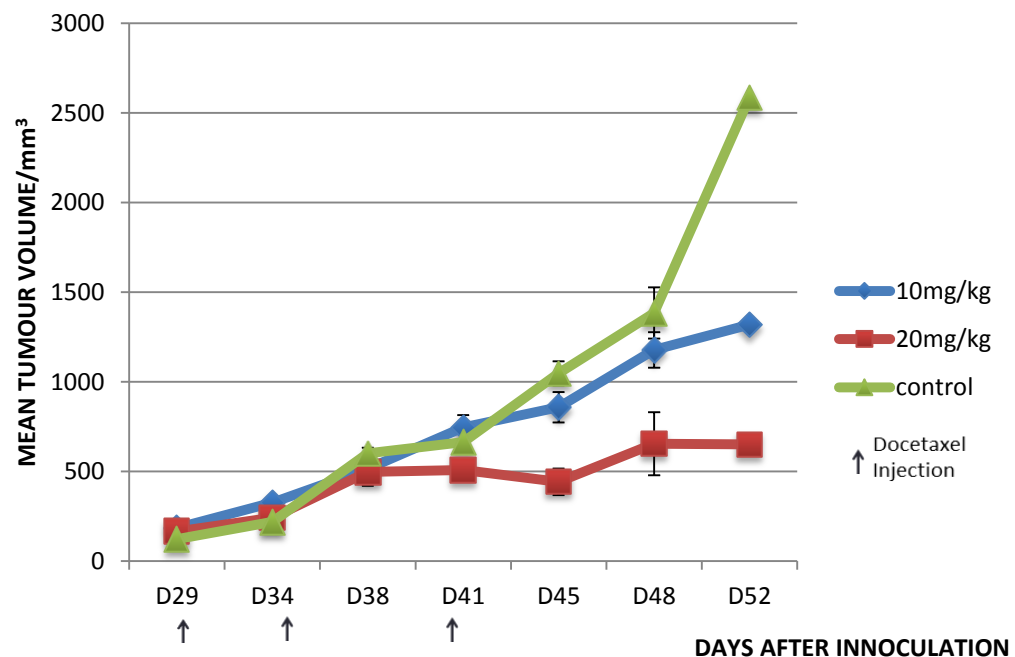


Figure 4.25: **Effect of docetaxel on PDX Y042 tumour growth.** Mice were administered with 10mg/kg docetaxel (n=20), 20mg/kg docetaxel (n=20), control (n=20) once tumour diameter reached 5mm. The results are represented as mean (\pm SD) tumour volumes. The black arrows below the x-axis indicate the dosing period.

Side effects were noted after the third injection, in the treatment groups but not in the control group. One mouse from each of the docetaxel groups was found dead. One mouse from the 10mg/kg group and seven from the 20mg/kg had side effects of weight loss, diarrhoea and pilo-erection. Since they lost more than 20% of their body weight, they were terminated earlier. Two mice from control group had a limp due to rapid tumour burden restricting their movement and therefore had to be culled early.

The survival curve shows that the average survival for mice in the control group was 46.9 days, 48.4 days for the 10mg/kg docetaxel group and 53 days for the 20mg/kg docetaxel group (Figure 4.26). This survival advantage was statistically significant with $p=0.005$ for the 20mg/kg compared to the control group and $p=0.029$ for the 10mg/kg and the control group (Figure 4.26 the Log Rank test).

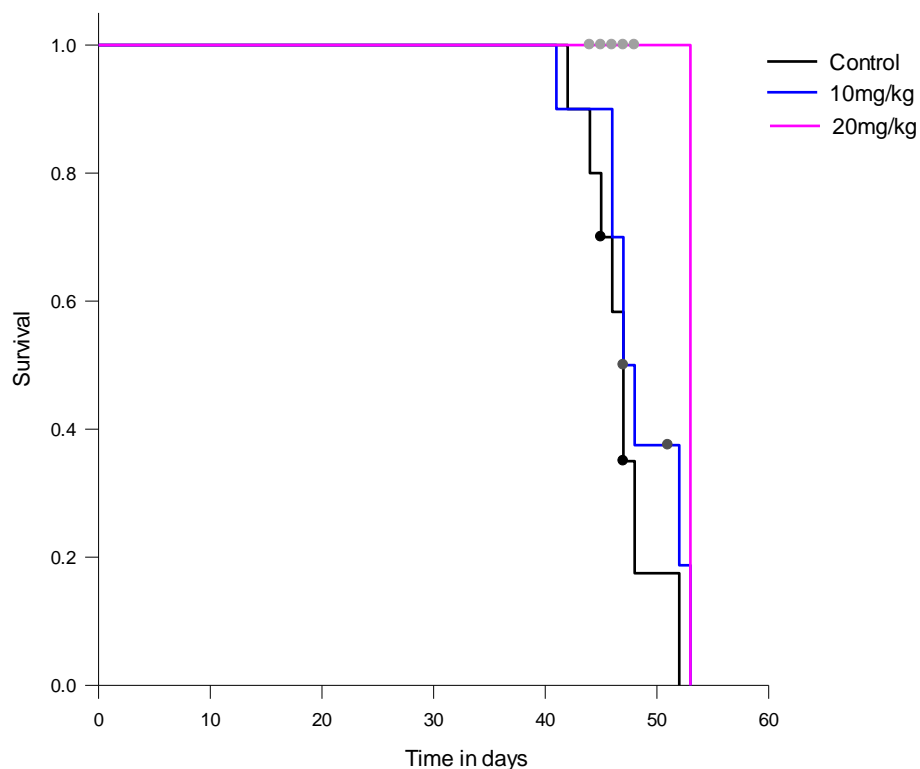


Figure 4.26: **Survival curves of Y042 xenograft after treatment with docetaxel.** A Kaplan-Meier curve of overall survival in the 3 groups was generated using Sigma Plot software. The dark circles indicate censored mice, due to severe side effects of therapy. The Log Rank test was used giving a p value < 0.05 ($p=0.005$ and $p=0.029$) showing that there is a statistically significant difference between both the treatment groups and control.

4.6.1 Histological analysis of Y042 xenograft post treatment

Prior to excising the tumour mass, a clear difference was noticed in their external appearance. Tumours from the control group were highly vascularised and invaded local surrounding structures. In contrast, tumours from the 20mg/kg group appeared devascularised with well-demarcated edges with no evidence of invasion of local structures (Figure 4.27 and see Figure 4.17 for comparison).

Tumour sections from all three groups were stained with H&E at the end of the experiment. Results are shown in Figure 4.28. As treatment dose increased, fewer actively dividing cells (mitotic nuclei) were seen. Blood vessels also became scarce in the tumour section. The control group had a mean of 49.7 (± 3.1) actively dividing cells compared to 9.7 (± 2.5) in the 20mg/kg group. This difference was statistically significant ($p=0.006$).

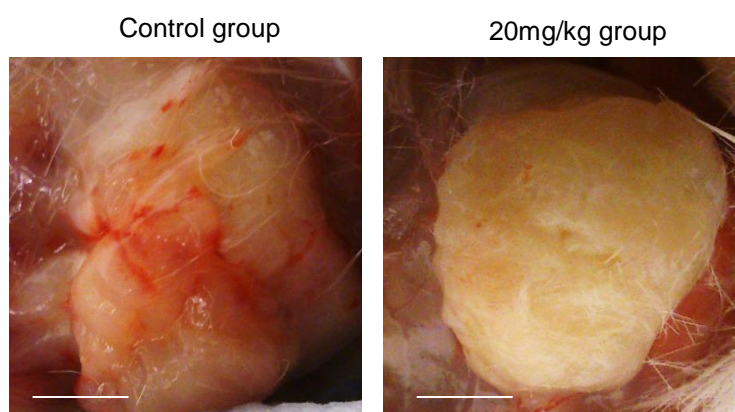


Figure 4.27: **External appearance of tumour mass of Y042 after treatment with docetaxel.** Control group: a markedly vascular tumour invading the abdominal muscles and thigh underneath compared to a less vascularized tumour with well-demarcated edges (20mg/kg group). Scale bars represent 5mm.

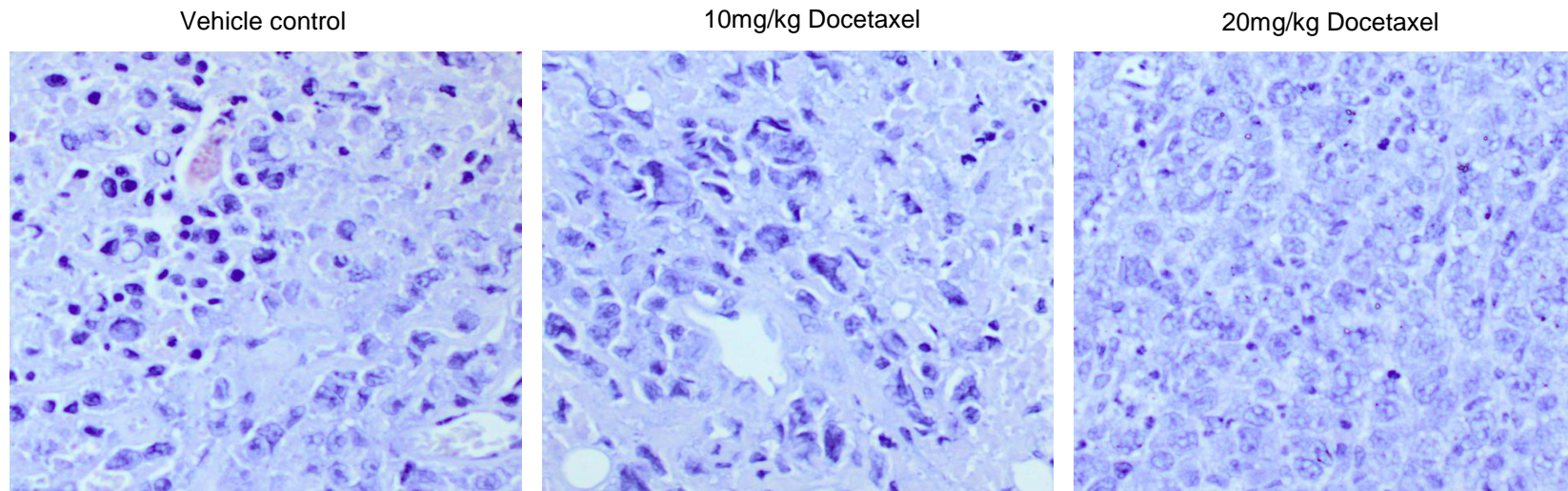


Figure 4.28: **H&E staining of Y042 xenograft paraffin embedded tissue sections.** Representative sections after treatment with vehicle control, 10mg/kg docetaxel and 20mg/kg docetaxel. A statistically significant difference was seen in the number of actively dividing cells between the control and 20mg/kg groups ($p=0.006$). Images were taken on an Olympus BX51 light microscope at x40 magnification, with scale bars representing 50 μ m.

4.6.2 Immunohistochemistry of Y042 xenograft post treatment

Immunohistochemistry for AR, p63 and Ki67 was performed on tumours from the three groups. Results from the control and 20mg/kg group are illustrated below as the latter produced the best response in slowing down tumour growth compared to the 10mg/kg group.

AR was expressed in both groups. The control group had a mean of 71.3 (± 1.5) positive cells compared to a significantly lower 13.7 (± 2.5) cells in the 20mg/kg group, Figure 4.29. This was a statistically significant decrease $p < 0.005$.

There was a significant change in the basal cell population as p63 was expressed in the control group and absent in the 20mg/kg group (Figure 4.30).

Despite a slowing down in the growth rate of tumours with treatment, Ki67 was still positive with a proliferative index of 51% (± 2) in the control group compared to 55% (± 3) in the 20mg/kg group (Figure 4.31). This was not statistically significant ($p = 0.3$).

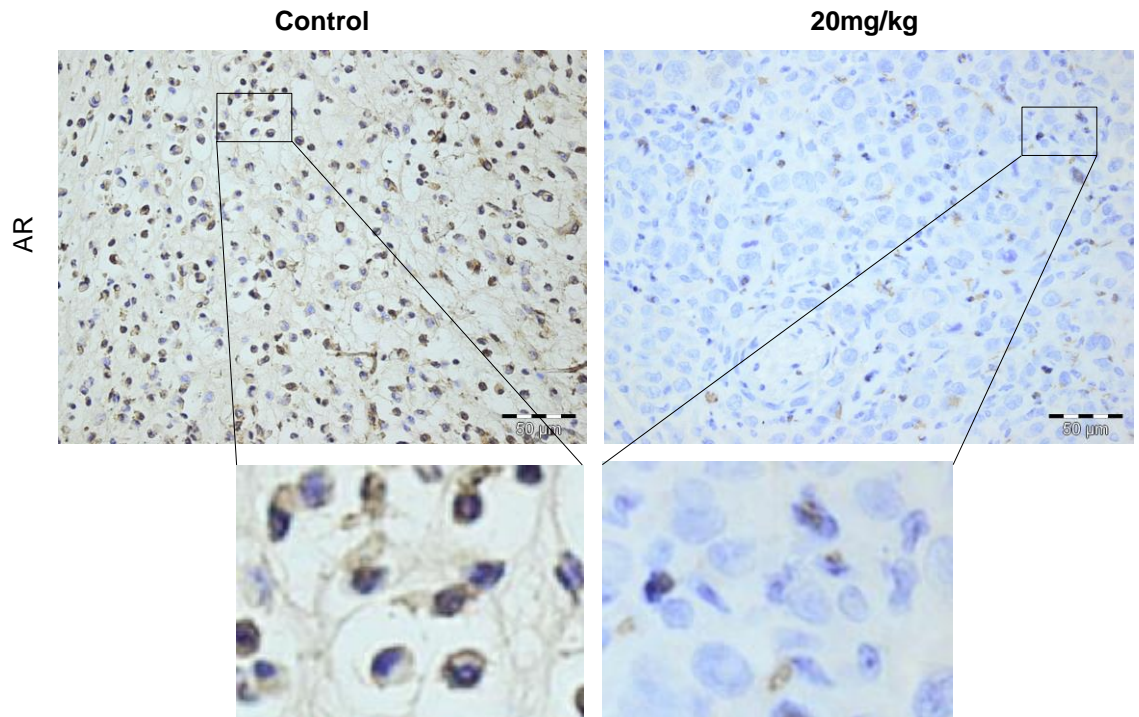


Figure 4.29: **AR staining of Y042 xenograft paraffin embedded tissue sections.** Tumours from both the control and 20mg/kg groups are positive for the androgen receptor. However there was a statistically significant decrease from a mean of 71.3 (± 1.5) to 13.7 (± 2.5) cells ($p < 0.005$). Staining and counting were all performed in triplicate. An isotype IgG negative control was used each time alongside the primary antibodies (Appendix 2 and 6). Images were taken at x40 and x200 magnification with scale bars representing 50 μ m. The pictures represent close ups of positive cells.

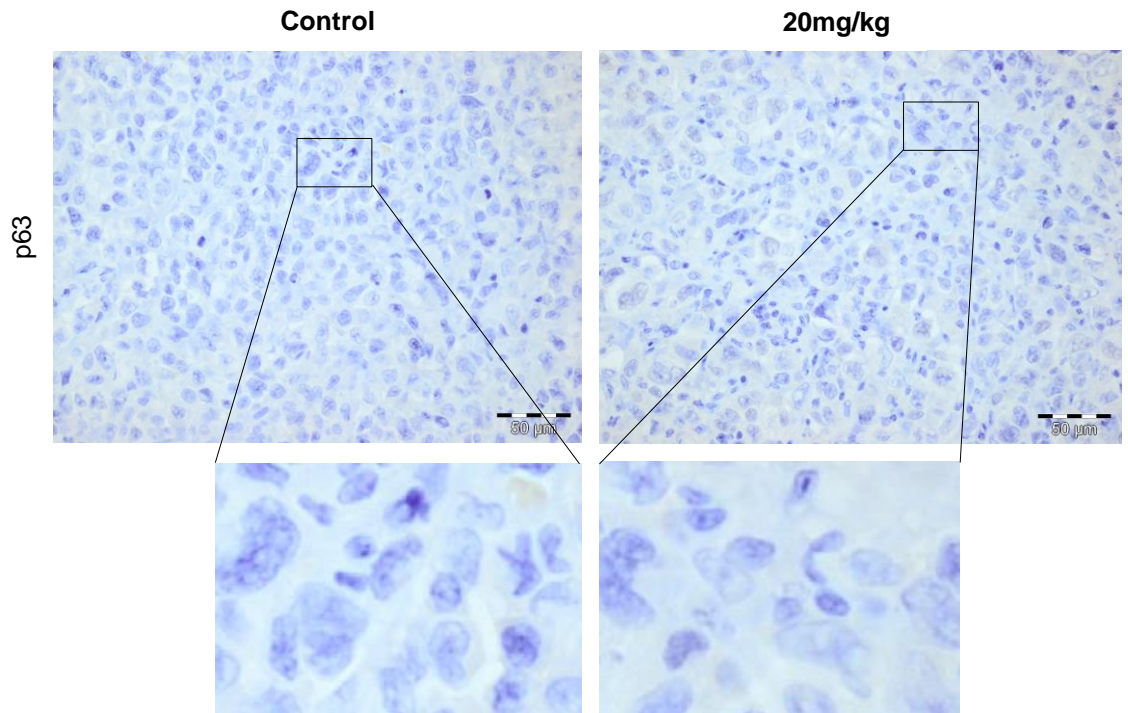


Figure 4.30: **p63 staining of Y042 xenograft paraffin embedded tissue sections.** Representative sections after treatment with p63 expression in the control group and no expression in the 20mg/kg group. An isotype IgG negative control was used each time alongside the primary antibodies (Appendix 2 and 6). Staining were performed in triplicate. Images were taken at x40 and x200 magnification with scale bars representing 50µm.

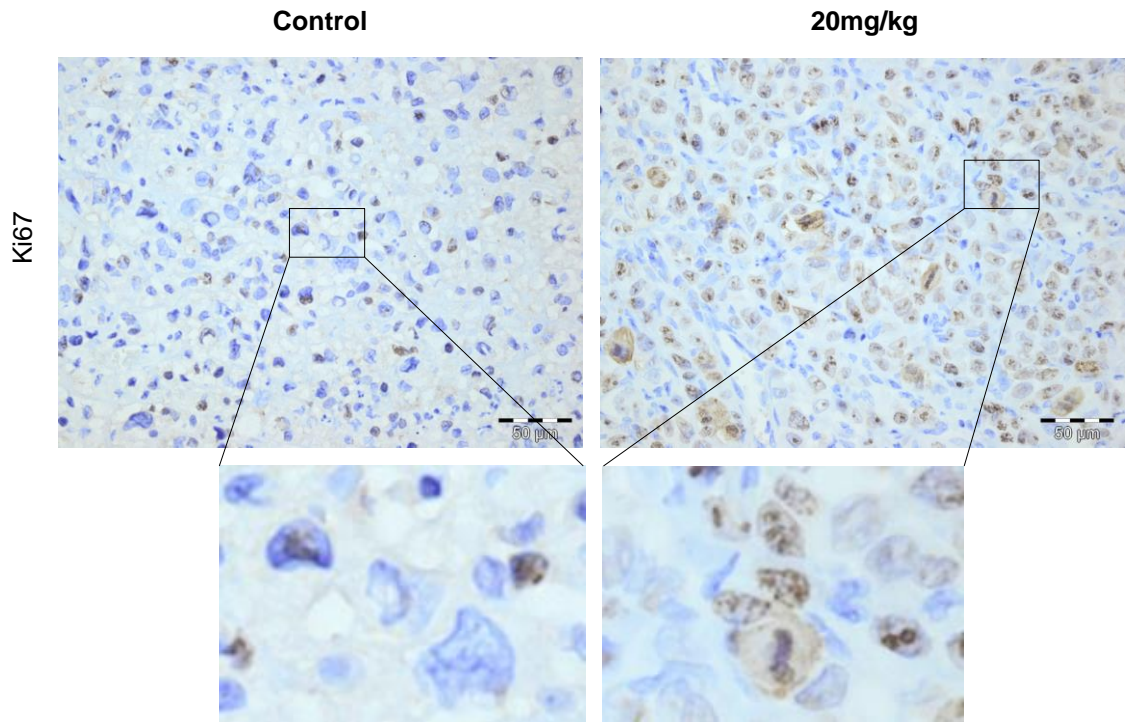


Figure 4.31: **Ki67 staining of Y042 xenograft paraffin embedded tissue sections.** Both groups were positive for Ki67 with a proliferative index of 51% (± 2) in the control group v/s 55% (± 3) in the 20mg/kg group. Staining and counting were all performed in triplicate. Images were taken at x40 and x200 magnification with scale bars representing 50µm. The pictures represent close ups of positive cells.

4.6.3 Flow cytometry analysis of PDX Y042 post treatment

Flow cytometry for CD24, CD44, AR and Ki67 were performed on tumours from the three groups. Results from the control and 20mg/kg group are illustrated below as the latter dose produced a better response in slowing down tumour growth.

4.6.3.1 Flow cytometry analysis of Y042 xenografts for CD24 and CD44

There was a significant reduction in the CD44 population (basal-like cells) (Figure 4.32) from 47.7% in the control group to 20.6% in the 20mg/kg group. The CD24 population (luminal-like cells) increased from 1.3% to 10.2%. Further analyses for CD24 and CD44 on Y042 xenografts are illustrated in appendix 11. They all show a consistent reduction in the basal-like cell population.

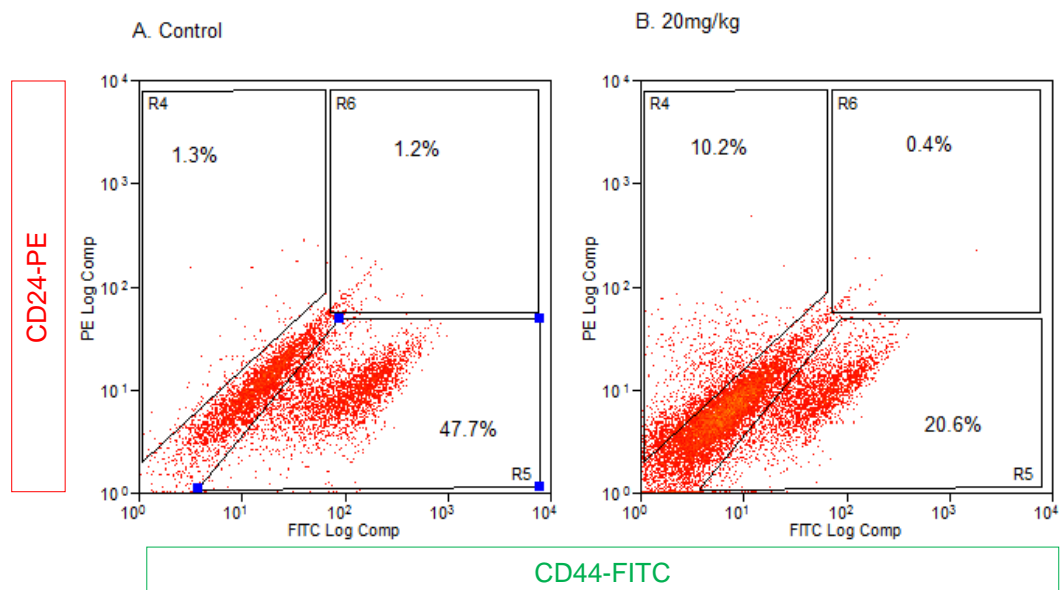


Figure 4.32: **Flow cytometry analysis for Y042 xenograft after treatment with docetaxel.** Tumours from the control (A) and 20mg/kg treatment group (B) were analysed. Dot plots of the LIN-/CD31- tumour cells dual labelled for CD44-FITC (x-axis), which labelled basal-like cells and CD24-PE (y-axis), which labelled luminal-like cells. With treatment a significant reduction of the CD44-FITC was seen (47.7% to 20.6%). The number of positively labelled cells was set against a control of IgG labelled cells or cells only.

4.6.3.2 FACS on Y042 xenografts for AR

Androgen receptor staining was present in both the control and 20mg/kg group. The AR population increased from 9.4% to 26.2% with docetaxel treatment (Figure 4.33). This increase in the luminal-like cell population corresponded to the CD24 increase seen above.

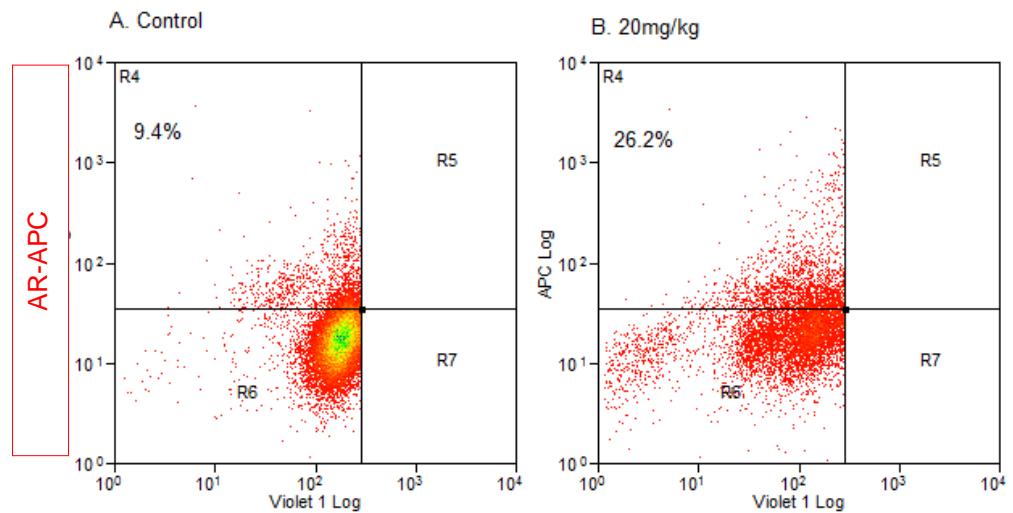


Figure 4.33: **Flow cytometry analysis for AR on Y042 xenograft after treatment with docetaxel.** Rectangles R4 represent the APC labelled AR positive cells (y-axis). An increase in the AR population was seen (9.4% to 26.2%). LNCaP cells were used as positive control for AR in the same experiment (Appendix 9).

4.6.3.3 Flow cytometry analysis of Y042 proliferation

More dead cells were sorted from the treatment groups confirming that the treatment had a beneficial response. Comparing a typical tumour from the control group to one from the 20mg/kg group showed an increase from 40.7% to 63% (Figure 4.34) in the dead cell fraction.

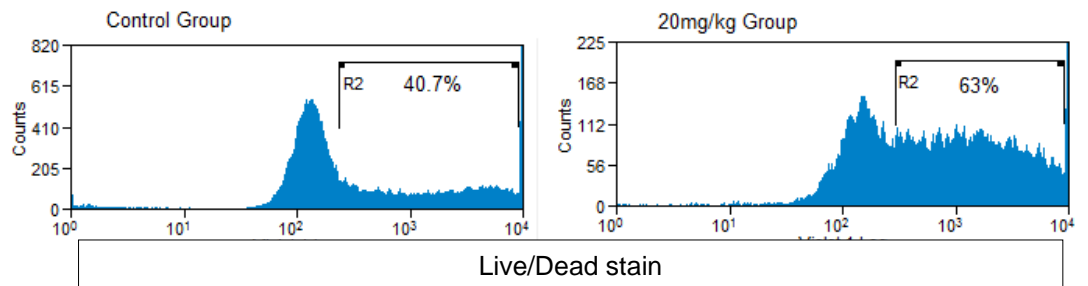


Figure 4.34: **Percentage of dead Y042 cells after docetaxel** using flow cytometry. The first peak represents the live cell population and region R2 represents the percentage of dead cells in the tumour analysed. The proportion of dead cells sorted increased from 40.7% to 63%. Experiments were repeated 3 times.

4.7 Summary of basal and luminal cells expression

Table 11 summarizes the effects of docetaxel on the basal (CD44) and luminal (CD24) cell populations on each of the 3 PDXs used as analysed by FACS.

PDX Id.	Pathology	Docetaxel	Effect on basal cells	Effect on luminal cells
Y019	CRPC	Responsive	Decrease	Slight reduction
H016	Hormone naïve	Resistant	No trend seen	No trend seen
Y042	Hormone naïve	Responsive	Decrease	Increase

Table 11: **Summary of the effect of docetaxel on basal and luminal cell populations** in the 3 PDXs analysed.

Table 12 summarizes the effects of docetaxel on the basal (p63) and luminal (AR) cell populations on each of the 3 PDXs used as analysed by IHC.

PDX Id.	Pathology	Docetaxel	Basal cells p63	Luminal cells AR
Y019	CRPC	Responsive	Decrease	Not expressed
H016	Hormone naïve	Resistant	Not expressed	Increase
Y042	Hormone naïve	Responsive	Decrease	Decrease

Table 12: **Summary of the effect of docetaxel on p63 and AR populations** in the 3 PDXs analysed.

4.8 Discussion

The aim of this part of the study was to investigate if the PDXs reaction to docetaxel corresponds to the heterogeneous responses seen when treating human PC. We looked at the differences in docetaxel response in hormone naïve and CRPC PDXs. Factors affecting their chemo sensitivity were also investigated.

CRPC occurs when hormone naïve cancers become refractory following a period of androgen ablation. Docetaxel belongs to the family of taxanes and has currently a European license as the first line chemotherapy for hormone refractory prostate cancer however this may soon change with the new AR-axis inhibitors. At the present time it is not possible to make a clear recommendation (EAU guidelines 2015) but ADT combined with upfront docetaxel may well be an option in metastatic hormone naïve tumours.

Although docetaxel currently represents an active chemotherapeutic agent it only gives a modest survival advantage, with most patients eventually progressing because of inherent or acquired drug resistance (O'Neill et al., 2011). CRPC patients ultimately manifest resistance to docetaxel and succumb to the disease (Mediavilla-Varela et al., 2009). Survival is not expected to exceed between 9 and 12 months and the aim of treatment is to improve symptoms, prolong life and slow progression of the disease (NICE Guidelines CG175) (NICE, 2014).

Limited data is available on the activity of docetaxel in animal models of PC (Navone et al., 1998). Previous studies on the cell line PC3 have shown sustained tumour regression over continued docetaxel treatment (Figure 4.35) (Fizazi et al., 2004). Interestingly, this does not correspond to the actual disease aggressiveness and metastatic potential in patients as not every patient responds to docetaxel or show continued disease regression.

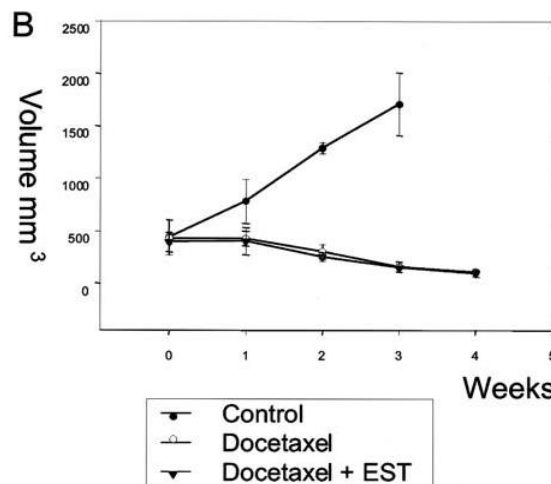


Figure 4.35: **Antitumour activity of docetaxel** with or without estramustine (EST) in subcutaneous xenografts from the PC3 cell line. (Reproduced from Fizazi et al, 2004)

As described in the above study, most studies are based on established cell lines, which are the traditional way to study PC. Although they represent an excellent basis for testing scientific hypotheses and optimising treatment, there are some concerns regarding how closely they represent the patient setting after over 40 years in culture. Neither cell lines nor xenografts derived from them give any indications about whether new prostate cancer therapies are likely to be successful in the longer term, although they frequently show potent cytotoxicity. Many potentially beneficial therapies that might be valuable in humans are also discarded if they fail to show efficacy in cell lines (Daniel et al., 2009). As a result, a preclinical model more closely mimicking patients' tumour characteristics appears more promising. PDXs (like the ones used in this study) represent a better tool for future preclinical studies, translation and management of the evolving CRPC aspects.

In this section, it was shown that treatment with docetaxel resulted in growth reduction in Y019 (CRPC xenograft) and Y042 (hormone naïve xenograft) tumours compared to vehicle control. This difference was statistically significant in the Y042 xenograft (Figure 4.26) but not in the Y019 xenograft (Figure 4.5 and 4.8). In contrast, H016 (hormone naïve xenograft) tumours were completely unresponsive to docetaxel (Figure 4.16), which made no difference to tumour progression.

Despite a clear reduction in tumour progression in the Y019 xenograft, statistical significance was not achieved mainly because the volume of tumours at the start of the injection period was highly variable. Ten mice per group with each mouse having two tumours on both flanks were used. The effective sample size was 20. The volume discrepancy was consistent in all three experiments. The tumour take in mouse experiments with PDXs is difficult to predict. Coordinated tumour growth is even harder to achieve than when using cell lines. This is despite the cells implanted being derived from the same xenograft, using the same number of cells, feeder STOs and injecting in the same way each time. Tumour initiation remained difficult to synchronise and some mice failed to produce tumours, 4/60 and 1/60 flanks in the Y019 experiments, 2/60 flanks in the Y042 experiment and 16/54 flanks in the H016 experiment. An explanation for this is the possible interactions between the host and the cells injected leading to rejection. An improvement, which we have already started using, is to implant a standard 4mm disc of tumour tissue subcutaneously in mice, which tends to give better results. However, in this setting host cells are not depleted and may compromise experiments with more mouse cell invasions in the PDXs.

In the H016 experiment, tumour initiation was asynchronous. The start of treatment had to be delayed until enough mice had measurable tumours. A compromise had to be reached as to when to initiate treatment, in order to get enough data and tumours. Another variable was the shape of the tumours, which affected the calculation of tumour volumes. Some tumours had a necrotic centre, which developed a wound or a hole. In drug response studies, direct calliper measurements are often affected due to variability of tumour shape, skin thickness and a subcutaneous fat layer. It has been shown that microCT (computed tomography) scanning is more accurate (Jensen et al., 2008). Unfortunately, this technology was not available to us.

Apart from varying tumour sizes, side effects of docetaxel also limited the duration of the experiments. In the Y019 experiment, mice from the 5mg/kg and 10mg/kg docetaxel treatment groups showed no clinical side effects (diarrhoea, piloerection and ill health) and gained weight, indicating possibly sub-optimum dosage. Increasing the dose caused more side effects. However, reduction in tumour growth was sustained (Figure 4.7). 8 mice from the repeated Y019 experiment, 7 from the H016 experiment and 8 from the Y042 experiment had

significant side effects and had to be censored. This is a well-known phenomenon in patients. In fact docetaxel is usually given together with steroids to boost appetite and reduce weight loss (NICE Guidelines CG175, (Tannock et al., 2004). If significant side effects occur, granulocyte colony stimulating factor (G-CSF) is administered and very often the dose is reduced or stopped. In fact in the Y042 and H016 experiment only three of the four planned docetaxel injections could be achieved.

To compare these results with the clinical picture, the results of the landmark study, which revolutionised CRPC treatment in 2004 (Tannock et al., 2004) is summarised. The TAX327 trial was an international, multicentre, open-label, phase III randomised control trial (RCT). The trial looked at 1006 men with metastatic prostate cancer with disease progression during hormonal therapy. The men were randomised to three chemotherapy arms, all of which received prednisolone 5mg orally twice daily. The chemotherapy regimens were: docetaxel at 75mg/m² administered every 3 weeks (335 patients); docetaxel at 30mg/m² administered weekly for the first 5 weeks in a 6-week cycle (334 patients); and mitoxantrone 12mg/m² administered every 3 weeks (337 patients). Up to 10 cycles of treatment were planned for the 3-weekly docetaxel group and the mitoxantrone group, and up to five cycles (of 6 weeks each) in the weekly docetaxel group. Patients in the docetaxel groups also received premedication with the steroid, dexamethasone. There was a statistically significant benefit for the 3-weekly docetaxel group compared with the mitoxantrone group ($p = 0.009$) in overall survival (OS). At the time of analysis 166/335 (50%) patients receiving 3-weekly docetaxel and 201/337 (60%) of patients receiving mitoxantrone had died. There was no statistically significant difference in OS between the weekly docetaxel group and the mitoxantrone group. Therefore their best OS was in the 3-weekly docetaxel group and even then ONLY 50% of the patients appeared to be sensitive. In their weekly docetaxel group, relapse was seen at 32 months after a period of good response (Summary from NICE guidelines TA101) (NICE, 2006) and (Tannock et al., 2004). Another RCT investigating the efficacy of docetaxel in CRPC (SWOG 9916) also showed that not all patients were sensitive to chemotherapy (Petrylak et al., 2004).

This PDX study can be compared with the two clinical RCTs, in that the Y019 and Y042 xenografts were sensitive and H016 inherently resistant. Y019

showed reduction in tumour growth but not statistical significant and relapse of tumour growth after completion of docetaxel treatment was also seen. It is common to see relapse after an initially good response with docetaxel in CRPC patients. Therefore our mouse experiments mimic the responses seen in patients and could be used to identify the possible mechanisms that define of docetaxel resistance.

4.9 Docetaxel effects on the basal cells of responsive tumours

H&E analysis saw a reduction in actively dividing cells in the responsive tumours Y019 and Y042, which was statistically significant. Cells became loosely arranged with less prominent nuclei. Since we were interested in the docetaxel effects on the phenotypes and their differentiation we looked at basal and luminal cell markers using FACS and IHC.

Following treatment with docetaxel, there was a decrease in the number of basal (CD44) cells in the responsive xenografts Y019 and Y042 (Figure 4.14 and 4.32). CD44 is enriched in prostate cancer stem/progenitor cells (Collins et al., 2005) and is known to promote their viability (Gotte and Yip, 2006). In the IHC experiments, the number of p63 cells (basal marker), reduced in Y042 and Y019 and was statistically significant in Y042. This decrease could explain the inhibition in tumour growth and associated inhibition of mitosis with docetaxel treatment. In fact, Signoretti et al. proposed that p63 is the stem cell factor because prostate development is absent in embryonic/newborn p63^{-/-} mice (Signoretti et al., 2000). There was no correlation with the hormone status as Y042 was from a hormone naïve sample and Y019 from a castrate resistant sample.

In the docetaxel resistant xenograft H016, there was no change in the number of CD44 cells (Figure 4.22) and the content stayed at a high level, signifying inherent resistance of the stem cells. A high expression of CD44 has been previously shown to correlate with invasiveness and metastatic potential in prostate cancer (Lokeshwar et al., 1995) and despite being a hormone naïve xenograft, H016 was still resistant. Moreover, IHC showed no change in the p63 expression before and after docetaxel treatment. Therefore docetaxel sensitivity is likely to be related to a basal cell reduction and not in the hormone status of the PDXs. This was further confirmed with Y019, which showed a reduction in basal cell content with growth reduction after docetaxel treatment.

4.10 Docetaxel effects on the luminal cells of responsive tumours

Looking at the luminal (CD24) cells, Y019 showed a decrease, H016 had no decrease and Y042 showed an increase with docetaxel treatment (Figure 4.14, 4.22 and 4.32 and Table 11). IHC showed AR expression in H016, and intracellular localisation changed from nuclear to cytoplasmic with docetaxel treatment but the tumours were still nonresponsive. In fact, this change of AR expression was seen in the orthotopic experiments of H016 (Figure 3.12) and Y018 (Figure 3.13). AR was also present after docetaxel treatment in Y042, but there was no change in the way it was expressed, though there was a reduction in numbers of AR⁺ cells. AR was absent in Y019.

Changing the way AR is expressed can be a mechanism of survival and resistance (Tan et al., 2015). AR could have been mutated to develop survival benefits as explained in section 1.5.

Our data show no clear trends of change in the luminal cell population with docetaxel treatment. The basal cells appeared to give rise to differentiation in prostate cancer and docetaxel targeted the proliferative cells. The key to docetaxel sensitivity and development of resistance may be explained by basal cell interactions. Our results confirmed that docetaxel leads to a decrease in basal cells however an increase in luminal cells can signify eventual resistance.

4.11 Off target effects of docetaxel

Docetaxel overall had a detrimental effect on live cell populations in all 3 PDXs. The number of dead cells was seen to rise with treatment (Figures 4.15, 4.24 and 4.34). The global cell numbers might have been reduced from docetaxel toxicity rather than any effects on the basal cell population. It is important to realize this as a limitation specially when looking at specific cell numbers.

Responsiveness to chemotherapy can be better assessed by looking at the impaired cell proliferation or reduction in Ki67 expression (Scholzen and Gerdes, 2000). In the Y019 experiment, mice treated with the docetaxel showed no Ki-67 staining compared to the control group, which was positive (Figure 4.12). There was no difference seen in the Ki67 staining in the Y042 and H016 experiments (Figure 4.21 and 4.31). The proliferative indices stayed high with docetaxel treatment. This is evident in the H016 experiment as no response to docetaxel was seen. However, in the Y042 tumours, no change in Ki67 staining was seen despite slower growth been maintained in the treatment groups.

Ki67 is a cell proliferation marker expressed during all phases of the cell cycle except G0 and early G1. Previous studies have reported an association between increased Ki67 staining and poor outcome (Gimotty et al., 2005, Ramsay et al., 1995). Other studies argue that Ki67 is not an independent prognostic factor (Hazan et al., 2002). Anti-mitotic protein monoclonal-2 (MPM-2) and anti-phosphohistone-H3 (PHH3) are two relatively new antibodies that differ from earlier surrogate markers of proliferation in that their respective epitopes are restricted to the M phase. Thus, they are potentially more specific and sensitive markers of mitosis than Ki67. An improvement for future PDX experiments would be to use PHH3 or MPM-2, which can be more docetaxel specific markers. The presence of Bcl-2 in tumour cells can also serve as a specific indicator for docetaxel responsiveness. Bcl-2 has been shown to be inactivated with docetaxel treatment (Kraus et al., 2003). These markers would have been more relevant to show on-target effects of docetaxel and should be considered in future PDX experiments.

CHAPTER 5

RESULTS III

5. Lentiviral transduction of PC3 and 'near patient' derived xenografts for tracking metastatic spread

5.1 Rationale

Metastases are a common feature of advanced cancer and the cause of significant patient morbidity and mortality (Coleman, 2006). Prostate cancer has a high prevalence for developing bone metastases. The cellular and molecular mechanisms involved are poorly understood. Hence the prevention of metastatic spread remains one of the main challenges as once tumours colonize distant sites, the disease is considered incurable (Coleman, 2012). There is a clear need to characterise the processes involved in the development and progression of metastases in order to identify new therapeutic targets and improve the outcome for patients. Progress in this area has been hampered by the lack of clinical samples being made available for research, as there is no routine sampling of metastases from tumours. Very often, patients die in hospices and at home and prompt tissue sampling is difficult. Therefore our understanding of tumour spread relies much on in vivo models, which represent our best source of information to this intricate process. Cell lines have been traditionally used in these models and therefore, I tried to develop a PDX model to look at the key events involved. A starting step is to identify and track the PDX cells when injected subcutaneously. I looked into lentiviral transduction of PDXs cells with fluorescent and luciferase markers, which would allow live monitoring and locating spread. PC3 cells were used to optimise this technique first. Once successful, transduced PDX cells could be used to look at orthotopic engraftment or to monitor therapy effects.

5.2 The AMSBio™ lentiviral system

The AMSBio lentivirus system was used in this study. It is a commercial toolkit that provides pre-made lentiviral particles, expressing specific kinds of luciferase and fluorescent proteins. Particles are in a high titre concentration in phosphate buffer solution (PBS) without any human or animal origin components. Virus in PBS solution is good for any cell type that requires non-serum media in the application. This is also a requirement for stem cell transduction where the presence of serum components can induce differentiation (Hager et al., 2008). The luciferase is expressed under a re-engineered EF1a promoter, which is non-tissue specific, highly expressed in all cell types and less likely to be silenced after long-term culture. Promoter silencing is a common feature of lentiviral vectors, which express transgenes from a strong viral promoter, like cytomegalovirus (CMV) (Frame et al., 2010). The fluorescent protein is also expressed under the same promoter. Together with luciferase they are expressed as individual proteins and not as fusions. Under a separate Rous sarcoma virus (RSV) promoter, each particle also contains an antibiotic marker, Blasticidin (Bsd). Figure 5.1 illustrates the vector map of a typical AMSBio™ lentivector used in this study. Transduced cells can be sorted via flow cytometry after established culture.

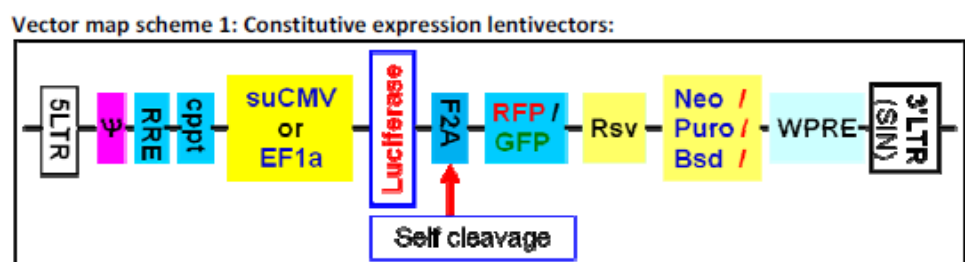


Figure 5.1: Luciferase can be expressed using the suCMV or EF1a promoter. The F2A element mediates the expression of the fluorescent marker and each particle also contains an antibiotic under the RSV promoter. Incorporation of Woodchuck Posttranscriptional Regulatory Element, (WPRE) from the woodchuck hepatitis virus, a central polypurine tract (cppt) and a Rev Responsive Element (RRE) into lentivirus vectors provide increased transduction efficiency and transgene expression. Long terminal repeats (LTRs) are identical sequences of DNA that repeat hundreds or thousands of times found at either ends. They are used by viruses to insert their genetic material into the host genomes. (Adapted from <http://www.amsbio.co.uk/datasheets>)

The incentive for using luciferase in this study was the added benefit of performing in vivo tracking of biological processes with D-luciferin. This is a powerful technique to track cell populations in mice (Greer and Szalay, 2002). It involves non-invasive visualisation inside a live mouse using a light sensitive apparatus (IVIS) after intraperitoneal injection of the substrate, D-luciferin. Luciferase catalyses the luciferin/ATP and luciferyl adenylate/oxygen reactions in tissues producing light emission which can be captured (Gould and Subramani, 1988). Carcinogenesis and response to tumour treatment can be followed in this way (Becher and Holland, 2006, Lyons et al., 2003).

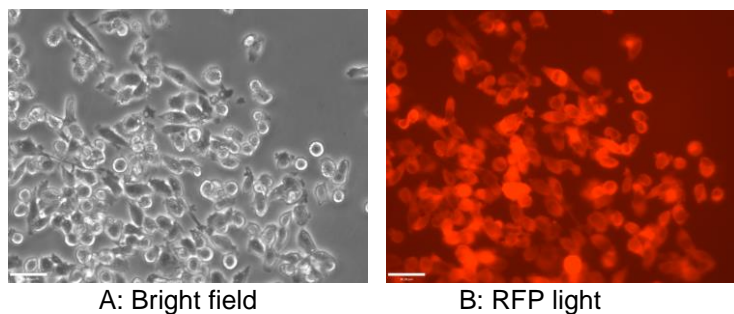
5.3 Generation of clonal, lentivirus transduced PC3 cell lines

The PC3 cell line was derived from bone metastasis of a high-grade prostate cancer of a 62 year old Caucasian male (Kaighn et al., 1979). PC3 cells have a high metastatic potential compared to other commonly used cell lines. They readily generate tumours in mice even when implanted at low cell numbers (Pulukuri et al., 2005).

An unselected population of PC3 cells was infected with an AM5Bio lentiviral expression cassette containing the EF1a-Luciferase- α -RFP indicator protein. Infections were performed from crude virus stocks for two hours with 1×10^5 PC3 cells. Pure populations of lentivirus transduced cells were selected by supplementing the culture media with 4 μ g/ml Blasticidin. Colonies consisted of rounded, loosely packed cells of variable size. However, they showed good expression from the transgene RFP (Figure 5.2) compared to negative controls.

To establish expression of a lentiviral transgene, the virus DNA must integrate into the cell chromosome (target DNA), which occurs in a semi-random fashion. Therefore, every PC3 cell genome would have been transduced at a different position (Laufs et al., 2006). Since the expression levels of lentivirus delivered transgenes are subject to positional effects (Ellis and Yao, 2005), a clonal selection of the PC3 cells was performed. Colonies consisting of smooth outlined, tightly packed cells with more uniform shapes highly expressing RFP were selected (Figure 5.3).

Transduced PC3 cells



Negative PC3 cells control

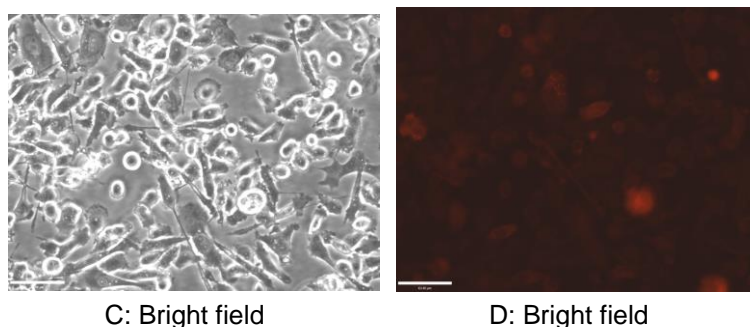


Figure 5.2: **Transduced PC3 cells post Blasticidin selection.** PC3 cells were infected with the AMSBio lentivirus containing an EF1a-RFP expression cassette. Infected cells were selected in the presence of 4 μ g/ml Blasticidin 2 days after transduction. Photographs were taken 13 days after selection and media was changed every 3 days. Cells were seen to express RFP (B) compared to negative PC3 control (D) in which non-specific auto-fluorescence could be seen. Images were taken using a Nikon Eclipse TE300 fluorescent microscope (Nikon, Surrey, UK) at x200 magnification with scale bars representing 90 μ m.

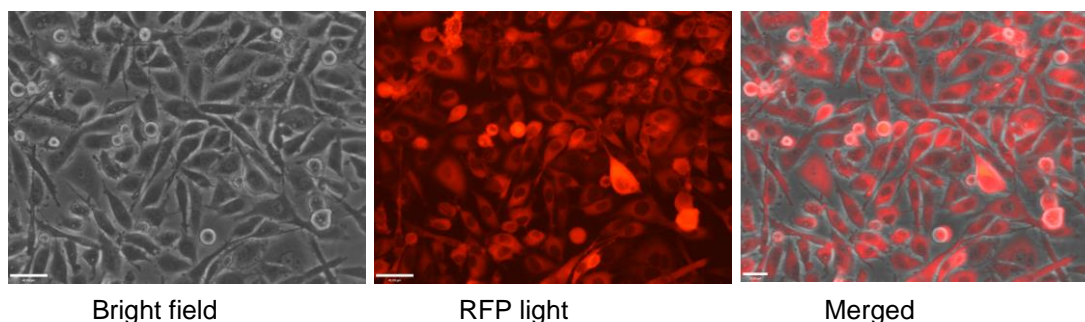


Figure 5.3: **Clonal selection of transduced PC3 cells.** Lentivirus-infected and Blasticidin selected PC3 cells formed colonies after plating. Photographs of colonies originating from EF1a-RFP PC3 cells (p6.4) were taken under bright light, RFP filter and merged. Passage number: p (total number of passages).(number of passages since lentivirus infection). Images were taken using a Nikon Eclipse TE300 fluorescent microscope (Nikon, Surrey, UK) at x200 magnification with scale bars representing 90 μ m.

5.4 Tumour initiation with transduced PC3 cells

Transduced PC3 cells were mixed with matrigel and injected subcutaneously in Rag2 $\gamma^{-/-}$ C $\gamma^{-/-}$ mice. Tumours started to appear after 31 days and grew at the same rate as untransduced PC3 tumours (data from previous experiments not shown). The mice were euthanised once tumour size reached 15mm. Some of the tumour tissue was put directly on a dish with media (explant) and examined under the fluorescent microscope (Figure 5.4). Various layers of cells were present, which appeared rounded, loosely packed, and not forming colonies. However, RFP was still present indicating stable integration (Fig 5.4 A, B) compared to an explant from an untransduced PC3 tumour as negative control (Fig 5.4 C, D).

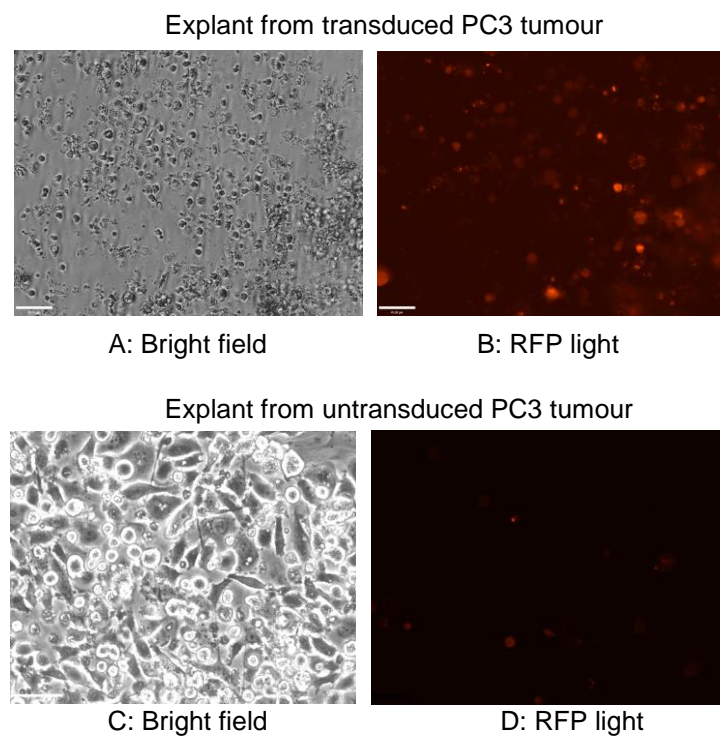


Figure 5.4: **Explant of a transduced PC3 tumour.** A piece of tumour was explanted directly in culture media. Cells were present in various layers and started spreading out after culture. Photographs were taken 4 days after explant under bright light, RFP filter and merged. A and B: Persistent expression of RFP fluorescent marker following in PC3 tumour growth. C and D: Explant from an untransduced PC3 tumour used as a negative control. Images were taken using a Nikon Eclipse TE300 fluorescent microscope (Nikon, Surrey, UK) at x200 magnification with scale bars representing 90 μ m.

5.5 Flow cytometry analysis of transduced PC3 tumours

The tumours were dissociated and the resultant LIN-/CD31- cells were analysed for RFP expression with fluorescence-activated cell sorting (FACS). There were a high proportion of RFP positive cells representing 62.9% of the overall cells present (Figure 5.5, rectangle R5). Untransduced PC3 cells were used as negative controls showing the absence of RFP expression (rectangle R5 in Figure 5.6). Successfully transduced clonal PC3 cells (cells from Figure 5.3) were used as positive control showing very high RFP expression (Figure 5.7, rectangle R5 with 99.6% positive cells).

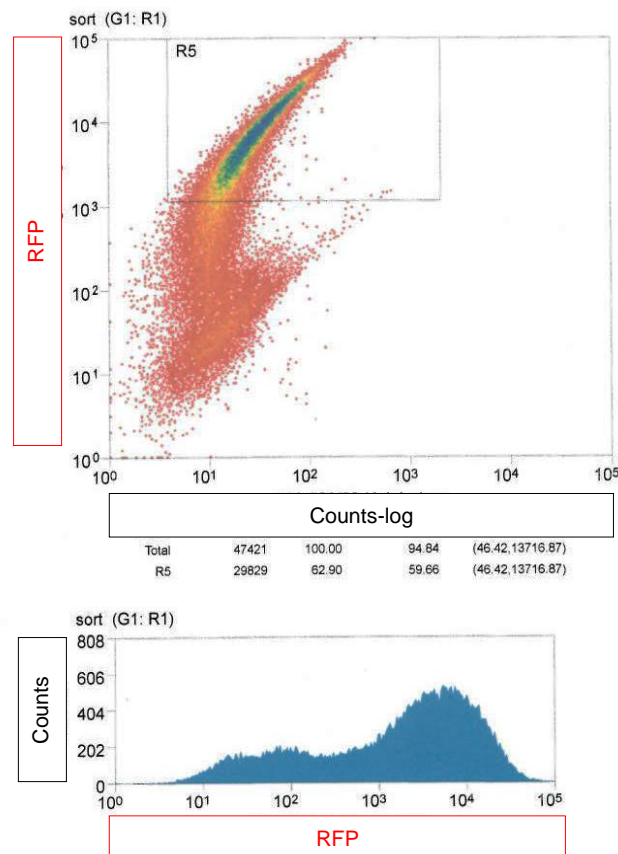


Figure 5.5: **Flow cytometry analysis of transduced PC3 cells.** Transduced PC3 cells expressed high levels of RFP with 62.9% of cells present in the R5 region. There was a significant shift of the positive cell population on the histogram below.

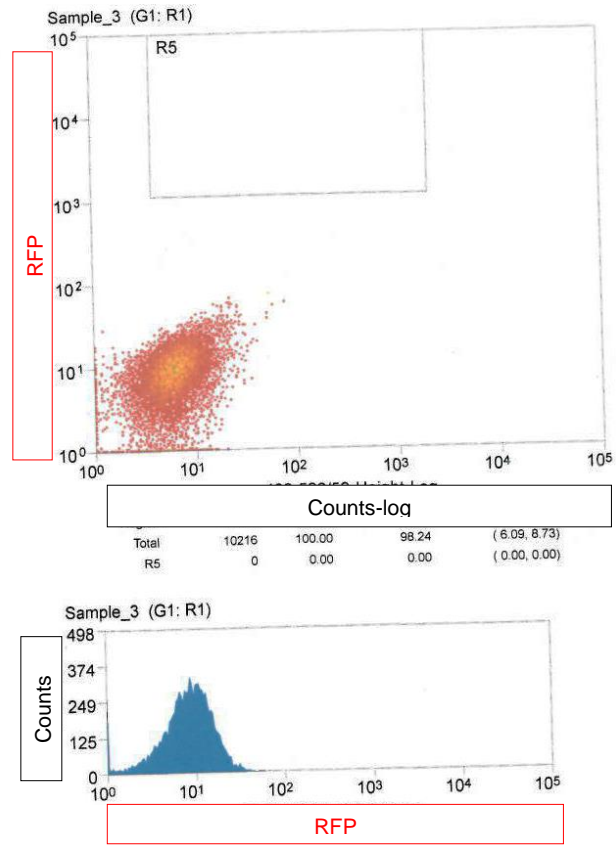


Figure 5.6: **Flow cytometry analysis of untransduced PC3 cells as negative controls.** PC3 cells were analysed in parallel showing no RFP positive cells (the R5 rectangle represented the area where RFP emission spectrum should be). No shift of population was seen in the histogram below.

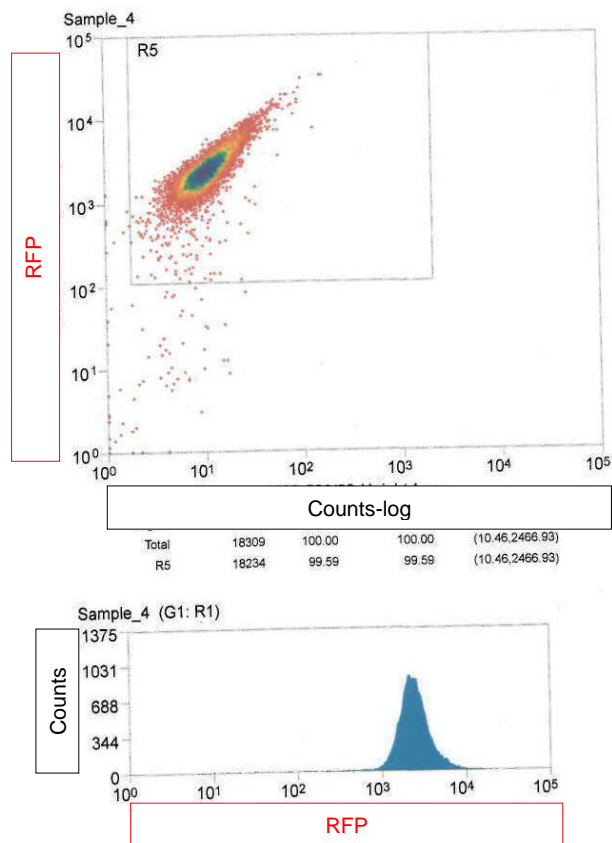


Figure 5.7: **Flow cytometry analysis of transduced PC3 clones as positive controls.** PC3 clones which had never been grafted in mice were used as positive controls. They were analysed in parallel showing very high RFP positive cells, rectangle R5 contained 99.6% of the cells. This is confirmed on the single population seen on the histogram below and retention of the original, high levels of RFP expression.

5.6 Generation of lentivirus transduced PDX cells

PDX Y042 was from a Gleason 3+4 adenocarcinoma of prostate and readily reproduced serially transplantable tumours at a low latency (Table 6). 4×10^4 (LIN-/CD31-) cells were transduced with AMsBio lentiviral particles for 2 hours. Figure 5.8 shows the transduced Y042 cells in culture media supplemented with 4 μ g/ml Blasticidin compared to Y042 cells, which were not transduced (negative control). The two did not look different under the RFP filter or bright field under the microscope. Successful RFP integration was not achieved (as further confirmed with FACS analysis, section 5.8) and the derivation of stable Y042 transduced cells was unsuccessful. These cells were hard to culture in vitro. They did not actively divide and did not adhere to the culture flasks.

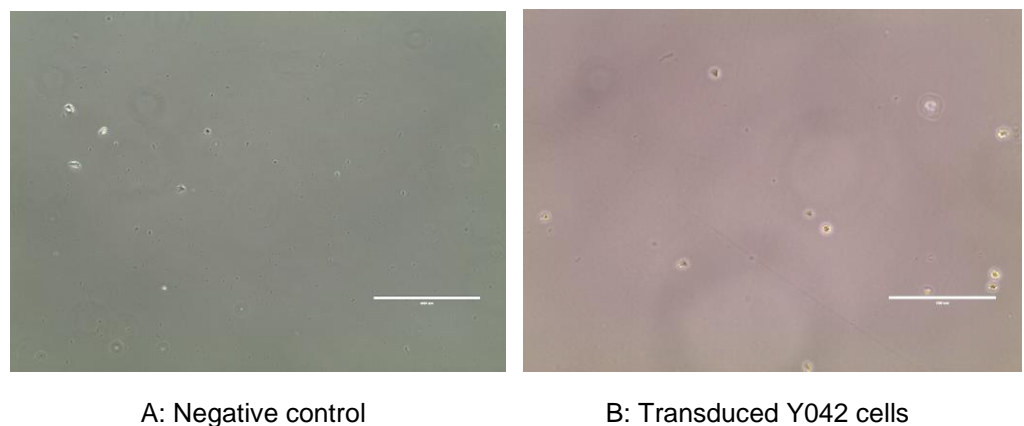


Figure 5.8: **Lentivirus transduction of Y042 PDX cells.** A: Untransduced LIN-/CD31- Y042 cells were used as negative control. B: Y042 cells after 2hrs transduction with the EF1a-Luciferase-A-RFP lentivirus. These cells were very difficult to grow on a culture dish. They remained floating, loosely packed without forming colonies or actively dividing but stayed alive. No RFP integration was seen despite the culture media supplemented with 4 μ g/ml Blasticidin. Photographs were taken using RFP light on a Nikon Eclipse TE300 fluorescent microscope (Nikon, Surrey, UK) at x200 magnification with scale bars representing 100 μ m.

5.7 Tumour initiation with transduced Y042 cells

After transduction, Y042 cells were mixed in matrigel and injected subcutaneously in mice. Tumours grew at the same rate as untransduced Y042 cells (data from previous experiments, section 4.6) and the first measurable tumours appeared after 16 days. Figure 5.9 shows explant pictures from the transduced Y042 tumours (Fig A, B) compared to untransduced Y042 tumour, negative control (Fig C, D). Explant tissues show various layers of cells, making it difficult to focus the microscope to give a clear image. Figures 5.9 A and B confirm no convincing RFP expression from transduced Y042 cells.

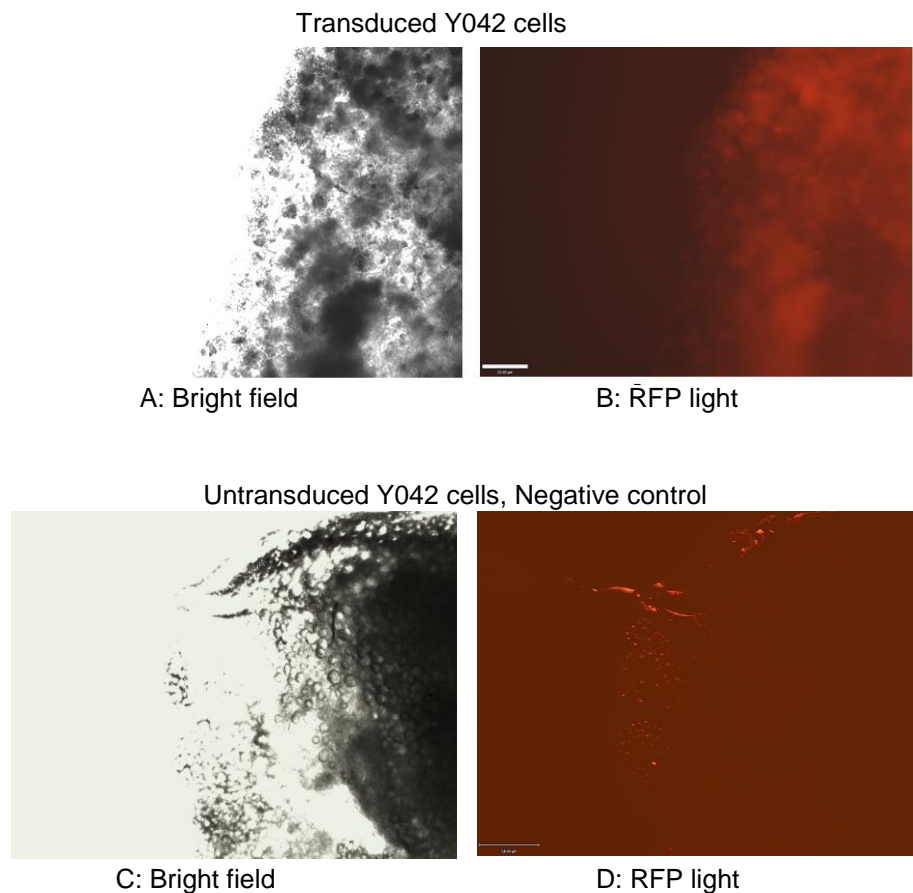


Figure 5.9: **Explant pictures.** A piece of freshly dissected tumour placed on a dish with media (explant) and analysed directly for RFP expression. B and D: non-specific red cells on the periphery of the explant, which represent auto-fluorescence under RFP light. They were not deemed to represent RFP expression as shown as in Fig 5.4B. Images were taken on a Nikon Eclipse TE300 fluorescent microscope (Nikon, Surrey, UK) at x10 magnification with scale bars representing 15 μ m.

5.8 Flow cytometry analysis of transduced Y042 tumours

The resultant Y042 tumours from section 5.7 were dissociated and the LIN-/CD31- cells analysed for RFP expression with FACS (Figure 5.10). No cells with high RFP expression were seen in polygon R3 compared to successfully transduced PC3 cells (positive control) in polygon R5 of Figure 5.10. There was also no shift in cell populations on the histogram (counts v/s RFP light) as seen in Figure 5.10B. Transduction of PDX cells did not lead to stable genomic integration of the RFP indicator protein although they still expressed tumour initiating capacity.

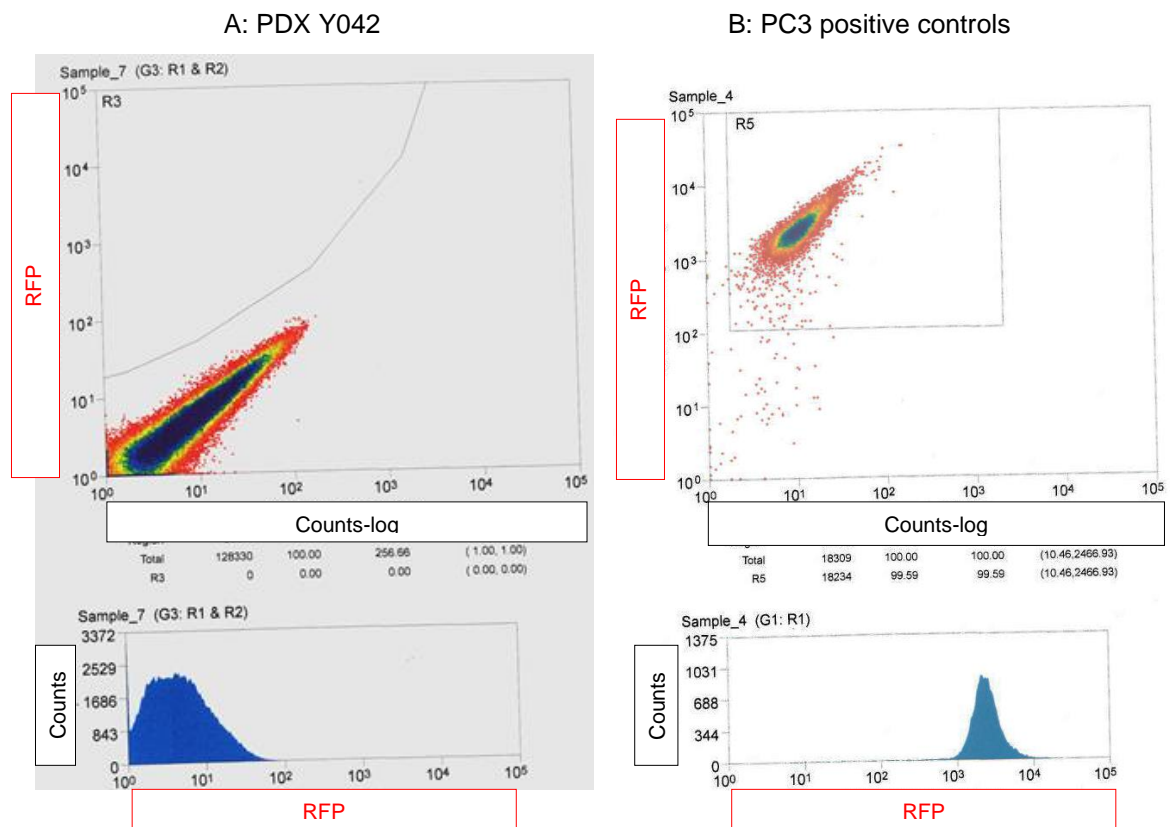


Figure 5.10: **LIN depleted Y042 tumour analysed by flow cytometry.** No RFP positive cells were detected in the R3 polygon, which represent the area where the RFP emission spectrum should be. In the PC3 positive controls there was a significant shift in cell population in the histogram below.

5.9 Discussion

The aim of this section of my research was to develop lentiviral transduced PDX cells, which could be transplanted to track early metastatic spread. Lentiviruses possess the ability to stably integrate into the genome of host cells, allowing long-term and stable transgene expression (Bukrinsky et al., 1992). Lentivirus transduction succeeded in PC3 cells with high genomic integration of the RFP fluorescent marker giving high expression (Figure 5.2). However, the Y042 PDX cells transduction proved more challenging. In fact no integration was apparent in these cells (Figure 5.8). It is possible that the transcription units have not integrated into the host genome even with a lentivirus to cell ratio of 5 to 1. Primary prostate epithelial cells have been proposed to originate from stem cells, which can differentiate into transit-amplifying cells, committed basal cells and terminally differentiated luminal cells (Collins et al., 2005, Richardson et al., 2004). It is important to target the stem cells before differentiation. However, they are significantly rare. This lentivirus might not have targeted the stem cells. Using differentiation stage-specific promoters, which become active when the stem cells differentiate has been recently investigated (Frame et al., 2010) and might be a potential development in PDX transduction. Frame et al. showed successful infection of stem cells and activation of late-stage promoters including prostate stem cell antigen (PSCA) and prostate specific antigen/probasin (PSA/Pb) in basal epithelial cultures following induction of differentiation.

High transgene expression from the lentivirus-delivered expression cassette is hindered by the promoter inactivation through methylation and changes in chromatin structure (Ellis and Yao, 2005, Xia et al., 2007, Zhang et al., 2007). In fact these gene delivery systems are commonly cloned without a polyadenylation signal to prevent disruption of full-length lentiviral genomes on mRNA maturation (Hager et al., 2008). Hager et al. showed a 3 to 6.5-fold increase in indicator protein expression in primary prostate epithelial cells when an internal polyadenylation signal was present. They also showed a 8 to 9-fold decrease of functional viral titre when the CMV and EF1a promoters were used in the presence of polyadenylation but titre was not affected when a β -actin and tissue specific

PSA/Pb were used. EF1a was the lentiviral promoter used in my experiments and it could have been silenced. Introducing a polyadenylation signal could considerably enhance transgene expression levels in the AMSBio lentiviral system. But particular attention has to be given to which promoter is being used.

In PDX cells there could also have been a global silencing of the integrated proviruses as this is thought to be an evolved mechanism to preserve the integrity of a cell's genetic information (Ellis and Yao, 2005, Pannell et al., 2000). Silencing of transgene expression can happen on a specific portion of the virus genome and can be the result of an unfavourable interaction between expression cassettes in multigene constructs (Emerman and Temin, 1984a, Emerman and Temin, 1984b). Indeed, in the AMSBio lentiviral system, the RSV-bsd resistant gene cassette was positioned downstream (3') of the EF1a transgene expression cassette (5') (Figure 5.1). It is possible that interference between the EF1a promoter (driving RFP expression) and the RSV promoter (driving blasticidin resistance) in the Y042 cells created selective pressure for inactivation when blasticidin selection was applied. However the method worked in PC3 cells and interference is less likely to explain the failure to transduce Y042 cells. But these cells are hard to culture in vitro. They do not actively divide and usually do not adhere to the culture flask as shown in figure 5.8. They could also be in a permanent G0 phase, which inherently is difficult to transduce. But it should be possible for lentiviruses to stably integrate non-dividing as well as terminally differentiated cells unlike retroviruses, which require cell division (Bukrinsky et al., 1993, Lewis and Emerman, 1994, Naldini et al., 1996).

Another explanation could be the inactivation of the fluorescent indicator protein due to toxicity of RFP. The latter was chosen as prostate cells elicit green auto fluorescence and therefore could easily be distinguished between. Indicator protein toxicity could be accounted by studies that have demonstrated the enhanced green fluorescent protein (EGFP) to disturb physiological processes and trigger apoptosis in mammalian cells (Baens et al., 2006, Liu et al., 1999). Therefore, other fluorescent markers might cause similar toxic effects and could be inactivated to confer growth advantage to the Y042 PDX cells. Of note, they yielded tumours at an unaltered rate to untransduced Y042 cells.

When using two expression cassettes within a single construct, problems have been frequently reported with interference between the two transcriptional units leading to unsatisfactory expression levels (Curtin et al., 2008, Eszterhas et al., 2002). Interference might have been a determining factor in the Y042 cells but convincing presence of RFP in PC3 cells makes this explanation unlikely.

Modifications according to the above explanation and further transduction attempts were planned, however, infections of cells generated from the FACS cell sorter (MoFlo, Astrios machine) affected several of my experiments and proved to be recurrent. This was a recognised problem from the supplying company and they made several internal modifications to the machine after quite a few months. Nevertheless, further experiments on this study were hampered due to the time taken to fix the MoFlo, Astrios. At the moment, the company are in the process of paying compensation back to the University of York and our lab for the liability caused. Therefore, after discussion with my supervisor and the thesis advisory panel (TAP), I decided to concentrate on the other sections of this study rather than taking this section of my research further.

5.10 Conclusion

The lentivirus used in this study is suitable for use in the PC3 cell line. The successfully transduced PC3 cells could be used for the live monitoring of prostate cancer progression in vivo and treatment strategies to hinder its spread. However, further optimisation is required in PDX cells before developing their diagnostic applications in tracking metastasis spread.

CHAPTER 6

FINAL DISCUSSION AND CONCLUSION

6.1 Final Discussion

The treatment of men with CRPC has evolved in the recent decades, based on a better understanding of the mechanisms of castrate resistance (Sonpavde et al., 2015). In 2004, docetaxel was approved for first line treatment of metastatic CRPC and was the first agent to prolong survival in patients with this disease (Tannock et al., 2004). Since 2010, there are several new agents available, although docetaxel chemotherapy continues to play an important role. However its timing may inevitably be affected due to the better adverse effects profile of the newer agents. Patient selection is therefore going to be very important in determining the optimal sequence of treatments as this remains undefined and requires further study.

Targeting the AR with abiraterone or enzalutamide improves survival in CRPC (de Bono et al., 2011, Scher et al., 2012), but resistance eventually develops and the response rate to sequential treatment appears lower when one agent is used after the other (Bianchini et al., 2014). A major question currently is whether AR-based progression is a predominant mechanism mediating resistance or whether CSCs are more responsible. CSCs are impervious to the start of ADT and are capable of regenerating the tumour mass (Collins et al., 2005). PDXs from hormone naïve and CRPC samples represent a good way to study CSC as a lot of the 'founder' characteristics are represented. They provide the opportunity to non-invasively and repeatedly sample tumour cells and thus can provide information concerning molecular interactions, tumour heterogeneity and changes that occur with treatment in PC.

I found that, basal and luminal cell markers in subcutaneous PDXs (compared to orthotopic PDX) were adequately expressed for conclusions to be possible when looking at treatment effects. A higher group number (n) could also be achieved which was not the case in the orthotopic method as it took considerable time to set up experiments in the latter method. By successfully engrafting several PDXs orthotopically and I showed that the tumour take rate was similar to the subcutaneous route with a reasonable latency period. Since fresh metastatic biopsy samples from living CRPC patients have been limited due to the

challenges in obtaining adequate tumour tissue, orthotopic PDXs represent a promising way to study metastatic spread in future.

The mechanisms that underlie resistance to docetaxel resistance and how to overcome these are largely unknown. Our data suggests that sensitivity to docetaxel is either pre-existing or starts very early (in the CSCs) and does not need the presence of androgen ablation. Some cancer cells may also already be predestined to be sensitive to docetaxel. The high presence of basal cells seems to confer docetaxel resistance, especially when they are predominantly present. Resistance could be intrinsic to certain tumours, which could explain why not all patients show response to docetaxel.

Even though some patients show sensitivity to docetaxel, eventually resistance develops through various mechanisms and there is also the potential for cross-resistance between different drug classes if used concomitantly. The PDXs responses to docetaxel mirror this. It is unknown whether treating patients with hormone therapies affects their subsequent response to chemotherapy. Recent reports suggest that tubulin-targeting drugs may be active, at least in part through cytoplasmic AR sequestration (Jiang and Huang, 2010). Another study has shown nuclear accumulation of the forkhead transcription factor family member (FOXO1, a potent repressor of AR function) with docetaxel treatment (Kuroda et al., 2009). In vitro data have also shown that docetaxel, cabazitaxel, abiraterone and enzalutamide all inhibit AR nuclear translocation (van Soest et al., 2013). Given that both taxanes and androgen targeting agents disrupts AR signalling, these data may have clinical implications when combining these drugs as proposed by the STAMPEDE and CHARTED trial. Cross-resistance also exists between abiraterone and enzalutamide (Schrader et al., 2014). Hence whilst some men will respond to docetaxel upfront, their chances on second line chemotherapy or AR axis inhibitors could become limited. In this setting, our PDX model could be useful in this assessing the cross-resistance mechanisms suggested.

6.2 Conclusion and Future Trends

The optimal sequence of treatment and timing of chemotherapy in advanced prostate cancer is unknown. There is no clear method to select treatment or treatment sequences for individual patients to maximise survival. Systemic chemotherapy remains an important therapeutic method although their toxicity can reduce the window of intervention. The strategy of implementing the most feasible sequence that permits the administration of all active agents should be adopted (Sonpavde et al., 2015).

To further improve patient outcomes with chemotherapy, several studies have looked at combining docetaxel with other biological agents. The RTOG 0521 (Radiation Therapy Oncology Group) trial looked at chemotherapy in locally advanced, non-metastatic, hormone naïve PC. It has shown improvement in OS when docetaxel was given after standard radiation therapy along with 2 years of ADT (Sandler, 2015). This is the first adjuvant chemotherapy trial for locally advanced PC showing reduction in recurrence and reduction in distant metastases. In this setting, the PDX model can help to decide whether this study will lead to routine use of adjuvant docetaxel to primary standard therapy.

Two phase II trials have looked at combination of platinum based chemotherapy with taxanes as second line chemotherapy following docetaxel failure (Lee et al., 2014, Ross et al., 2008). They showed that a subset of patients with mCRPC could be still responsive. As our models have potentially generated docetaxel resistant PDXs, they can be used to test new combinations and provide valuable information in setting up future clinical trials.

Finally, the PDX model can help in predicting treatment responses for a specific patient if there is enough time between establishing his xenograft and his clinical relapse of disease progressing to mCRPC. We can then test the possible sequences in vivo and evaluate which one is best suited for him. They are a better representation of the actual patients' tumour and hence can provide credible results to guide treatment.

REFERENCES

- ABATE-SHEN, C. & SHEN, M. M. 2002. Mouse models of prostate carcinogenesis. *Trends Genet*, 18, S1-5.
- ARAGON-CHING, J. B., WILLIAMS, K. M. & GULLEY, J. L. 2007. Impact of androgen-deprivation therapy on the immune system: implications for combination therapy of prostate cancer. *Front Biosci*, 12, 4957-71.
- AUMULLER, G. 1991. Postnatal development of the prostate. *Bull Assoc Anat (Nancy)*, 75, 39-42.
- AYRES, B. E., MONTGOMERY, B. S., BARBER, N. J., PEREIRA, N., LANGLEY, S. E., DENHAM, P. & BOTT, S. R. 2012. The role of transperineal template prostate biopsies in restaging men with prostate cancer managed by active surveillance. *BJU Int*, 109, 1170-6.
- BAENS, M., NOELS, H., BROECKX, V., HAGENS, S., FEVERY, S., BILLIAU, A. D., VANKELECOM, H. & MARYNEN, P. 2006. The dark side of EGFP: defective polyubiquitination. *PLoS One*, 1, e54.
- BANSAL, N. & BANERJEE, D. 2009. Tumor initiating cells. *Curr Pharm Biotechnol*, 10, 192-6.
- BARQAWI, A. B., STOIMENOVA, D., KRUGHOFF, K., EID, K., O'DONNELL, C., PHILLIPS, J. M. & CRAWFORD, E. D. 2014. Targeted Focal Therapy for the Management of Organ Confined Prostate Cancer. *J Urol*.
- BECHER, O. J. & HOLLAND, E. C. 2006. Genetically engineered models have advantages over xenografts for preclinical studies. *Cancer Res*, 66, 3355-8, discussion 3358-9.
- BEER T.M, A. A. J., STERNBERG C.N, HIGANO C.S, PETER IVERSEN, YOHANN LORIOT, DANA E. RATHKOPF, SUMAN BHATTACHARYA, JOAN CARLES, JOHANN S. DE BONO, CHRISTOPHER P. EVANS, ANTHONY M. JOSHUA, CHOUNG-SOO KIM, GO KIMURA, PAUL N. MAINWARING, HARRY H. MANSBACH, KURT MILLER, SARAH B. NOONBERG, PETER M. VENNER, BERTRAND TOMBAL 2014. Enzalutamide in men with chemotherapy-naive metastatic prostate cancer (mCRPC): results of phase III PREVAIL study. *Clin Adv Hematol Oncol*, 12, 3-4.
- BEN-SHLOMO, Y., EVANS, S., IBRAHIM, F., PATEL, B., ANSON, K., CHINEGWUNDOH, F., CORBISHLEY, C., DORLING, D., THOMAS, B., GILLATT, D., KIRBY, R., MUIR, G., NARGUND, V., POPERT, R., METCALFE, C., PERSAD, R. & GROUP, P. S. 2008. The risk of prostate cancer amongst black men in the United Kingdom: the PROCESS cohort study. *Eur Urol*, 53, 99-105.
- BERRY, W., DAKHIL, S., MODIANO, M., GREGURICH, M. & ASMAR, L. 2002. Phase III study of mitoxantrone plus low dose prednisone versus low dose prednisone alone in patients with asymptomatic hormone refractory prostate cancer. *J Urol*, 168, 2439-43.
- BERTHON, P., CUSSENOT, O., HOPWOOD, L., LEDUC, A. & MAITLAND, N. 1995. Functional expression of sv40 in normal human prostatic epithelial and fibroblastic cells - differentiation pattern of nontumorigenic cell-lines. *Int J Oncol*, 6, 333-43.
- BIANCHINI, D., LORENTE, D., RODRIGUEZ-VIDA, A., OMLIN, A., PEZARO, C., FERRALDESCHI, R., ZIVI, A., ATTARD, G., CHOWDHURY, S. & DE BONO, J. S. 2014. Antitumour activity of enzalutamide (MDV3100) in patients with metastatic castration-resistant prostate cancer (CRPC) pre-treated with docetaxel and abiraterone. *Eur J Cancer*, 50, 78-84.
- BLANPAIN, C., LOWRY, W. E., GEOGHEGAN, A., POLAK, L. & FUCHS, E. 2004. Self-renewal, multipotency, and the existence of two cell populations within an epithelial stem cell niche. *Cell*, 118, 635-48.
- BLO, M., MICKLEM, D. R. & LORENS, J. B. 2008. Enhanced gene expression from retroviral vectors. *BMC Biotechnol*, 8, 19.
- BOLLA, M., COLLETTE, L., BLANK, L., WARDE, P., DUBOIS, J. B., MIRIMANOFF, R. O., STORME, G., BERNIER, J., KUTEN, A., STERNBERG, C., MATTELAER, J., LOPEZ TORECILLA, J., PFEFFER, J. R., LINO CUTAJAR, C., ZURLO, A. & PIERART, M. 2002. Long-term results with immediate androgen suppression and external irradiation in patients with locally advanced prostate cancer (an EORTC study): a phase III randomised trial. *Lancet*, 360, 103-6.

- BONNET, D. & DICK, J. E. 1997. Human acute myeloid leukemia is organized as a hierarchy that originates from a primitive hematopoietic cell. *Nat Med*, 3, 730-7.
- BOSMA, M. J. & CARROLL, A. M. 1991. The SCID mouse mutant: definition, characterization, and potential uses. *Annu Rev Immunol*, 9, 323-50.
- BOWER, M. & WAXMAN, J. 2010. *Lecture Notes: Oncology*, Wiley-Blackwell.
- BOYLE, P. & FERLAY, J. 2005. Cancer incidence and mortality in Europe, 2004. *Ann Oncol*, 16, 481-8.
- BROOKE, G. N. & BEVAN, C. L. 2009. The role of androgen receptor mutations in prostate cancer progression. *Curr Genomics*, 10, 18-25.
- BUKRINSKY, M. I., HAGGERTY, S., DEMPSEY, M. P., SHAROVA, N., ADZHUBEL, A., SPITZ, L., LEWIS, P., GOLDFARB, D., EMERMAN, M. & STEVENSON, M. 1993. A nuclear localization signal within HIV-1 matrix protein that governs infection of non-dividing cells. *Nature*, 365, 666-9.
- BUKRINSKY, M. I., SHAROVA, N., DEMPSEY, M. P., STANWICK, T. L., BUKRINSKAYA, A. G., HAGGERTY, S. & STEVENSON, M. 1992. Active nuclear import of human immunodeficiency virus type 1 preintegration complexes. *Proc Natl Acad Sci U S A*, 89, 6580-4.
- BUONERBA, C., POND, G. R., SONPAVDE, G., FEDERICO, P., RESCIGNO, P., PUGLIA, L., BOSSO, D., VIRTUOSO, A., POLICASTRO, T., IZZO, M., VACCARO, L., FERRO, M., AIETA, M., PERDONA, S., PALMIERI, G., DE PLACIDO, S. & DI LORENZO, G. 2013. Potential value of Gleason score in predicting the benefit of cabazitaxel in metastatic castration-resistant prostate cancer. *Future Oncol*, 9, 889-97.
- CHEUNG, F. Y., LEUNG, K. C. & NGAN, R. K. 2013. Docetaxel chemotherapy for Chinese patients with castrate-resistant prostate cancer. *Hong Kong Med J*, 19, 237-41.
- CHOI, N., ZHANG, B., ZHANG, L., ITTMANN, M. & XIN, L. 2012. Adult murine prostate basal and luminal cells are self-sustained lineages that can both serve as targets for prostate cancer initiation. *Cancer Cell*, 21, 253-65.
- CHU, P. G. & WEISS, L. M. 2002. Keratin expression in human tissues and neoplasms. *Histopathology*, 40, 403-39.
- CHUNG, L. W. K., ISAACS, W. B. & SIMONS, J. W. 2007. *Prostate cancer : biology, genetics, and the new therapeutics*, Totowa, N.J., Humana Press.
- CLARKE, S. J. & RIVORY, L. P. 1999. Clinical pharmacokinetics of docetaxel. *Clin Pharmacokinet*, 36, 99-114.
- COHEN, R. J., SHANNON, B. A., PHILLIPS, M., MOORIN, R. E., WHEELER, T. M. & GARRETT, K. L. 2008. Central zone carcinoma of the prostate gland: a distinct tumor type with poor prognostic features. *J Urol*, 179, 1762-7; discussion 1767.
- COLEMAN, R. A., P-A; HADJI, P 2012. *Handbook od cancer-related bone disease*, Bristol UK, BioScientifica.
- COLEMAN, R. E. 2006. Clinical features of metastatic bone disease and risk of skeletal morbidity. *Clin Cancer Res*, 12, 6243s-6249s.
- COLLINS, A. T., BERRY, P. A., HYDE, C., STOWER, M. J. & MAITLAND, N. J. 2005. Prospective identification of tumorigenic prostate cancer stem cells. *Cancer Res*, 65, 10946-51.
- COLLINS, A. T., HABIB, F. K., MAITLAND, N. J. & NEAL, D. E. 2001. Identification and isolation of human prostate epithelial stem cells based on alpha(2)beta(1)-integrin expression. *J Cell Sci*, 114, 3865-72.
- COLLINS, A. T. & MAITLAND, N. J. 2006. Prostate cancer stem cells. *Eur J Cancer*, 42, 1213-8.
- COOKSON, M. S., ROTH, B. J., DAHM, P., ENGSTROM, C., FREEDLAND, S. J., HUSSAIN, M., LIN, D. W., LOWRANCE, W. T., MURAD, M. H., OH, W. K., PENSON, D. F. & KIBEL, A. S. 2013. Castration-resistant prostate cancer: AUA Guideline. *J Urol*, 190, 429-38.
- COOPERBERG, M. R., BROERING, J. M. & CARROLL, P. R. 2009. Risk assessment for prostate cancer metastasis and mortality at the time of diagnosis. *J Natl Cancer Inst*, 101, 878-87.
- COOPERBERG, M. R., PASTA, D. J., ELKIN, E. P., LITWIN, M. S., LATINI, D. M., DU CHANE, J. & CARROLL, P. R. 2005. The University of California, San Francisco Cancer of the Prostate Risk

- Assessment score: a straightforward and reliable preoperative predictor of disease recurrence after radical prostatectomy. *J Urol*, 173, 1938-42.
- COOPERBERG, M. R., SIMKO, J. P., COWAN, J. E., REID, J. E., DJALILVAND, A., BHATNAGAR, S., GUTIN, A., LANCHBURY, J. S., SWANSON, G. P., STONE, S. & CARROLL, P. R. 2013. Validation of a cell-cycle progression gene panel to improve risk stratification in a contemporary prostatectomy cohort. *J Clin Oncol*, 31, 1428-34.
- COREY, E., QUINN, J. E. & VESSELLA, R. L. 2003. A novel method of generating prostate cancer metastases from orthotopic implants. *Prostate*, 56, 110-4.
- CRAMER, S. D. 2013. *Stem cells and prostate cancer*, New York, Springer.
- CRUK. 2012. *Cancer Research UK statistics* [Online]. Available: <http://www.cancerresearchuk.org/>.
- CURTIN, J. A., DANE, A. P., SWANSON, A., ALEXANDER, I. E. & GINN, S. L. 2008. Bidirectional promoter interference between two widely used internal heterologous promoters in a late-generation lentiviral construct. *Gene Ther*, 15, 384-90.
- D'AMICO, A. V., WHITTINGTON, R., MALKOWICZ, S. B., SCHULTZ, D., BLANK, K., BRODERICK, G. A., TOMASZEWSKI, J. E., RENSCHAW, A. A., KAPLAN, I., BEARD, C. J. & WEIN, A. 1998. Biochemical outcome after radical prostatectomy, external beam radiation therapy, or interstitial radiation therapy for clinically localized prostate cancer. *JAMA*, 280, 969-74.
- DANIEL, V. C., MARCHIONNI, L., HIEMAN, J. S., RHODES, J. T., DEVEREUX, W. L., RUDIN, C. M., YUNG, R., PARMIGIANI, G., DORSCH, M., PEACOCK, C. D. & WATKINS, D. N. 2009. A primary xenograft model of small-cell lung cancer reveals irreversible changes in gene expression imposed by culture in vitro. *Cancer Res*, 69, 3364-73.
- DAVIS, J. W. 2014. Novel commercially available genomic tests for prostate cancer: a roadmap to understanding their clinical impact. *BJU Int*, 114, 320-2.
- DE BONO, J. S., LOGOTHETIS, C. J., MOLINA, A., FIZAZI, K., NORTH, S., CHU, L., CHI, K. N., JONES, R. J., GOODMAN, O. B., JR., SAAD, F., STAFFURTH, J. N., MAINWARING, P., HARLAND, S., FLAIG, T. W., HUTSON, T. E., CHENG, T., PATTERSON, H., HAINSWORTH, J. D., RYAN, C. J., STERNBERG, C. N., ELLARD, S. L., FLECHON, A., SALEH, M., SCHOLZ, M., EFSTATHIOU, E., ZIVI, A., BIANCHINI, D., LORIOT, Y., CHIEFFO, N., KHEOH, T., HAQQ, C. M., SCHER, H. I. & INVESTIGATORS, C.-A.-. 2011. Abiraterone and increased survival in metastatic prostate cancer. *N Engl J Med*, 364, 1995-2005.
- DE BONO, J. S., OUDARD, S., OZGUROGLU, M., HANSEN, S., MACHIELS, J. P., KOCAK, I., GRAVIS, G., BODROGI, I., MACKENZIE, M. J., SHEN, L., ROESSNER, M., GUPTA, S., SARTOR, A. O. & INVESTIGATORS, T. 2010. Prednisone plus cabazitaxel or mitoxantrone for metastatic castration-resistant prostate cancer progressing after docetaxel treatment: a randomised open-label trial. *Lancet*, 376, 1147-54.
- DE CREMOUX, P., JOURDAN-DA-SILVA, N., COUTURIER, J., TRAN-PERENNOU, C., SCHLEIERMACHER, G., FEHLBAUM, P., DOZ, F., MOSSERI, V., DELATTRE, O., KLIJANIENKO, J., VIELH, P. & MICHON, J. 2007. Role of chemotherapy resistance genes in outcome of neuroblastoma. *Pediatr Blood Cancer*, 48, 311-7.
- DE MARZO, A. M., DEWEESE, T. L., PLATZ, E. A., MEEKER, A. K., NAKAYAMA, M., EPSTEIN, J. I., ISAACS, W. B. & NELSON, W. G. 2004. Pathological and molecular mechanisms of prostate carcinogenesis: implications for diagnosis, detection, prevention, and treatment. *J Cell Biochem*, 91, 459-77.
- DE MARZO, A. M., MARCHI, V. L., EPSTEIN, J. I. & NELSON, W. G. 1999. Proliferative inflammatory atrophy of the prostate: implications for prostatic carcinogenesis. *Am J Pathol*, 155, 1985-92.
- DE MARZO, A. M., PLATZ, E. A., SUTCLIFFE, S., XU, J., GRONBERG, H., DRAKE, C. G., NAKAI, Y., ISAACS, W. B. & NELSON, W. G. 2007. Inflammation in prostate carcinogenesis. *Nat Rev Cancer*, 7, 256-69.
- DEKLERK, D. P. & COFFEY, D. S. 1978. Quantitative determination of prostatic epithelial and stromal hyperplasia by a new technique. Biomorphometrics. *Invest Urol*, 16, 240-5.

- EASTON, D. F., STEELE, L., FIELDS, P., ORMISTON, W., AVERILL, D., DALY, P. A., MCMANUS, R., NEUHAUSEN, S. L., FORD, D., WOOSTER, R., CANNON-ALBRIGHT, L. A., STRATTON, M. R. & GOLDGAR, D. E. 1997. Cancer risks in two large breast cancer families linked to BRCA2 on chromosome 13q12-13. *Am J Hum Genet*, 61, 120-8.
- EAU. 2014. *EAU Guidelines for Radical Prostatectomy* [Online]. Available: www.uroweb.org/guidelines/online-guidelines.
- EL-ALFY, M., PELLETIER, G., HERMO, L. S. & LABRIE, F. 2000. Unique features of the basal cells of human prostate epithelium. *Microsc Res Tech*, 51, 436-46.
- ELLIS, J. & YAO, S. 2005. Retrovirus silencing and vector design: relevance to normal and cancer stem cells? *Curr Gene Ther*, 5, 367-73.
- EMERMAN, M. & TEMIN, H. M. 1984a. Genes with promoters in retrovirus vectors can be independently suppressed by an epigenetic mechanism. *Cell*, 39, 449-67.
- EMERMAN, M. & TEMIN, H. M. 1984b. High-frequency deletion in recovered retrovirus vectors containing exogenous DNA with promoters. *J Virol*, 50, 42-9.
- EPSTEIN, J. I. 2010. An update of the Gleason grading system. *J Urol*, 183, 433-40.
- EPSTEIN, J. I. 2011. Prognostic significance of tumor volume in radical prostatectomy and needle biopsy specimens. *J Urol*, 186, 790-7.
- EPSTEIN, J. I., ALLSBROOK, W. C., JR., AMIN, M. B., EGEVAD, L. L. & COMMITTEE, I. G. 2005. The 2005 International Society of Urological Pathology (ISUP) Consensus Conference on Gleason Grading of Prostatic Carcinoma. *Am J Surg Pathol*, 29, 1228-42.
- ESZTERHAS, S. K., BOUHASSIRA, E. E., MARTIN, D. I. & FIERING, S. 2002. Transcriptional interference by independently regulated genes occurs in any relative arrangement of the genes and is influenced by chromosomal integration position. *Mol Cell Biol*, 22, 469-79.
- FELDMAN, B. J. & FELDMAN, D. 2001. The development of androgen-independent prostate cancer. *Nat Rev Cancer*, 1, 34-45.
- FICHTNER, I., ROLFF, J., SOONG, R., HOFFMANN, J., HAMMER, S., SOMMER, A., BECKER, M. & MERK, J. 2008. Establishment of patient-derived non-small cell lung cancer xenografts as models for the identification of predictive biomarkers. *Clin Cancer Res*, 14, 6456-68.
- FINLAN, L. E. & HUPP, T. R. 2007. p63: the phantom of the tumor suppressor. *Cell Cycle*, 6, 1062-71.
- FIZAZI, K., CARDUCCI, M., SMITH, M., DAMIAO, R., BROWN, J., KARSH, L., MILECKI, P., SHORE, N., RADER, M., WANG, H., JIANG, Q., TADROS, S., DANSEY, R. & GOESSL, C. 2011. Denosumab versus zoledronic acid for treatment of bone metastases in men with castration-resistant prostate cancer: a randomised, double-blind study. *Lancet*, 377, 813-22.
- FIZAZI, K., SCHER, H. I., MOLINA, A., LOGOTHETIS, C. J., CHI, K. N., JONES, R. J., STAFFURTH, J. N., NORTH, S., VOGELZANG, N. J., SAAD, F., MAINWARING, P., HARLAND, S., GOODMAN, O. B., JR., STERNBERG, C. N., LI, J. H., KHEOH, T., HAQQ, C. M., DE BONO, J. S. & INVESTIGATORS, C.-A.-. 2012. Abiraterone acetate for treatment of metastatic castration-resistant prostate cancer: final overall survival analysis of the COU-AA-301 randomised, double-blind, placebo-controlled phase 3 study. *Lancet Oncol*, 13, 983-92.
- FIZAZI, K., SIKES, C. R., KIM, J., YANG, J., MARTINEZ, L. A., OLIVE, M. C., LOGOTHETIS, C. J. & NAVONE, N. M. 2004. High efficacy of docetaxel with and without androgen deprivation and estramustine in preclinical models of advanced prostate cancer. *Anticancer Res*, 24, 2897-903.
- FRAME, F. M., HAGER, S., PELLACANI, D., STOWER, M. J., WALKER, H. F., BURNS, J. E., COLLINS, A. T. & MAITLAND, N. J. 2010. Development and limitations of lentivirus vectors as tools for tracking differentiation in prostate epithelial cells. *Exp Cell Res*, 316, 3161-71.
- GARBER, K. 2009. From human to mouse and back: 'tumorgraft' models surge in popularity. *J Natl Cancer Inst*, 101, 6-8.
- GEROLAMI, R., UCH, R., FAIVRE, J., GARCIA, S., HARDWIGSEN, J., CARDOSO, J., MATHIEU, S., BAGNIS, C., BRECHOT, C. & MANNONI, P. 2004. Herpes simplex virus thymidine kinase-mediated

- suicide gene therapy for hepatocellular carcinoma using HIV-1-derived lentiviral vectors. *J Hepatol*, 40, 291-7.
- GIMOTTY, P. A., VAN BELLE, P., ELDER, D. E., MURRY, T., MONTONE, K. T., XU, X., HOTZ, S., RAINES, S., MING, M. E., WAHL, P. & GUERRY, D. 2005. Biologic and prognostic significance of dermal Ki67 expression, mitoses, and tumorigenicity in thin invasive cutaneous melanoma. *J Clin Oncol*, 23, 8048-56.
- GINGRICH, J. R., BARRIOS, R. J., KATTAN, M. W., NAHM, H. S., FINEGOLD, M. J. & GREENBERG, N. M. 1997. Androgen-independent prostate cancer progression in the TRAMP model. *Cancer Res*, 57, 4687-91.
- GLEASON, D. F. 1966. Classification of prostatic carcinomas. *Cancer Chemother Rep*, 50, 125-8.
- GOLDMAN, J. P., BLUNDELL, M. P., LOPES, L., KINNON, C., DI SANTO, J. P. & THRASHER, A. J. 1998. Enhanced human cell engraftment in mice deficient in RAG2 and the common cytokine receptor gamma chain. *Br J Haematol*, 103, 335-42.
- GOLDSTEIN, A. S., DRAKE, J. M., BURNES, D. L., FINLEY, D. S., ZHANG, H., REITER, R. E., HUANG, J. & WITTE, O. N. 2011. Purification and direct transformation of epithelial progenitor cells from primary human prostate. *Nat Protoc*, 6, 656-67.
- GOTTE, M. & YIP, G. W. 2006. Heparanase, hyaluronan, and CD44 in cancers: a breast carcinoma perspective. *Cancer Res*, 66, 10233-7.
- GOULD, S. J. & SUBRAMANI, S. 1988. Firefly luciferase as a tool in molecular and cell biology. *Anal Biochem*, 175, 5-13.
- GRAVIS, G., FIZAZI, K., JOLY, F., OUDARD, S., PRIOU, F., ESTERNI, B., LATORZEFF, I., DELVA, R., KRAKOWSKI, I., LAGUERRE, B., ROLLAND, F., THEODORE, C., DEPLANQUE, G., FERRERO, J. M., POUESSEL, D., MOUREY, L., BEUZEBOC, P., ZANETTA, S., HABIBIAN, M., BERDAH, J. F., DAUBA, J., BACIUCHKA, M., PLATINI, C., LINASSIER, C., LABOUREY, J. L., MACHIELS, J. P., EL KOURI, C., RAVAUD, A., SUC, E., EYMARD, J. C., HASBINI, A., BOUSQUET, G. & SOULIE, M. 2013. Androgen-deprivation therapy alone or with docetaxel in non-castrate metastatic prostate cancer (GETUG-AFU 15): a randomised, open-label, phase 3 trial. *Lancet Oncol*, 14, 149-58.
- GREENBERG, N. M., DEMAYO, F., FINEGOLD, M. J., MEDINA, D., TILLEY, W. D., ASPINALL, J. O., CUNHA, G. R., DONJACOUR, A. A., MATUSIK, R. J. & ROSEN, J. M. 1995. Prostate cancer in a transgenic mouse. *Proc Natl Acad Sci U S A*, 92, 3439-43.
- GREER, L. F., 3RD & SZALAY, A. A. 2002. Imaging of light emission from the expression of luciferases in living cells and organisms: a review. *Luminescence*, 17, 43-74.
- GREY, A. D., CHANA, M. S., POPERT, R., WOLFE, K., LIYANAGE, S. H. & ACHER, P. L. 2015. Diagnostic accuracy of magnetic resonance imaging (MRI) prostate imaging reporting and data system (PI-RADS) scoring in a transperineal prostate biopsy setting. *BJU Int*, 115, 728-35.
- GROSSMANN, M., CHEUNG, A. S. & ZAJAC, J. D. 2013. Androgens and prostate cancer; pathogenesis and deprivation therapy. *Best Pract Res Clin Endocrinol Metab*, 27, 603-16.
- GUNTHER, U., STAUDER, R., MAYER, B., TERPE, H. J., FINKE, L. & FRIEDRICH, K. 1995. Are CD44 variant isoforms involved in human tumour progression? *Cancer Surv*, 24, 19-42.
- HAESE, A., DE LA TAILLE, A., VAN POPPEL, H., MARBERGER, M., STENZL, A., MULDER, P. F., HULAND, H., ABBOU, C. C., REMZI, M., TINZL, M., FEYERABEND, S., STILLEBROER, A. B., VAN GILS, M. P. & SCHALKEN, J. A. 2008. Clinical utility of the PCA3 urine assay in European men scheduled for repeat biopsy. *Eur Urol*, 54, 1081-8.
- HAGER, S., FRAME, F. M., COLLINS, A. T., BURNS, J. E. & MAITLAND, N. J. 2008. An internal polyadenylation signal substantially increases expression levels of lentivirus-delivered transgenes but has the potential to reduce viral titer in a promoter-dependent manner. *Hum Gene Ther*, 19, 840-50.
- HALL, J. & GUYTON, A. 2000. *Textbook of Medical Physiology* W. B. Saunders Company.

- HAN, M., WALSH, P. C., PARTIN, A. W. & RODRIGUEZ, R. 2000. Ability of the 1992 and 1997 American Joint Committee on Cancer staging systems for prostate cancer to predict progression-free survival after radical prostatectomy for stage T2 disease. *J Urol*, 164, 89-92.
- HARME LIN, A., DANON, T., KELA, I. & BRENNER, O. 2005. Biopsy of the mouse prostate. *Lab Anim*, 39, 215-20.
- HARRIS, W. P., MOSTAGHEL, E. A., NELSON, P. S. & MONTGOMERY, B. 2009. Androgen deprivation therapy: progress in understanding mechanisms of resistance and optimizing androgen depletion. *Nat Clin Pract Urol*, 6, 76-85.
- HAZAN, C., MELZER, K., PANAGEAS, K. S., LI, E., KAMINO, H., KOPF, A., CORDON-CARDO, C., OSMAN, I. & POLSKY, D. 2002. Evaluation of the proliferation marker MIB-1 in the prognosis of cutaneous malignant melanoma. *Cancer*, 95, 634-40.
- HE, H. C., HAN, Z. D., DAI, Q. S., LING, X. H., FU, X., LIN, Z. Y., DENG, Y. H., QIN, G. Q., CAI, C., CHEN, J. H., JIANG, F. N., LIU, X. & ZHONG, W. D. 2013. Global analysis of the differentially expressed miRNAs of prostate cancer in Chinese patients. *BMC Genomics*, 14, 757.
- HEIDENREICH, A., BELLMUNT, J., BOLLA, M., JONIAU, S., MASON, M., MATVEEV, V., MOTTET, N., SCHMID, H. P., VAN DER KWAST, T., WIEGEL, T., ZATTONI, F. & EUROPEAN ASSOCIATION OF, U. 2011. EAU guidelines on prostate cancer. Part 1: screening, diagnosis, and treatment of clinically localised disease. *Eur Urol*, 59, 61-71.
- HOROSZE WICZ, J. S., LEONG, S. S., CHU, T. M., WAJSMAN, Z. L., FRIEDMAN, M., PAPSIDERO, L., KIM, U., CHAI, L. S., KAKATI, S., ARYA, S. K. & SANDBERG, A. A. 1980. The LNCaP cell line--a new model for studies on human prostatic carcinoma. *Prog Clin Biol Res*, 37, 115-32.
- HUNTLY, B. J. & GILLILAND, D. G. 2005. Leukaemia stem cells and the evolution of cancer-stem-cell research. *Nat Rev Cancer*, 5, 311-21.
- HURWITZ, M. D., HALABI, S., ARCHER, L., MCGINNIS, L. S., KUETTEL, M. R., DIBIASE, S. J. & SMALL, E. J. 2011. Combination external beam radiation and brachytherapy boost with androgen deprivation for treatment of intermediate-risk prostate cancer: long-term results of CALGB 99809. *Cancer*, 117, 5579-88.
- HUSS, W. J., MADDISON, L. A. & GREENBERG, N. M. 2001. Autochthonous mouse models for prostate cancer: past, present and future. *Semin Cancer Biol*, 11, 245-60.
- ISAACS, J. T. & COFFEY, D. S. 1989. Etiology and disease process of benign prostatic hyperplasia. *Prostate Suppl*, 2, 33-50.
- IVERSEN, P., TYRRELL, C. J., KAISARY, A. V., ANDERSON, J. B., VAN POPPEL, H., TAMMELA, T. L., CHAMBERLAIN, M., CARROLL, K. & MELEZINEK, I. 2000. Bicalutamide monotherapy compared with castration in patients with nonmetastatic locally advanced prostate cancer: 6.3 years of followup. *J Urol*, 164, 1579-82.
- JACKSON, R. J. & STANDART, N. 1990. Do the poly(A) tail and 3' untranslated region control mRNA translation? *Cell*, 62, 15-24.
- JAMES, N. D., SPEARS, M. R., CLARKE, N. W., DEARNALEY, D. P., DE BONO, J. S., GALE, J., HETHERINGTON, J., HOSKIN, P. J., JONES, R. J., LAING, R., LESTER, J. F., MCLAREN, D., PARKER, C. C., PARMAR, M. K., RITCHIE, A. W., RUSSELL, J. M., STREBEL, R. T., THALMANN, G. N., MASON, M. D. & SYDES, M. R. 2015. Survival with Newly Diagnosed Metastatic Prostate Cancer in the "Docetaxel Era": Data from 917 Patients in the Control Arm of the STAMPEDE Trial (MRC PR08, CRUK/06/019). *Eur Urol*, 67, 1028-38.
- JENSEN, M. M., JORGENSEN, J. T., BINDERUP, T. & KJAER, A. 2008. Tumor volume in subcutaneous mouse xenografts measured by microCT is more accurate and reproducible than determined by 18F-FDG-microPET or external caliper. *BMC Med Imaging*, 8, 16.
- JIANG, J. & HUANG, H. 2010. Targeting the Androgen Receptor by Taxol in Castration-Resistant Prostate Cancer. *Mol Cell Pharmacol*, 2, 1-5.
- JONES, J. M. & GELLERT, M. 2004. The taming of a transposon: V(D)J recombination and the immune system. *Immunol Rev*, 200, 233-48.

- KAIGHN, M. E., NARAYAN, K. S., OHNUKI, Y., LECHNER, J. F. & JONES, L. W. 1979. Establishment and characterization of a human prostatic carcinoma cell line (PC-3). *Invest Urol*, 17, 16-23.
- KANTOFF, P. W., HALABI, S., CONAWAY, M., PICUS, J., KIRSHNER, J., HARS, V., TRUMP, D., WINER, E. P. & VOGELZANG, N. J. 1999. Hydrocortisone with or without mitoxantrone in men with hormone-refractory prostate cancer: results of the cancer and leukemia group B 9182 study. *J Clin Oncol*, 17, 2506-13.
- KANTOFF, P. W., HIGANO, C. S., SHORE, N. D., BERGER, E. R., SMALL, E. J., PENSON, D. F., REDFERN, C. H., FERRARI, A. C., DREICER, R., SIMS, R. B., XU, Y., FROHLICH, M. W., SCHELLHAMMER, P. F. & INVESTIGATORS, I. S. 2010. Sipuleucel-T immunotherapy for castration-resistant prostate cancer. *N Engl J Med*, 363, 411-22.
- KAPLAN-LEFKO, P. J., CHEN, T. M., ITTMANN, M. M., BARRIOS, R. J., AYALA, G. E., HUSS, W. J., MADDISON, L. A., FOSTER, B. A. & GREENBERG, N. M. 2003. Pathobiology of autochthonous prostate cancer in a pre-clinical transgenic mouse model. *Prostate*, 55, 219-37.
- KEIL, K. P., ABLER, L. L., MEHTA, V., ALTMANN, H. M., LAPORTA, J., PLISCH, E. H., SURESH, M., HERNANDEZ, L. L. & VEZINA, C. M. 2014. DNA methylation of E-cadherin is a priming mechanism for prostate development. *Dev Biol*, 387, 142-53.
- KLEIN, E. A., COOPERBERG, M. R., MAGI-GALLUZZI, C., SIMKO, J. P., FALZARANO, S. M., MADDALA, T., CHAN, J. M., LI, J., COWAN, J. E., TSIATIS, A. C., CHERBAVAZ, D. B., PELHAM, R. J., TENGGARA-HUNTER, I., BAEHNER, F. L., KNEZEVIC, D., FEBBO, P. G., SHAK, S., KATTAN, M. W., LEE, M. & CARROLL, P. R. 2014. A 17-gene assay to predict prostate cancer aggressiveness in the context of Gleason grade heterogeneity, tumor multifocality, and biopsy undersampling. *Eur Urol*, 66, 550-60.
- KLOTZ, L. & EMBERTON, M. 2014. Management of low risk prostate cancer-active surveillance and focal therapy. *Nat Rev Clin Oncol*, 11, 324-34.
- KORETS, R., MOTAMEDINIA, P., YESHCHINA, O., DESAI, M. & MCKIERNAN, J. M. 2011. Accuracy of the Kattan nomogram across prostate cancer risk-groups. *BJU Int*, 108, 56-60.
- KRAUS, L. A., SAMUEL, S. K., SCHMID, S. M., DYKES, D. J., WAUD, W. R. & BISSERY, M. C. 2003. The mechanism of action of docetaxel (Taxotere) in xenograft models is not limited to bcl-2 phosphorylation. *Invest New Drugs*, 21, 259-68.
- KURODA, K., LIU, H., KIM, S., GUO, M., NAVARRO, V. & BANDER, N. H. 2009. Docetaxel down-regulates the expression of androgen receptor and prostate-specific antigen but not prostate-specific membrane antigen in prostate cancer cell lines: implications for PSA surrogacy. *Prostate*, 69, 1579-85.
- KYPRIANOU, N. & ISAACS, J. T. 1988. Activation of programmed cell death in the rat ventral prostate after castration. *Endocrinology*, 122, 552-62.
- LAUFS, S., GUENECHEA, G., GONZALEZ-MURILLO, A., ZSUZSANNA NAGY, K., LUZ LOZANO, M., DEL VAL, C., JONNAKUTY, S., HOTZ-WAGENBLATT, A., JENS ZELLER, W., BUEREN, J. A. & FRUEHAUF, S. 2006. Lentiviral vector integration sites in human NOD/SCID repopulating cells. *J Gene Med*, 8, 1197-207.
- LAWSON, D. A. & WITTE, O. N. 2007. Stem cells in prostate cancer initiation and progression. *J Clin Invest*, 117, 2044-50.
- LEE, C., KOZLOWSKI, J. M. & GRAYHACK, J. T. 1995. Etiology of benign prostatic hyperplasia. *Urol Clin North Am*, 22, 237-46.
- LEE, J. L., AHN, J. H., CHOI, M. K., KIM, Y., HONG, S. W., LEE, K. H., JEONG, I. G., SONG, C., HONG, B. S., HONG, J. H. & AHN, H. 2014. Gemcitabine-oxaliplatin plus prednisolone is active in patients with castration-resistant prostate cancer for whom docetaxel-based chemotherapy failed. *Br J Cancer*, 110, 2472-8.
- LEONG, K. G., WANG, B. E., JOHNSON, L. & GAO, W. Q. 2008. Generation of a prostate from a single adult stem cell. *Nature*, 456, 804-8.
- LEVINE, A. J., TOMASINI, R., MCKEON, F. D., MAK, T. W. & MELINO, G. 2011. The p53 family: guardians of maternal reproduction. *Nat Rev Mol Cell Biol*, 12, 259-65.

- LEWIS, P. F. & EMERMAN, M. 1994. Passage through mitosis is required for oncoretroviruses but not for the human immunodeficiency virus. *J Virol*, 68, 510-6.
- LIN, D., XUE, H., WANG, Y., WU, R., WATAHIKI, A., DONG, X., CHENG, H., WYATT, A. W., COLLINS, C. C., GOUT, P. W. & WANG, Y. 2014. Next generation patient-derived prostate cancer xenograft models. *Asian J Androl*, 16, 407-12.
- LIU, A. Y., NELSON, P. S., VAN DEN ENGH, G. & HOOD, L. 2002. Human prostate epithelial cell-type cDNA libraries and prostate expression patterns. *Prostate*, 50, 92-103.
- LIU, H. S., JAN, M. S., CHOU, C. K., CHEN, P. H. & KE, N. J. 1999. Is green fluorescent protein toxic to the living cells? *Biochem Biophys Res Commun*, 260, 712-7.
- LOKESHWAR, B. L., LOKESHWAR, V. B. & BLOCK, N. L. 1995. Expression of CD44 in prostate cancer cells: association with cell proliferation and invasive potential. *Anticancer Res*, 15, 1191-8.
- LUBAROFF, D. M., COHEN, M. B., SCHULTZ, L. D. & BEAMER, W. G. 1995. Survival of human prostate carcinoma, benign hyperplastic prostate tissues, and IL-2-activated lymphocytes in scid mice. *Prostate*, 27, 32-41.
- LYONS, S. K., MEUWISSEN, R., KRIMPENFORT, P. & BERNS, A. 2003. The generation of a conditional reporter that enables bioluminescence imaging of Cre/loxP-dependent tumorigenesis in mice. *Cancer Res*, 63, 7042-6.
- MADAN, R. A., ARLEN, P. M., MOHEBTASH, M., HODGE, J. W. & GULLEY, J. L. 2009. Prostavac-VF: a vector-based vaccine targeting PSA in prostate cancer. *Expert Opin Investig Drugs*, 18, 1001-11.
- MAITLAND, N. 2015. Why does anti-androgens therapy fail? *European Urology Today*, 27, 10-11.
- MAITLAND, N., CHAMBERS, K., GEORGOPOULOS, L., SIMPSON-HOLLEY, M., LEADLEY, R., EVANS, H., ESSAND, M., DANIELSSON, A., VAN WEERDEN, W., DE RIDDER, C., KRAAIJ, R., BANGMA, C. H. & CONSORTIUM, G. F. 2010. Gene transfer vectors targeted to human prostate cancer: do we need better preclinical testing systems? *Hum Gene Ther*, 21, 815-27.
- MAITLAND, N. J. & COLLINS, A. 2005. A tumour stem cell hypothesis for the origins of prostate cancer. *BJU Int*, 96, 1219-23.
- MAITLAND, N. J., MACINTOSH, C. A., HALL, J., SHARRARD, M., QUINN, G. & LANG, S. 2001. In vitro models to study cellular differentiation and function in human prostate cancers. *Radiat Res*, 155, 133-142.
- MAKAROVSKIY, A. N., SIRYAPORN, E., HIXSON, D. C. & AKERLEY, W. 2002. Survival of docetaxel-resistant prostate cancer cells in vitro depends on phenotype alterations and continuity of drug exposure. *Cell Mol Life Sci*, 59, 1198-211.
- MANDAIR, D., ROSSI, R. E., PERICLEOUS, M., WHYAND, T. & CAPLIN, M. E. 2014. Prostate cancer and the influence of dietary factors and supplements: a systematic review. *Nutr Metab (Lond)*, 11, 30.
- MANI, S. A., GUO, W., LIAO, M. J., EATON, E. N., AYYANAN, A., ZHOU, A. Y., BROOKS, M., REINHARD, F., ZHANG, C. C., SHIPITSIN, M., CAMPBELL, L. L., POLYAK, K., BRISKEN, C., YANG, J. & WEINBERG, R. A. 2008. The epithelial-mesenchymal transition generates cells with properties of stem cells. *Cell*, 133, 704-15.
- MARANGONI, E., VINCENT-SALOMON, A., AUGER, N., DEGEORGES, A., ASSAYAG, F., DE CREMOUX, P., DE PLATER, L., GUYADER, C., DE PINIEUX, G., JUDDE, J. G., REBUCCI, M., TRANPERENNOU, C., SASTRE-GARAU, X., SIGAL-ZAFRANI, B., DELATTRE, O., DIERAS, V. & POUPON, M. F. 2007. A new model of patient tumor-derived breast cancer xenografts for preclinical assays. *Clin Cancer Res*, 13, 3989-98.
- MASSARD, C., DEUTSCH, E. & SORIA, J. C. 2006. Tumour stem cell-targeted treatment: elimination or differentiation. *Ann Oncol*, 17, 1620-4.
- MATTIE, M., CHRISTENSEN, A., CHANG, M. S., YEH, W., SAID, S., SHOSTAK, Y., CAPO, L., VERLINSKY, A., AN, Z., JOSEPH, I., ZHANG, Y., KUMAR-GANESAN, S., MORRISON, K., STOVER, D. & CHALLITA-EID, P. 2013. Molecular characterization of patient-derived human pancreatic

- tumor xenograft models for preclinical and translational development of cancer therapeutics. *Neoplasia*, 15, 1138-50.
- MAZERSKI, J., MARTELLI, S. & BOROWSKI, E. 1998. The geometry of intercalation complex of antitumor mitoxantrone and ametantrone with DNA: molecular dynamics simulations. *Acta Biochim Pol*, 45, 1-11.
- MCNEAL, J. E. 1981. Normal and pathologic anatomy of prostate. *Urology*, 17, 11-6.
- MCNEAL, J. E. 1988. Normal anatomy of the prostate and changes in benign prostatic hypertrophy and carcinoma. *Semin Ultrasound CT MR*, 9, 329-34.
- MEDIAVILLA-VARELA, M., PACHECO, F. J., ALMAGUEL, F., PEREZ, J., SAHAKIAN, E., DANIELS, T. R., LEOH, L. S., PADILLA, A., WALL, N. R., LILLY, M. B., DE LEON, M. & CASIANO, C. A. 2009. Docetaxel-induced prostate cancer cell death involves concomitant activation of caspase and lysosomal pathways and is attenuated by LEDGF/p75. *Mol Cancer*, 8, 68.
- MHAWECH-FAUCEGLIA, P., ZHANG, S., TERRACCIANO, L., SAUTER, G., CHADHURI, A., HERRMANN, F. R. & PENETRANTE, R. 2007. Prostate-specific membrane antigen (PSMA) protein expression in normal and neoplastic tissues and its sensitivity and specificity in prostate adenocarcinoma: an immunohistochemical study using multiple tumour tissue microarray technique. *Histopathology*, 50, 472-83.
- MONTGOMERY, R. B., MOSTAGHEL, E. A., VESSELLA, R., HESS, D. L., KALHORN, T. F., HIGANO, C. S., TRUE, L. D. & NELSON, P. S. 2008. Maintenance of intratumoral androgens in metastatic prostate cancer: a mechanism for castration-resistant tumor growth. *Cancer Res*, 68, 4447-54.
- MOORE, K. & DALLEY, A. 1999. *Clinically Oriented Anatomy*, Philadelphia, Lippincott Williams & Wilkins.
- MORSE, D. L., GRAY, H., PAYNE, C. M. & GILLIES, R. J. 2005. Docetaxel induces cell death through mitotic catastrophe in human breast cancer cells. *Mol Cancer Ther*, 4, 1495-504.
- MOTTET, N., BELLMUNT, J., BOLLA, M., JONIAU, S., MASON, M., MATVEEV, V., SCHMID, H. P., VAN DER KWAST, T., WIEGEL, T., ZATTONI, F. & HEIDENREICH, A. 2011. EAU guidelines on prostate cancer. Part II: Treatment of advanced, relapsing, and castration-resistant prostate cancer. *Eur Urol*, 59, 572-83.
- MUIR, C. S., NECTOUX, J. & STASZEWSKI, J. 1991. The epidemiology of prostatic cancer. Geographical distribution and time-trends. *Acta Oncol*, 30, 133-40.
- NAGLE, R. B., AHMANN, F. R., MCDANIEL, K. M., PAQUIN, M. L., CLARK, V. A. & CELNIKER, A. 1987. Cytokeratin characterization of human prostatic carcinoma and its derived cell lines. *Cancer Res*, 47, 281-6.
- NALDINI, L., BLOMER, U., GALLAY, P., ORY, D., MULLIGAN, R., GAGE, F. H., VERMA, I. M. & TRONO, D. 1996. In vivo gene delivery and stable transduction of nondividing cells by a lentiviral vector. *Science*, 272, 263-7.
- NAVONE, N. M., LOGOTHETIS, C. J., VON ESCHENBACH, A. C. & TRONCOSO, P. 1998. Model systems of prostate cancer: uses and limitations. *Cancer Metastasis Rev*, 17, 361-71.
- NESLUND-DUDAS, C., LEVIN, A. M., BEEBE-DIMMER, J. L., BOCK, C. H., NOCK, N. L., RUNDLE, A., JANKOWSKI, M., KRAJENTA, R., DOU, Q. P., MITRA, B., TANG, D., REBBECK, T. R. & RYBICKI, B. A. 2014. Gene-environment interactions between JAZF1 and occupational and household lead exposure in prostate cancer among African American men. *Cancer Causes Control*, 25, 869-79.
- NICE 2006. Docetaxel for the treatment of hormone-refractory metastatic prostate cancer. *NICE Guidelines*, TA101, Prostate cancer, Jun 2006.
- NICE 2014. Prostate cancer: diagnosis and treatment. *NICE Guidelines*, CG 175, Prostate cancer, Jan 2014.
- NUPPONEN, N. & VISAKORPI, T. 1999. Molecular biology of progression of prostate cancer. *Eur Urol*, 35, 351-4.

- O'NEILL, A. J., PRENCIPE, M., DOWLING, C., FAN, Y., MULRANE, L., GALLAGHER, W. M., O'CONNOR, D., O'CONNOR, R., DEVERY, A., CORCORAN, C., RANI, S., O'DRISCOLL, L., FITZPATRICK, J. M. & WATSON, R. W. 2011. Characterisation and manipulation of docetaxel resistant prostate cancer cell lines. *Mol Cancer*, 10, 126.
- OHBO, K., SUDA, T., HASHIYAMA, M., MANTANI, A., IKEBE, M., MIYAKAWA, K., MORIYAMA, M., NAKAMURA, M., KATSUKI, M., TAKAHASHI, K., YAMAMURA, K. & SUGAMURA, K. 1996. Modulation of hematopoiesis in mice with a truncated mutant of the interleukin-2 receptor gamma chain. *Blood*, 87, 956-67.
- OLIVER, R. T. & GALLAGHER, C. J. 1995. Intermittent endocrine therapy and its potential for chemoprevention of prostate cancer. *Cancer Surv*, 23, 191-207.
- OUSSET, M., VAN KEYMEULEN, A., BOUVENCOURT, G., SHARMA, N., ACHOURI, Y., SIMONS, B. D. & BLANPAIN, C. 2012. Multipotent and unipotent progenitors contribute to prostate postnatal development. *Nat Cell Biol*, 14, 1131-8.
- PANNELL, D., OSBORNE, C. S., YAO, S., SUKONNIK, T., PASCERI, P., KARAIKAKIS, A., OKANO, M., LI, E., LIPSHITZ, H. D. & ELLIS, J. 2000. Retrovirus vector silencing is de novo methylase independent and marked by a repressive histone code. *EMBO J*, 19, 5884-94.
- PARKER, C., NILSSON, S., HEINRICH, D., HELLE, S. I., O'SULLIVAN, J. M., FOSSA, S. D., CHODACKI, A., WIECHNO, P., LOGUE, J., SEKE, M., WIDMARK, A., JOHANNESSEN, D. C., HOSKIN, P., BOTTOMLEY, D., JAMES, N. D., SOLBERG, A., SYNDIKUS, I., KLIMENT, J., WEDEL, S., BOEHMER, S., DALL'OGGIO, M., FRANZEN, L., COLEMAN, R., VOGELZANG, N. J., O'BRYAN-TEAR, C. G., STAUDACHER, K., GARCIA-VARGAS, J., SHAN, M., BRULAND, O. S., SARTOR, O. & INVESTIGATORS, A. 2013. Alpha emitter radium-223 and survival in metastatic prostate cancer. *N Engl J Med*, 369, 213-23.
- PARSONS, J. K., GAGE, W. R., NELSON, W. G. & DE MARZO, A. M. 2001. p63 protein expression is rare in prostate adenocarcinoma: implications for cancer diagnosis and carcinogenesis. *Urology*, 58, 619-24.
- PATRAWALA, L., CALHOUN, T., SCHNEIDER-BROUSSARD, R., LI, H., BHATIA, B., TANG, S., REILLY, J. G., CHANDRA, D., ZHOU, J., CLAYPOOL, K., COGHLAN, L. & TANG, D. G. 2006. Highly purified CD44+ prostate cancer cells from xenograft human tumors are enriched in tumorigenic and metastatic progenitor cells. *Oncogene*, 25, 1696-708.
- PCUK. 2013. *Prostate Cancer UK* [Online]. Available: www.prostatecanceruk.org/.
- PETRYLAK, D. P. 2014. Practical guide to the use of chemotherapy in castration resistant prostate cancer. *Can J Urol*, 21, 77-83.
- PETRYLAK, D. P., TANGEN, C. M., HUSSAIN, M. H., LARA, P. N., JR., JONES, J. A., TAPLIN, M. E., BURCH, P. A., BERRY, D., MOINPOUR, C., KOHLI, M., BENSON, M. C., SMALL, E. J., RAGHAVAN, D. & CRAWFORD, E. D. 2004. Docetaxel and estramustine compared with mitoxantrone and prednisone for advanced refractory prostate cancer. *N Engl J Med*, 351, 1513-20.
- POLSON, E. S., LEWIS, J. L., CELIK, H., MANN, V. M., STOWER, M. J., SIMMS, M. S., RODRIGUES, G., COLLINS, A. T. & MAITLAND, N. J. 2013. Monoallelic expression of TMPRSS2/ERG in prostate cancer stem cells. *Nat Commun*, 4, 1623.
- PORRES, D., PFISTER, D. & HEIDENREICH, A. 2012. Minimally invasive treatment for localized prostate cancer. *Minerva Urol Nefrol*, 64, 245-53.
- POSTMA, R., SCHRODER, F. H., VAN LEENDERS, G. J., HOEDEMAEKER, R. F., VIS, A. N., ROOBOL, M. J. & VAN DER KWAST, T. H. 2007. Cancer detection and cancer characteristics in the European Randomized Study of Screening for Prostate Cancer (ERSPC)--Section Rotterdam. A comparison of two rounds of screening. *Eur Urol*, 52, 89-97.
- PRASAD, S. M., GU, X., LAVELLE, R., LIPSITZ, S. R. & HU, J. C. 2011. Comparative effectiveness of perineal versus retropubic and minimally invasive radical prostatectomy. *J Urol*, 185, 111-5.
- PULUKURI, S. M., GONDI, C. S., LAKKA, S. S., JUTLA, A., ESTES, N., GUJRATI, M. & RAO, J. S. 2005. RNA interference-directed knockdown of urokinase plasminogen activator and urokinase

- plasminogen activator receptor inhibits prostate cancer cell invasion, survival, and tumorigenicity in vivo. *J Biol Chem*, 280, 36529-40.
- RAFFO, A. J., PERLMAN, H., CHEN, M. W., DAY, M. L., STREITMAN, J. S. & BUTTYAN, R. 1995. Overexpression of bcl-2 protects prostate cancer cells from apoptosis in vitro and confers resistance to androgen depletion in vivo. *Cancer Res*, 55, 4438-45.
- RAGHAVAN, D., KOCZWARA, B. & JAVLE, M. 1997. Evolving strategies of cytotoxic chemotherapy for advanced prostate cancer. *Eur J Cancer*, 33, 566-74.
- RAMSAY, J. A., FROM, L., ISCOE, N. A. & KAHN, H. J. 1995. MIB-1 proliferative activity is a significant prognostic factor in primary thick cutaneous melanomas. *J Invest Dermatol*, 105, 22-6.
- RICHARDSON, G. D., ROBSON, C. N., LANG, S. H., NEAL, D. E., MAITLAND, N. J. & COLLINS, A. T. 2004. CD133, a novel marker for human prostatic epithelial stem cells. *J Cell Sci*, 117, 3539-45.
- RIVIERE, J., BERNHARD, J. C., ROBERT, G., WALLERAND, H., DETI, E., MAURICE-TISON, S., ARDIET, J. M., MAIRE, J. P., RICHAUD, P., FERRIERE, J. M., BALLANGER, P., GELET, A. & PASTICIER, G. 2010. Salvage radiotherapy after high-intensity focussed ultrasound for recurrent localised prostate cancer. *Eur Urol*, 58, 567-73.
- ROSS, R. W., BEER, T. M., JACOBUS, S., BUBLEY, G. J., TAPLIN, M. E., RYAN, C. W., HUANG, J., OH, W. K. & PROSTATE CANCER CLINICAL TRIALS, C. 2008. A phase 2 study of carboplatin plus docetaxel in men with metastatic hormone-refractory prostate cancer who are refractory to docetaxel. *Cancer*, 112, 521-6.
- ROTHKE, M., BLONDIN, D., SCHLEMMER, H. P. & FRANIEL, T. 2013. [PI-RADS classification: structured reporting for MRI of the prostate]. *Rofo*, 185, 253-61.
- ROUSE, P., SHAW, G., AHMED, H. U., FREEMAN, A., ALLEN, C. & EMBERTON, M. 2011. Multi-parametric magnetic resonance imaging to rule-in and rule-out clinically important prostate cancer in men at risk: a cohort study. *Urol Int*, 87, 49-53.
- RYAN, C. J., SMITH, M. R., DE BONO, J. S., MOLINA, A., LOGOTHETIS, C. J., DE SOUZA, P., FIZAZI, K., MAINWARING, P., PIULATS, J. M., NG, S., CARLES, J., MULDER, P. F., BASCH, E., SMALL, E. J., SAAD, F., SCHRIJVERS, D., VAN POPPEL, H., MUKHERJEE, S. D., SUTTMANN, H., GERRITSEN, W. R., FLAIG, T. W., GEORGE, D. J., YU, E. Y., EFSTATHIOU, E., PANTUCK, A., WINQUIST, E., HIGANO, C. S., TAPLIN, M. E., PARK, Y., KHEOH, T., GRIFFIN, T., SCHER, H. I., RATHKOPF, D. E. & INVESTIGATORS, C.-A.-. 2013. Abiraterone in metastatic prostate cancer without previous chemotherapy. *N Engl J Med*, 368, 138-48.
- SABBISSETTI, V., DI NAPOLI, A., SEELEY, A., AMATO, A. M., O'REGAN, E., GHEBREMICHAEL, M., LODA, M. & SIGNORETTI, S. 2009. p63 promotes cell survival through fatty acid synthase. *PLoS One*, 4, e5877.
- SANDLER, H. M. 2015. A phase III protocol of androgen suppression (AS) and 3DCRT/IMRT versus AS and 3DCRT/IMRT followed by chemotherapy (CT) with docetaxel and prednisone for localized, high-risk prostate cancer (RTOG 0521). *J Clin Oncol* 33.
- SCHER, H. I., FIZAZI, K., SAAD, F., TAPLIN, M. E., STERNBERG, C. N., MILLER, K., DE WIT, R., MULDER, P., CHI, K. N., SHORE, N. D., ARMSTRONG, A. J., FLAIG, T. W., FLECHON, A., MAINWARING, P., FLEMING, M., HAINSWORTH, J. D., HIRMAND, M., SELBY, B., SEELY, L., DE BONO, J. S. & INVESTIGATORS, A. 2012. Increased survival with enzalutamide in prostate cancer after chemotherapy. *N Engl J Med*, 367, 1187-97.
- SCHOENWOLF, G., BLEYL, S., BRAUER, P. & FRANCIS-WEST, P. 2008. *Larsen's Human Embryology*, Churchill Livingstone.
- SCHOLZEN, T. & GERDES, J. 2000. The Ki-67 protein: from the known and the unknown. *J Cell Physiol*, 182, 311-22.
- SCHRADER, A. J., BOEGEMANN, M., OHLMANN, C. H., SCHNOELLER, T. J., KRABBE, L. M., HAJILI, T., JENTZMIK, F., STOECKLE, M., SCHRADER, M., HERRMANN, E. & CRONAUER, M. V. 2014. Enzalutamide in castration-resistant prostate cancer patients progressing after docetaxel and abiraterone. *Eur Urol*, 65, 30-6.

- SCHRODER, F. H., CARTER, H. B., WOLTERS, T., VAN DEN BERGH, R. C., GOSSELAAR, C., BANGMA, C. H. & ROOBOL, M. J. 2008. Early detection of prostate cancer in 2007. Part 1: PSA and PSA kinetics. *Eur Urol*, 53, 468-77.
- SCHRODER, F. H., HERMANEK, P., DENIS, L., FAIR, W. R., GOSPODAROWICZ, M. K. & PAVONE-MACALUSO, M. 1992. The TNM classification of prostate cancer. *Prostate Suppl*, 4, 129-38.
- SCHRODER, F. H., HUGOSSON, J., ROOBOL, M. J., TAMMELA, T. L., CIATTO, S., NELEN, V., KWIATKOWSKI, M., LUJAN, M., LILJA, H., ZAPPA, M., DENIS, L. J., RECKER, F., PAEZ, A., MAATTANEN, L., BANGMA, C. H., AUS, G., CARLSSON, S., VILLERS, A., REBILLARD, X., VAN DER KWAST, T., KUJALA, P. M., BLIJENBERG, B. G., STENMAN, U. H., HUBER, A., TAARI, K., HAKAMA, M., MOSS, S. M., DE KONING, H. J., AUVINEN, A. & INVESTIGATORS, E. 2012. Prostate-cancer mortality at 11 years of follow-up. *N Engl J Med*, 366, 981-90.
- SCHRODER, F. H., VAN DER MAAS, P., BEEMSTERBOER, P., KRUGER, A. B., HOEDEMAEKER, R., RIETBERGEN, J. & KRANSE, R. 1998. Evaluation of the digital rectal examination as a screening test for prostate cancer. Rotterdam section of the European Randomized Study of Screening for Prostate Cancer. *J Natl Cancer Inst*, 90, 1817-23.
- SEER. 2010. *Surveillance, Epidemiology, and End Results Program* [Online]. Available: seer.cancer.gov/csr/1975_2010/.
- SHAH, R., MUCCI, N. R., AMIN, A., MACOSKA, J. A. & RUBIN, M. A. 2001. Postatrophic hyperplasia of the prostate gland: neoplastic precursor or innocent bystander? *Am J Pathol*, 158, 1767-73.
- SHAO, R., SHI, J., LIU, H., SHI, X., DU, X., KLOCKER, H., LEE, C., ZHU, Y. & ZHANG, J. 2014. Epithelial-to-mesenchymal transition and estrogen receptor alpha mediated epithelial dedifferentiation mark the development of benign prostatic hyperplasia. *Prostate*, 74, 970-82.
- SHARIFI, N., KAWASAKI, B. T., HURT, E. M. & FARRAR, W. L. 2006. Stem cells in prostate cancer: resolving the castrate-resistant conundrum and implications for hormonal therapy. *Cancer Biol Ther*, 5, 901-6.
- SHEN, F. R., YAN, C. Y., LIU, M., FENG, Y. H. & CHEN, Y. G. 2013. Relationship between multidrug resistance 1 polymorphisms and the risk of prostate cancer in Chinese populations. *Genet Mol Res*, 12, 3806-12.
- SHEN, M. M. & ABATE-SHEN, C. 2007. Pten inactivation and the emergence of androgen-independent prostate cancer. *Cancer Res*, 67, 6535-8.
- SHULTZ, L. D., SCHWEITZER, P. A., CHRISTIANSON, S. W., GOTT, B., SCHWEITZER, I. B., TENNENT, B., MCKENNA, S., MOBRAATEN, L., RAJAN, T. V., GREINER, D. L. & ET AL. 1995. Multiple defects in innate and adaptive immunologic function in NOD/LtSz-scid mice. *J Immunol*, 154, 180-91.
- SIGNORETTI, S., WALTREGNY, D., DILKS, J., ISAAC, B., LIN, D., GARRAWAY, L., YANG, A., MONTIRONI, R., MCKEON, F. & LODA, M. 2000. p63 is a prostate basal cell marker and is required for prostate development. *Am J Pathol*, 157, 1769-75.
- SIMENTAL, J. A., SAR, M., LANE, M. V., FRENCH, F. S. & WILSON, E. M. 1991. Transcriptional activation and nuclear targeting signals of the human androgen receptor. *J Biol Chem*, 266, 510-8.
- SINNATAMBY, C. 1999. *Last's Anatomy: Regional and Applied*, Churchill Livingstone.
- SJOQUIST, K. M., CHIN, V. T., CHANTRILL, L. A., O'CONNOR, C., HEMMINGS, C., CHANG, D. K., CHOU, A., PAJIC, M., JOHNS, A. L., NAGRIAL, A. M., BIANKIN, A. V. & YIP, D. 2014. Personalising pancreas cancer treatment: When tissue is the issue. *World J Gastroenterol*, 20, 7849-63.
- SONPAVDE, G., WANG, C. G., GALSKEY, M. D., OH, W. K. & ARMSTRONG, A. J. 2015. Cytotoxic chemotherapy in the contemporary management of metastatic castration-resistant prostate cancer (mCRPC). *BJU Int*, 116, 17-29.
- STONE, K. R., MICKEY, D. D., WUNDERLI, H., MICKEY, G. H. & PAULSON, D. F. 1978. Isolation of a human prostate carcinoma cell line (DU 145). *Int J Cancer*, 21, 274-81.

- SUN, S., SPRENGER, C. C., VESSELLA, R. L., HAUGK, K., SORIANO, K., MOSTAGHEL, E. A., PAGE, S. T., COLEMAN, I. M., NGUYEN, H. M., SUN, H., NELSON, P. S. & PLYMATE, S. R. 2010. Castration resistance in human prostate cancer is conferred by a frequently occurring androgen receptor splice variant. *J Clin Invest*, 120, 2715-30.
- SUTER, D. M., CARTIER, L., BETTIOL, E., TIREFORT, D., JACONI, M. E., DUBOIS-DAUPHIN, M. & KRAUSE, K. H. 2006. Rapid generation of stable transgenic embryonic stem cell lines using modular lentivectors. *Stem Cells*, 24, 615-23.
- SWEENEY CJ, C. Y., CARDUCCI MA 2014. Impact on overall survival with chemohormonal therapy versus hormonal therapy for hormone sensitive newly metastatic PC (mPrCa), an ECOG ledphase II randomised trial. *J Clin Oncol*, 32.
- TAN, M. H., LI, J., XU, H. E., MELCHER, K. & YONG, E. L. 2015. Androgen receptor: structure, role in prostate cancer and drug discovery. *Acta Pharmacol Sin*, 36, 3-23.
- TANNOCK, I. F., DE WIT, R., BERRY, W. R., HORTI, J., PLUZANSKA, A., CHI, K. N., OUDARD, S., THEODORE, C., JAMES, N. D., TURESSON, I., ROSENTHAL, M. A., EISENBERGER, M. A. & INVESTIGATORS, T. A. X. 2004. Docetaxel plus prednisone or mitoxantrone plus prednisone for advanced prostate cancer. *N Engl J Med*, 351, 1502-12.
- TANNOCK, I. F., OSOBA, D., STOCKLER, M. R., ERNST, D. S., NEVILLE, A. J., MOORE, M. J., ARMITAGE, G. R., WILSON, J. J., VENNER, P. M., COPPIN, C. M. & MURPHY, K. C. 1996. Chemotherapy with mitoxantrone plus prednisone or prednisone alone for symptomatic hormone-resistant prostate cancer: a Canadian randomized trial with palliative end points. *J Clin Oncol*, 14, 1756-64.
- TAPLIN, M. E., BUBLEY, G. J., KO, Y. J., SMALL, E. J., UPTON, M., RAJESHKUMAR, B. & BALK, S. P. 1999. Selection for androgen receptor mutations in prostate cancers treated with androgen antagonist. *Cancer Res*, 59, 2511-5.
- TAPLIN, M. E., BUBLEY, G. J., SHUSTER, T. D., FRANTZ, M. E., SPOONER, A. E., OGATA, G. K., KEER, H. N. & BALK, S. P. 1995. Mutation of the androgen-receptor gene in metastatic androgen-independent prostate cancer. *N Engl J Med*, 332, 1393-8.
- TAYLOR, B. S., SCHULTZ, N., HIERONYMUS, H., GOPALAN, A., XIAO, Y., CARVER, B. S., ARORA, V. K., KAUSHIK, P., CERAMI, E., REVA, B., ANTIPIN, Y., MITSIADES, N., LANDERS, T., DOLGALEV, I., MAJOR, J. E., WILSON, M., SOCCI, N. D., LASH, A. E., HEGUY, A., EASTHAM, J. A., SCHER, H. I., REUTER, V. E., SCARDINO, P. T., SANDER, C., SAWYERS, C. L. & GERALD, W. L. 2010. Integrative genomic profiling of human prostate cancer. *Cancer Cell*, 18, 11-22.
- THOMPSON, D., EASTON, D. F. & BREAST CANCER LINKAGE, C. 2002. Cancer Incidence in BRCA1 mutation carriers. *J Natl Cancer Inst*, 94, 1358-65.
- THOMPSON, I. M., PAULER, D. K., GOODMAN, P. J., TANGEN, C. M., LUCIA, M. S., PARNES, H. L., MINASIAN, L. M., FORD, L. G., LIPPMAN, S. M., CRAWFORD, E. D., CROWLEY, J. J. & COLTMAN, C. A., JR. 2004. Prevalence of prostate cancer among men with a prostate-specific antigen level ≤ 4.0 ng per milliliter. *N Engl J Med*, 350, 2239-46.
- TILLEY, W. D., BUCHANAN, G., HICKEY, T. E. & BENTEL, J. M. 1996. Mutations in the androgen receptor gene are associated with progression of human prostate cancer to androgen independence. *Clin Cancer Res*, 2, 277-85.
- TOMLINS, S. A., MEHRA, R., RHODES, D. R., CAO, X., WANG, L., DHANASEKARAN, S. M., KALYANA-SUNDARAM, S., WEI, J. T., RUBIN, M. A., PIENTA, K. J., SHAH, R. B. & CHINNAIYAN, A. M. 2007. Integrative molecular concept modeling of prostate cancer progression. *Nat Genet*, 39, 41-51.
- VALKENBURG, K. C. & WILLIAMS, B. O. 2011. Mouse models of prostate cancer. *Prostate Cancer*, 2011, 895238.
- VAN BRUSSEL, J. P. & MICKISCH, G. H. 2003. Multidrug resistance in prostate cancer. *Onkologie*, 26, 175-81.

- VAN DEN BRANDT, J., WANG, D., KWON, S. H., HEINKELEIN, M. & REICHARDT, H. M. 2004. Lentivirally generated eGFP-transgenic rats allow efficient cell tracking in vivo. *Genesis*, 39, 94-9.
- VAN SOEST, R. J., DE MORREE, E. S., SHEN, L., TANNOCK, I. F., EISENBERGER, M. A. & DE WIT, R. 2014. Initial biopsy Gleason score as a predictive marker for survival benefit in patients with castration-resistant prostate cancer treated with docetaxel: data from the TAX327 study. *Eur Urol*, 66, 330-6.
- VAN SOEST, R. J., VAN ROYEN, M. E., DE MORREE, E. S., MOLL, J. M., TEUBEL, W., WIEMER, E. A., MATHIJSSSEN, R. H., DE WIT, R. & VAN WEERDEN, W. M. 2013. Cross-resistance between taxanes and new hormonal agents abiraterone and enzalutamide may affect drug sequence choices in metastatic castration-resistant prostate cancer. *Eur J Cancer*, 49, 3821-30.
- VAN WEERDEN, W. M., BANGMA, C. & DE WIT, R. 2009. Human xenograft models as useful tools to assess the potential of novel therapeutics in prostate cancer. *Br J Cancer*, 100, 13-8.
- VAN WEERDEN, W. M., DE RIDDER, C. M., VERDAASDONK, C. L., ROMIJN, J. C., VAN DER KWAST, T. H., SCHRODER, F. H. & VAN STEENBRUGGE, G. J. 1996. Development of seven new human prostate tumor xenograft models and their histopathological characterization. *Am J Pathol*, 149, 1055-62.
- VAN WEERDEN, W. M. & ROMIJN, J. C. 2000. Use of nude mouse xenograft models in prostate cancer research. *Prostate*, 43, 263-71.
- VYAS, L., ACHER, P., KINSELLA, J., CHALLACOMBE, B., CHANG, R. T., STURCH, P., CAHILL, D., CHANDRA, A. & POPERT, R. 2014. Indications, results and safety profile of transperineal sector biopsies (TPSB) of the prostate: a single centre experience of 634 cases. *BJU Int*, 114, 32-7.
- WANG, X., KRUIHOF-DE JULIO, M., ECONOMIDES, K. D., WALKER, D., YU, H., HALILI, M. V., HU, Y. P., PRICE, S. M., ABATE-SHEN, C. & SHEN, M. M. 2009. A luminal epithelial stem cell that is a cell of origin for prostate cancer. *Nature*, 461, 495-500.
- WANG, Y., REVELO, M. P., SUDILOVSKY, D., CAO, M., CHEN, W. G., GOETZ, L., XUE, H., SADAR, M., SHAPPELL, S. B., CUNHA, G. R. & HAYWARD, S. W. 2005. Development and characterization of efficient xenograft models for benign and malignant human prostate tissue. *Prostate*, 64, 149-59.
- WARMUTH, M., JOHANSSON, T. & MAD, P. 2010. Systematic review of the efficacy and safety of high-intensity focussed ultrasound for the primary and salvage treatment of prostate cancer. *Eur Urol*, 58, 803-15.
- WATSON, P. A., CHEN, Y. F., BALBAS, M. D., WONGVIPAT, J., SOCCI, N. D., VIALE, A., KIM, K. & SAWYERS, C. L. 2010. Constitutively active androgen receptor splice variants expressed in castration-resistant prostate cancer require full-length androgen receptor. *Proc Natl Acad Sci U S A*, 107, 16759-65.
- WEBBER, M. M., BELLO, D. & QUADER, S. 1996. Immortalized and tumorigenic adult human prostatic epithelial cell lines: characteristics and applications. Part I. Cell markers and immortalized nontumorigenic cell lines. *Prostate*, 29, 386-94.
- WILT, T. J. 2012. The Prostate Cancer Intervention Versus Observation Trial: VA/NCI/AHRQ Cooperative Studies Program #407 (PIVOT): design and baseline results of a randomized controlled trial comparing radical prostatectomy with watchful waiting for men with clinically localized prostate cancer. *J Natl Cancer Inst Monogr*, 2012, 184-90.
- WINTER, S. F., COOPER, A. B. & GREENBERG, N. M. 2003. Models of metastatic prostate cancer: a transgenic perspective. *Prostate Cancer Prostatic Dis*, 6, 204-11.
- WOLFF, J. M. & MASON, M. 2012. Drivers for change in the management of prostate cancer - guidelines and new treatment techniques. *BJU Int*, 109 Suppl 6, 33-41.
- XIA, X., ZHANG, Y., ZIETH, C. R. & ZHANG, S. C. 2007. Transgenes delivered by lentiviral vector are suppressed in human embryonic stem cells in a promoter-dependent manner. *Stem Cells Dev*, 16, 167-76.

- XU, J., QIU, Y., DEMAYO, F. J., TSAI, S. Y., TSAI, M. J. & O'MALLEY, B. W. 1998. Partial hormone resistance in mice with disruption of the steroid receptor coactivator-1 (SRC-1) gene. *Science*, 279, 1922-5.
- YADAV, N. & HEEMERS, H. V. 2012. Androgen action in the prostate gland. *Minerva Urol Nefrol*, 64, 35-49.
- YANG, A., KAGHAD, M., WANG, Y., GILLETT, E., FLEMING, M. D., DOTSCHE, V., ANDREWS, N. C., CAPUT, D. & MCKEON, F. 1998. p63, a p53 homolog at 3q27-29, encodes multiple products with transactivating, death-inducing, and dominant-negative activities. *Mol Cell*, 2, 305-16.
- YOSHINO, H., UEDA, T., KAWAHATA, M., KOBAYASHI, K., EBIHARA, Y., MANABE, A., TANAKA, R., ITO, M., ASANO, S., NAKAHATA, T. & TSUJI, K. 2000. Natural killer cell depletion by anti-asialo GM1 antiserum treatment enhances human hematopoietic stem cell engraftment in NOD/Shi-scid mice. *Bone Marrow Transplant*, 26, 1211-6.
- ZHANG, F., THORNHILL, S. I., HOWE, S. J., ULAGANATHAN, M., SCHAMBACH, A., SINCLAIR, J., KINNON, C., GASPAR, H. B., ANTONIOU, M. & THRASHER, A. J. 2007. Lentiviral vectors containing an enhancer-less ubiquitously acting chromatin opening element (UCOE) provide highly reproducible and stable transgene expression in hematopoietic cells. *Blood*, 110, 1448-57.
- ZHANG, M., LATHAM, D. E., DELANEY, M. A. & CHAKRAVARTI, A. 2005. Survivin mediates resistance to antiandrogen therapy in prostate cancer. *Oncogene*, 24, 2474-82.
- ZHOU, B. B., ZHANG, H., DAMELIN, M., GELES, K. G., GRINDLEY, J. C. & DIRKS, P. B. 2009. Tumour-initiating cells: challenges and opportunities for anticancer drug discovery. *Nat Rev Drug Discov*, 8, 806-23.
- ZHOU, H. J., YAN, J., LUO, W., AYALA, G., LIN, S. H., ERDEM, H., ITTMANN, M., TSAI, S. Y. & TSAI, M. J. 2005. SRC-3 is required for prostate cancer cell proliferation and survival. *Cancer Res*, 65, 7976-83.

APPENDICES

Appendix 1: List of primary antibodies

Target	Isotype	Clone	Manufacturer	Application	Concentration
Ki67	Mouse mAb	MIB-1	DAKO	IHC	1:50
				FC	1:10
Ki67-FITC	Mouse mAb	MIB-1	DAKO	FC	1:10
Vimentin	Mouse mAb	V9	DAKO	IHC	1:100
PSA	Mouse mAb	ER-PR8	DAKO	IHC	1:25
AR	Rabbit	SC-816X	Santa Cruz	IHC	1:50
				FC	1:50
Pancytokeratin	Mouse mAb	Mixture	Sigma C2562	IHC	1:800
p63	Mouse mAb	DAK-p63	DAKO	IHC	1:50
CD24-PE	Mouse mAb	32D12	Miltenyi Biotec	FC	1:10
CD44-FITC	Mouse mAb	DB105	Miltenyi Biotec	FC	1:10

IHC- immunohistochemistry, FC- flow cytometry

Appendix 2: Negative control antibodies

Target	Isotype	Clone	Manufacturer	Application	Concentration
IgG mouse	IgG1	Not provided	DAKO	IHC	1:100
IgG Goat	Goat	Not provided	DAKO	IHC	1:100

IHC- immunohistochemistry

Appendix 3: Secondary antibodies

Target	Conjugate	Manufacturer	Application	Concentration
Rabbit anti-Mouse	Biotin	DAKO	IHC	1:100
Goat anti-Rabbit	Biotin	DAKO	IHC	1:100
Goat anti-Rabbit	Alexa	Invitrogen	FC	1:200

IHC- immunohistochemistry, FC- flow cytometry

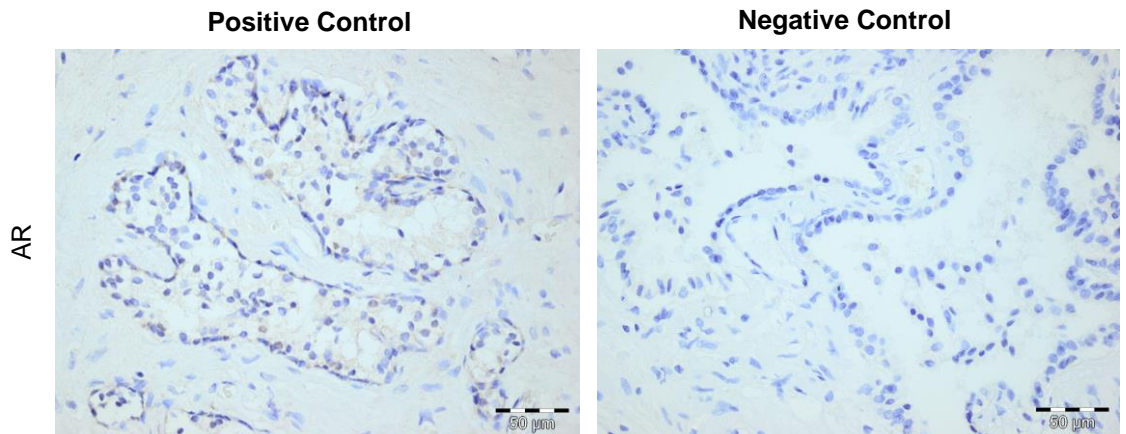
Appendix 4: Table showing the different lasers used for flow cytometry and their emission spectra.

Secondary Antibody	Excitation/nm	Emission/nm
Violet 1	405	425-475
FITC	488	510-550
PE	488	560-590
Alexa 288	488	510-550
Alexa 647	633	645-685
APC	633	645-685

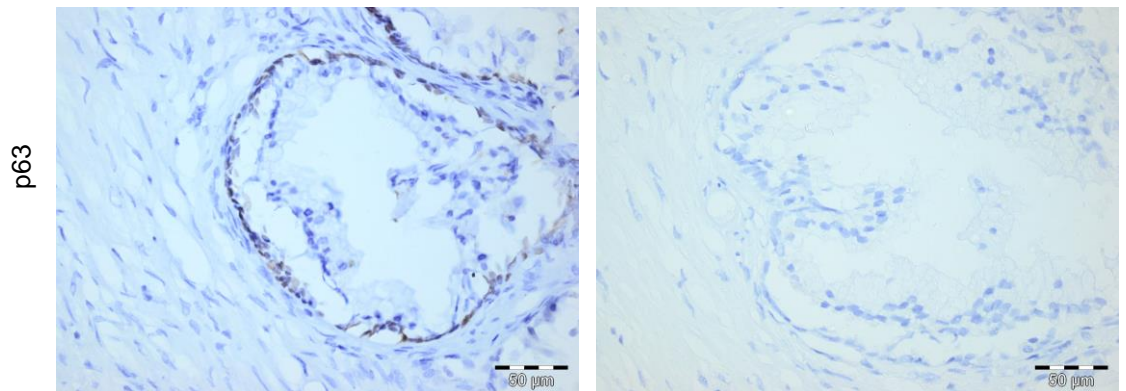
Appendix 5: List of culture medium and composition of buffers

Name	Content of culture media for cell biology
H7	Ham's F-12 medium (Lonza) 7% FCS (PAA) 2mM L-Glutamine (Invitrogen)
R10	Roswell Park Memorial Institute 1640 10% FCS 2mM L-Glutamine
D10	Dulbecco's Modified Eagle Media 10% FCS 2mM L-Glutamine
K2	Keratinocyte Serum-Free Media 2% FCS 2mM L-Glutamine 5ng/ml EGF 50ug/ml bovine pituitary extract
Freezing medium	90% D10 10% DMSO
	Composition of buffers for molecular biology
MACS buffer	PBS, pH 7.2 0.5% FCS 2mM EDTA
	Immunocytochemistry
TBS	50mM Tris-HCl 150mM NaCl

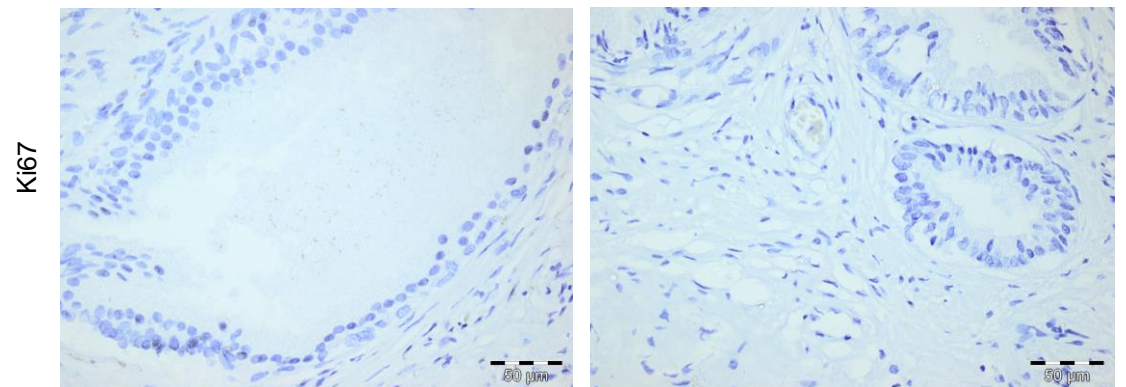
Appendix 6: Supplementary images of immunohistochemistry on BPH positive controls for AR, p63, Ki67, PSA, PCK and Vimentin with the respective IgG negative control. All images were taken on an Olympus BX51 light microscope at x40 magnification with scale bars representing 50µm.



AR staining in the luminal cells of BPH glands compared to its absence in the negative control.

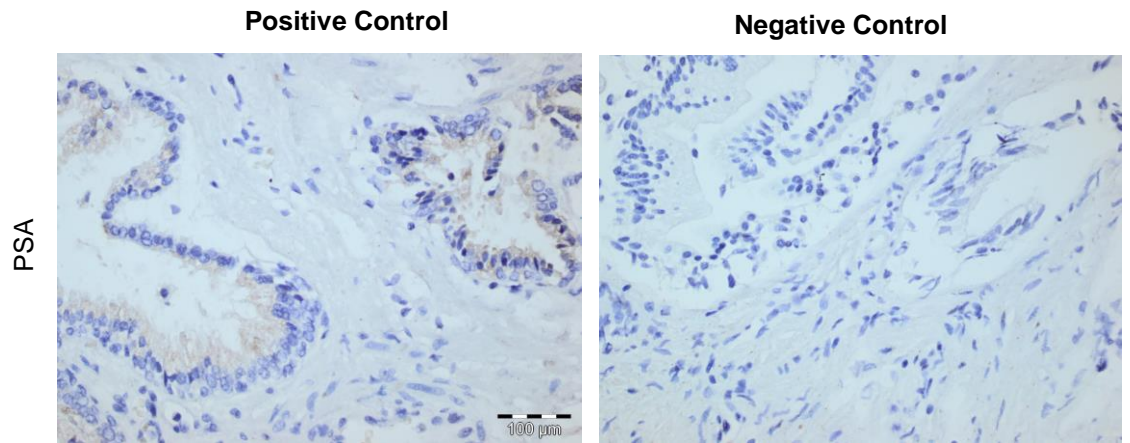


p63 staining in the basal cells of BPH glands compared to its absence in the negative control.

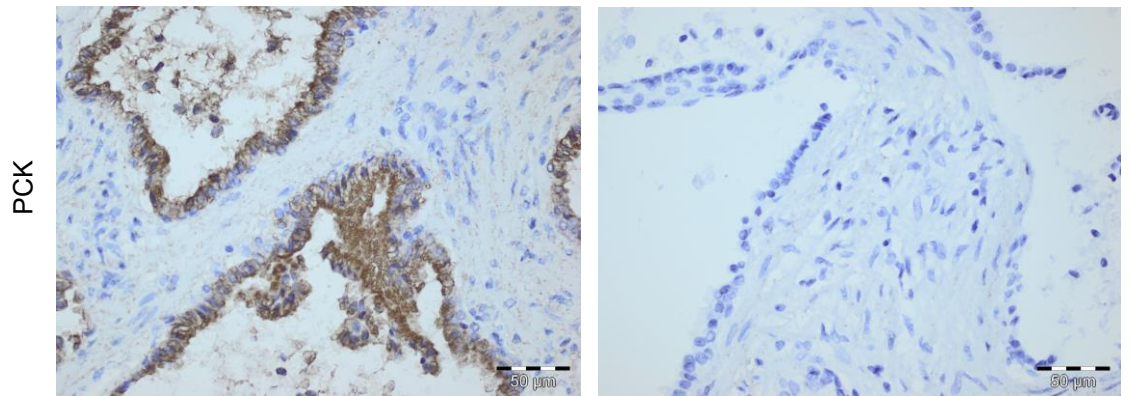


Ki67 staining in BPH cells compared to its absence in the negative control.

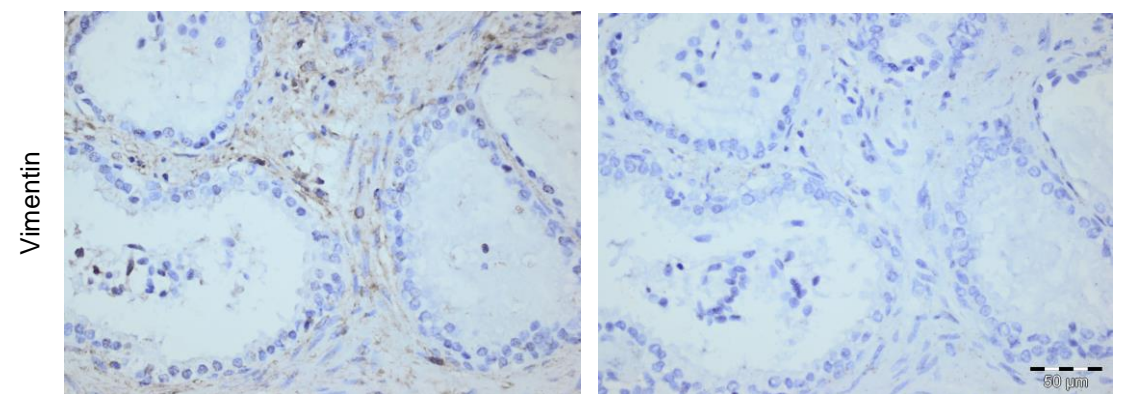
Appendix 6 (continued):



PSA staining in the luminal cells of BPH glands compared to its absence in the negative control.

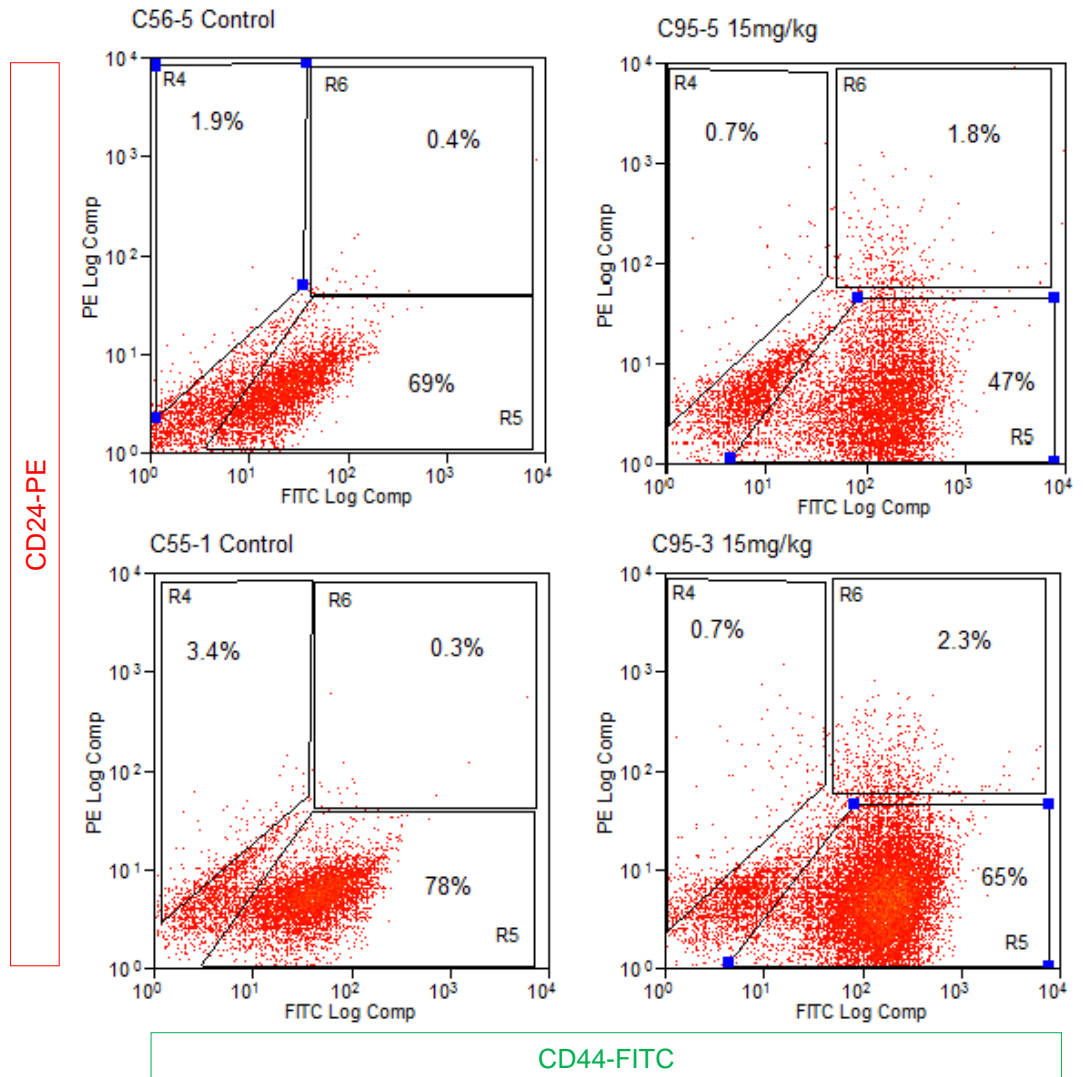


PCK staining in both luminal and basal cells compared to its absence in the negative control.

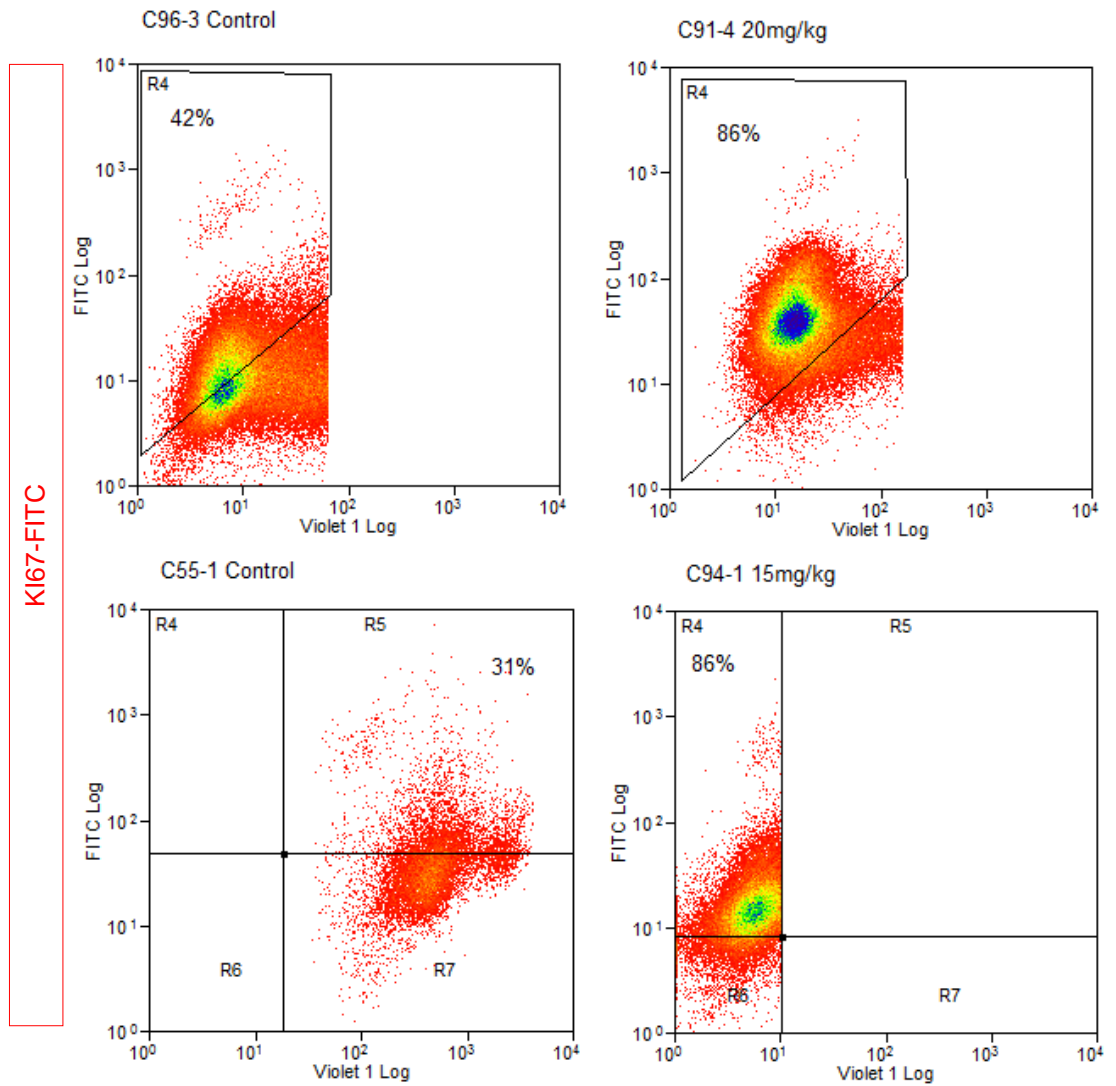


Vimentin staining BPH cells compared to its absence in the negative control.

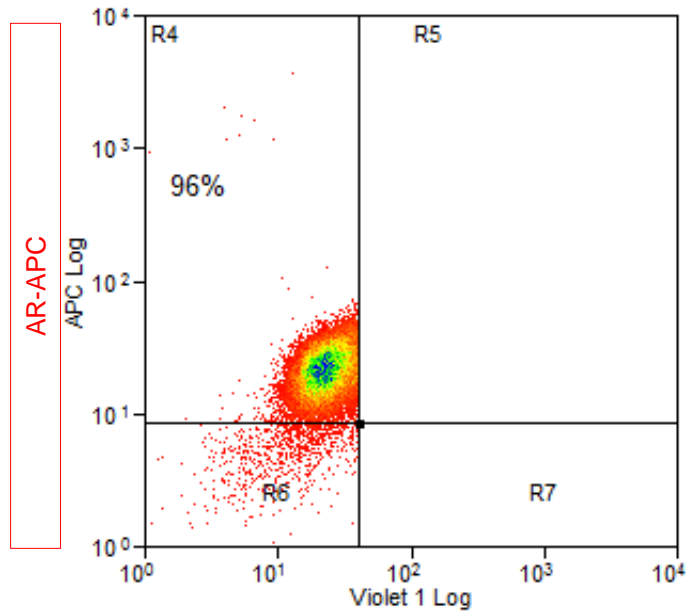
Appendix 7: Flow cytometry analysis of PDX Y019 after treatment with docetaxel. Tumours from the control and 15mg/kg treatment group were analysed. Dot plots of the LIN-/CD31- tumour cells dual labelled for CD44-FITC (x-axis), which labelled basal-like cells and CD24-PE (y-axis) which labelled luminal-like cells. The number of positive cells was set against a control of IgG labelled cells or cells only.



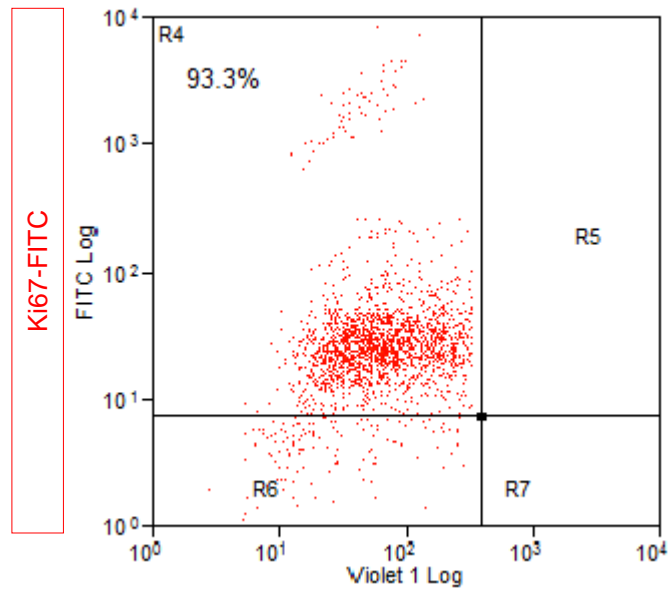
Appendix 8: Flow cytometry analysis of Y019 xenografts after treatment with docetaxel. Dot plots represent the FITC labelled Ki67 positive cells (y-axis), indicating a consistent increase in Ki67 staining with docetaxel treatment. The number of positive cells was set against a control of IgG labelled cells or cells only.



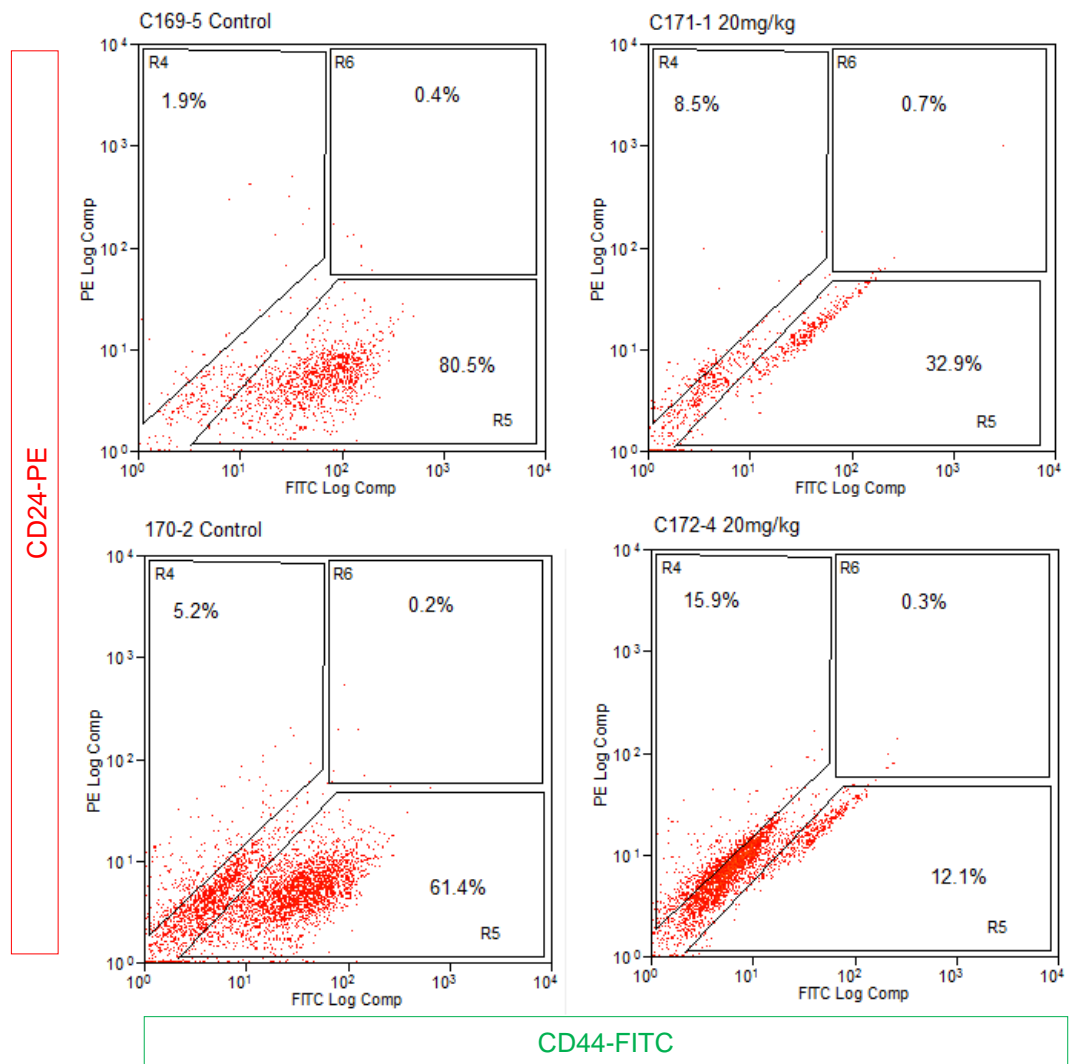
Appendix 9: Flow cytometry analysis of LNCaP cells after staining with AR acting as positive control. Strong positivity (96%) was shown in the R4 rectangle. The number of positive cells was set against a control of IgG labelled cells or cells only.



Appendix 10: Flow cytometry analysis of LNCaP cells after staining with Ki67 acting as positive control. Strong positivity (93.3%) was shown in the R4 rectangle. The number of positive cells was set against a control of IgG labelled cells or cells only.



Appendix 11: Flow cytometry analysis of PDX Y042 after treatment with docetaxel. Tumours from the control and 20mg/kg treatment group were analysed. Dot plots of the LIN-/CD31- tumour cells dual labelled for CD44-FITC (x-axis), which labelled basal-like cells and CD24-PE (y-axis) which labelled luminal-like cells. The number of positive cells was set against a control of IgG labelled cells or cells only.



ABBREVIATIONS

AA	Abiraterone acetate
ABM	antibiotic-antimycotic
ABC	ATP-binding cassette
ADT	androgen deprivation therapy
ACTH	adrenocorticotrophic hormone
AMACR	alpha-methylacyl-CoA racemase
APC	allophycocyanin
APES	3'aminopropyl triethoxysaline
AR	androgen receptor
ARE	androgen responsive elements
ASCO	American society of clinical oncology
ASiT	Association of surgeons in training
AUA	American Urological Association
BAUS	British Association of Urological Surgeons
BPH	benign prostatic hyperplasia
CAPRA	cancer of the prostate risk assessment
CARN	castration-resistant Nkx3-1-expressing cell
CHAARTED	chemo-hormonal therapy vs androgen ablation randomised trial for extended disease
CK	cytokeratin
CMV	cytomegalovirus
CO ₂	carbon dioxide

CRPC	castrate resistant prostate cancer
CRUK	Cancer research UK
CSC	cancer stem cells
CSM	cancer specific mortality
CYP-17	cytochrome P-450-17
DAB	3,3'diaminobenzidine
DAPI	4',6' diamino-2-phenylindole2HCl
DHT	dihydrotestosterone
DMSO	dimethyl sulfoxide
DNA	deoxyribonucleic acid
DPX	Distrene, Plasticiser, Xylene
DRE	digital rectal examination
DWI	diffuse weighted imaging
EAU	European Association of Urology
EBRT	external beam radiotherapy
EF1a	elongation factor 1 alpha
EGF	epidermal growth factor
EMA	European Medicines Agency
EMT	epithelial to mesenchymal transition
EtOH	ethanol
EU	European Union
EDTA	ethylene-diamine-tetra-acetic acid
FACS	Fluorescence-activated cell sorting

FDA	food and drug administration
FITC	fluorescein isothiocyanate
FCS	foetal calf serum
g	gram
GEMM	genetically engineered mouse model
GnRH	Gonadotropin-releasing hormone
GP	general practitioner
GPS	Genomic prostate score
G-CSF	granulocyte colony stimulating factor,
hr	hour
H&E	haematoxylin and eosin
HCl	hydrogen chloride
HIFU	high intensity focused ultrasound
HRP	horseradish peroxidase
HYMS	Hull York Medical School
IHC	Immunohistochemistry
IPTG	Isopropyl β -D-1-thiogalactopyranoside
IMRT	intensity modulated radiotherapy
JCMS	Jackson Laboratory's Colony Management System
KSFM	Keratinocyte serum-free medium
LSM	lymphocyte separation medium
LUTS	lower urinary tract symptoms
M	molar

MDR	multidrug resistance
mg	milligram
ml	millilitre
mm	millimetre
NaCl	sodium chloride
NCOA2	nuclear receptor co-Activator 2
NCRI	National Cancer Research Institute
NICE	National Institute for Health and Care Excellence
NK	natural killer
NOD/SCID	non obese diabetic/SCID
OM	overall mortality
OS	overall survival
p	P-value
PAP	prostatic acid phosphatase
PBS	phosphate buffer solution
PCA3	prostate cancer antigen 3
PC	prostate cancer
PCK	pancytokeratin
PCUK	Prostate cancer UK
PDX	'near patient' derived xenograft
PE	phycoerythrin
PFA	paraformaldehyde
PFS	progression free survival

PIA	proliferative inflammatory atrophy
PIN	prostatic intraepithelium neoplasia
PIRADS	Prostate Imaging Reporting and Data System
PIVOT	PC Intervention versus Observational trial
PSA	prostate specific antigen
PSMA	prostate specific membrane antigen
PTEN	phosphatase and tensin homolog
qRT-PCR	quantitative reverse transcription polymerase chain reaction
RAG2	recombinase activating gene 2
RCT	randomised control trial
RNA	ribonucleic acid
RFP	red fluorescent protein
Rpm	revolutions per minute
RPMI	roswell park institute-1640
RSV	Rous sarcoma virus
RT	room temperature
SC	stem cells
SCID	severe combined immunodeficiency
SD	standard deviation
SEER	Surveillance, Epidemiology and End Results
SEM	standard error of the mean
SHBG	Sex hormone-binding globulin
sh	short hairpin

si	short interfering
STO	a continuous line of SIM mouse embryonic fibroblasts
STR	short tandem repeats
SV40	simian virus 40
SWOG	Southwest Oncology Group
T	testosterone
TA	transcription activating
TAP	thesis advisory panel
TBS	tris-buffered solution
TM	trade mark
TMPRSS2	transmembrane protease serine 2
TNM	Tumour-Node-Metastasis
TRAMP	transgenic adenocarcinoma of the mouse prostate
TRUS	transrectal ultrasound scan
TURP	transurethral resection of the prostate
UCSF	university of California, San Francisco
UK	United Kingdom
V	volt
YUAG	Yorkshire urology group
YCR	Yorkshire Cancer Research
%	percentage
°C	degree celcius
α	alpha

β	beta
μ	micro
Δ	delta
γ	gamma